PROFILE OF RETINAL PIGMENT EPITHELIUM RESPONSE TO ETHANOL: ROLE OF CYP2E1

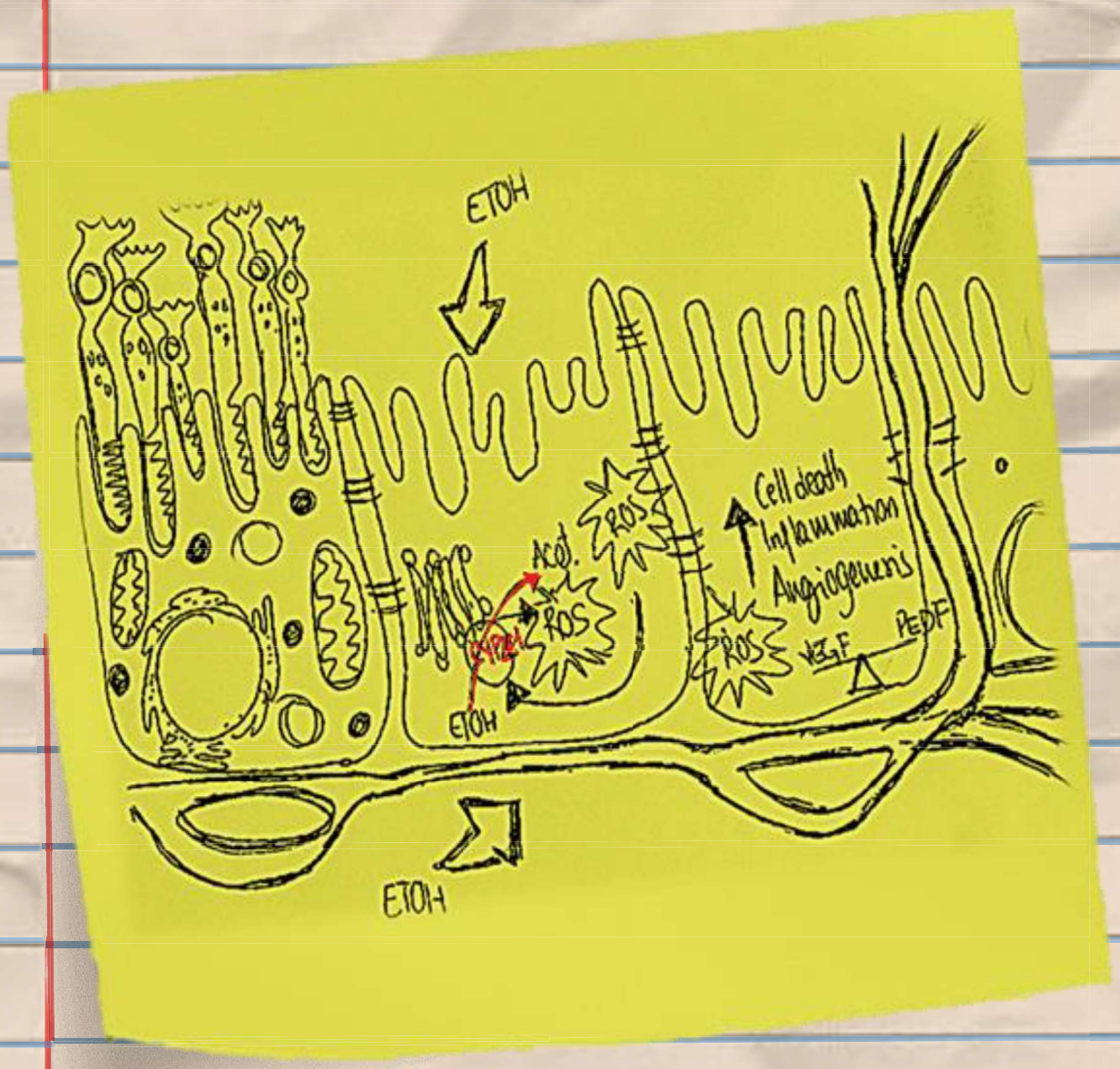

Natalia Martínez Gil
Valencia 2017

Supervised By:
Prof. Dr. F. J. Romero
Dr. J. M. Barcia

Universidad Católica de Valencia
San Vicente Mártir

Profile of Retinal Pigment Epithelium Response to Ethanol: Role of CYP2E1

Natalia Martínez Gil

Doctoral Thesis

Supervised By:
Dr. F. J. Romero
Dr. J. M. Barcia

La presente tesis doctoral titulada “Profile of Retinal Pigment Epithelium Response to Ethanol: Role of CYP2E1” ha sido realizada gracias a la financiación concedida por las siguientes instituciones: Generalitat Valenciana (FPA/2013/034, Acomp/2013/036, GV/2014/106, PROMETEO/2016/094). Universidad Católica de Valencia San Vicente Mártir (2013/128/005, 2015-128-003)

To those who support and trust in science to make a better world.

"[...] In the laboratory I become from a girl into a scientist, just like Peter Parker becoming Spider-Man [...] My lab is the place where I can be the child that I still am"

Hope Jahred.
Lab Girl

Acknowledgements

El camino que he recorrido para llegar hasta aquí comenzó hace más de 10 años. El día que decidí ser investigadora. Nunca lo hubiera logrado sin la ayuda de muchísimas personas. Sólo tengo palabras de agradecimiento y también de admiración. Pues saben que este no es el final, sino una etapa más, y siguen brindándome su apoyo. Así que corregiré mi primera frase; El camino que hemos recorrido para llegar hasta aquí comenzó hace más de 10 años, ¡GRACIAS por estos maravillosos años!

No quiero olvidarme de nadie, por ello me gustaría daros las gracias en el orden en el que habéis ido apareciendo y participando en esta aventura.

Gracias al Dr. Mateo Tolosa, porque no sólo me abriste las puertas de tu laboratorio cuando aún era estudiante de tercer curso de Biología, sino que también me abriste las del increíble mundo de la investigación… y desde ese día, ya no he vuelto a salir.

Gracias al Dr. Hermenegildo y a la Dra. Novella, ha sido un placer formar parte de vuestro grupo. Con vosotros no sólo aprendí de ciencia… gracias por vuestro constante apoyo y cariño y por enseñarme a ser esa flecha roja! También a vosotros Pascual y Gloria, ¡Muchas gracias! A ti Carlos Bueno, mejor dicho, "Chechu" porque fueron tantas horas, días de comida-cena, fines de semana… gracias por tu paciencia y por convertirte en un amigo. Al resto de LINCES, Maca, Xavi y Ana, fue corto pero intenso, gracias por hacerme sentir siempre una más. A los "raros", Isa, Marta y Santi y menos rara Jessica. Da gusto compartir penas y glorias con vosotros, bien sea en París, Sevilla, Granada, o Càlig City.

Por supuesto, esta tesis no habría sido posible sin el Dr. Romero y el Dr. Barcia. Gracias por haberme dado esta gran oportunidad. Javier, confiaste en mí desde el primer día y me diste alas para plasmar mis locas ideas en experimentos. Tanto Jorge como tú me habéis permitido equivocarme, dejándome aprender de mis errores, ¡Que han sido millones! Ha sido un placer ser vuestra alumna.

Gracias al resto del grupo RETOS. Miguel, que decirte que no sepas, ¡Cuánto te he echado de menos!, Sancho, tu despacho fue un antes y un después en esta tesis, mucha ciencia y ganas de investigar se respiran en ese sitio! Dani, gracias por ayudarme en todo, aunque eso suponga que un químico acabe hablando de biología molecular. Lorena, qué bien ha estado compartir contigo estos últimos momentos!. Gracias por tu apoyo incondicional. A Luis, Sandra, María Benlloch, Albita, Javi, María, Gema y a todos los alumnos que han pasado por el laboratorio incluyendo a la internacional Rosa, también a Saúl. He aprendido mucho de vosotros, ha sido un placer compartir tantos momentos, gracias por vuestra ayuda. Bea y Nuria gracias también por vuestro apoyo tanto técnico como personal.

Hemos vivido muchos momentos juntos, yo me quedo con las celebraciones acompañadas de Cardhu, las barbacoas, las comidas de grupo, los viajes en coche y los experimentos infinitos que requerían de todos nosotros. Esa es nuestra mejor versión.

Leti, Paulita y María, gracias por vuestra paciencia y ayuda en tantas gestiones administrativas, también por enseñarme tanto. A los compañeros de batalla del laboratorio "53120" por compartir conmigo horas de trabajo, también penas, alegrías y alguna que otra "omelette of science".

También a las chicas del IVP, FOM, IIBB-CSIC, y Fernando del IBV gracias por vuestro soporte técnico, disponibilidad y colaboración. No me puedo olvidar de Patri, Quique, Javi y Reyes, ¡Gracias, habéis conseguido sacarme una sonrisa a cualquier hora del día!

I wanted to thank my "American Families" in Baltimore and Boston, because without knowing me they offered me a lot.

Thank you so much to Dra. Canto Soler from Wilmer Eye Institutye at Johns Hopkins University for giving me the opportunity to learn and enjoy science with her team. Thanks to Valeria, Natalia, Minda, Miguel, Silvia, also Marisol, Dr. Handa, Dr. Sinha, and all the students who helped me. It was an awesome experience. Especially thanks to Miguel and Silvia for your generosity, for helping me and welcoming me.

Thank you so much to Dr. Vavvas from Mass Eye and Ear at Harvard Medical School for letting me to learn a lot about animal models. Thank you to all of his postdoctoral fellows Daniel, Eleni, Ahmad, Shoji, Pavlina, Peggy, Bo, Takashi, Nick also Cassandra and Chris. Thank you to all of you for your patient and kindness. I felt at home from day one. Here too, I must thank Daniel for your time, affection and your good advices.

Y no dejo para el final a los últimos en llegar, sino a aquellas personas que me han acompañado desde el principio y que sé que seguirán haciéndolo. A mis amigos de toda la vida y a los que he ido conociendo, a mis compañeras de piso, Eli, Cris, Ele y Glo. Me habéis ayudado a focalizar y desconectar cuando me ha hecho falta. ¡Qué suerte haberos encontrado!. Gracias especialmente a aquellos que han vivido conmigo mis mejores y peores momentos, Miguel y Guillem gracias por vuestro apoyo, por tantos e incontables buenos momentos y por las risas, por la risas siempre! Patri, Ale, Luci, Vivi, Cris y Silvi, habéis sido un pilar fundamental en esta última etapa, gracias por hacer que un día cualquiera acabara siendo el mejor.

Gracias a mi familia de Elda, Petrer y comarca, también de la contorná. A mis abuelas y a mi iaio, de los que sigo aprendiendo cada día. A mis tíos, a los más peques y a mis primos, especialmente a Sandra, gracias por tu ayuda tan profesional. A Ruth, Bernardo y María. Esta tesis también es gracias a todos vosotros, por cambiar las fechas de comidas y celebraciones familiares, por las videollamadas, por esas fiestas de despedida y también de bienvenida en los aeropuertos. ¡Me lo habéis puesto muy fácil!

Gracias Papá y Mamá, recuerdo perfectamente el día que os dije que quería venir Valencia para ser bióloga. No tengo palabras para agradeceros el esfuerzo que habéis hecho para que llegue hasta aquí. Me habéis acompañado, literalmente, en cada escalón que he subido. A mi "geme" Cristina, que aprendiste a dibujar una célula sólo para entender de qué iba esta historia. Gracias por todas y cada una de vuestras palabras de aliento a horas intempestivas, aquí y en la Luna, siempre que os he necesitado. Me siento muy orgullosa de teneros.

Y a ti Daniel, que entiendes cada una de estas líneas mejor que nadie. Que esta tesis no nos ha robado ningún minuto porque has querido estar conmigo en cada paso. Porque me has regalado tus tiempos de incubaciones y tus tiempos de espera para dibujar juntos nuestras hipótesis. Gracias por esquivar las piedras y compartir conmigo este maravilloso camino.

Resumen y Palabras clave

Abstract and Keywords

RESUMEN:

El epitelio pigmentario de la retina (RPE) es esencial para la visión. Como parte de la barrera hematorretiniana (BRB) su papel principal es el mantenimiento de la homeostasis de la retina y coroides. El alcohol se ha convertido en la droga adictiva más aceptada por la sociedad causando problemas de salud, sociales y económicos. El estrés oxidativo (OS) inducido por etanol (EtOH) genera toxicidad celular aumentando la aparición de especies reactivas del oxígeno (ROS) que activan respuestas en el organismo como pueden ser inflamación y muerte celular. El enzima citocromo p450 2E1 (CYP2E1) tiene una alta afinidad por el EtOH. Su actividad es la principal fuente de ROS durante la oxidación del EtOH por las células. A pesar de que el CYP2E1 ha sido identificado en el RPE humano y que podría jugar un papel fundamental en la función del ciclo visual del RPE, no se conoce nada sobre su regulación y la respuesta celular que desencadena. Nuestro objetivo fue estudiar el rol del CYP2E1 en el RPE, en respuesta al tratamiento con EtOH.

Fueron empleadas células ARPE-19, hRPE y hiPSC-RPE como modelos de RPE. Simultáneamente al EtOH, se realizaron tratamientos con DAS (inhibidor específico del CYP2E1) y con NAC (como antioxidante) para bloquear el efecto del EtOH en las células. Se realizaron estudios de viabilidad y citotoxicidad con EthD-1, calcein y XTT. El ROS intracelular y los aniones superóxido fueron cuantificados usando sondas fluorescentes (DCF y DHE respectivamente). Los marcadores de estrés celular, angiogénesis e inflamación fueron determinados con kits de expresión proteica. La integridad de la función de la barrera formada por el RPE se determinó midiendo la resistencia eléctrica transepitelial (TER) y el estado de las uniones intercelulares por inmunofluorescencia (IF). Se utilizaron western blot (WB), qPCR, IF y ELISA para cuantificar la expresión del CYP2E1 y los principales factores y moléculas liberadas por el RPE. La actividad del CYP2E se midió mediante HPLC.

El EtOH aumentó los niveles ROS en las células del RPE, dando lugar a la muerte celular por apoptosis. Provocó una disfunción del RPE disminuyendo la integridad de las uniones intercelulares y modificando el perfil de expresión y liberación de factores de crecimiento, inflamación y angiogénesis. El EtOH aumentó la expresión del CYP2E1. El uso de DAS y NAC revirtió el daño causado en la células del RPE revelando que el CYP2E1 en el RPE estaría regulado por el OS. Finalmente, la presencia del CYP2E1 refuerza el papel protector del RPE y sugiere otros roles diferentes del CYP2E1 relacionados con la degeneración del RPE.

PALABRAS CLAVE: Epitelio pigmentario de la retina; Barrera hematorretiniana; Etanol; Estrés oxidativo; Citocromo p450 2E1.

ABSTRACT:

The retinal pigment epithelium (RPE) is essential for the vision. As a part of blood retinal barrier (BRB) its main role is the retinal and choroid homeostasis maintenance. Alcohol has become the more socially accepted addictive drug, it can result in a health, social and economic problems. Oxidative stress (OS) induced by ethanol (EtOH), generates reactive oxygen species (ROS) activating inflammation and cell death process. Cytochrome p450 2E1 (CYP2E1) enzyme has a high EtOH affinity. Its catalytic activity results in the production of large amounts of ROS during EtOH oxidation. In spite of CYP2E1 has been identify in human RPE and could be implicated in a RPE visual cycle, nothing is known about its regulation and implication in cellular response. Our aim was study the role of CYP2E1 in RPE, triggered by EtOH treatment.

ARPE-19, hRPE y hiPSC-RPE cells were used as a RPE cellular models. Cells were treated at the same time with EtOH, DAS (specific inhibitor of CYP2E1), and NAC (as antioxidant) to block the EtOH cellular effects. Cell viability and cytotoxicity studies were carried out by EthD-1, calcein and XTT. Intracellular ROS and superoxide anions were quantified using fluorescence probes (DCF and DHE respectively). Cell stress, angiogenic and inflammation biomarkers were determined by proteome profile arrays. The integrity of RPE barrier function was determined measuring transepithelial electrical resistance (TER) and intercellular junctions state by immunofluorescence (IF). Western blot (WB), qPCR, IF and ELISA was assayed to quantify CYP2E1 expression and also the main molecules and factors released by RPE. The activity of CYP2E1 was measured by HPLC.

EtOH increased the formation of ROS in RPE cells triggering cell death by apoptosis. EtOH induced RPE dysfunction decreasing intercellular junctions integrity and modifying the release and expression profile of inflammation, angiogenesis and growth factors. EtOH treatment induced CYP2E1 expression. The use of DAS and NAC reverted RPE cellular damage, this revealed that CYP2E1 is regulated by OS. Finally, the presence of CYP2E1 reinforces the protective role of RPE and strongly suggests additional CYP2E1 roles related to vision.

KEYWORDS: Retinal pigment epithelium; Blood retinal barrier; Ethanol; Oxidative stress; Cytochrome p450 2E1.

Table of Contents

TABLE OF CONTENTS

4-HNE: 4-hydroxynonenal

ADH: Alcohol dehydrogenase

AIF: Apoptosis inducing factor

ALDH: Aldehyde dehydrogenase

AMD: Age macular degeneration

AREs: Antioxidant response elements

ARPE-19: Human RPE cell line

Bax: Bcl-2-associated X

Bcl-2: B-cell lymphoma 2

BMP4: Bone morphogenetic protein 4

BRB: Blood-retinal barrier

CA9: Carbonic anhydrase 9

CMZ: Clomethiazole

CNS: Central Nervous System

CNV: Choroidal neovascularization

CRABP: Cellular retinaldehyde binding protein

CRBP: Cellular retinol binding protein

CYP2E1: Cytocrome P450 2E1

CYT-C: Cytocrome C

DAS: Diallyl Sulfide

DHA: Docosahexaenoic acid

DMEM: Dulbecco's modified Eagle's medium

DNA: Deoxyribonucleic acid

DR: Diabetic retinopathy

ECM: Extracellular matrix

FGF: Fibroblast growth factor

GSH: Glutation

GSH-Px: Glutathione peroxidase

GSSG: Oxidized GSH

HB-EGF: Heparin-binding epidermal growth factor

HEPG2: Human Hepatocellular carciroma cell line

HGF: Hepatocytes growth factor

HIF-1α: Hypoxia inducible factor 1α

HO-1: Heme oxygenase-1

hRPE: Human retinal pigment epithelium

HSP: Heat shock protein

IL: Interleukin

ILM: Inner limiting membrane

INL: Inner nuclear layer

IPL: Inner plexiform layer

IS: Photoreceptor inner segments

JNK: c-Jun N-terminal kinases

LCFAs: Long-chain fatty acids

LPO: Lipid peroxidation

LPS: Lipopolysaccharides

MAPK: Mitogen-activated protein kinases

MEOS: Microsomal EtOH-oxidizing system

MITF: Microphthalmia-associated transcriptor factor

MMPs: Matrix metalloproteinases

mRNA: Messenger RNA

EGFR: Epidermal growth factor receptor

ELM: External limiting membrane

ER: Endoplasmic reticulum

ERK: Extracellular signal-regulated kinases

EtOH: Ethanol

NOX: NADPH oxidase

NPD1: Neuroprotectin D1

Nrf2: Nuclear factor erythroid-2 related factor-2

NV: Neovascularization

ONL: Outer plexiform layer

OS: Oxidative stress

OTX2: Homeodomain-containing transciptor factor

PEDF: Pigment epithelium derived factor

POS: Photoreceptor outer segments

PUFAs: Polyunsaturated fatty acids

RAR: Retioic acid receptor

RIPK: Protein kinase receptor

RNA: Ribonucleic acid

ROS: Reactive oxygen species

RP: Retinitis pigmentosa

mtDNA: Mitochondrial DNA

NAC: N-acetylcysteine

NFL: Nerve fiber layer

NFKB: Nuclear factor KB

NO: Nitric oxide

RPE: Retinal pigment epithelium

RPE65: Retinal pigment epithelium specific 65 kDa protein

RT: Room temperature

SIRT-2: Sirtuin-2: CYT-C

SOD: Superoxide dismutase

TER: Transepithelial electrical resistance

TGF-β1: Transforming growth factor β1

TIMPs: MMPs inhibitors

TJ: Tight junctions

TNF-α: Tumor necrosis factor alpha

TSP-1: Thrombospondin-1

uPA: Urokinase type plasminogen activator

VEGF: Vascular endothelial growth factor

VEGFR: VEGF receptors

ZO: Zonula ocludens

FIGURES **PAGE**

TABLES **PAGE**

ANNEXED FIGURES **PAGE**

CHAPTER 1

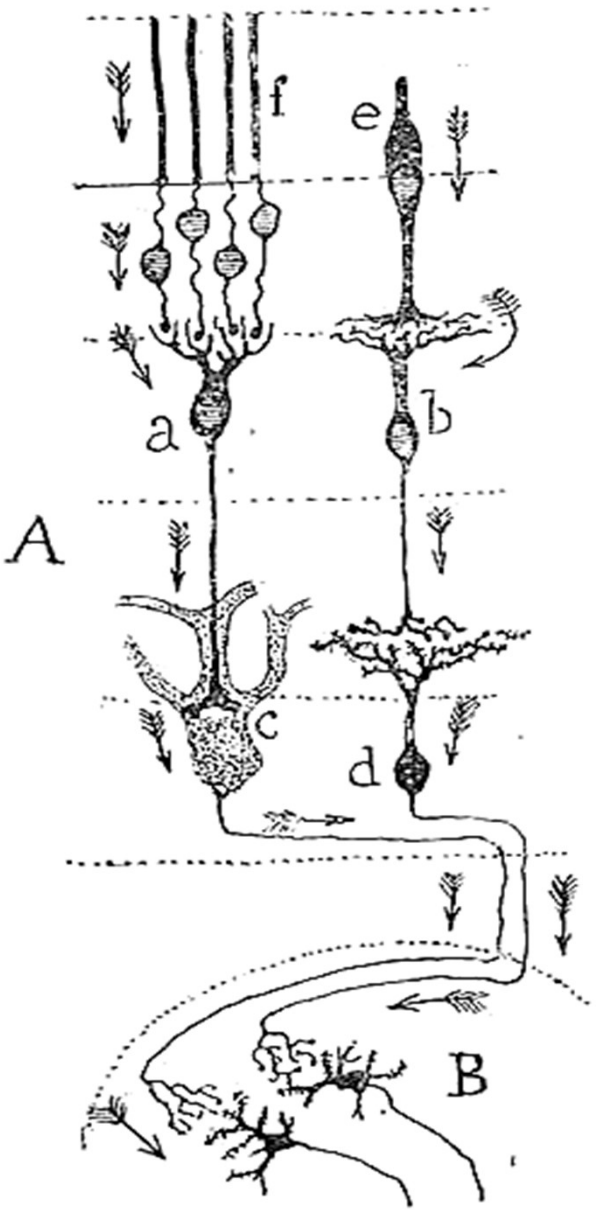

Nervous impulse in vertebrates retina

S. Ramón y Cajal

Introduction

1. ANATOMICAL STRUCTURE OF HUMAN EYE

One of the most valuable senses for humans is the sight. Among the several vision-related structures, the eye can be considered the most important, as it is responsible of the first step on a complicated process. The human eye presents an organized and complex structure with a high level of specialization and it is also considered an immunological privileged organ (1). It has developed molecular and cellular mechanisms to limit the immune response in order to preserve the sight.

In a lateral section of the ocular globe, three layers can be observed: The external tunica, the media tunica and the sensorial internal tunica. The external tunica is constituted by collagen and also includes the cornea on the anterior part. The cornea extends back to the sclera, a dense fibrous and opaque tissue that surrounds the ocular globe until it reaches the optic nerve. The media tunica, which is mainly vascular, is also known as uvea. This layer is composed of the iris in the anterior part, the ciliary body in the center, and the choroid in the posterior part, which is in contact with the retina, **figure 1** (2).

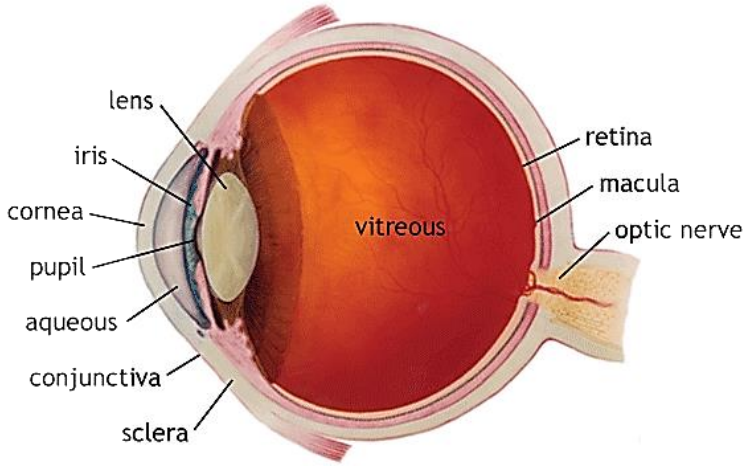

Figure 1. Human eye anatomy. In the image it is possible to distinguish the different parts of the human eye pointed with arrows. Obtained from Tian J, et al. 2013 (2).

In addition, the eye is divided in three different compartments or chambers:

1. The anterior chamber, located between the cornea and the iris, contains the aqueous humor.

2. The posterior chamber, between the iris, ciliary body, and crystalline, contains the aqueous humor.

3. The vitreous chamber, between the crystalline and the retina, contains a gelatin mass called vitreous humor or vitreous body.

The extraocular muscles give the ability to rotate the eyeball in the orbits and allow the image to be focused at all times on the fovea of the central retina (3).

1.2. THE RETINA

The retina is a prolongation of the central nervous system (CNS). As **figure 2** shows (3), it derives from the neural tube and it is formed during development of the embryo, from optic vesicles outpouching from two sides of the developing neural tube (2). The primordial optic vesicles fold back upon themselves to form the optic cup, with the inside of the cup becoming the retina and the outside remaining a single monolayer of epithelium, which is known as the retinal pigment epithelium (RPE), (3). Initially both walls of the optic cup are just one cell, but the cells of the inner wall divide themselves to form a neuroepithelial layer composed by many cells: the retina.

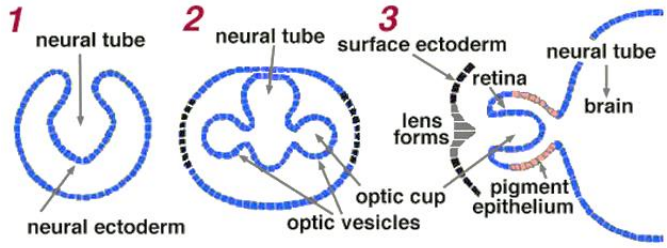

Figure 2. Embryonic origin of the retina. Necessary and complex stpes for the formation of the retina and RPE. Obtained and modified from http://webvision.med.utah.edu/ (3).

The retina is a very complex anatomical and functional tissue because it is here where the analysis of the light information process starts (4). Besides, about the 80% of all sensorial information comes from the retina. The retina extends over the back of the eyeball, from the inner surface to the ciliary body. It is in contact with the vitreous body internally and with the choroid externally (4).

This part of the eye is composed of ten layers, **figure 3** (5): Inside out we can find the RPE; the photoreceptor outer segments (POS); the photoreceptor inner segments (IS); the external limiting membrane (ELM); the photoreceptor outer nuclear layer (ONL); the outer plexiform layer (OPL), where photoreceptor cells synapse with interneurons; the inner nuclear layer (INL), containing bipolar, amacrine and horizontal cells; the inner plexiform layer (IPL), where interneurons synapse with the ganglion cell layer (GCL); the nerve fiber layer (NFL); and the inner limiting membrane (ILM).

The inner layers of the retina are often cited as a neural retina. It consists of seven main types of neurons: photoreceptors (rod and cones), bipolar cells, horizontal cells, amacrine cells, retinal ganglion cells and Müller cells, **figure 3** (5). The neural retina transforms light into electrical impulses through the optic nerve. The non-neural retina, that includes RPE and Bruch´s membrane, maintains the integrity of the retina and is part of the barrier between the choroid and the retina, known as external blood-retinal barrier (BRB).

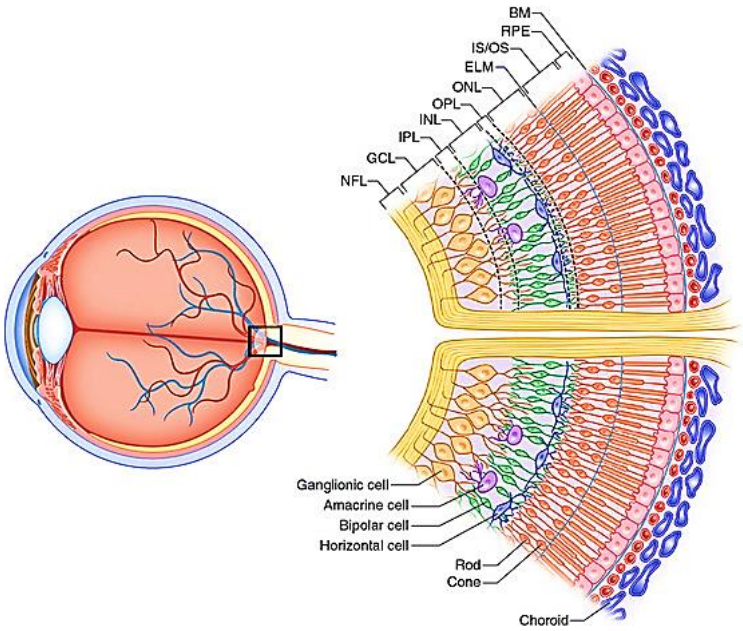

Figure 3. Retinal histology. Cellular composition and distribution of human retinal layers. Obtained and modified from http://www.retinareference.com/anatomy/ (5).

1.3. THE CHOROID

The choroid consists of blood vessels, melanocytes, fibroblasts, resident immunocompetent cells, and connective tissue. It is located between the retina and the sclera, being the main blood supply source to the outer part of retina (6). Thicker in the posterior part of the eye, it reaches the middle portion of the eye where it becomes the ciliary body (7). The choroid is the major blood supply to the outer retina. Choroid circulation presents fenestrated capillaries with especially large pores. These fenestrations present high permeability not only for glucose but for other low molecular weight molecules (7). Additionally, the choroid presents another set of functions such as light absorption, thermoregulation through heat dissipation, retinal position adjustments, changes in choroid thickness, intraocular pressure modulation by vasomotor control blood flow, and drainage of aqueous on the anterior chamber through the uveoscleral pathway (8).

2. THE RETINAL PIGMENT EPITHELIUM

2.1. EMBRYONIC ORIGIN AND ANATOMY

The RPE is essential for the proper development of the retina. For this purpose, the RPE was found to secrete factors promoting photoreceptor survival and differentiation. The correct development of the retina appears to be dependent on the genes involved in the proper development of RPE (9).

After the invagination of the optic cup, two layers opposed to each other and separated by a thin remnant of lumen are still able to differentiate into the RPE or neural retina. The following developmental steps depend on the interaction of the retina and the RPE. The maturation of the RPE begins with the activation of the tyrosinase promoter, which marks the onset of melanogenesis (3).

Several factors were found to be essential for the determination of RPE differentiation. In its early development, before the formation of the two layers, the region destined to form the anterior parts of the eye express cellular retinol binding protein (CRBP), cellular retinaldehyde binding protein (CRABP), and several enzymes in the retinal metabolism pathway. The embryonic retina anlage releases retinoic acid. RPE cells, in turn, express receptors for retinoic acid (RAR-β2), CRBP, and CRABP (9).

From that point onwards, neuroectodermal cells begin to differentiate into the RPE as **figure 4** shows (9). The RPE basement membrane and the basement membrane of the endothelium form Bruch's membrane.

The expression of the transcription factors e.g. homeodomain-containing transcription factor (OTX2) and microphthalmia-associated transcription factor (MITF) appear to be the critical initial steps of the determination and differentiation of the RPE (9).

The RPE was described in 1861 by Rudolf von Kölliker and since then, many researchers have devoted their efforts to get to know its anatomy and describe its function (10). It is a simple cuboidal epithelium of pigmented cells with neuroectodermal origin. The RPE presents a regular hexagonal form with intercellular tight junctions (TJ) (6).

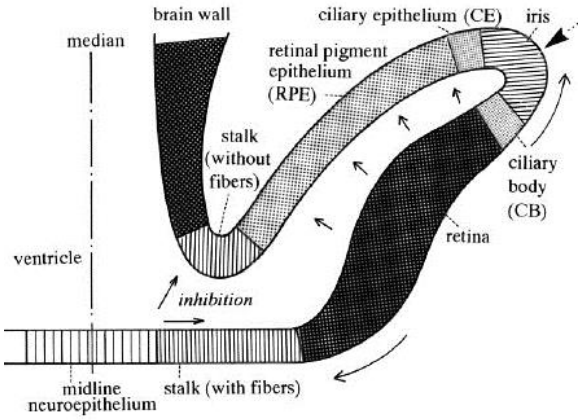

Figure 4. Embryonic origin of the RPE. The arrows indicate how neuroepithelium designated to become the RPE and neuroepithelium designated to become retina move into an opposed position. Obtained and modified from Strauss O. 2005 (9).

The inner limit, also known as apical membrane, interdigitates with POS. The outer one, or basolateral membrane, faces the Bruch's membrane, separating the RPE from the choroid fenestrated capillaries, **figure 5** (11). In the apical side, long microvilli are directly in contact with the outer photoreceptor segments. In this side, the RPE cells can form tight junctions, gap junctions or macula adherens.

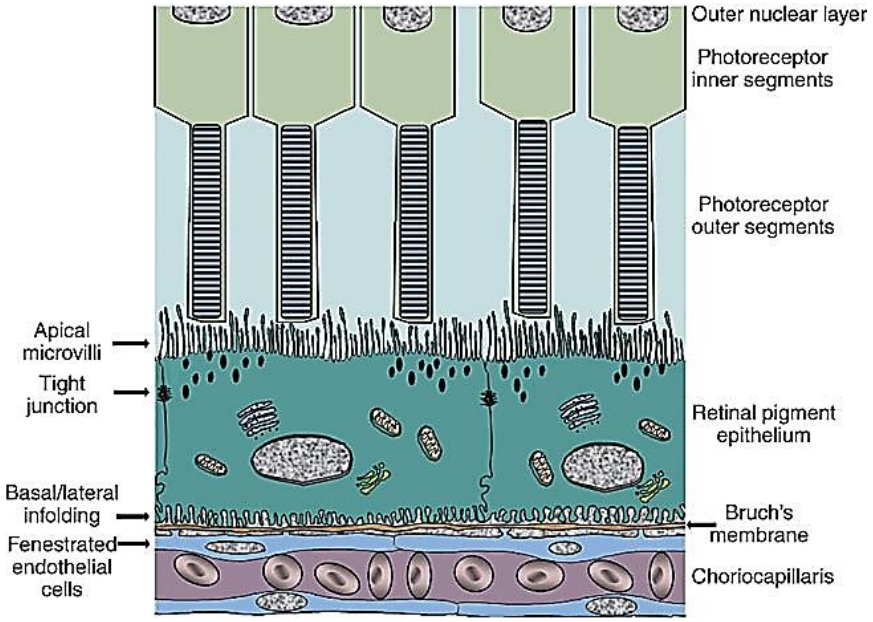

Figure 5. Anatomy of the RPE. RPE barrier is formed by TJs. RPE is separated from choriocapillaris by Bruch's membrane. On the apical side, POS outer segment are phagocytosed by RPE cells. Obtained from Sonoda S, et al. 2009 (11).

2.2. RPE FUNCTIONS

The RPE is one of the most metabolically active tissues in the human body, **figure 6** (12). Despite not being directly involved in vision, the loss of the RPE leads to secondary photoreceptor and choroid atrophy. Functional RPE alterations typically lead to retina degeneration and decreased visual acuity, eventually leading to blindness (9-12).

2.2.1. Blood retinal barrier (BRB) component

The RPE and Bruch's membrane form the outer BRB while the inner one consists of a group of endothelial cells (13). The BRB consists of a restrictive physiological barrier that regulates the passage of ions, proteins, and the water flow that goes in and out of the retina.

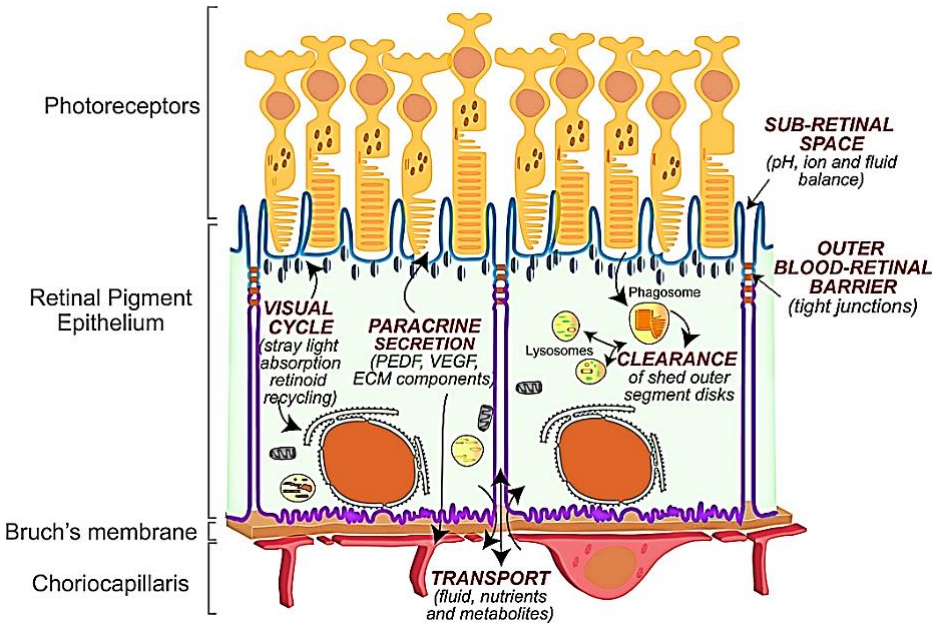

Figure 6. RPE functions. Schematic drawing with principal RPE functions: Viscual cycle, paracrine secretion, transport through Bruch's membrane and POS disk clearance. Obtained from Toops KA, et al. 2014 (12).

The presence of TJ between the RPE cells and the vascular endothelium is essential to control the molecular transport through the BRB and to prevent the entry of toxic molecules or plasma components in the retina. Therefore, it is essential for the retina integrity and its maintenance for a normal visual function (12).

In addition, the RPE stabilizes the ionic concentration in the subretinal space, **figure 6** (12) which results crucial for photoreceptors excitability, helping to the eye immune response by the secretion of immunosuppressive factors (6).

2.2.2. Transepithelial transport

The RPE has an active transport of ions modulating the extracellular environment balance of the outer retina. The numerous pleats in the basal and apical area increase the RPE surface facilitating active transport (9). The transport occurs in two directions, from the blood to the photoreceptors (subretinal space) and from the photoreceptors to the blood.

From the blood to the photoreceptors: The RPE provides nutrients such as glucose, retinol, ascorbic acid and fatty acids from the blood to the photoreceptors, **figure 6**. This transport is vital for the visual cycle (12), during the phagocytosis of the outer segments on photoreceptors. Delivery of organic acids, such as docosahexaenoic (DHA), to the photoreceptors is another important function. DHA is an omega-3 type fatty acid that cannot be synthesized by the nervous tissue, but it is essential for the structure of the photoreceptors. In addition to its role on the functional RPE integrity, DHA acid is a neuroprotectin D1 (NPD1) precursor that protects the RPE against **oxidative stress (OS)** (14).

From the photoreceptors to the blood: Amounts of water are accumulated in the subretinal space because of the high metabolic activity of neurons and photoreceptors. Moreover, the intraocular pressure generates a movement of water from the vitreous body to the retina. These two processes require the constant removal of water from the inner layer of the retina towards the choroid. The RPE is capable of promoting the flow of ions and water from the subretinal space (at the apical side) into the blood (basolateral side). This transport is carried out by the energy provided from the Na^+/K^+ ATPase pump. This water within the retina is carried by Müller glia, while the water present in the subretinal space is removed through the RPE. The transport of metabolic products requires an efficient pH regulation, such as the HCO_3- transport system (15).

2.2.3. Light absorption and photooxidation protection

The retina is constantly exposed to large amounts of light and oxygen (16,17) leading to photooxidation and generating **reactive oxygen species (ROS)** (18). The RPE is essential to counteract the retinal OS by two mechanisms: On the one hand, light absorption and filtration, and on the second hand, by the production of antioxidant molecules, proteins or vitamins (6).

To carry out the first functions, the RPE presents two pigments that absorb and filter light: lipofuscin (outer segments) and melanin (in RPE melanosomes). Melanin is in the apical side of the cell, while the lipofuscin is located in the basal area (19). Melanin absorbs light and eliminates free radicals, helping photoreceptors and RPE to prevent the photooxidative damage (17). There is an inverse relationship between melanin and lipofuscin in the human eye. Lipofuscin levels are increased by age and cell damage, being a marker of senility or disease (20).

2.2.4. The visual cycle

The visual process in the retina begins when light is absorbed by photoreceptor visual pigments. The visual pigments, **rhodopsin** and **opsin**, are integral membrane proteins located in the highly specialized outer segments of rods and cones, respectively. The light-sensitive chromophore, 11-*cis*-retinal, is covalently attached to opsin by a specific lysine residue located in one of the seven transmembrane alpha helical segments. The capture of a single photon results in the isomerization from 11-*cis*-retinal to all-t*rans*-retinal, and the formation of photoactive visual pigment that decays through a number of conformational intermediates, **figure 7** (21).

The visual cycle starts with the circulation of vitamin A (all-*trans*-retinol) on the blood stream. Once vitamin A is incorporated to RPE cells, all-*trans*-retinol is converted to retinyl ester through the activity of the lecithin retinol acyl transferase enzyme. The resulting all-*trans*-retinyl ester represents a form of vitamin A storage. All-*trans*-retinyl ester is converted to 11-*cis*-retinol by RPE65. Finally, 11-*cis*-retinol is oxidized by 11-*cis*-specific retinol dehydrogenase to form the visual chromophore, 11-*cis*-retinal (21).

The visual chromophore is transferred to rod and cone outer segments where it combines with opsins, giving as a restult visual pigments (e.g., rhodopsin). Light activation of rhodopsin initiates visual transduction processes and liberates all-*trans*-retinal as a photoproduct. Reduction of all-*trans*-retinal, via all-*trans*-retinal dehydrogenase, produces all-*trans*-retinol, which is transferred back to the RPE for recycling. The continued activity of RPE65 in the light state ensures sustained levels of rhodopsin, closure of ion channels through transducin activation, and reduced oxygen demand (**Figure 7**) (22). Rhodopsin is converted by photoabsorption to meta-rhodopsin, and the latter is reconverted to rhodopsin by light. It is well known that rhodopsin can be formed from opsin only when 11-*cis*-retinal is present (22).

The photoisomerization of the retinal released during the degradation of meta-rhodopsin is catalyzed by an unknown isomerase and this photoisomerization is stereospecifically directed toward the formation of 11-*cis*-Retinal. Retinal is also reduced in the reaction catalyzed by all-*trans*-retinal specific retinol dehydrogenases and also alcohol dehydrogenases (ADH) (23).

On the other hand, retinal in turn is rapidly oxidized to retinoic acid by different dehydrogenases including mitochondrial aldehyde degydrogenase (ALDH). Then, retinoic acid is metabolized to 4-Hydroxy-retinoic acid, 4-Oxo-retinoic acid, and 5,6-Epoxy-retinoic acid. Finally the oxidation of retinoic acid to 4-Hydroxy-retinoic acid is catalyzed by cytochrome P-450 enzymes, including the **CYP2E1** isoform (23 ,24).

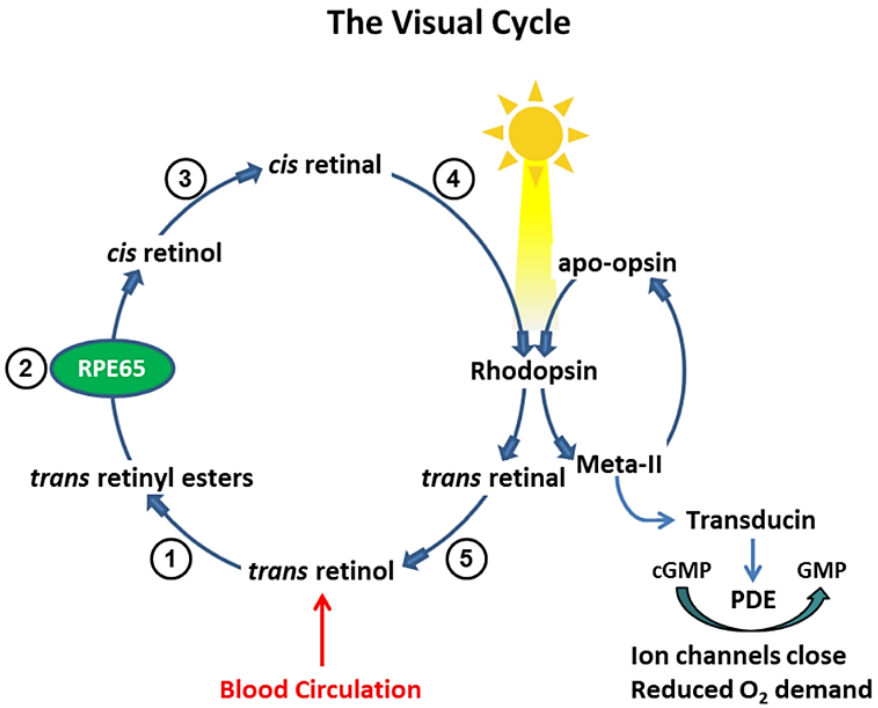

Figure 7.Visual cycle. Schematic drawing of the visual cycle steps. Obtained from Bavik C, et al. 2015 (22)

2.2.5. Photoreceptor outer segment phagocytosis

POS phagocytosis of is a highly complex process involving the RPE. Mechanistically, this RPE-related phagocytosis (RPE-POS) belongs to a non-inflammatory clearance phagocytosis pathway aimed to remove apoptotic cells and debris. (25, 26). This RPE-POS is a renewal mechanism, where the RPE microvilli is able to phagocyte the POS. Just important molecules, such as the retinal ones, are redelivered to photoreceptors. In order to maintain photoreceptors' excitability, POS are newly built at the connecting cilia from the inner segments (27). Because of photooxidation, POS are continuously exposed to ROS. Inefficient RPE lysosomal function causes accumulation of debris in RPE that result in toxic for cells (26).

2.2.6. Essential proteins and factors secretion

RPE secrete a host of growth factors and structure-related proteins. These secretions result in extreme relevance supporting photoreceptor survival, as well as in maintenance of the retinal blood supply (28). The polarized nature of the RPE is essential for the health of the eye, not only regarding nutrient and waste transport, but also in the synthesis and directional secretion of proteins required to maintain retinal homoeostasis and a good function (28).

High levels of particular growth factors and structural proteins beneficial in one compartment can be detrimental in the other. Maintaining the correct concentrations of particular factors, in the correct location and timing, is therefore of critical importance for retinal health (9).

The choroid is also capable of secreting angiogenic factors such as **vascular endothelial growth factor (VEGF)** and extravasation related molecules. Directly related to neovascularization (NV) changes, some **matrix metalloproteinases (MMPs)** and **MMPs inhibitors (TIMPs)** can be also synthesized (7). On this line, choroidal defects cause degenerative changes on the retina (8).

The table 1 lists some of this essential proteins and factors released by RPE. Nevertheless it is important to emphasize by their function the following:

- Fibroblast growth factor (FGF): There are around 19 members of the FGF family. They can participate in different processes such as inflammation and epithelial tissue regeneration (29).

- Heparin-binding epidermal growth factor (HB-EGF): In the eye, HB-EGF plays a central role in the stimulation of cell growth as the proliferation-stimulatin action of various growth factors and agonists of G protein coupled receptors depends on the transactivation of receptor tyrosine kinases, specially of the epidermal growth factor receptor (EGFR) (30). This factor represents an autocrine/paracrine migration. HB-EGF activates at least three signal transduction pathways in RPE cells: Proliferation (mitogenic activity), migration and secretion of VEGF. Finally, it has an indirect role in the choroidal NV (CNV) via influence on VEGF expression (29).

- Hepatocytes growth factor (HGF): Is a growth factor involved in growth, motility and morphogenesis. It provides protection to RPE cells under OS (29). HGF partially blocks the induction of cell death by apoptosis activation up-regulating cellular redox status and by inhibiting caspase-3- dependent cell death (31).

- Transforming growth factor β1 (TGF-β1): It is a peptide analog of EGF (32). It can be presented as three isoforms; TGF-β1, TGF-β2, and TGF-β3. Each isoform is encoded by a distinct gene and is expressed in both a tissue-specific and a developmentally

regulated fashion. TGF-β1 messenger RNA (mRNA) is expressed in endothelial, hematopoietic, and connective-tissue cells (33).

It is a multifunctional cytokine with different cellular effects. It can either stimulate or inhibit cell proliferation, stimulate or inhibit cell differentiation, and other critical processes for cell function, e.g. deposition of extracellular matrix (ECM) and apoptosis. For this reason, it is involved in numerous diseases such as tumorigenesis; angiogenesis development; fibrotic disease of kidney, lung, and liver and even atherosclerosis (33). Regarding TGF-β1 signaling, it is well known that its activation in RPE cells can also be caused by various stimuli including: environmental stress, pro-inflammatory cytokines, such as **tumor necrosis factor-alpha (TNF-α), interleukins (ILs)** and lipopolysaccharides (LPS) (34).

- MMPs and TIMPs: MMPs and TIMPs are apically secreted by the RPE. MMPs are a family of at least 20 zinc endopeptidases (35) and play a crucial role in the ECM turnover throughout the body. Their activity is normally tightly regulated at several levels, including functional inhibition by TIMPs. It has been suggested that apically secreted MMPs/TIMPs could play a crucial role in the turnover and structural maintenance of the interphotoreceptor matrix, or also be involved in degrading the tips of POS, signaling their readiness for phagocytosis by RPE (28). MMPs and TIMPs are also present basally on the RPE, in the Bruch's membrane (35).

MMP-2 and MMP-9 preferentially degrade basement membrane components such as type IV collagen, and the levels of these increase with aging (35). A second set of targets, for MMP activity, are growth factors. Matrix-bound VEGF seems to be mobilized by MMP, in particular MMP-9, whereas PEDF is a substrate for MMP-2 and MMP-9. On the other hand, OS has been shown to increase MMP-1 and MMP-3 expression and secretion (35), this indicates potential basolateral secretion of MMPs. It is possible that the RPE are able to secrete certain MMPs/ TIMPs in opposite directions depending on external cues such as cytokine stimulation or signals from the ECM (28).

MMP activity was found PEDF as net result, the ratio of VEGF/PEDF was significantly altered, shifting the balance to pro-angiogenic state (30). Alternatively, MMPs/TIMPs present in Bruch's membrane could be secreted by choroidal cells. Malfunctions in controlled, directional secretion of MMPs/ TIMPs could disrupt the balance of proteolytic activity on either side of the RPE, contributing to age-related changes in Bruch's membrane (28). There is expression of MMP-1, MMP-3 and MMP-9, located between the matrix and photoreceptor. MMP-2 participates in the phototoxic processes and its expression is increased upon exposure to light (36).

Table 1. Essential proteins and factors secreted by RPE

PROTEIN	MAIN FUNCTION	POLARITY
A/B CRYSTALLIN	Molecular chaperone, cytoprotection	Apical
BDNF	Neurotrophic growth factor	Unknown
CFH	Inhibitor of the complement pathway	Unknown
CNTF	Neurotrophic growth factor	Unknown
CYSTATIN C	Cysteine protease inhibitor	Basal
ENDOTHELIN I	Vasoconstriction/vasodilation	Basal
FIBULIN 3	ECM protein involved in elastogenesis (fibulin 5)	Unknown
FGF 2	Growth factor involved in mitogenesis, angiogenesis and cell survival	Unknown
FGF 5	Growth factor involved in mitogenesis, angiogenesis and cell survival	Basal
HB-EGF	Mitogenic growth factor	Unknown
HGF	Growth factor involved in growth, motility and morphogenesis	Unknown
HYALURONAN	Major component of ECM	Apical
IGF-I	Growth factor involved in growth and development	Unknown
LIF	Cytokine involved in differentiation	Unknown
MMP-2	Zinc-dependent endopeptidase involved in ECM degradation	Apical
MMP-9	Zinc-dependent endopeptidase involved in ECM degradation	Unknown
NGF	Neurotrophic growth factor	Unknown
PEDF	Growth factor with neurotrophic and anti-angiogenic properties	Apical
TGF-B	Growth factor involved in proliferation and differentiation	Apical
TIMP-I	Inhibitor of MMPs	Apical
TROPOELASTIN	Involved in formation of elastin fibres (such as in Bruch's membrane)	Unknown
VEGF	Angiogenic growth factor	Basal

Summary table of proteins and factors by RPE and its release side. Modified from Kay P, et al. 2013 (28).

- VEGF: Was originally described as an angiogenic factor and helps conferring vascular permeability. Under physiological conditions, the RPE secretes low levels of VEGF and has been shown to act not only as a factor for endothelial cell survival, but also in other cell types such as photoreceptors and Müller cells (34).

There are described different types of VEGF; VEGF-A, VEGF-B, VEGF-C (37). Among these, we find the most studied factor, and often referred to as VEGF is VEGF-A. Differences in pre-mRNA splicing give rise to different isoforms, as the VEGF-A_{165} isoform (38-41). The "downstream" VEGF signals occur by binding the tyrosine kinases receptor. These are the **VEGF receptor 1** (**VEGFR-1**, also known as FLT-1), the **VEGF receptor 2** (**VEGFR-2**, also known as KDR / Flk-1), and the **VEGF receptor 3** (**VEGFR-3**) (37).

In the healthy RPE tissue, PEDF is secreted into the apical side, while VEGF secretion is performed in the basolateral side. Thus, PEDF acts on neurons and photoreceptors. Most of the secreted VEGF act on the endothelium of the choroid (28, 37). Previous studies have shown that with age the RPE begins to lose its metabolic capacity and stress factors such as light, hypoxia and inflammation, which cause the pigment epithelial barrier to be compromised. Furthermore, these stressful stimuli lead to increased angiogenic factors (39).

- Pigment epithelium derived factor (PEDF): Also known as serpin F1 (SERPINF1), is a multifunctional secreted protein. It is an important factor for the survival and function of the retina and ocular tissues, **table 2** (42). This factor is secreted apicolaterally from the retinal pigment epithelium to act on photoreceptor morphogenesis and retinal neuroprotection.

Additionally, it is well established as a neurotrophic activity, PEDF has potent antiangiogenic properties that prevent neo-vascular invasion in the eye (43). Low levels of PEDF below the basal surface of the RPE may aid in preventing vascularization in this compartment as well. A delicate balance exists in the expression and concentration of PEDF and VEGF. Disrupting this balance can produce vascularization of the retina, whilst simultaneously decreasing photoreceptor support (28).

Table 2. Effects of PEDF.

CELL TYPE	EFFECTS OF PEDF
ENDOTHELIAL	Inhibits formation of new vessels
PHOTORECEPTORS	Enhances development and survival
NEURONS	Protects against cell death
RETINAL PIGMENT EPITHELIUM	PEDF production high in young cells, decreases with age
RETINOBLASTOMA TUMOR CELLS	Stimulates differentiation to less malignant phenotype

Summary table of PEDF function in different ocular cells. Modified from Bouk N. 2002 (42).

2.3. EXPERIMENTAL MODELS FOR RETINAL PIGMENT EPITHELIUM STUDIES

This thesis focuses on the RPE study and its dysfunction due to oxidative stress. For this aim it has been developed cellular models to use them *in vitro* experiments.

2.3.1. RPE cell lines

Because of the difficulty to study in human and animals retinal diseases and testing possible treatments, it is necessary to resort to *in vitro* studies. These offer certain advantages, such as the need for a smaller working space and cost reduction benefits.

There are different cell types and they can also be differentiated according to the techniques used for their generation. The most commonly used in laboratories are immortalized cell lines. On the other hand, research laboratories also can use primary cell cultures. Cell lines have an advantage, they have an increased or unlimited proliferative capacity showing a higher rate of renewal. Until today, there are a variety of RPE cell lines, but the hypothesis that experiments developed with cell lines mimic the physiology of real RPE tissue does not seem very strong. It is possible to find different cell lines e.g.: H80HrPE-6, ARPE-19, D407 and RPE-340; some of these cellular transformation models are spontaneous, such as ARPE-19 cells (44). But others are immortalized, for example hTERT-RPE-1 is a line derived from cell line 340-RPE. Cell lines h1RPE-7 and h1RPE-116 were generated from a 50 years woman by SV40 T plasmid transfection. These cells do not have normal **transepithelial electrical resistance (TER**) and have been used in a few studies (45).

TER is a widely accepted quantitative technique to measure the integrity of tight junction dynamics in cell culture models of endothelial and epithelial monolayers. TER values are strong indicators of the integrity of the cellular barriers before they are evaluated for the transport of drugs or chemicals. TER measurements can be performed in real time without cell damage and generally are based on measuring ohmic resistance or measuring impedance across a wide spectrum of frequencies (46).

ARPE-19 is a RPE cell line that appeared spontaneously in 1986 derived from the normal eyes of a 19-year-old male. These cells express specific markers of RPE, like RPE65 and CRALBP (44). The ARPE-19 cells seem to present a normal phenotype and grow at a steady pace. Furthermore, they are capable of forming stable layers which exhibit morphological and functional polarity (44). ARPE-19 cells have been used in studies of OS (47), cell communication (48), study of cell toxicity drugs, autophagy (49), inflammation, and diseases such as age macular degeneration (AMD), diabetic retinopathy (RD) or retinitis pigmentosa (RP), among others (50).

2.3.2. Primary cultures of RPE

When we obtain cells from a piece of tissue, we are talking about primary culture, and they could come from an animal or a human (**hRPE**). These are always going to be more real, as they can recreate a more faithful and cell physiology and environment. But these crops have large experimental limitations, and this fact coupled with the limited availability and heterogeneity among donors makes it difficult to work with them, emphasizing the value of cell lines.

There are different protocols to obtain these primary cultures, but in all of them it is necessary to use big pieces of tissue, which increases the difficulty to obtain them. Additionally, it is very important to consolidate a proper protocol that validates the primary culture, always making sure that the culture is not contaminated with others retinal cells. Knowing the limitations of cell lines, some of the experiments should be tested with both kind of cells at the same time.

2.3.3. Human Induced Pluripotent Stem Cells (hiPSC)

hiPSC are a type of pluripotent stem cells that can be generated directly from adult cells. The iPSC technology was pioneered by Shinya Yamanaka's lab in Kyoto, Japan, who showed in 2006 that the introduction of four specific transcription factors could turn adult cells into pluripotent stem cells in mice (51).

There are different protocols to induce RPE cells from hiPSC. But recently Flores-Bellver M, describes a protocol to generate RPE cells from retinal cups (RC) (51).These retinal cups are produced in *in vitro* conditions with a specific protocol from hiPSC (52). Basically, this **hiPSC-RPE** could be like a primary culture because it is obtained from retinal cups generated by hiPSC, with the advantage that it is possible to generate them without needing a donation of human tissue (taking into account how complicated it is).

3. OXIDATIVE STRESS

According to the definition, OS is a disturbance in the balance between the production of free radicals, ROS and antioxidant defenses (53).

3.1. REACTIVE OXYGEN SPECIES GENERATION

Usually, an atom is composed of a central nucleus with pairs of electrons orbiting around it. However, some atoms and molecules have unpaired electrons and these are called free radicals. Free radicals are usually unstable and highly reactive as the unpaired electrons tend to form pairs with other electrons. An oxygen molecule (O_2) undergoes a four-electron reduction when it is metabolized “in vivo”. During this process, reactive oxygen metabolites are generated by the excitation of electrons secondary to the addition of energy or interaction with transition elements (54).

ROS are derived from many sources including mitochondria, xanthine oxidase, uncoupled nitric oxide synthases and nicotinamide adenine dinucleotide phosphate (NADP) oxidase (NOX) (53). The oxygen metabolism, cell respiration, cell signaling and other homeostatic processes produce ROS within the cell, **figure 8** (55). In addition to generalized oxidation resulting in cell dysfunction and cell death (necrosis or apoptosis).

If active oxygen species or free radicals are generated excessively or at abnormal sites, the balance between formation and removal is lost, resulting in OS. Consequently, active oxygen species and free radicals can attack molecules in biological membranes and tissues, thus inducing diseases.

3.2. SOURCES OF ROS

In cells, various organelles can generate ROS. These include mitochondria, the endoplasmic reticulum (ER), particularly relevant for ER stress, and peroxisomes (as part of their role in metabolizing long-chain fatty acids (LCFAs). In addition, various enzymes, including oxidases and oxygenases, generate ROS as part of their enzymatic reaction cycles as hydrogen peroxide (H_2O_2), **figure 8** (55).

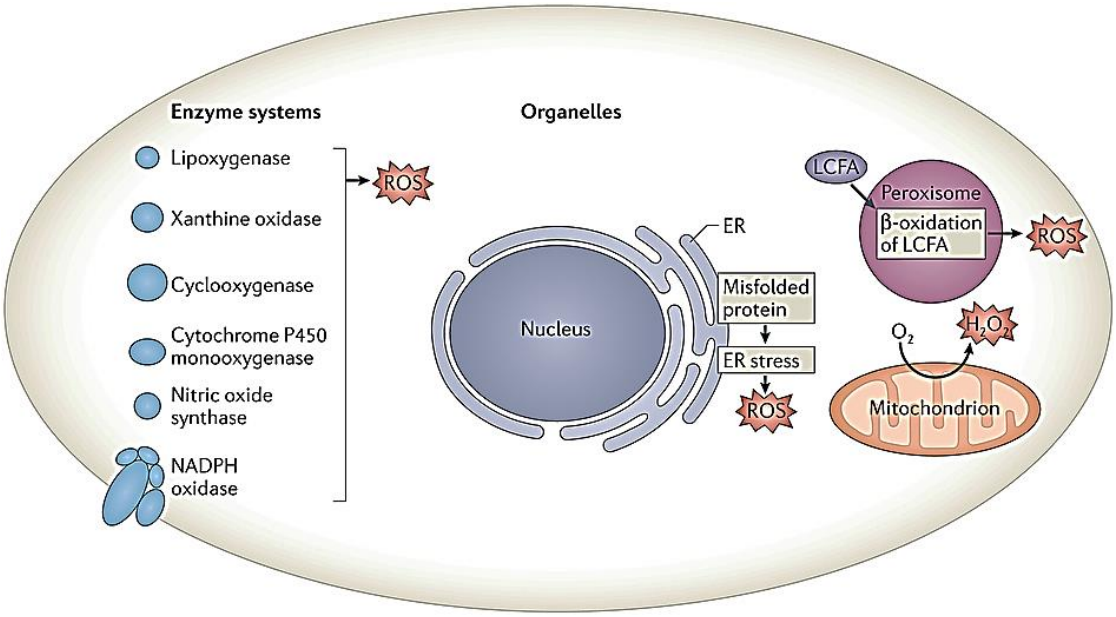

Figure 8. Intracellular sources of ROS. All cellular organelles and enzymatic systems are susceptible to generate ROS. Particularly, ER and mitochondria are the major sources of ROS. Obtained from Holmstrom KM, et al. 2014 (55).

3.2.1. Mitochondria

Mitochondria generates ATP in an oxygen-dependent manner. Throughout this process, molecular oxygen can also undergo a one-electron reduction to generate a superoxide anion. The major sites of superoxide production are generally believed to be within complex I and complex III of the electron transport chain (55).

Similarly, other organelles such as the peroxisome and ER, can produce oxidants. The relative contribution of these additional sources of ROS varies according to cellular metabolism that can vary as well depending on the cell type (55).

3.2.2. NADPH oxidases

NOX is an enzyme family first described in the context of neutrophils. In this context, the major source of ROS generation is a flavin- and heme-containing protein complex that transfers electrons from cytosolic NADPH to molecular oxygen in order to deliberately produce superoxide anions. The catalytic subunit of this complex is commonly referred to as NOX2. NOX2 does not generate superoxide on its own; rather, its stimulation causes the recruitment of cytosolic factors. These cytosolic factors combine with the membrane-bound factors NOX2 and p22phox to generate the classic phagocyte response to stimulation known as the respiratory burst (55).

3.2.3. Cytochrome P450 enzymes

This superfamily of monooxygenases is in the ER microsomes. CYP450´s are highly conserved across species implying that, in addition to their function in the metabolism of xenobiotics, these enzymes possibly exert broader physiological functions in the haem-dependent oxidation of various metabolic intermediates (55).

Consistent with this view, the **CYP450-2E1** or **CYP2E1** isoenzyme has been implicated in a variety of diseases, possibly as a result of its capacity to produce high levels of ROS. In fact, CYP2E1 assumes an important role as a major component of the microsomal ethanol- (EtOH) oxidizing system (MEOS) (56, 57). This issue will be developed and expanded along this thesis.

3.3. BIOMARKERS OF OXIDATIVE STRESS

The term biomarker has been defined by The National Institute of Health as “a characteristic that is objectively measured and evaluated as an indicator of normal biological processes, pathogenic processes, or pharmacological responses to a therapeutic intervention” (58).

Many markers have been proposed, including lipid peroxides, malondialdehyde (MDA), and 4-hydroxynonenal (4-HNE) as markers for oxidative damage to lipids; isoprostan as a product of the free radical oxidation of arachidonic acid; 8-oxoguanine (8-hydroxyguanine) and thymineglycol as indicators of oxidative damage to DNA; and various products of the oxidation of protein and amino acids including carbonyl protein, hydroxyleucine, hydrovaline, and nitrotyrosine (59).

3.3.1. Lipid peroxidation

Lipid peroxidation (LPO) is a free radical-related process that, in biological systems, may occur under enzymatic control or non-enzymatically. This later form is associated mostly with cellular damage as a result of OS, and a great variety of aldehydes are formed when lipid hydroperoxides break down. In other words, LPO can be described as a process under which oxidants, such as free radicals, attack lipids, especially polyunsaturated fatty acids (PUFAs), resulting in the oxidative degradation of them and, thereby producing cell damage (59).

PUFAs are intensified in cells subjected to OS, and result in the generation of various bioactive compounds such as MDA, 4-HNE, propanal, and hexanal (49, 59). In fact, MDA and 4-HNE have been indirectly liked to the pathogenesis of several diseases. The main challenge in the field of pathological processes is that it is often difficult to determine whether these LPO-derived aldehydes are actually causing the disease or are a consequence of it (60).

3.3.2. Protein damage

Free radicals and non-radical ROS attack proteins leading to serious disorders of metabolism and cellular structure. ROS-associated protein modification can lead to loss of biological functions and to the change of protein forms. Modified proteins have increased sensitivity to intracellular proteolysis and they are quickly degraded by endogenous proteases, particularly by multi-catalytic system (60).

ROS can lead to oxidation of amino acid residue side chains, formation of protein-protein cross-linkages, and oxidation of the protein backbone, resulting in protein fragmentation. In the meantime, it has been shown that other forms of ROS may yield similar products and that transition metal ions can substitute for ·OH and $O^{\cdot -}_2$ in some of the reactions (60). These changes can result in different secondary effects, including protein fragmentation, aggregation, and unfolding.

These processes are ordinarily connected with loss or change of protein activity and function. Increased oxidative damage of proteins results in (61):

- An increased production of ROS.
- A decreased capacity to scavenge ROS.
- An increased sensitivity of damaged proteins to become oxidized as a consequence of transcriptional and translational errors.
- Decreased levels or activities of the proteasome or proteases which degrade oxidized proteins.

3.3.3. DNA damage

Nucleic acids are particularly sensitive to oxidative damage. ROS can damage DNA by direct chemical attack of purine and pyrimidine bases and deoxyribose sugars and also by indirect mechanisms.

Mitochondrial DNA (mtDNA) is excessively sensitive under oxidative damage because mtDNA is close to the inner mitochondrial membrane, where ROS are formed. Damage of mtDNA can be potentially more important than nuclear DNA damage because all mitochondrial genes are expressed, whereas nuclear DNA includes a great number of un-transcribed sequences (61). At this point, mitochondrial chaperons, such as **heat shock protein (HSP)**, have an important role. For example, mitochondria HSP60 is relevant to assist in folding linear amino acid chains into their respective three-dimensional structure and it is also implicated in mitochondrial protein import and macromolecular assembly (62).

A well-known transcriptor factor inducible by DNA damage under OS conditions is **p53**. It is a tumor suppressor protein and can activate DNA repair proteins when DNA has sustained damage (63). The critical event leading to the activation of p53 is the phosphorylation of its N-terminal domain, triggering the disruption with Mdm2-binding (64). Recent reports show that the acetylation status of p53 plays a crucial role in the modulation of p53 levels and transcription factor activity. **Sirtuin-2 (SIRT-2)**, has a deacylase activity and can prevent deacetylation of p53, regulating its activation (64). Alike, **CITED-2** can induce the acetylation of p53. This protein is induced by cytokines such as ILs, as its downregulation contributes to TGF-β- mediated cellular quiescence (65).

3.4. ANTIOXIDANT DEFENSE

To counteract the large number of mechanisms producing ROS, the cell is equipped with various potent antioxidant defenses. These can be differentiated in 3 groups: enzymatic, non-enzymatic and other exogenous antioxidants.

3.4.1. Enzymatic defense

- Superoxide dismutase (SOD): Since superoxide is the primary ROS produced from a variety of sources, its dismutation by SOD is of primary importance for each cell. All 3 forms of SOD, that is, CuZn- SOD, Mn-SOD, and EC-SOD, are widely expressed in the human lung. Mn-SOD is located in the mitochondria matrix. EC-SOD is primarily located in the ECM. H_2O_2 that is produced by the action of SODs or the action of oxidases is reduced to water by catalase (CAT) and the glutathione peroxidase (GSH-Px), (66).

- **Catalase**: Is an enzyme which is present mainly in the peroxisomes of mammalian cells. CAT exists as a tetramer composed of 4 identical monomers, each of them contains a heme group at the active site. Degradation of H_2O_2 is accomplished via the

conversion between 2 conformations of catalase-ferricatalase (iron coordinated to water) and compound I (iron complexed with an oxygen atom). CAT also binds NADPH as a reducing equivalent to prevent oxidative inactivation of the enzyme (formation of compound II) by H_2O_2 as it is reduced to water (66).

- GSH-Pxs: Are mainly cytosolic, but also present in mitochondria. GSH-Pxs are a family of tetrameric enzymes that contain the unique amino acid selenocysteine within the active sites and use low-molecular-weight thiols, such as GSH, to reduce H_2O_2 and lipid peroxides to their corresponding alcohols and water reducing glutathione (GSH) to form oxidized glutathione (GSSH) (66).

- ALDH: The aldehyde dehydrogenase superfamily represents a group of enzymes that catalyze the $NAD(P)^+$-dependent oxidation of a wide variety of aldehydes to their corresponding carboxylic acids (67). For example, MDA and 4-HNE are removed by detoxification reactions mediated by ALDH. In addition to their catalytic roles, ALDHs have been shown to possess non-catalytic roles, e.g. cavenging of hydroxy radicals by CYS sulfhydryl groups, protein-protein interaction. Also, members of the ALDH1, ALDH2, and ALDH3 families serve as lens and corneal crystallins (67).

- Heme oxygenase-1 (HO-1): HO-1 is the rate limiting enzyme within the heme catabolism pathway resulting in the formation of biliverdin, carbon dioxide, and iron. Several results support the hypothesis that HO-1 induction plays an important role in cellular protection against oxidant injury and also maintaining cellular homeostasis (68).

3.4.2. Non-Enzymatic defense

- GSH: It is a potent cellular reducing agent and an important substrate for the enzymatic antioxidant systems as well as a direct antioxidant. It is the most abundant cellular thiol antioxidant, which exhibits numerous and versatile functions and therefore protects cells against toxicity (69). GSH acts as a scavenger of peroxides and also serves as storage and transport for reduced sulfur. In such reactions, the thiol group is oxidized to form a disulfide bond between two molecules of GSH and the oxidized GSH is therefore designated as GSSG. GSSG can be reduced back to GSH by the NADPH dependent GSSG reductasa (69).

- Vitamin C (ascorbate): Is the most abundant aqueous-phase antioxidant in blood and it is a critical water-soluble metabolite in the cell. It is essential for a range of physiological functions, including acting as an important enzyme co-factor and an efficient antioxidant, scavenging ROS and protecting cells from free radical-mediated oxidative damage and stress (70).

- Vitamin E: Lipid-soluble vitamin E is concentrated in the hydrophobic interior site of cell membrane and is the principal defense against oxidant-induced membrane injury. Vitamin E donates electron to peroxyl radical, which is produced during LPO. α-Tocopherol is the most active form of vitamin E and it is the major membrane-bound antioxidant in cell. Vitamin E triggers apoptosis of cancer cells and inhibits free radical formation (66).

3.4.3. Other exogenous antioxidants

There are many other substances with antioxidant capacity which can be derived from the diet. For example, **Vitamin A (retinol)** is a fat-soluble vitamin from the group of carotenoids. It is rapidly oxidized in the presence of oxygen, transient metals, and light. As previously mentioned, vitamin A is also an important molecule for a correct visual cycle in RPE cells (22).

There are some other antioxidants with excellent properties commonly used as co-adjuvant therapies: **N-acetylcysteine (NAC)**, and **Diallyl Sulfide (DAS)** as specific CYP2E1 inhibitor.

- **NAC:** It has an optimal thiol redox state, which is of great importance to optimize the protective ability of cells to counterbalance OS and inflammation. It acts directly increasing intracellular GSH. Administration of NAC has been reported to be beneficial in other chronic clinical conditions, such as inflammatory diseases, HIV infection, diabetes and hepatic injuries (69).

- **DAS:** Is an organosulfur compound typically found in garlic. It is a selective CYP2E1 inhibitor. Taking into account that CYP2E1 is one of the major ROS producers in the cells under xenobiotic metabolism, the use of this inhibitor could be essential to maintain the redox balance status. CYP2E1 is also induced in HIV, diabetic, and Parkinson patients, who regularly consume alcohol, analgesic drugs and other xenobiotics (71). Thus, DAS by inhibiting CYP2E1, has the potential to be used as a novel therapeutic in alcohol and analgesic drug users, as well as in HIV, diabetic, and Parkinson's disease patients who suffer from liver toxicity and toxicity of other extra hepatic cells (71).

3.5. RPE ANTIOXIDANT DEFENSE

SOD, **GPx**, and **CAT** are key enzymes of the antioxidant RPE cell defense (6, 17). SOD, CAT and GPx activity is decreased in RPE cells after the addition of H_2O_2 compared with control cells. Resveratrol treatment as antioxidant resulted in a significant increasing of the enzyme activity (72).

It was shown that a short-term exposure of nonadapted RPE cells to a higher H_2O_2 concentration had as a result a very severe decrease in CAT, GPx, and CuZnSOD activities. By contrast, MnSOD showed no adaptive behavior (72). In the same way, OS inducing by H_2O_2 increase the HO-1 expression in RPE cells. Besides, this study also relates the activation of nuclear factor erythroid-2 related factor-2 (Nrf2) and its interactions with antioxidant response elements (AREs), which mediated transcriptional induction of various antioxidants, including SOD, GSH-PX and HO-1 (73).

RPE cells have different response to OS depending on the damage or stimuli. For example, the oxidative damage caused by exposure of RPE cells to H_2O_2 was significantly reduced by vitamin C, vitamin E, and DHA, while hyperoxia-induced damage was decreased by vitamin E and DHA, but not vitamin C, and paraquat-induced damage was not reduced by any of the three antioxidants (74). In addition, the RPE cell takes up DHA from the blood stream through the choriocapillaris. RPE have the capacity to synthesize NPD1 from DHA, and this NPD1 can modify the expression of the proteins that challenge cell survival (75). Under OS conditions NPD1, a DHA-derived mediator endogenously synthesized by neuroepithelium-derived RPE cells, is a modulator of signaling pathways that promote cell survival (75).

3.6. RPE SIGNALING ACTIVATED BY OXIDATIVE STRESS

As we know, intense illumination from focal light, LPO from the degradation of rod outer segments, and high oxygen tension in the macular area, all provide conditions for OS to the RPE. ROS can induce expression of several genes involved in signal transduction in RPE cells. Activation of transcription factors via ROS is achieved by signal transduction cascades that transmit the information from outside to the inside of cell. Tyrosine kinase receptors, growth factor receptors, such EGFR, VEGFRs, and serine/threonine kinases such as **mitogen activated protein kinases (MAPKs)** are targets of ROS, **figure 9** (76).

3.6.1. MAPKs signaling

MAPKs are a family of serine/threonine kinases which are strongly involved in OS. In mammalian cells, there are three well-defined subgroups of MAPKs: the **extracellular signal-regulated kinases (ERKs)**, the **c-Jun N-terminal kinases (JNKs)**, and the **p38 MAPKs** (77). Each of these kinases mediates different reactions (adaptive and apoptotic), integrating external signals in order to organize the appropriate response of the cell.

A number of cellular stimuli that induce ROS production in parallel can activate MAPK pathways in multiple cell types. But in general, ERKs are essentially an activated response to growth factors, while the JNKs and p38 MAPKs are more responsive to stress stimuli and inflammation, just like cytokines (77). Additionally, blockade of p38 or ERK provides significant protection from retinal ischemic damage, suggesting a novel therapeutic role for MAPK inhibition in neuroprotection (78). And recently, Qiu Y, et al. (79) published that the activation of MAPK and **nuclear factor KB (NFKB)** plays vital roles in regulating proinflammatory genes in RPE cells. Also, combination of NFKB and p38 inhibitors abolishes VEGF secretion in RPE cells (80).

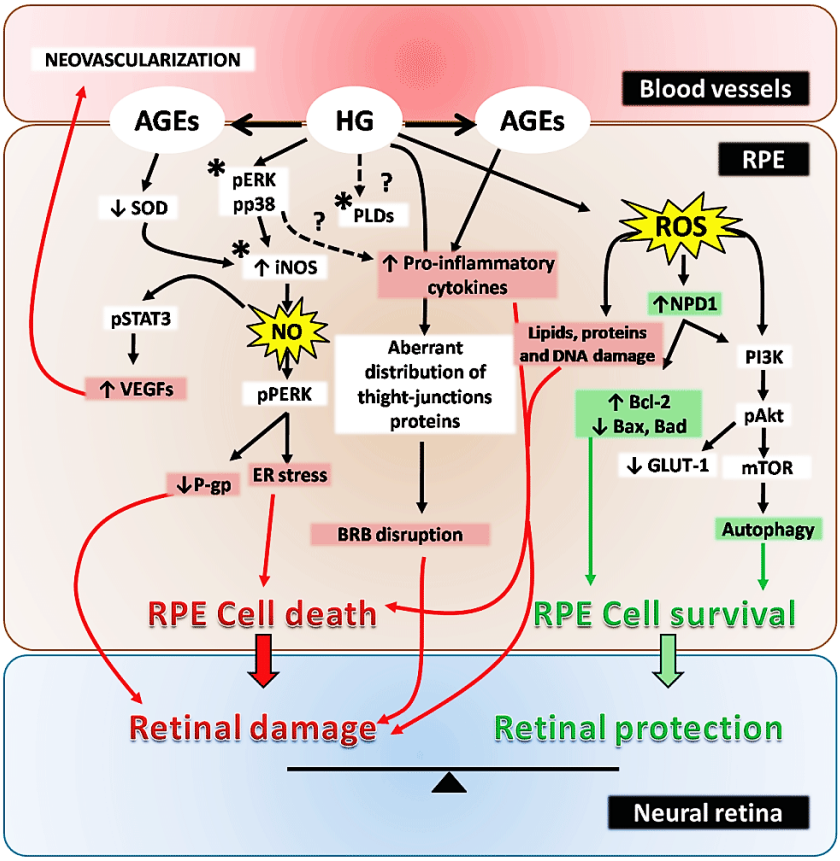

Figure 9. ROS targets in RPE cells. Several pathways can be activated by ROS in RPE cells. The balance between survival (autophagy, increase of Bcl-2 and NPD1) and cell death processes (apoptosis, increase of ER stress, BRB disruption) is essential to maintain healthy the retinal tissue. Obtained from Mateos MV, et al. 2015 (76).

Several pathways activated by OS are implicated in antioxidant defense. For example, NFKB activation is initiated by the signal-induced degradation of IκB proteins via activation of a kinase called the IκB kinase (IKK). With the degradation of IκB, the NF-κB complex is then freed to enter the nucleus where it can 'turn on' the expression of specific genes. NPD1 can indirectly inhibit NFKB activation in RPE cells (75). Additionally, NPD1 promotes RPE cell survival inhibiting low and repetitive OS-induced apoptosis by inducing the activation of PI3K/Akt and mTOR/p70S6K pathways (81). PI3K/Akt pathway has been proposed to protect RPE cells against the deleterious effects of OS. In Faghiri Z, et al. work (81), apoptosis was unaffected and phosphorylation of Akt, mTOR, and p70S6K occurred in a sustained manner, in low OS conditions. During repetitive OS, RPE showed a rapid increase, followed by a decrease of Akt, mTOR, and p70S6K expression and less than 50% of the cells showed apoptosis (81).

3.6.2. Apoptosis

Some evidence suggests that OS is involved in RPE cell death. Apoptosis is one of the mechanism than RPE cells can activate to control the retinal tissue damage (57). The intracellular machinery responsible for apoptosis depends on a family of proteases called **caspases**. Caspases are synthesized in the cell as inactive precursors, or procaspases, which are usually activated by cleavage at aspartic acids by other caspases. This activation can be triggered from outside or inside the cell, **figure 10** (82).

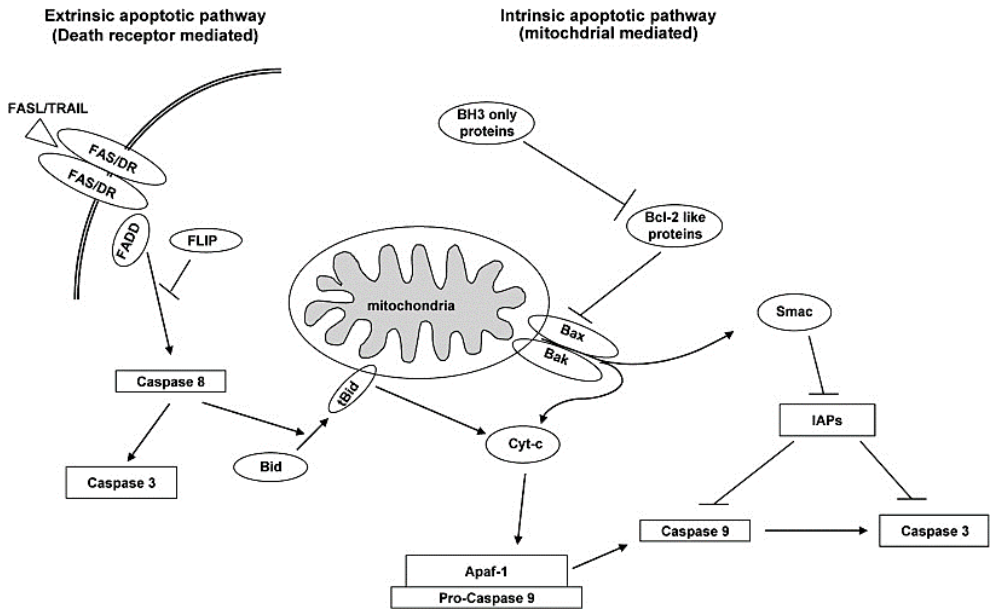

Figure 10. Apoptosis activation. Induction of apoptosis by either extracellular or intracellular stimuli. Obtained from Hector S, et al. 2009 (82).

The Bcl-2 family of intracellular proteins helps regulate the activation of procaspases. This family contains pro-apoptotic members (**Bax**, Bak, Bad, Bik, Bim, Noxa, and Puma) and anti-apoptotic members (Bcl-xL, **Bcl-2**, and Mcl-1). The release of **cytochrome c (CYT-C)** to the cytosol, mediated by Bax, activates a protein complex called "apoptosoma," which directly activates caspase-9, developing the apoptosis pathway. Bcl-2 inhibits apoptosis at least partly by blocking the release of CYT-C (82). The balance of anti- and pro-apoptotic proteins determines whether a cell lives or dies.

Another important family of intracellular apoptosis regulators is the inhibitor of apoptosis family. These proteins are thought to inhibit apoptosis in two ways: they bind to some procaspases to prevent their activation, and they bind to caspases to inhibit their activity (83). The intracellular cell death program is also regulated by extracellular signals, which can either activate apoptosis or inhibit it. These signal molecules mainly act by regulating the levels or activity of members of the Bcl-2 and IAP families (82).

There is an important apoptosis regulator in RPE cells; the bone morphogenetic protein 4 (BMP4). BMP4 mediates OS inducing senescence *in vitro* via Smad and p38 pathways. BMP4 can also be either pro-angiogenic or anti-angiogenic, depending on the context of cell types and associated microenvironment. In the RPE, over-expression of BMP4 inhibits experimental CNV by modulating VEGF and MMP-9 (84).

There are many studies that support this affirmation. In 2007 Yang demonstrated the possible implication of caspase-8 levels to protect RPE cells from apoptosis in AMD (56). They also showed that exposure to hydrogen peroxide (H_2O_2) on RPE cells leads to transcription of Bax. Bax overexpression is accompanied by an increase of caspases (9 and 3) and OS, inducing Bax translocation to the mitochondria, which results in the release of apoptosis inducing factor (AIF) (85).

Another important apoptosis regulator in RPE cells is p53. This p53 pathway responds to stress signal which lead to cell cycle arrest, cell senescence or cellular apoptosis. p53 induces some proapoptotic proteins and suppresses the transcription of Bcl-2 and Bcl-xL. In humans RPE, the basal rate of p53-dependent apoptosis increases in an age-dependent manner. Moreover, H_2O_2 induces an elevation of p53 and 4-HNE increasing the level and phosphorylation of p53 in the RPE (63).

On the other hand, it has been shown that the addition of NPD1 protects human RPE cells in culture from OS injury (**Figure 9**) and also upregulates the expression of anti-apoptotic proteins, such as Bcl-2 and Bcl-xL, and downregulates levels of pro-apoptotic markers, such as Bax and Bad.

The inhibition of caspase 3 and a diminished COX-2 expression have also been shown to be triggered by NPD1 during OS events (76).

3.6.3. Necroptosis

For many years, apoptosis was considered to be the only form of regulated cell death, whereas necrosis was seen as an unregulated accidental cell death process. Regulated necrosis includes several cell-death modalities such as necroptosis (86).

Necroptosis is mediated by interacting with the protein kinase-3 receptor (RIPK3) and its substrate mixed lineage kinase like (MLKL), is the best-characterized form of regulated necrosis. During necrosis induction, RIP3 interacts with RIP1 to form a pro-necrotic complex (86). Some data demonstrates that RIPK-mediated programmed necrosis is a redundant mechanism of photoreceptor death in addition to apoptosis, and that simultaneous inhibition of RIP kinases and caspases is essential for effective neuroprotection (87). Besides, RIP3 has a critical role in inducing necrosis to the RPE and photoreceptors, as well as in sustaining retinal inflammation during retinal degeneration. This publication also suggests that necrotic pathways may be crucial in RPE cell death in AMD and in others retinal degenerative diseases associated with inflammation (88).

3.6.3. Autophagy

The study of this cellular pathway has been awarded with a Nobel prize in Physilogy or Medicine 2016 to Yoshinori Ohsumi. The concept emerged during the 1960s, when researchers found that the cells could destroy their own content, membrane enclosing and sending the resulting vesicles to the lysosome, a cellular organelle responsible for recycling (89).

Cumulative evidence demonstrates that during OS, RPE can also trigger the activation of survival signaling pathways for self-protection as well as for cell death prevention e.g. synthesis of neuroprotective compounds such as NPD1 or autophagy activation by the inhibition of PI3K-Akt-mTOR pathway has been reported in RPE cells (81).

In RPE cells, autophagy is involved in development, cell survival, melanin degradation, as well as in the degradation of toxic cellular components and damaged organelles (47). RPE cells maintain basal autophagy levels for cellular homeostasis, with variations, commonly observed in aged and damaged cells (47, 49). Autophagy plays an important role in the pathogenesis of blinding retinal diseases due to defective lysosomal-autophagic degradation in the RPE (90). Recently, several research

groups showed advances in understanding the role that autophagy plays in RPE, AMD development (91) or glaucoma (92).

3.6.4. Release of cytokines

The release of cytokines and chemokines by cells of the immune system occurs in order to recruit other cells in the place where the damage has developed (93-95). There are proinflammatory cytokines such as interleukin 1, 2, 6, and 8 (IL-1, IL-2, IL-6, IL-8), together with TNF-α and also antiinflammatory such as IL-10 and IL-6. The first cytokines of the inflammatory cascade are TNF-α and IL-1β to stimulate the production of IL-6 (96).

ROS production is essential for the progression of an inflammatory process, this is produced by the same cells above mentioned, involved in carrying out the immune response. Therefore, we can say that the ROS acts as a signaling molecule and as a mediator of inflammation (96). In addition, it acts as secondary messenger modulating transcription factors in a variety of inflammatory signaling ways including MAPK, NFKB, and the signaling pathway JAK-STAT in different cell types (97).

There are studies that relate the production of ROS in the RPE specifically with inflammatory processes and release of VEGF. This has been studied in diseases such as DR and AMD (98, 99). Besides, taking into account the important role of VEGF in maintaining the RPE tissue stability, the imbalance of VEGF release can induce retinal damage.

Recently, Vatsyayan and collaborators (100), have published that the expression and function of VEGF in RPE cells is regulated by 4-HNE. On the other hand, NAC treatment in hyperglycemia rescued the severity of this CNV by inhibiting overexpression of p-STAT3 and VEGF in RPE cells (101).

3.6.5. MMPs activation

It has been observed the presence of MMPs, in particular MMP-1, MMP-3 and MMP-9, in the matrix located between the photoreceptor; subsequently it was confirmed that the presence of MMP-2 is increased upon exposure to light. The participation of these proteases is proved in the phototoxic processes (102).

As mentioned before, overexpression of MMP-9 is implicated in CNV development via VEGF (84). On the other hand, PEDF-treated mice underwent a reduction in MMP activity reflecting a normalization of ocular VEGF levels (103).

3.6.6. TJ disruption

The TJ form a barrier for the movement of substances into the cellular space, limiting the passage of substances between the basement membrane and the basolateral membrane in RPE cells. Three transmembrane proteins in TJ have been identified: occludins, claudins and adhesion molecules. Among these, the occludin seems to be the most important and, therefore, it has been extensively characterized (104, 105). Occludin, binds to members of the family of **zonula ocludens** (**ZO-1**, ZO-2, ZO-3) (95, 106) through its C-terminal and interaction with these proteins appears to be crucial in the assembly of the TJ and in the maintenance of barrier function. Recent studies show that OS is capable of interfering with the integrity of the barrier because it affects negatively to TJ inducing, among other things, the dissociation between occludin and ZO-1 (76). On the other hand, there are studies that say that the expression of ZO-1 decreases under hypoxic conditions, **figure 9** (76, 106).

4. OXIDATIVE STRESS AND OCULAR DISEASES

Oxidative stress plays a central role in the most common eye diseases, including RP, AMD, and DR (107). As mentioned previously, the eye is one of the most metabolically active tissues and it is exposed to high levels of light and oxygenation. These characteristics favor the production of ROS in RPE and neural retina. Excessive accumulation of this species contributes to the retinal pathogenesis (17), leading to LPO processes, protein oxidation and DNA damage. These effects are related in turn to mitochondrial damage that can result in apoptosis or cell necrosis (108).

It has been shown that some retinal diseases can produce changes in the extracellular tissue environment, this increases OS, stimulating ROS production. Excessive accumulation of ROS is related to a decrease in the production of antioxidant enzymes (108). ROS formation also appears to be related to processes of hypoxia and inflammation (109), ischemia, EtOH consumption (73), actin reorganization, and cell migration (48). Furthermore, it has been observed that the onset of angiogenic activity mediated by inflammatory cells also appears related to ROS production (48).

4.1. RETINITIS PIGMENTOSA

Retinitis pigmentosa is defined as an inherited retinal condition that gradually leads to visual field loss and retinal degeneration. RP results from harmful changes in any one of more than 50 genes limiting the cells function. It is considered a rare disorder that affects roughly 1 in 4,000 people (110).

The progressive rod degeneration is later followed by abnormalities in the adjacent RPE and the deterioration of cone photoreceptor cells. As peripheral vision becomes increasingly compromised, patients experience progressive "tunnel vision" and eventual blindness (111).

In 2005 Shen J and collaborators described in a pig model of RP the presence of acrolein- and 4-HNE-adducts on proteins like a specific indicator of LPO (112). Also, decreased oxygen consumption and hyperoxia in the outer retina, resulting in gradual cone cell death (112). This cell death could be caspase-independent apoptosis induced by OS (113). According to OS implication in the death of retinal cells, other research group published that antioxidants reduce cone cell death in RPE (114).

4.2. CHORIOCAPILLAR AND RETINAL MICROVASCULATURE ALTERATIONS

Ocular angiogenesis is a cause of severe worldwide visual loss and ocular morbidity. These include retinopathy of prematurity, DR, and AMD, which are leading causes of vision loss in children, working-age adults, and the elderly in the developed world (115).

In these CNV and retinal NV diseases the **VEGF/VEGFR-2** axis promotes endothelial cell function and proliferation, leading to increased pathological neovessels in proliferative eye diseases (48). The evolution of CNV begins with a break or defect in Bruch's membrane. This may be secondary to a traumatic break, a degenerative process, tissue traction and/or inflammation. When this occurs, choriocapillary endothelial cells, pericytes, fibrocytes and inflammatory cells are introduced into the sub-retinal pigment epithelium and/or sub-retinal spaces. There are inflammatory, angiogenic and ECM components of the CNV competing to induce or suppress the processes (116).

Several inflammatory subsystems have been implicated in CNV, including the complement system, cytokines, and chemokines (117). Pro-angiogenic factors that stimulate the proliferation of endothelial cells in CNV include **VEGF**, **FGF** and **PDGF** (116). PEDF is a naturally occurring anti-angiogenic protein. Interestingly, PEDF also exhibits anti-inflammatory properties by modulating macrophage activity (42). The MMPs and TIMPs are involved with pro- and anti-angiogenesis as well as pro- and anti-tissue degradation (28, 35).

We can describe all of this like a system with three general categories: inflammation, angiogenesis and proteolysis. These systems are interrelated and allow the initiation, maintenance and progress of CNV. In the case of NV, the principal promoter is the hypoxia. Numerous clinical and experimental observations have indicated that ischemia and hypoxia is the main cause for retinal NV (117). Hypoxia increases the accumulation of **hypoxia inducible factor 1α (HIF-1α)**, a transcription factor, which can promote the expression and secretion of the VEGF. Exposure to hypoxia may also induce changes in the levels of OS in the body, generating an increase in ROS (118). It has been observed that HIF-1 is closely related to VEGF and this, in turn with different growth factors (EGF, TGF-α and β, IGF-1, FGF and PDGF), activates oncogenes as well as various cytokines (IL-1-α and IL-6), and the resale of nitric oxide (NO) (76).

One of the best characterized targets of HIF-1 is **carbonic anhydrase 9 (CA9)**. It has been shown that CA9 contributes to the acidification of the extracellular

environment during hypoxia, and low extracellular pH is associated with the angiogenic process. This makes CA9 a potential marker of hypoxia (119).

ROS production appears to be involved in the initiation of angiogenesis, and it also has a crucial role in triggering intracellular signals (120). Like inflammatory processes, it has been demonstrated that there is an increase of hypoxia markers in many retinal diseases that eventually trigger angiogenic processes. (98, 121). It has been demonstrated that not only VEGF can regulate angiogenesis process; there are different molecules and process involved (76, 89 120, 121). But other proteins not mentioned before are strongly associated with the regulation of angiogenesis.

Thrombospondin-1 (TSP-1) is a glycoprotein of ECM and it has multiple functional domains that have been attributed to different biological activities (122). These activities should be noted as a potent inhibitor of angiogenesis (123, 124).

Others endogenous inhibitors of angiogenesis are angiostatin, that it is resulting from the degradation of plasminogen and endostatin (collagen XVIII fragment). On the other hand, inhibitors of ECM e.g. tumstatin, vasoinhibin and vasostatin (125), can act as indirect inhibitors of angiogenesis.

AMD is a disease associated with age that gradually destroys sharp, central vision (110). The treatment and therapy for AMD is constantly evolving. In the past, the only way to seal leaking blood vessels in wet AMD was using a laser in a procedure. In 2004, an even more effective type of treatment, called “Targeted Therapy” was developed. These treatments called anti-VEGF therapies have now revolutionized the treatment of wet AMD (112). But VEGF is not only the target for the treatments, it is necessary to take into account the important role of OS in this disease.

Previous studies demonstrate that OS induces VEGF liberation in RPE and endothelial cells (48). OS also promotes the NV and angiogenesis in different AMD models (126). Chronic elevated ROS level, OS, pathophysiological inflammation, and long stay hypoxia decrease the ability of RPE cells to remove damaged or nonfunctional proteins via the lysosomal clearance system, including macroautophagy (66). In addition, superoxide anions are involved in the regulation of cell adaptation to hypoxia via HIF-1α and are involved in the regulation of mitochondrial autophagy process (68).

The major cause of blindness in working age people is DR. It is a chronic and progressive complication in the course of diabetes mellitus type 1 or type 2. It is characterizes by gradual and progressive alterations in the retinal microvasculature, accompanied by damage of glia and neurons (127). Vision loss occurs from the breakdown of the BRB, resulting in macular edema, inner retinal and vitreous hemorrhages, and tractional retinal detachment (128).

The role of OS in this disease is more complicated to define. This is a multifactorial disease and the excess of glucose in the blood does not only have damage in the retinal tissue. In RPE hyperglycemia, the levels of ROS are increased with a persistent mtDNA damage (129), releasing to cytokines and activating signaling pathway such as NFKB (130). Similar to AMD, DR triggers an inflammation response in the retinal tissue, resulting ultimately in an uncontrolled angiogenic process.

5. ALCOHOL AND RETINAL DEGENERATION

Alcohol consumption is a risk factor that causes death worldwide. Its consumption can lead to more than 60 different diseases (131). In fact, alcohol dependence correlates with a broad spectrum of diseases, psychological, behavioral and social problems (132). Alcohol has become the more socially accepted addictive drug worldwide (133), and it can result in the damage and functional impairment of many organs of the body.

But this is not only a major health problem, it also is an economic burden, due to the increased and many costs that chronic diseases related with alcohol have. These alcohol related diseases go from heart disease (134), strokes (135), liver disease (136), cancer (137), chronic respiratory diseases (138) to neurodegenerative disease (139). It has been shown that acute and chronic EtOH increases ROS production in a variety of systems, cells, and different species, including humans (136).

5.1. EtOH METABOLISM

The metabolism of alcohol, mainly referred as EtOH (CH_3CH_2OH), is closely linked with the stimulation of ROS generation and thus OS. The effects of EtOH on biological tissue depends on its concentration in blood over time (57). Elimination of absorbed EtOH occurs primarily through metabolism (98%), with small fractions (1-2%) excreted by breath, sweat, and urine (140). Although the main focus of EtOH-induced alterations is the liver, there are also clear indications of the existence of an extrahepatic oxidative EtOH metabolism in different organs.

EtOH exerts its deleterious effects metabolically via oxidative (producing acetaldehyde) and non-oxidative (formation of ethyl esters of fatty acids) pathways (141), involving free radical production and LPO (128, 142-144).

In cellular EtOH metabolism there are three enzymes responsible, **figure 11** (145). The principal EtOH-metabolizing enzymes are ADH in cytosol, but there are two others as well. One of them is CYP2E1 on microsomes, and CAT on peroxisomes. Both contribute to the metabolism of alcohol in specific circumstances, such as in high concentrations. The acetaldehyde produced by the EtOH oxidation is transformed to acetate by ALDH, which can be further metabolized through the tricarboxylic acid cycle to generate energy, although these metabolites can be deposited in the plasma (146).

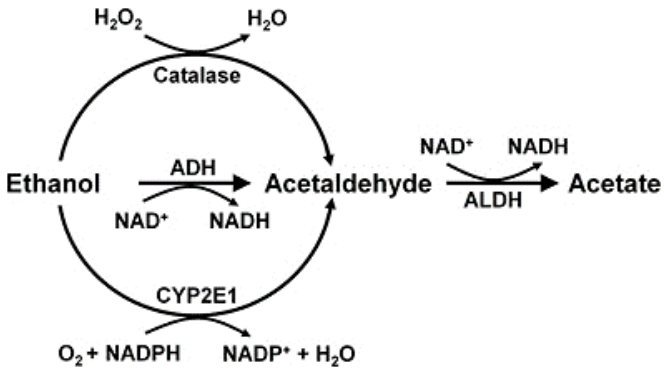

Figure 11. EtOH metabolism. EtOH is metabolized to acetaldehyde by ADH, Catalase and CYP2E1. The activity of ALDH transform acetaldehyde in acetate. Obtained from Israel Y, et al. 2013 (145).

5.1.1. Alcohol dehydrogenase

ADH is a zinc-containing enzyme, consisting of two subunits of 40 kDa each. Its function is to oxidize endogenous alcohol and exogenous alcohols consumed in the diet. The enzyme has broad substrate specificity, oxidizing many primary or secondary alcohols. It is located in the cytosolic fraction of the cell. ADH is found in its highest amount in the liver, followed by the estomach, kidneys, nasal mucosa, testes, uterus (147), and also in RPE tissue (51).

To maintain effective rates of alcohol oxidation by ADH, it is important to regenerate NAD+ from the NADH produced by the ADH reaction, **figure 11** (145). Under certain conditions, the rate of oxidation of alcohol can be limited by the reoxidation of NADH. The major system for reoxidizing NADH is the mitochondrial electron transfer system (145).

Alcohol oxidation is generally limited by the maximum capacity of ADH (147). To date, there are seven different ADH genes; Class I: ADH1A, ADH1B, ADH1C; Class II: ADH4; Class III: ADH5; Class IV: ADH6 and Class V: ADH7. All of these have been identified clustered together on the same chromosome.ADH1A, ADH1B and ADH1C genes encode the majority of the ADH enzymes that metabolize alcohol in the liver (148). Additionally ADH5, ADH7 were found in RPE cell line called ARPE-19 (51).

5.1.2. Catalase

Catalase (CAT) is capable of oxidizing EtOH *in vitro* in the presence of a hydrogen peroxide (H_2O_2)-generating system, such as the enzyme complex NADPH oxidase or the enzyme xanthine oxidase. Quantitatively, however, is considered a minor pathway of alcohol oxidation (149).

The increase in CAT activity following EtOH intake, and its effects in the CNS, are associated with weak ADH activity. This increase in CAT activity in the CNS may be an adaptive process induced by the increase in the hydrogen peroxide generated, as that which occurs in the CNS of animals exposed to high EtOH concentrations (147). In the same experiments with ARPE-19 cells, also the expression of catalase was found (51).

5.1.3. MEO System: CYP2E1

This is a system capable to metabolize EtOH on microsomes and sometimes in mitochondria. This system referred to as MEOS contains different members of the CYPP450 family. The CYP2E1 distribution in human body is well known, there is expression of this enzyme not only in liver, also in CNS (143), in the digestive system (150), heart (151), lung (152) and the eyes (51, 153, 154). The gene is located on chromosome 10q26.3 and is composed by 9 exons.

CYP2E1 is a P450 which has the highest activity for oxidizing alcohol to acetaldehyde. Besides, CYP2E1 can oxidize many other xenobiotic compounds including acetone, benzene, other alcohols and drugs (147). The Michaelis constant, Km of CYP2E1 for EtOH is 10-fold higher than the Km of ADH. Km is the substrate concentration at which the reaction rate is half of Vmax (the maximum rate achieved by the system, at saturating substrate concentration). At low alcohol concentrations, CYP2E1 may account for about 10% of the total alcohol oxidizing capacity of the liver. However in view of its higher Km, the relevance of CYP2E1 in EtOH oxidation increases as blood alcohol concentrations increase (147).

5.2. CYP2E1 AND OXIDATIVE STRESS GENERATION

The generation of these ROS by CYP2E1 contributes to the OS observed after alcohol consumption. CYP2E1 is unique P450s found in humans will readily accept electrons and generate these ROS even in the absence of a substrate (155). The production of these ROS by CYP2E1 is referred to as an “uncoupled reaction”. Thus, in the presence or even in the absence of substrate, CYP2E1, with O_2 and NADPH, it can produce ROS that may cause cell toxicity (155). In general, ROS are generated during P450 catalysis when either the ferrous oxy species decays to produce superoxide or the hydroperoxy form is protonated to release hydrogen peroxide. Collapse of these species could occur if electron or proton delivery is delayed or if the substrate is not positioned for attack. It has been proposed that during uncoupling, the substrate could

migrate away from the heme and the activated oxygen, thus allowing the oxygen to react in other ways (156).

The CYP2E1 catalytic activity results in the production of large amounts of reactive oxygen with intermediates such as the superoxide radical and hydrogen peroxide (146). Additionally the activity of CYP2E1 produces LPO products such as 4-HNE and MDA (146). For this reason, the activation of CYP2E1 could be toxic for the cell, **figure 12** (157).

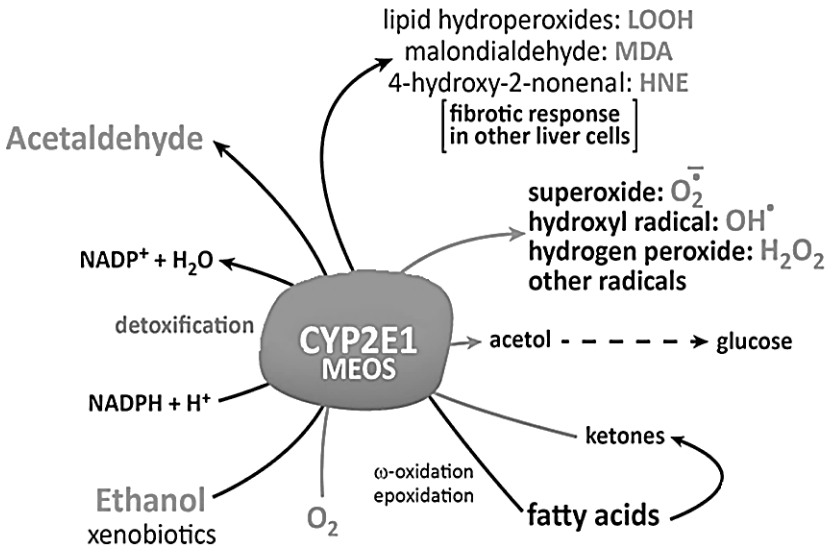

Figure 12. CYP2E1 and generation of oxidative stress. CYP2E1 activity increase the levels of OS producing ROS, increasing glucose levels and lipid peroxidation products. Obtained and modified from http://themedicalbiochemistrypage.org (157)

5.2.1. CYP2E1 induction

CYP2E1 is induced in the liver and several extrahepatic tissues by small organic molecules such as **EtOH**, pyrazole, acetone, or isoniazide. Consequently, the tissue levels of this heme protein are significantly increased (158).

CYP2E1 can also be induced under a variety of metabolic or nutritional conditions. For example, CYP2E1 levels were elevated in chronically obsesses rats, also in rats in which the levels of CYP2E1 were increased by prolonged starvation (159). The most significant chemical inducer of CYP2E1 is EtOH, a compound which is also a substrate for the protein. Debate still exists as to the precise mechanism of CYP2E1 induction by alcohol, with some reports indicating that EtOH stabilizes CYP2E1 *in vitro* and another group suggesting that EtOH induces CYP2E1 by increasing protein synthesis (159).

Induction of CYP2E1 expression by EtOH is complex and involves both transcriptional and post-transcriptional mechanisms (160, 161). EtOH, at very high levels can also increase CYP2E1 by a transcriptional mechanism and increase mRNA synthesis. Thus, multiple mechanisms can exist by which a cytochrome P450 such as CYP2E1 can be induced. In many cases, induction of a specific P450 by a chemical inducer requires binding of the inducer to a nuclear receptor, followed by translocation of the receptor-inducer complex into the nucleus and subsequent interaction and activation of the gene for the P450 (160).

5.2.2. CYP2E1 regulation

The regulation of CYP2E1 activity can be modulated at several levels, ranging from transcriptional to post-translational induction and inhibition. The net result is in fact not "induction" per se, but the accumulation of substrate-stabilized CYP2E1 (162).

The signaling pathways involved in CYP2E1 regulation by EtOH are unclear, especially in extra-hepatic cells. Jin M and collaborators demonstrate the strong evidence of the involvement of the **PKC/JNK/SP1 pathway** in EtOH-mediated regulation of CYP2E1 in astrocytes and monocytes (161). Their results are supported in recent monocytes studies (163). The OS generated by CYP2E1 activates the inflammatory pathways. This mechanism can regulate also CYP2E1 expression.

Previous studies have shown that anti-inflammatory cytokine IL-4 can induce CYP2E1 in hepatic cells through PKC pathway. In fact, the pro-inflammatory cytokines IL-1β, IL-6 and TNF-α down-regulate CYP2E1 gene expression (164). Abdel-Razzak and collaborators realized a complete study about possible transcriptional factors for CYP2E1. They found that there are several putative binding locations for transcription factors e.g. AP-1 and NFKB (164). Also nuclear factor 1 (NF-1) binding sites are found in CYP2E1 gene promoter region, suggesting that CYP2E1 gene expression is also regulated by NF-1 (165, 166). Most of them are known for their involvement in IL-4 response in other cell systems. IL-1β slightly inhibits CYP2E1 promoter activity through a sequence independent from the IL-4 responsive region.

NFKB is an important transcription factor that regulates a wide spectrum of genes including CYP450. NFKB can directly regulate the expression of CYP2E1 through binding to the promoter region. Also indirectly, it regulates the transcription of CYP genes through mutual repression with some nuclear receptors, and finally it can regulate the activity at post-transcriptional level by inducing heme oxygenase or by affecting the protein stability (167).

On the other hand, ROS accumulation and a pro-oxidant environment generated by CYP2E1, trigger activation of transcription factors NFKB and AP-1 (168). In addition to the role of ROS in activating NFKB and AP-1, it is conceivable that carbonyls resulting from the LPO caused by EtOH may also play a role in modulating the DNA binding of NFKB and AP-1 (168).

Different CYP2E1 inhibitors have been described. On one side we find the endogenous cell inhibitors, and in the other side, the exogenous or drugs inhibitors. The first ones are proteins, transcriptional factors or molecules induced by cell signaling response under OS situations. The second ones are drugs or molecules that can block the CYP2E1 activity. There are many in this last group, but the most used in cellular and animal experiments are DAS, disulfiram or clomethiazole (CMZ), like synthetic antioxidants or drugs.

As previously mentioned, the regulation of CYP2E1 and the cell signaling implicated is a complex process that implicates a lot of cell signaling proteins, factors, processes and pathways, **figure 13**. For this reason it is still under investigation.

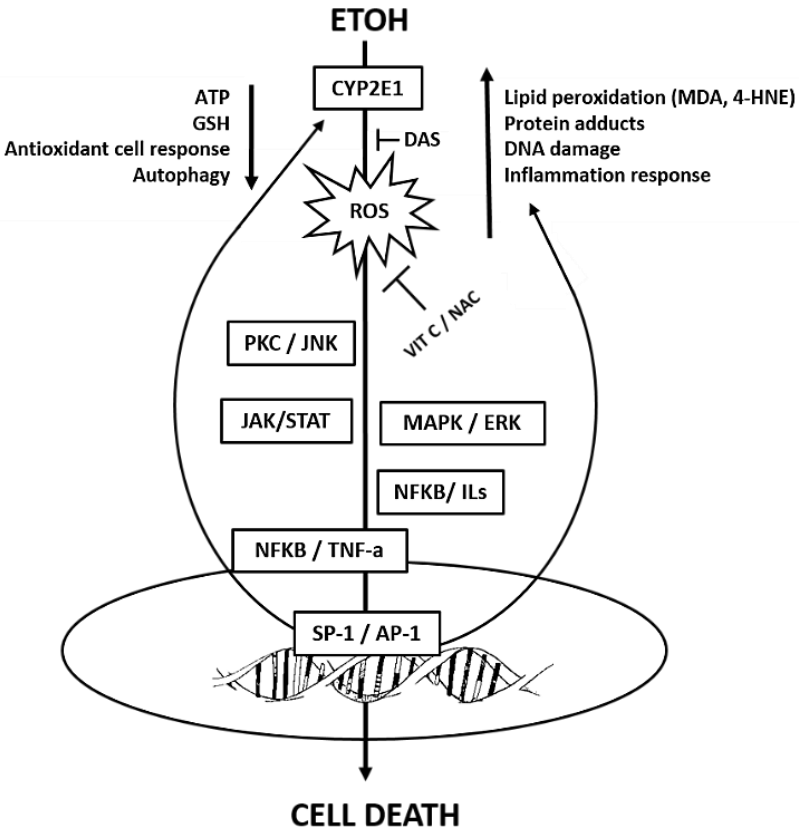

Figure 13. Regulation of CYP2E1 and cell signaling involved. The increase of OS by CYP2E1 activity induced by EtOH, activates a ROS-induced MAPKs and cytokines pathways. That results in a CYP2E1 gene promoter activation increasing CYP2E1 expression as a positive feedback regulation.

Background
And
State Of The Art

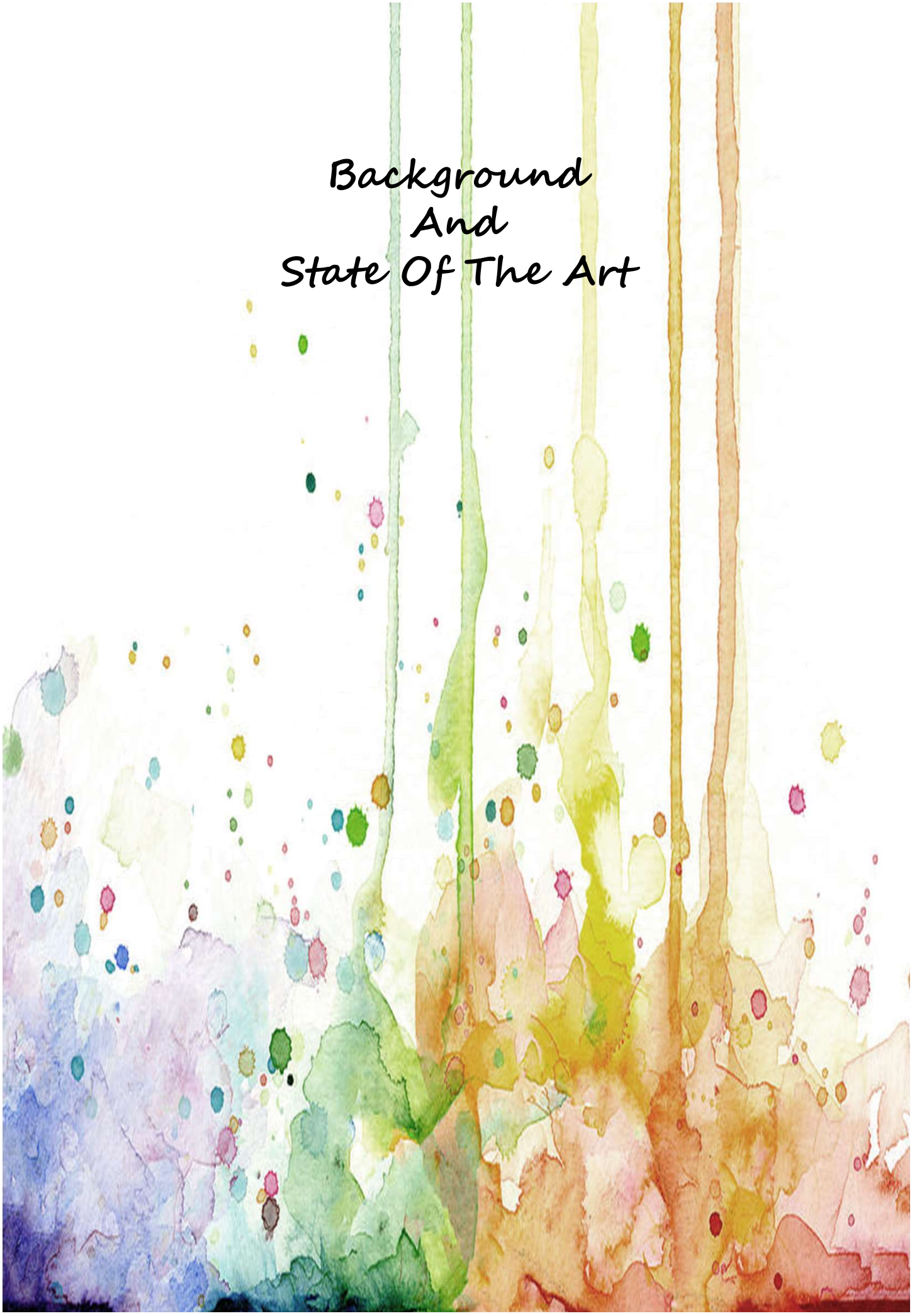

Alcohol consumption is a risk factor for death worldwide important because consumption of this leads to more than 60 different diseases (131). In fact, alcohol dependence correlates with a broad spectrum of diseases, psychological, behavioral and social problems (132). Alcohol has become more socially acceptable addictive drug worldwide (133), resulting in damage and functional impairment of many organs of the body.

As is mentioned before, alcohol-mediated upregulation of pro-inflammatory cytokines occurs through the MAPK pathway (ERK1/2, p-38, and JNK), which triggers the downstream activation of oxidant-sensitive transcription factors NFKB and AP-1 (161-168). It has been demonstrated that low alcohol concentrations can increase cellular antioxidant defense to combat the OS. But high EtOH concentrations and consistent abuse can cause alcohol-induced toxicity and liver damage through the PKC/JNK pathway (161).

It has been also reported that the inhibition of CYP2E1 activity by DAS prevented the induction of collagen I gene expression in rat stellate cells overexpressing CYP2E1 (169). Also the same study demonstrate the MMP-2 and TGF-β induction by EtOH in a concentration dependent manner in hepatic stellate cells. The same occur with NFKB, the increase of this factor is accompanied by decrease of its inhibitor, IKBα.

Is well known that exposure to high EtOH treatment induce apoptosis in several tissues and cells (170-172). This EtOH, induces caspase-3 expression, not only in hepatocytes for example in RPE cells (170) and astrocytes (161). In addition, knocking down CYP2E1 expression through CYP2E1 siRNA abolished ethanol-induced caspase-3 cleavage. The same occur with the use of DAS , vitamin C, as well as vitamin E suggesting that ethanol-induced apoptosis is mediated through ROS production (161). Similar results were found in our group in RPE cells under EtOH treatment using DAS and CMZ as an inhibitor (51). This process could be activated because mitochondria appear to be among the critical cellular organelles damaged by CYP2E1-derived oxidants (159). On the other hand in neurons, EtOH induces apoptosis by inhibition of phosphatidylserine accumulation (173).

The role of LPO products in apoptosis activation, It has been well studied. And its ability to form protein adducts, and aggresomes is an important key in this process. For example 4-HNE can promote organelle and protein damage, apoptosis or necrosis programmed cell death at high or very high levels, respectively, and cells die.

These processes eventually lead to molecular cell damage which may facilitate development of various pathological states. High levels of 4-HNE can also react with proteins and/or DNA to form adducts resulting in a variety of cytotoxic and genotoxic consequences (47).

Autophagy has been identified as cytoprotector in nervous and liver cells under EtOH-induced toxicity. Oxidative-damaged mitochondria, a main source of ROS, seem to be removed by autophagy in order to guarantee cell survival. Autophagy can modulate CYP2E1-dependent ethanol toxicity. Inhibition of autophagy increased binge ethanol-induced steatosis in wild type and CYP2E1 knocking mice but not CYP2E1 knockout mice (174).

In vitro inhibition of autophagy in CYP2E1-expressing HepG2 cells increases levels of active JNK that promote liver injury, suggesting that autophagy may also regulate the effects of CYP2E1 on JNK activation (175). CYP2E1 increase the activity of SOD, HO-1 and Nrf2. All of them protect the cells against oxidative stress. In presence of DAS is possible to reduce their expression and also ROS (176).

There is another cytoprotective mechanism that is affect by OS induced by CYP2E1. They are ubiquitious and highly conserved proteins which their function is assistance in the correct folding of nascent and stress-accumulated misfolded proteins, HSPs (177). This kind of protein have been related with ethanol tolerance and neuronal adaptation. Studies have also shown that acute and chronic alcohol induces HSP activation and differentially induces HSP70 and HSP90 to affect inflammatory cytokine production in macrophages (177).

CHAPTER II

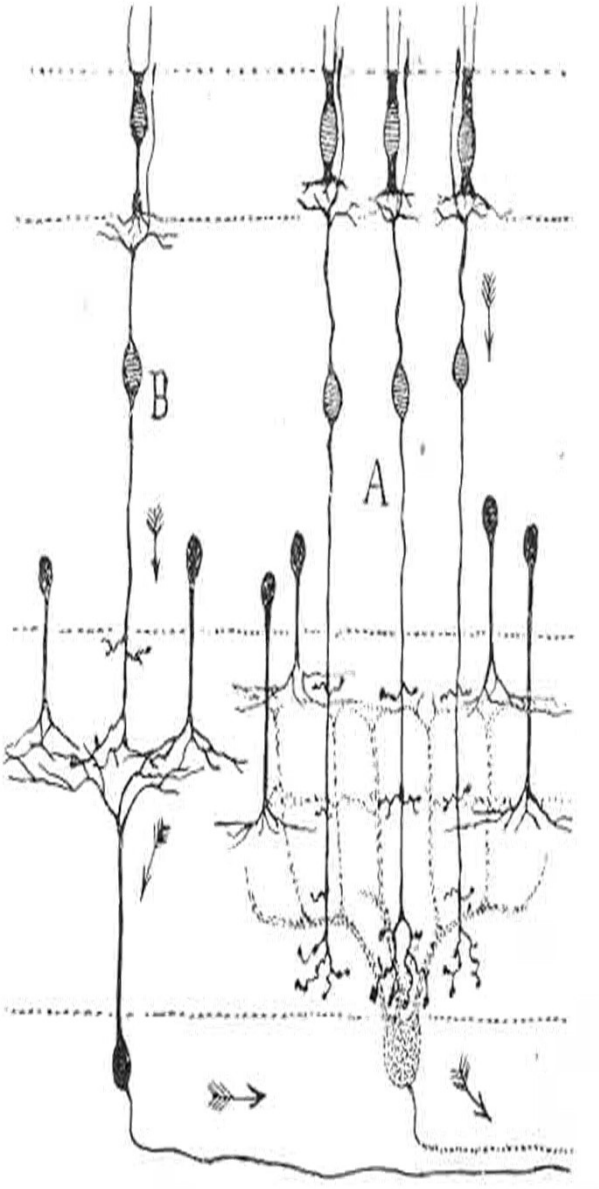

Bird retina

S. Ramón y Cajal

Hypothesis

It is difficult to find studies that directly link the consumption of alcohol with retinal degeneration. There are some that classify different risks factors for retinal diseases prevalence, and at this point alcohol consumption could be one of them. For example heavy EtOH consumption has been associated with elevated intraocular pressure and glaucoma, cataract formation, AMD (178-179). In contrast with that, low or moderate alcohol consumption has a protective role in these same diseases (180).

Oxidative stress plays a crucial role in retinal degeneration and retinal diseases such as RP (113), RD (129) and AMD (48,127). It is also well known that EtOH increases OS production unleashing an inflammatory response (164) with NFKB as the main intermediary (125,126). The implication of CYP2E1 in pathological processes and diseases has been studied not only in EtOH abuse. It has been related with cancer (181), cirrhosis (182), with healthy problems induced by cigarette smoke (183), and also with neurodegeneration (184).

Focusing in ocular diseases, the relationship between ocular diseases and CYP2E1 is really clear; CYP2E1 is involved in visual cycle (24), but surprisingly few studies have been conducted on this respect. It has been described the CYP2E1 presence and participation in blindness caused by methanol poisoning (185), in the pathogenesis of drug-induced retinopathy (186) and in retinal metabolism of ω-3-Polyunsaturated fatty acids (187).

As already described, this enzyme is induced by EtOH, triggering the increase of intracellular ROS (155,157). It has also been described the implications of ROS in the RPE cellular response, loss of function and integrity (107,166) causing retinal degeneration. Taking together all this information, it is plausible to establish the hypothesis proposed herein that, **oxidative stress generated by EtOH could be directly involved in the regulation of CYP2E1 in RPE.**

Objectives

The current study is aimed at producing knowledge concerning mechanisms implicated in vision loss using ARPE-19 cells as in vitro model after EtOH exposure. Nowadays alcohol is one of the most commonly consumed drugs. This problem also increasingly affects young people. Blindness is a terrible disease with huge impacts both socially and economically. Hence, the purpose of this thesis is to find out the pathophysiological mechanisms involved in the deleterious effect of EtOH and EtOH-induced OS on RPE and therefore in vision, that could also help understand this same mechanisms of other retinal diseases.

The general and specific objectives:

1. To evaluate ARPE-19 as a cellular model to study the effects of EtOH on RPE cells:

1.1 To generate primary cell culture of RPE from human tissue (hRPE).

1.2 To generate RPE cell culture from 3D retinal model generated from hiPSC (hiPSC-RPE).

1.3 To generate mature ARPE-19 cells.

1.4 To evaluate the cytotoxicity of EtOH, in RPE all cellular models developed, by XTT cell viability assay.

2. To evaluate the OS dependent cellular response in ARPE-19 cells:

2.1 To study the OS biomarkers expression after acute EtOH exposure by human cell stress array.

2.2 To characterize OS status measuring total of intracellular ROS by DCFH fluorescence and superoxide anions by DHE fluorescence after different EtOH concentrations treatment.

2.3 To relate the generated OS to cell death using XTT and DCFH fluorescence.

3. To study ARPE-19 cell death process:

3.1 To characterize apoptosis activation, depending on EtOH concentration used, by WB using specific apoptosis biomarkers such as Caspase-3, Bax, and Bcl-2.

3.2 To evaluate plasma membrane integrity after EtOH treatment by calcein/EthD-1 fluorescence.

4. To evaluate the RPE barrier function:

4.1 To study the TJ integrity by ZO-1 immunofluorescence (IF) in ARPE-19 cells and TER assay in mature ARPE-19 cells. Using different EtOH concentrations treatment on ARPE-19 cells.

4.2 To characterize the profile of secreted molecules, growth factors and proteins expression under non-lethal EtOH treatment by human proteome profile array.

4.3 To characterize the expression of specific RPE growth factors such as PEDF and VEGF by qPCR and its receptors VEGFR-1 and VEGFR-2 by WB, under non-lethal EtOH treatment.

4.4. To characterize the profile expression of MMPs, under non-lethal EtOH treatment by ELISA.

4.5 To characterize the EtOH-induced NFKB expression modification and activation by IF and WB.

5. To corroborate CYP2E1 expression in all RPE cellular models by WB, IF and PCR using HEPG2 cells as a positive control of its expression.

6. To monitor CYP2E1 induction in ARPE-19 cells:

6.1 To evaluate the time dependent EtOH-induced CYP2E1 expression by qPCR and IF.

6.2 To evaluate the concentration dependent EtOH-induced CYP2E1 expression by qPCR, IF and WB.

6.3 To evaluate the enzymatic CYP2E1 activity induced by EtOH in ARPE-19 microsomes compared with HEPG2 microsomes by HPCL.

7. To study the CYP2E1 implication in RPE cell death:

7.1 To monitor apoptosis activation when CYP2E1 is overexpressed by toxic concentrations of EtOH, measuring Caspase-3, Bax and Bcl-2 by WB in ARPE-19 cells.

7.2 To describe the implication of CYP2E1 in ROS increase after EtOH treatment using DAS like a selective CYP2E1 inhibitor (XTT, DCFH, and HPLC).

7.3 To characterize the EtOH-induced CYP2E1 expression, using DAS to block the EtOH effect, by WB and qPCR.

7.4 To validate the cellular model replicating experiments with EtOH and DAS treatment with hRPE, mature ARPE-19 and hiPSC-RPE (XTT, DCFH, and IF).

8. To demonstrate the CYP2E1 implication in OS cellular response in RPE cells:

8.1 To study the OS biomarkers expression after acute EtOH exposure combined with DAS treatment by human cell stress array in ARPE-19 cells.

8.2 To study the possible NFKB regulation by EtOH-induced CYP2E1 by IF and WB.

9. To investigate the CYP2E1 regulation in RPE cells:

9.1 To validate NAC as an antioxidant using EtOH treatment in ARPE-19 cells to induce cell death and ROS (XTT, DCFH, and DHE).

9.2 To demonstrate that ROS generated by CYP2E1 modulates its self-expression, using DAS and NAC combined with EtOH, (WB).

9.3 To study the possible CYP2E1 regulation by EtOH –induced NFKB (IF and WB)

CHAPTER III

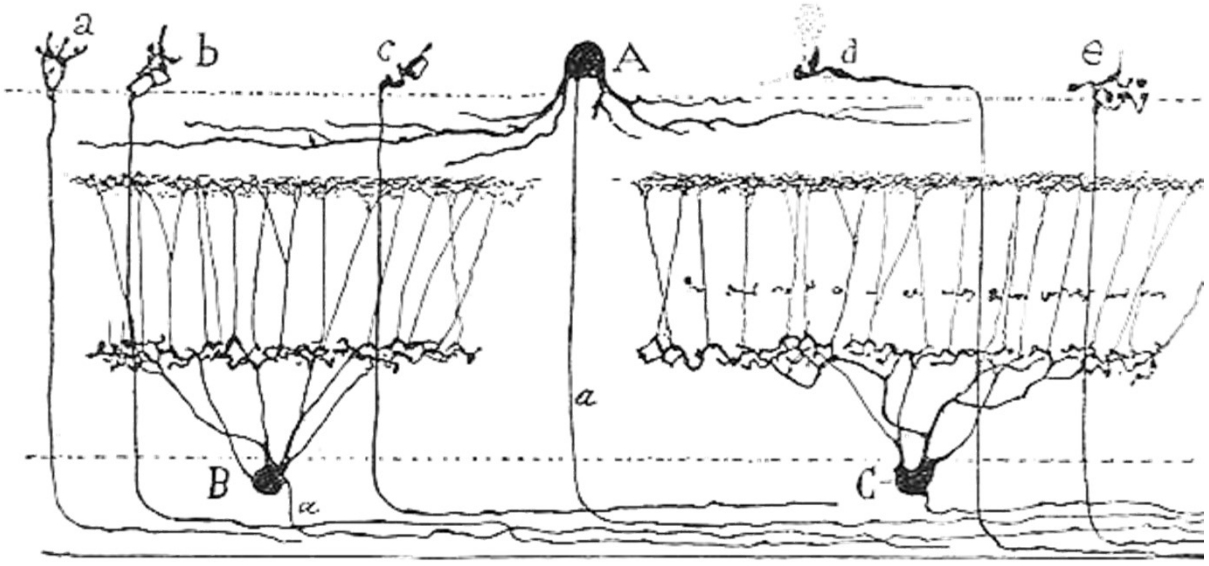

Bird retina ganglion cells

S. Ramón y Cajal

Materials and Methods

1. CELL CULTURE AND TREATMENTS

Human RPE cell line ARPE-19 was cultured according to supplier's protocol (American Type Culture Collection; ATCC) and were used from passages 18 to 20.

Human hepatocellular liver carcinoma (HEPG2-E47) cells were donated generously from the laboratory of Mª Carmen García-Ruiz, PhD (IIBB-CSIC, Barcelona, Spain), and cultured according to supplier's protocol (ATCC). HEPG2 cells were used as a positive control for CYP2E1 experiments (**See figure 1 annexed**).

Human RPE (hRPE) was obtained from human donors at the Fundación Oftalmológica Del Mediterráneo (FOM; Valencia, Spain) according with the Spanish regulations for the handling of human samples. Human RPE cells were isolated by collagenase and trypsin treatment as described previously (188). Briefly, after removal of the neural retina, sheets of RPE cells were washed with sterile phosphate-buffered saline (PBS; Sigma Aldrich) and then incubated with 1% collagenase (Thermo Fisher) in Dulbecco's modified Eagle's medium/nutrient mixture F12 (DMEM/F12; Thermo Fisher) at 37°C and 5% CO_2 for 20 min.

Then, the cells were incubated with trypsin-EDTA solution (Thermo Fisher) in the same conditions as above for 10 min. Finally, cells were recovered by centrifugation and seeded in the same conditions used for ARPE-19 cells. Cells were used from passages 2 to 4. In these passages, cells maintained typical hexagonal morphology, did not lose pigmentation, and all were positively labeled with RPE65, specific RPE marker (**see figure 2 annexed**).

hiPSC-RPE cells were generated in Canto-Soler lab. Starting from RCs generated in this laboratory (52) the RPE tissue is attached at the tip of RCs were microdissected (51) Then, this hiPSC-RPE were seeded, after enzyme digestion with trypsin-EDTA, onto matrigel (Corning) -coated dishes. All hiPSC-RPE procedures were performed under the supervision and assistance of Miguel Flores Bellver PhD from Wilmer Eye Institute (Johns Hopkins University).

ARPE-19 and hRPE cells were cultured in DMEM/F12 supplemented with 5 mM 2-[4-(2-hydroxyethyl)piperazin-1-yl] ethanesulfonic acid (HEPES; Thermo Fisher), 7.5% $NaHCO_3$ (Thermo Fisher), 10% fetal bovine serum (FBS; Thermo Fisher) and 1% penicillin/streptomycin (Thermo Fisher). hiPSC-RPE cells were cultured in DMEM/F12 (3:1) (Invitrogen) supplemented with 2% B27 nutrient (Sigma Aldrich) and 1% penicillin/streptomycin. All cells were maintained at 37°C and 5% CO_2.

ARPE-19 cells and hRPE cells were cultured at a seeding density of 1×10^3 cells/cm^2 as a "common" density. 1×10^5 were used for hiPSC-RPE and ARPE-19 cells as a "high density" condition. After 2 days at 80% of confluence, cells were ready to use. In case of mature ARPE-19 cells, cells were maintained 2 months in the same conditions previously described but reducing serum content in the media to 1% (44). After this time, cells were treated as described below.

Cells were treated for 24 hours at different EtOH (Biosolve, Valkenswaard) concentrations. For CYP2E1 Inhibition, diallyl sulfide (DAS; Santa Cruz), a known selective CYP2E1 inhibitor (161), was added (20 mM in dimethyl sulfoxide [DMSO], 0.1% in all samples) to the culture media without FBS. Moreover, cells were treated with 4 mM of an antioxidant N-acetylcysteine (NAC; Sigma Aldrich) (161). For both drugs, a viability assay was performed to select the used concentration, (**See figure 3 annexed**). Pictures of RPE cells morphology were taken under phase-contrast microscopy (Eclipse Ti; Nikon) to assess the efficiency, correct growth and the effects of drugs treatments into the cells.

2. CELLULAR PASSAGE AND MAINTENANCE

Because RPE are adherent cells, for a subculture to grow them, medium was aspirated, cells were rinsed with PBS. Following, trypsin-EDTA was added and cells were incubated at 37°C for 5 to 10 min for cell detachment.

To discard trypsin solution, a double volume of complete medium was added and cells were centrifuged for 5 min at 500 g. Cells were divided into different flasks at desired density, renewing it with fresh medium the next day.

3. HEAT INACTIVATION OF FETAL BOVINE SERUM

Because FBS is an important supplement of all culture media used, heat inactivation FBS should be strictly monitored and performed using a repeatable procedure. FBS was heated to 56°C for 30 min in a water bath mixing every 10 min. After cooling it to room temperature (RT), FBS was aliquoted and stored at -20°C.

4. COUNTING CELLS

Cells were detached with trypsin-EDTA solution. Pellet was suspended in corresponding medium and counted using a Neubauer haemacytometer (Fisher). 10 µL of cells were mixed with 10 µL of 0.4% trypan blue solution (Thermo Fisher) to make a 1:1 dilution. The cells were counted using the grid on the haemocytometer. The mean number of cells was calculated and multiplied by the dilution factor and then by 10^4 to scale the volume of the haemocytometer (0.1 mm^3) to cells/mL.

5. CELLULAR CRYOGENIC STORAGE

To freeze for future use, cells were detached using trypsin-EDTA as mentioned above. The detached cells were washed with complete medium and pelleted by centrifugation at 1200 xg for 3 min. The supernatant was aspirated and cells were resuspended in cryogenic solution (9:1 FBS: DMSO (v/v); Sigma Aldrich).

Approximately 1.5 x 10^6 cells were transferred with 1 ml cryogenic solution into each cryogenic vial (Thermo Fisher). They were stored in -80°C no more than 48 h into freezer container, then transferred (-150°C) for storage. Cells were thawed at 37°C in a water bath, then transferred to new tubes with complete medium, after that cells were centrifuged at 500 xg for 5 min. The medium was changed with fresh one and cells were placed into desired plate or flask and maintained at 37°C, 5% CO_2. The medium was replaced next day, once cells had attached.

6. XTT ASSAY

Sodium 3´-[1-phenylaminocarbonyl-3,4-tetrazolium]-bis(4-methoxy-6-nitro) benzene sulfonic acid hydrate, (XTT, Cell Proliferation Kit II; Roche) was used to determine cell viability as mitochondrial activity. RPE cells were seeded at 6 × 10^3 per well in a 96-cell culture well plate for 24 h. After washing step (twice with PBS) the XTT labeling reagent was mixed with electron coupling reagent. 0.3 mg/ml of XTT final solution was added to each well and incubated for 6 h at 37°C in 5% CO_2. Then, absorbance was read at 550 nm by microplate reader (Victor, Perkin Elmer). 3 independent experiments were carried out. Results were expressed as percentage relative to the control group.

7. DETERMINATION OF ROS LEVELS

ROS levels were measured by two different fluorescent probes. Using 2-7-dichlorodihydrofluorescein diacetate (H_2DCFDA; Santa Cruz Biotechnology), for the total intracellular ROS. Which is converted to a non-fluorescent derivative (H_2DCF) by intracellular esterases. This molecule can be oxidized by ROS producing intracellular dichlorofluorescein (DCF), which is a fluorescent compound.

The other fluorescent probe used is dihydroethidium, (DHE; Thermo Scientific). Cytosolic DHE exhibits blue fluorescence; however, once this probe is oxidized to ethidium, it intercalates within DNA, staining the cell nucleus a bright fluorescent red. DHE is a superoxide indicator because is oxidized by superoxide anions to 2-hydroxyethidium.

Cells were seeded in a 96 multiwell plate with same density as previously described in XTT assay. Cells were rinsed with PBS twice and then were incubated with 15 µM of H_2DCFDA for 15 min at 37°C. Total intracellular ROS production was measured by fluorescence multiplate reader (Victor X5; Perkin Elmer) excited at 485 nm and read at 530 nm. Pictures were also recorded with fluorescence inverted microscope (Eclipse Ti; Nikon). Images were taken with the assistance of Daniel Pérez Cremades, from University of Valencia.

Superoxide anions were measured by incubating with 5 µM of DHE during 20 min at 37°C. Then with a fluorescence multiplate reader excited at 518 nm and read at 605 nm. Total of 3 independent experiments were carried out for both methods. Results were expressed as percentage relative to the control group.

8. CELL STRESS BIOMARKERS MEASUREMENT

Human Cell Stress Array (R&D Systems) provides a rapid, sensitive tool to simultaneously detect the relative levels of different cell stress-related proteins in a single sample. Briefly, in this assay capture antibodies have been spotted in duplicate on nitrocellulose membranes. According to facture manual, 3 independent ARPE-19 cells protein samples of each treatment group were pooled. Final amount of 100 µg of protein for each experimental group was mixed with biotinylated antibodies and incubated with the array overnight at 4°C with gentle agitation. The next day, after washing step to discard non bounded antibodies, a Streptavidin-HRP solution was incubated 2 h.

Chemiluminescent signal is produced in proportion to the amount of analyte bound. Chemiluminescence was detected in the same manner as in western blot. The

signal intensity was quantified by densitometry using ImageQuant TL (GE) software. Results were expressed as percentage relative to the control group using one of the markers, which was not affected by the treatment, HIF-2α, used as an internal control to standardize the results.

9. VIABILITY/CYTOTOXICITY KIT

The LIVE/DEAD Viability/Cytotoxicity Assay Kit (Molecular Probes, Invitrogen, Thermo Fisher) provides a two-color fluorescence cell viability assay that is based on the simultaneous determination of live and dead cells with two probes that measure recognized parameters of cell viability intracellular esterase activity and plasma membrane integrity.

The polyanionic dye calcein is well retained within live cells, producing an intense uniform green fluorescence in live cells (ex/em 495 nm/515 nm). EthD-1 enters cells with damaged membranes and undergoes a 40-fold enhancement of fluorescence upon binding to nucleic acids, thereby producing a bright red fluorescence in dead cells (ex/em ~495 nm/~635 nm). EthD-1 is excluded by the intact plasma membrane of live cells.

Briefly, cells were seeded in a 96 multiwell plate with same density as previously described in XTT assay. According to manufacturer protocol, cells were rinsed with PBS twice and then were cells were exposed for 30 min to calcein AM, to measures cell viability, and EthD-1, to measure cell death. Afterwards, cells were rinsed again and fluorescence pictures were recorded with ArrayScan VTI HCS Reader (Thermo Scientific) under the supervision and assistance of Natalia Vergara from Wilmer Eye Institute (Johns Hopkins University). Total of 3 independent experiments were carried out. Images showed in results section are a representative pictures.

10. PROTEIN QUANTIFICATION

Protein quantification was carried out with Bicincroninc acid assay kit (BCA; Thermo Scientific). This method mainly depends on an alkaline medium, the peptide bonds of the proteins reduce Cu^{2+}. The Cu^{+} ions produced, bind to two molecules of BCA and in doing so, they change the structure, so that it now absorbs light at 562 nm and appears purple.There is proportionality between color intensity and protein concentration.

To establish this relationship a known concentration of bovine serum albumin (BSA; Thermo Fisher) was used for standard curve. The absorbance was measured at 550 nm with Victor X5 multilabel plate reader. Finally the samples absorbance values was calculated using standard curve where the protein concentration of each unknown sample was determined.

11. WESTERN BLOT (WB) ANALYSIS

This technique, SDS-PAGE mode, allows separating the proteins under denaturing and reducing conditions allowing proteins to migrate only according to their molecular weight. For protein isolation, cells were scraped with ice-cold PBS and lysed with RIPA buffer (Sigma Aldrich) containing 50 mM Tris-HCl, pH 8.0, 150 mM sodium chloride, 1.0% Igepal CA-630 (NP-40), 0.5% sodium deoxycholate, 0.1% sodium dodecyl sulfate and Protease Inhibitor Cocktail (Sigma Aldrich).

Samples were sonicated 3 pulses during 10 seconds spacing after each pulse the samples on ice to avoid the protein degradation. The supernatant (proteins), after 20 min at 4°C centrifugation, was collected.

For sample preparation, to equal amount of protein (25 mg) was added sample buffer with sodium dodecyl sulfate (SDS) and β-mercaptoethanol (**See table 3, below**). SDS acts breaking non-covalent bonds in the proteins, denaturing them and, by providing them with negative charge. β-mercaptoethanol, break the disulfide bonds, glycerol increases density and bromophenol blue gives blue color to the buffer. Later, samples were heated to 96 °C during 10 min to promote the denaturalization.Each sample was migrated on acrylamide/bisacrylamide (29:1; Thermo Fisher) gels. Gels were made manually using two acrylamide proportions. 4% acrylamide/bisacrylamide for stacking part of the gel and 12% for the resolving (the bottom part of the gel) (**See table 3, below**). Gels were prepared with SDS also. The acrylamide polymerization is catalyzed by the addition of (10 µl) N,N,N,N´-tetrametilen-diamina (TEMED; Sigma Aldrich) and (100 µl) 10% fresh ammonium persulfate (APS; Sigma Aldrich), to both stacking and resolving solution with acrylamide.

After electrophoresis, samples were electroblotted onto polyvinylidene difluoride membranes (PVDF; Millipore) by wet transfer with specific buffer (**See table 3, below**). Subsequently membranes were blocked with blocking buffer (**See table 3, below**) during 30 min at RT. The antibody incubation was the next step. For this, the same buffer was used overnight at 4°C, with the addition of the specific antibody (**See table 4, below**). To corroborate the successful blotting, gels were stained with coomassie blue solution (Thermo Fisher).

To discard excess antibody, membranes were washed 3 times with T-TBS, after incubation. Subsequently, membranes were incubated 2 hours at RT with secondary antibodies horseradish peroxidase-conjugated (HRP; Dilution 1:10,000) prepared in T-TBS. A stripping solution (Roche) was used, according to manufacturer's protocol, to eliminate the attached antibodies in order to reuse the membranes.

Finally, the same antibody wash process mentioned before was applied. Bands were visualized with ECL (Pierce, Thermo Fisher) and detected with Image Quant LAS-4000 mini (GE Healthcare). Protein levels were quantified by densitometry using ImageJ software (National Institutes of Health). Protein expression intensity was normalized to β-Actin or α-Tubulin. Total of 3 independent experiments were carried out. Results were expressed as percentage relative to the control group.

12. IMMUNOFLUORESCENCE (IF)

After desired treatment, cells were rinsed 3 times with PBS during 5 min each. For fixing step, 2 different compounds were used; in case of NFKB antibody the fixation agent used was methanol during 20 min at -20°C. Additionally a positive control of P65 NFKB nuclear translocation was used, ARPE-19 cells were exposed to 100 mM of H_2O_2 (**See figure 4 annexed**).

The fixation method for the rest of antibodies was at RT during 10 min with 4% Paraformaldehyde (PFA) in PBS. Then, samples were rinsed with PBS as mentioned before. Subsequently, samples were blocked in blocking solution (**See table 3, below**) during 1h at RT. After a washing step, were incubated with primary antibody in the same blocking solution reducing the FBS at 1%. The specific antibodies were incubated overnight at 4°C (**See table 4, below**). Afterward, cells were rinsed 3 times with PBS and incubated with fluorescent-conjugated secondary antibodies Alexa Fluor 555 and Alexa Fluor 488 (Dilution 1:500; Molecular Probes, Invitrogen, Thermo Fisher) for 2 h at RT.

Finally, F-Actin staining cells were incubated with Alexa Fluor 568 conjugated phalloidin (Thermo Fisher) during 10 min according to manufacturer's protocol. At the same time, for DNA staining, cells were incubated with 4,6-diamidino-2-phenylindole (DAPI; Sigma Aldrich). After washing step, fluorescence images were recorded with fluorescence inverted microscope (Eclipse Ti; Nikon).

Images were taken with the assistance of Daniel Pérez Cremades from University of Valencia. Images were processed with Image J software (National Institutes of Health). Total of 3 independent experiments were carried out. Results were expressed as percentage relative to the control group. Images showed in results section are a representative pictures.

13. TER MEASUREMENT

TER was measured with STX2/chopstick electrodes in mature ARPE-19 seeded in a transwell permeable inserts under the supervision and assistance of Marisol Cano PhD, from Wilmer Eye Institute (Johns Hopkins University). The total electrical resistance includes the ohmic resistance of the cell layer R_{TER}, the cell culture medium R_M, the semipermeable membrane insert R_I and the electrode medium interface R_{EMI} (46) (**See figure 5 annexed**). To calculate the total TER blank measure (well without cells) was taken into account. Values were obtained from 3 independent experiments.Results were expressed as percentage relative to the control group.

14. REVERSE TRANSCRIPTION POLYMERASE CHAIN REACTION (RT-PCR) AND QUANTITATIVE RT-PCR (qRT-PCR)

hRPE tissue, ARPE-19, hRPE, HEPG2-E47 and hiPSC-RPE cells were incubated in RNA Protect (Qiagen, Hilden, Germany) to attenuate endogenous RNAse activity and mRNA synthesis, and scraped off the plate into a 1.5 mL tube. Cells then were centrifuged at 2,500 xg for 10 min and the pellet was resuspended in buffer RLT plus (RNeasy Plus Micro/Mini Kits; Qiagen) with 2-mercaptoethanol (1:100; Sigma Aldrich). RNA was harvested from the cells according to manufacturer's protocol (RNeasy Micro/Mini Kits; Qiagen). RT-PCR reactions were performed with SuperScript III First-Strand Synthesis System (Life Technologies, Thermo Fisher) Gene-specific primers used are in **table 5, below.**

The amplified PCR products were electrophoresed on 1.6% (v/v) agarose gel prepared in with Tris/Borate/EDTA buffer (TBE), stained with Real Safe at 90 V for 35 min. The same TBE was used like running buffer. Following electrophoresis, the agarose gel was exposed to UV light to visualize DNA.

For qRT-PCR, reactions were performed with Sybr Green Supermix (Applied Biosystems) and a LightCycler 480 II (Roche). Reactions of RT-PCR were run at either 30 or 35 cycles, and all qRT-PCRs reactions were run at 40 cycles. Samples were run in triplicate. X-fold change in mRNA levels was determined by applying $2-\Delta\Delta CT$ method.

ΔCt values were calculated using endogenous control genes: β-Actin and GAPDH. The geometric mean of both reference genes was used to standardize the results. Total of 3 independent experiments were carried out. Results were expressed as percentage relative to the control group.

15. ANGIOGENESIS AND INFLAMMATION BIOMARKERS MEASUREMENT

Human Angiogenesis Antibody Array (R&D Systems) provides a rapid, sensitive tool to simultaneously detect the relative levels of angiogenesis and inflammation-related proteins in a single sample. Analytes include soluble growth and differentiation factors, ECM components, proteases, receptors, and signaling molecules.

As previously described in ROS biomarkers measurement, this array was carried out according to facture manual, 3 independent ARPE-19 cells protein samples of each EtOH treatment group were mixed as a pull. Final amount of 100 µg of protein was assayed using basic FGF, as an internal control to standardize the results.

16. MMPs ELISA

The determination of MMPs (MMP-1, MMP-2, MMP-3, MMP-7, MMP-8, MMP-9 and MMP-13) quantitatively was carried out by an ELISA kit, Mosaic ™ ELISA Human MMP Panel, (R & D Systems).

According to the manufacturer, the cellular supernatants (treatment culture medium) of the ARPE-19 cells were collected. The kit has a 96-well plate, each containing the 7 antibodies for each MMP.

The same amount of sample was deposited in a well containing fixed specific capture antibodies for each MMP. At the same time a standard curve of each MMP has been made. After washing step to eliminate non fixed material the well was then washed and HRP-conjugated detection antibodies were added to each well to form the "Sandwitch" (Antibody capture-MMP-Antibody-HRP).

Finally chemiluminescent signal was detected by CCD camera (ImageQuant LAS 4000 Mini, GE). Signal intensity was quantified by densitometry using the ImageQuant

TL (GE) software. Samples MMPs concentration values were calculated using each standard curve. Total of 3 independent experiments were carried out. Results were expressed in pg/ml and as percentage relative to the control group.

17. MICROSOME ISOLATION

Microsomes from ARPE-19 and HEPG2 cells were prepared with minor modifications as described previously (189). The protocol used was developed for hepatocytes, for this reason HEPG2 cells were used as a positive control. Briefly, 0.05 xg of cells were homogenized in 100 µL homogenization buffer (**See table 3, below**) with protease inhibitor cocktail. First, the homogenate was centrifuged at 600 xg for 3 min at 4°C). The supernatant was transferred carefully to clean centrifuge tubes, diluted 2-fold with distilled water, and centrifuged again at 21,000 xg for 2 hours at 4°C. The pellet was washed in 150 µL of wash buffer (**See table 3, below**) with protease inhibitor cocktail and centrifuged once more at 21,000 xg for 45 min at 4°C. The pellet then was resuspended in 100 µL of activity assay buffer (**See table 3, below**) and stored at −80°C until further use.

18. CYP2E1 ACTIVITY ASSAY

Activity assay of CYP2E1 was determined by quantification of 4-nitrocatechol (4NC) formation (190) under the supervision and assistance of Daniel Lopez-Malo PhD, from Catholic University of Valencia. Preliminary experiments were conducted to determine linear metabolite formation kinetics with respect to time and microsomal protein concentration (**See figure 6 annexed**).

Microsomal incubation mixtures consisted of 100 µM p-nitrophenol (PNP; Acros Organics), activity assay buffer, cofactor-generating system (**See table 3, below**), and 2 mg of microsomal protein in activity assay buffer at final volume of 0.5 mL. That amount of microsomes provides a good compromise microsome preparation time vs. activity observed. After a preincubation period of 1 minute at 37°C, the reaction was started by addition of microsomal protein and incubated at 37°C for 4 h mixing gently (to avoid microsomes precipitation) in a Thermomixer comfort (Eppendorf). The reaction was finished by addition of 20% ice-cold trichloracetic acid (TCA; Sigma) and centrifuged at 10,000 xg for 5 min at 4°C. Metabolite formation rate was calculated using known concentrations of 4NC (Acros Organics, Thermo Fisher) as calibration standards (0 –1000 nM) and dividing the amount of the metabolite formed by the incubation time and microsomal protein content (nmol/min.mg).

To be sure that DAS concentration used blocked CYP2E1 activity, an inhibition assay was carried out. 2 mg of isolated ARPE-19 microsomes were used as described above with 2 different DAS concentrations; 10 mM and 20 mM, to quantify 4NC formation, (**See results, figure 29D, chapter 4**) A blank test by thermal denaturalization of the enzyme by heating it at 95 °C during 10 min was carried out. There is not appreciate signal at the 4NC retention time (**See figure 7A annexed**). A thoroughly study of a wide range of time and amount of microsome were done. There is an unambiguous peak 4NC retention time (tR = 3.27 min) (**See figure 7B annexed**).

The quantification of the metabolite formed was assayed by HPLC (**See figure 7C annexed**) using a 1200 series chromatographic system (Agilent Technologies) equipped with a quaternary pump, automatic injection system, and a DAD UV-Vis detector. A Zorbax Eclipse Plus C-18 column (4.6 × 150 mm, 3.5 µm particle size; Agilent Technologies) was used, operated at room RT. Experimental conditions were based on previous reports (191, 192) absorbance was monitored at 334 nm. The mobile phase, delivered at a flow rate of 1.5 mL/min, consisted of 25% ACN, 0.1% TCA, and 74.9% Milli-Q water. The injection volume was 100 µL, the retention time for PNP was 3.27 min. The total running time was 8 min.

To corroborate our data the disappearance of the substrate (PNP) was also monitored (**See figure 7D annexed**).Total of 3 independent experiments were carried out.

19. STATISTICAL ANALYSIS

Statistical analyses were performed by using Prism 5.04 software (GraphPad, San Diego, CA, USA), by means of 1- and 2-way ANOVA, and Student's *t*-test. Statistically significant differences were set at $P<0.05$.

TABLES:

Table 3. Buffers composition

BUFFER	COMPOSITION
5x Sample Buffer (WB)	10% SDS, 25% 2-mercaptoethanol, 50% glycerol, 0.01% bromophenol blue, 0.5 M Tris-HC, pH 6.8
Stacking Buffer (WB)	0.5 M Tris-HCl, 10% SDS, 4% Acryl/Bis pH 6.8
Resolving Buffer (WB)	1.5 M Tris-HCl, 10% SDS, 12% Acryl/Bis pH 8.8
Running Buffer (WB)	25 mM Tris-HCl, 190 mM glycine, 0.1% SDS; pH 8.3
Transfer Buffer (WB)	20% Methanol Running Buffer, pH 8.3
TBS	20 mM Tris, 150 mM NaCl pH 7.5
T-TBS	20 mM Tris, 150 mM NaCl, 0.1% Tween 20 pH 7.5
Blocking Buffer (WB)	3% BSA, in T-TBS
Blocking Buffer (IC)	5% of FBS, 0.3% Triton X-100 in PBS
TBE	0.1 M Tris, 0.09 M boric acid, 0.001 EDTA pH 8
Homogenization buffer (MI)	100 mM Tris-HCl buffer, 5 mM KCl, 1 mM DTT, 10 mM EDTA, 5% glycerol, 25% sucrose pH 7.5
Wash Buffer (MI)	20 mM Tris-HCl, 5 mM EDTA pH 7
Activity assay buffer (CA)	50 mM potassium phosphate buffer pH = 6.8
Cofactor generation system (CA)	1.3 mM NADP, 3.3 mM D-glucose-phosphate, 3.3 mM MgCl2; $4x10^{-4}$U D-glucose-6-phosphate dehydrogenase in 0.05 mM sodium citrate

MI: Microsome isolation; **CA**: CYP2E1 activity

Table 4: Antibodies specifications

APPLICATION	NAME	DILUTION	DISTRIBUTOR
WB	**Caspase-3**	1:500	Santa Cruz Biotech
WB	**Bax**	1:250	Santa Cruz Biotech
WB	**Bcl-2**	1:500	Santa Cruz Biotech
WB	**VEGFR-1**	1:250	Abcam
WB	**VEGFR-2**	1:250	Abcam
WB/IC	**CYP2E1**	1:250	Abcam
WB/IC	**P65 NFKB**	1:250/1:200	Santa Cruz Biotech
WB	**β-Actin**	1:500	Santa Cruz Biotech
WB	**α- Tubulin**	1:500	Santa Cruz Biotech
IC	**RPE65**	1:200	Abcam
IC	**ZO-1**	1:200	Abcam

Table 5. Primer sequences

NAME	FORWARD SEQUENCE	REVERSE SEQUENCE
β-Actin	5'-CATGTACGTTGCTATCCAGGC-3'	5'-CTCCTTAATGTCACGCACGAT-3'
GAPDH	5'-TGAAGGTCGGAGTCAACGGAT-3'	5'-TTCTCAGCCTTGACGGTGCCA-3'
CYP2E1	5'-CCTACATGGATGCTGTGGTG-3'	5'-TGGGGATGAGGTATCCTCTG-3'
VEGF	5'-AGGAGGAGGGCAGAATCATCA-3'	5'-CTCGATTGGATGGCAGTAGCT-3'
PEDF	5'-AACCTTACAGGGGCAGCCTT-3'	5'-TGAGGGACACAGACACAGGG-3'

CHAPTER IV

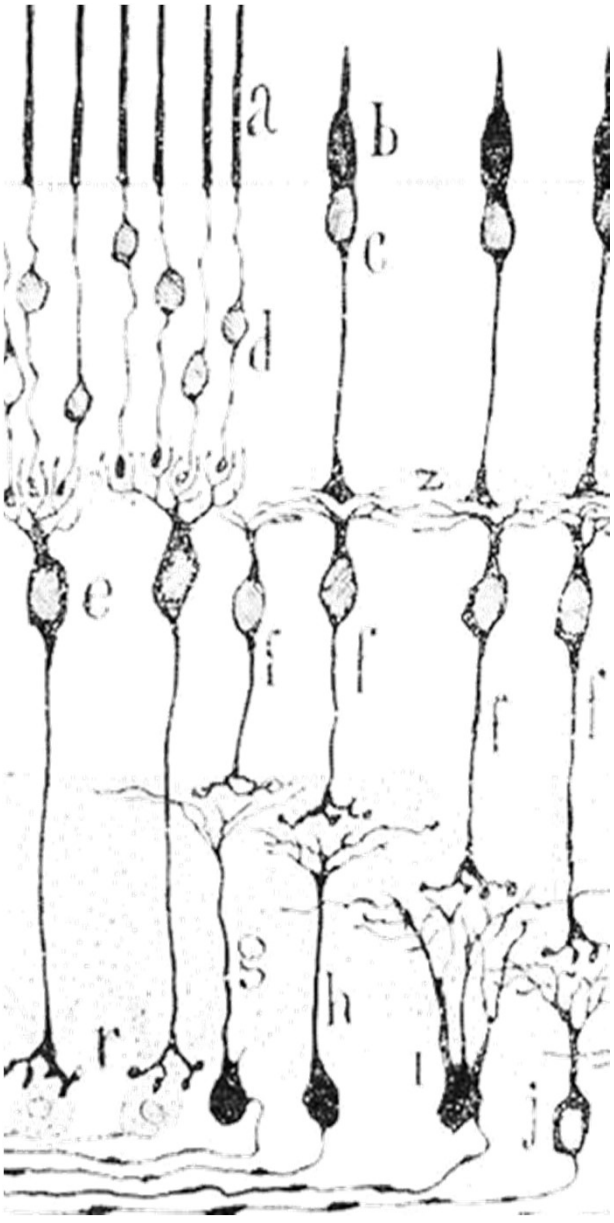

Mammals retina

S. Ramón y Cajal

Results

1. EtOH INDUCES SIMILAR CYTOTOXICITY PATTERN IN DIFFERENT RPE CELLS

24 hours after different EtOH concentration treatments, ARPE-19 cells presented high resistance to EtOH toxicity. It was necessary 600 mM EtOH to find a significant cell death compared with control group (CTL), (p. value < 0.01), **figure 14A**. Besides, 1200 mM EtOH, was unable to reach the median lethal dose (LD 50), only 40% of cell viability was significantly decreased (p. value < 0.001).

On the other hand, hRPE presented less resistance to EtOH toxicity. Significant differences on cell viability can be found at 400 mM EtOH compared with CTL, **figure 14B**. However, cell death rate was similar than ARPE-19 cells at the same EtOH concentrations. As seen in **figure 14A and 14B**, hRPE cell viability at 800 mM and 1200 mM EtOH were 82% and 59% respectively. ARPE-19 cells showed 80% and 64% respectively.

In order to check hRPE cells resistance to EtOH toxicity, these cells were compared with mature ARPE-19 cells (**see the procedure on materials and methods, chapter 3**). After 24 hours of 200 mM EtOH, mature ARPE-19 cells showed significant toxicity, compared with non-treated cells, (p. value < 0.01), **figure 14C**. As previously shown, the same cell response was observed when 800 and 1200 mM EtOH were compared.

The **figure 14D** shows how EtOH toxicity promotes the same cell viability profile in all the cellular models. Significant differences were found at 1200 mM EtOH when compared mature ARPE-19 cells versus immature ARPE-19 cells (p. value < 0.05).

Finally ARPE-19 cells were compared with a novel model of RPE cells, RPE derived from hiPSC (**see the procedure on materials and methods, chapter 3**). Cells were treated, as described before.

Taking into account that hiPSC-RPE cells need different seeding density, ARPE-19 cells were seeded at same conditions. Significant differences at 400 mM EtOH were observed in ARPE-19 cells seeded at high density, (20% of cell death, p. value < 0.05) compared to CTL group. By contrast, hiPSC-RPE cells were more resistant, **figure 15B**. Significant differences in cell death values were found at 800 mM EtOH (20% of cell death, p. value < 0.00001).

200 mM EtOH did not promote same cytotoxic response in ARPE-19 and hiPSC-RPE cells, **figure 15C**. hiPSC-RPE cells were more resistant than ARPE-19 cells under higher ethanol concentration conditions.

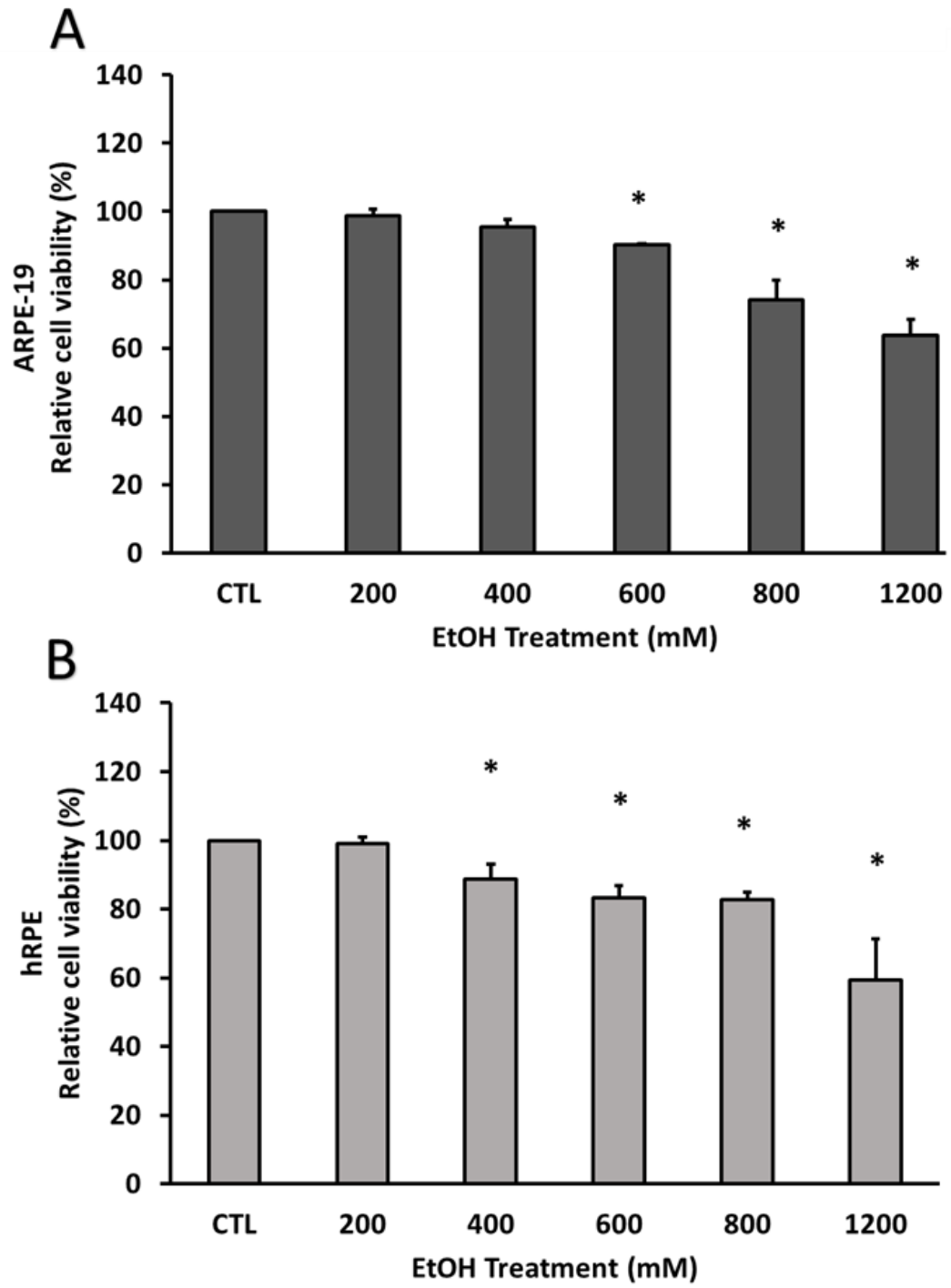
A
ARPE-19
Relative cell viability (%)
140
120
100
80
60
40
20
0
*
*
*
CTL
200
400
600
800
1200
EtOH Treatment (mM)
B
hRPE
Relative cell viability (%)
140
120
100
80
60
40
20
0
*
*
*
*
CTL
200
400
600
800
1200
EtOH Treatment (mM)

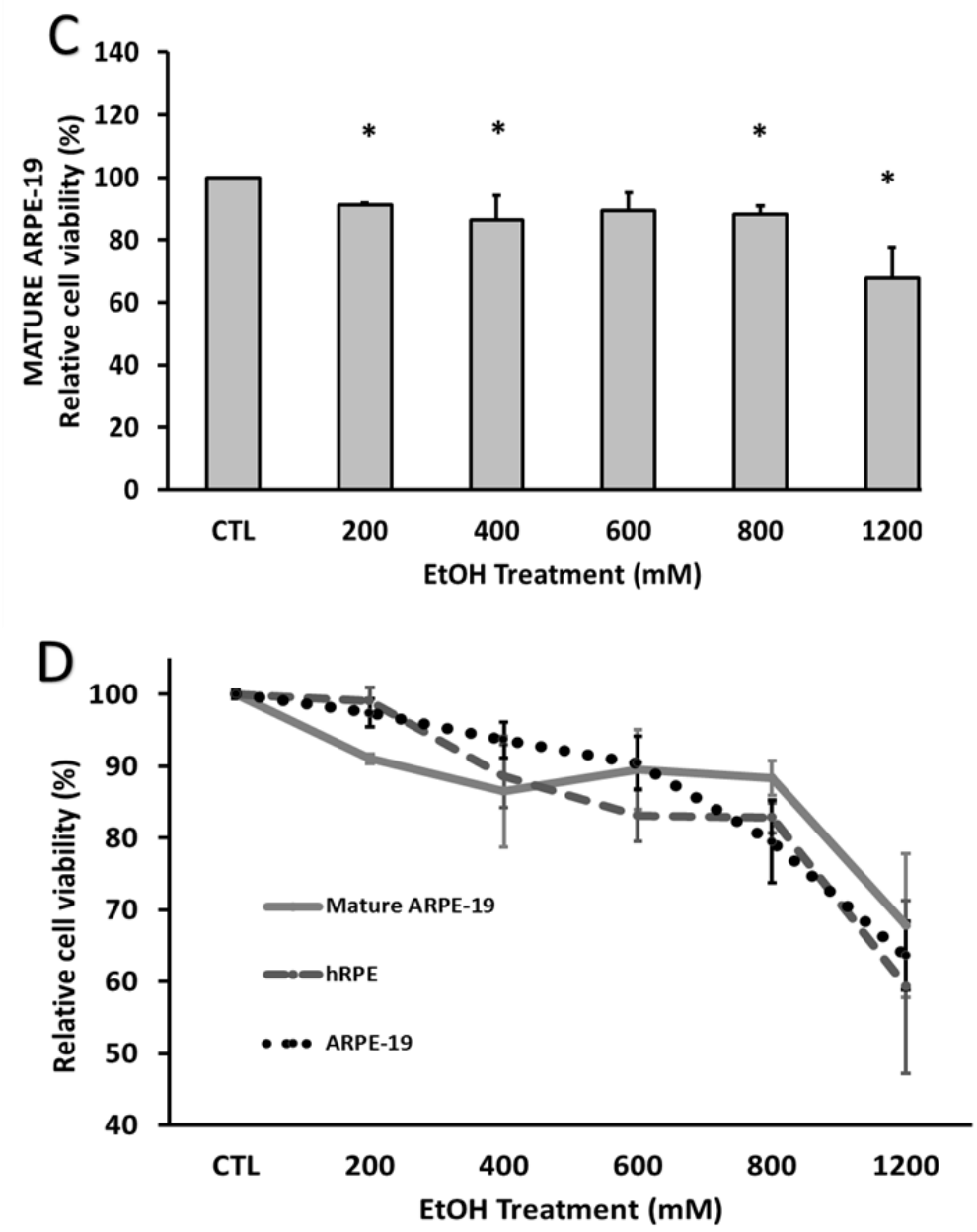

Figure 14. Cell viability in different RPE cell types and culture conditions. The cell viability assay were performed by XTT after 24 h of increasing EtOH concentrations treatment. ARPE-19 cells presented a high resistance to the toxic effect of EtOH (**A**). hRPE cells presented less resistance (**B**) and very similar behavior showed mature ARPE-19 cells (**C**). The same trend was observed comparing the three types of cells (**D**). Values are expressed as mean ± SEM (N=3). Statistical significance was determined by means of 1-and-2-way ANOVA, and Student's t-test. Statistically significant differences were set at *p<0.05 vs. CTL group.

After finding these differences, a comparison of cytotoxicity was carried out between hiPSC-RPE and the other studied cells. Figure **15D** shows that mature ARPE-19 cells response was more similar to hiPSC-RPE than immature ARPE-19 cells at high seeding density. Interestingly, the same response was found in hRPE cells, **figure 15E**. However, ARPE-19 at low seeding density showed the greatest similarity to hiPSC-RPE, **figure 15F**.

Finally, it is noticeable that cell seed density affects the cellular response to EtOH. High density ARPE-19 seeded cells, were less resistant to EtOH compared to low density ones, **figure 15G**. In addition there was a significant difference at 600 mM EtOH (p. value < 0.01). After considering these results, immature ARPE-19 cells seeded at low density were used to study EtOH-induced toxicity.

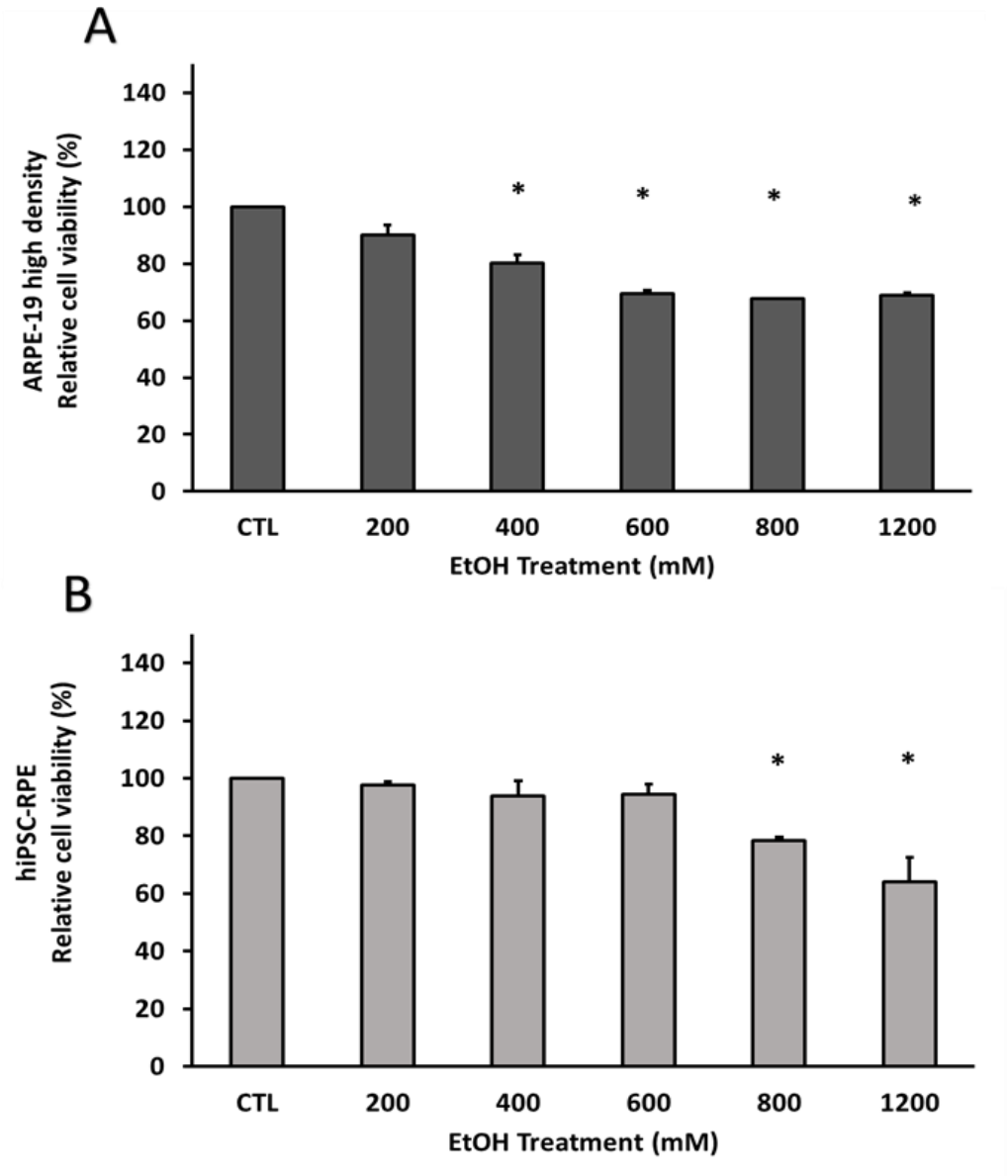

C

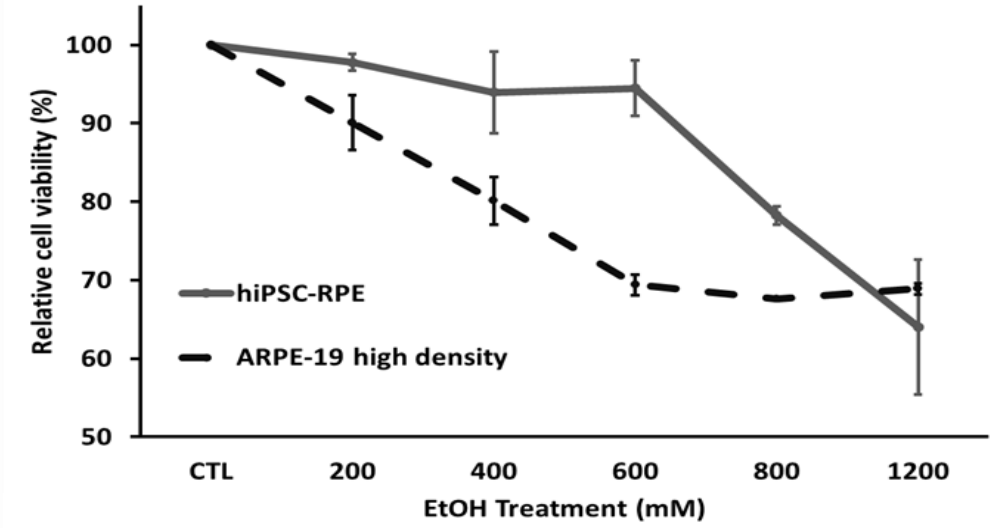
100
90
80
70
60
50
Relative cell viability (%)
hiPSC-RPE
ARPE-19 high density
CTL
200
400
600
800
1200
EtOH Treatment (mM)

D

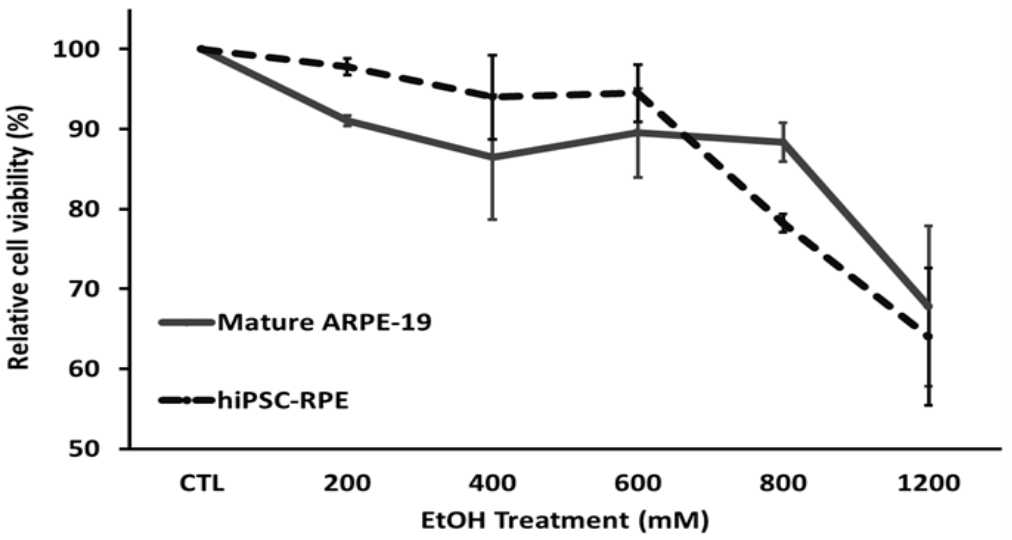
100
90
80
70
60
50
Relative cell viability (%)
Mature ARPE-19
hiPSC-RPE
CTL
200
400
600
800
1200
EtOH Treatment (mM)

E

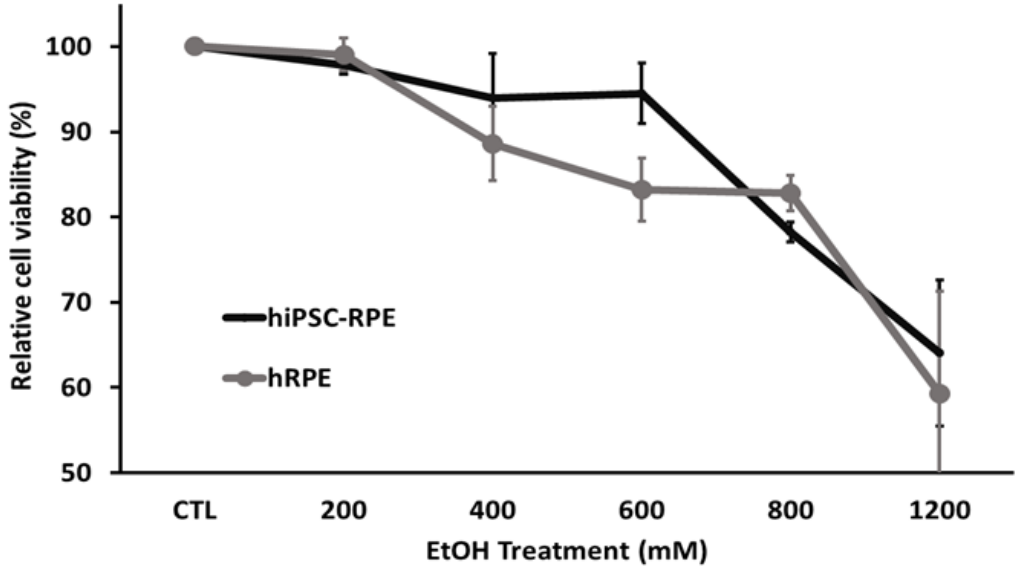
Relative cell viability (%)
100
90
80
70
60
50
hiPSC-RPE
hRPE
CTL
200
400
600
800
1200
EtOH Treatment (mM)

F

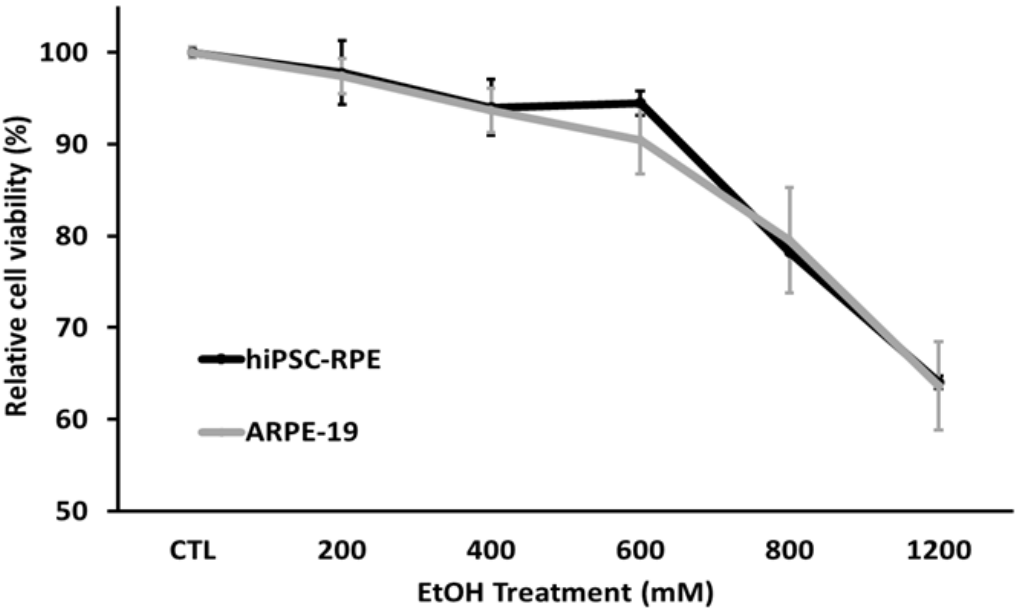
Relative cell viability (%)
100
90
80
70
60
50
hiPSC-RPE
ARPE-19
CTL
200
400
600
800
1200
EtOH Treatment (mM)

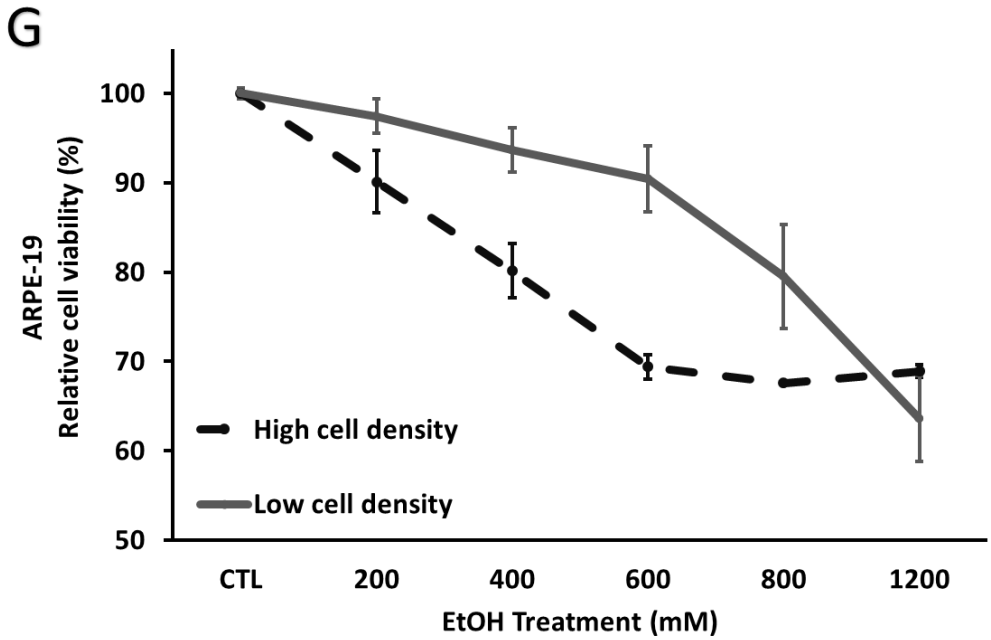

Figure 15. RPE-hiPSC cells as a RPE cell line. The cell viability assay by XTT after 24 h of EtOH treatment. ARPE-19 cells presented a lower resistance to EtOH (**A**). hiPSC-RPE cells presented more (**B**). The difference is showed in a comparative cell viability curve (**C**). Mature ARPE-19 (**D**) and hRPE were studied also (**E**). hiPSC-RPE and ARPE-19 comparative curve (**F**). Low vs. high cell seeding density of seeding in ARPE-19 cells (**G**). Values are expressed as mean ± SEM (N=3). Statistical significance was determined by means of 1-and-2-way ANOVA, and Student's t-test. Statistically significant differences were set at *p<0.05 vs. CTL group.

2. EtOH ACTIVATES A ROS DEPENDENT CELLULAR RESPONSE IN RPE CELLS

2.1. EtOH MODIFIES CELL STRESS BIOMARKERS EXPRESSION

The cell stress array revealed that 1200 mM EtOH induced changes in the expression of cell stress biomarkers in ARPE-19 cells, **figure 16**.

Surprisingly, some of the cell stress biomarkers were increased or decreased after EtOH challenge. CA9, CYT-C, HSP60 and P-JNK PAN were increased, **figure 16A**. Whereas, CITED-2, SIRT-2, P21/CIP1, HIF-1α, P27, p-P53 and PON2 (Paraoxonase/arylesterase 2) decreased, **figure 16B**. It should be noted that increased cell stress markers, CYT-C and HSP60, are involved in mitochondrial maintaining function. Additionally, CA9 and P-JNK PAN, are both implicated in cellular stress activation pathway (**Figure 16A**). In contrast, the survival-related biomarkers P21 and SIRT-2, were decreased (**Figure 16B**).

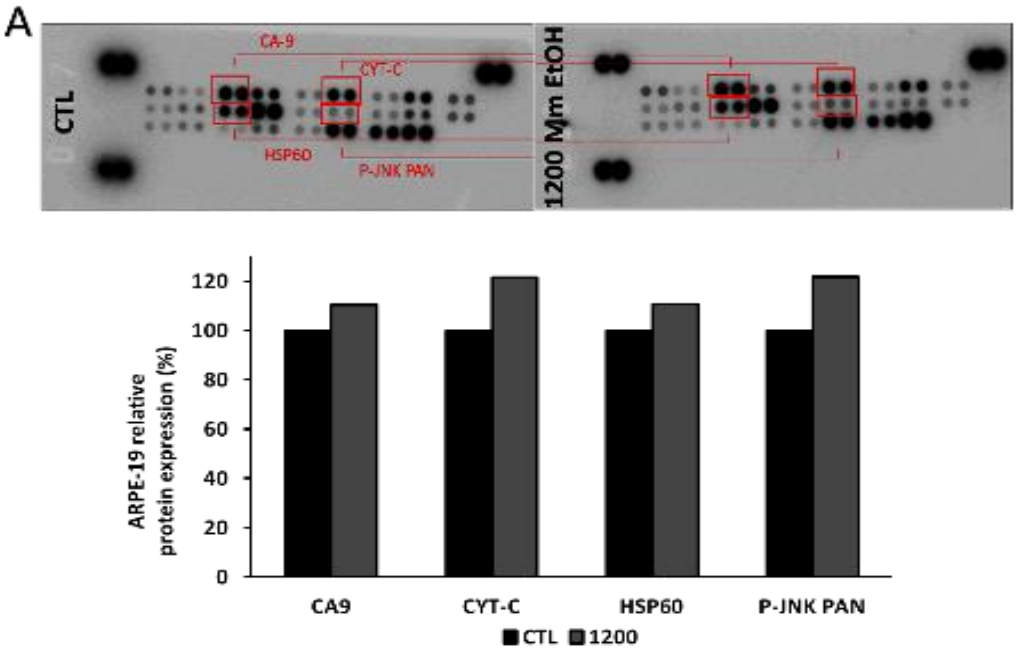

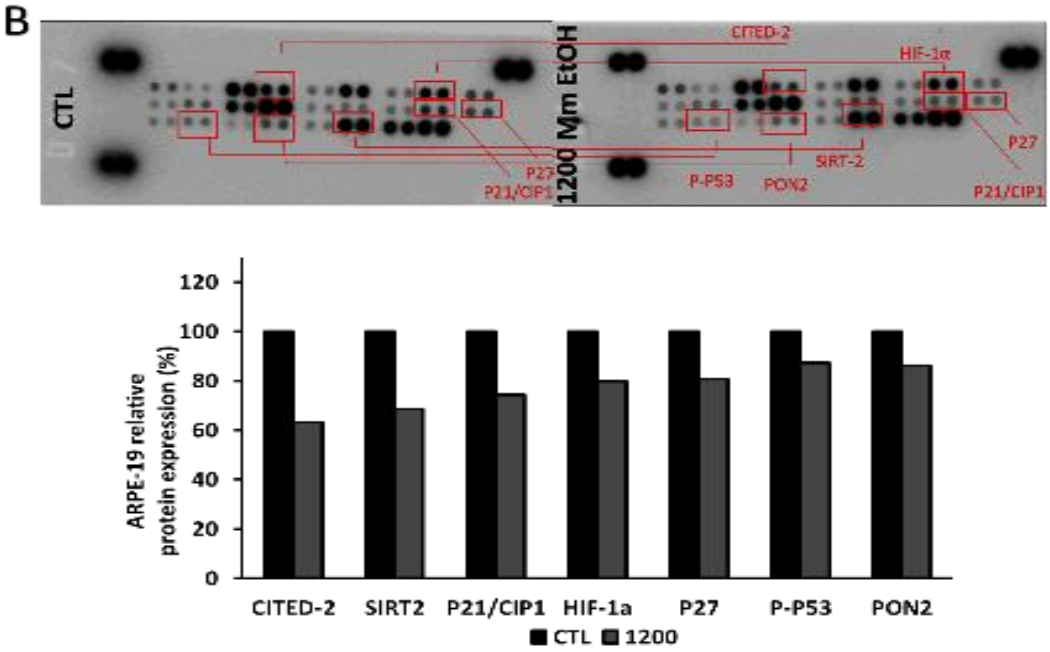

Figure 16. ARPE-19 cell stress profile after EtOH treatment. After 24 hours of EtOH treatment, the ARPE-19 cell survival and stress markers profile was increased (**A**) or decreased (**B**) depending on the concentrations used. Values are expressed as average of an N= 3 pooled samples.

2.2. EtOH INDUCES ROS PRODUCTION IN A CONCENTRATION DEPENDENT MANNER

After considering previous results indicating that RPE cells are resistant to OS, the intracellular ROS production was measured as the same conditions of EtOH treatment during 24 h, **figure 17.** EtOH treatment significantly increased intracellular ROS in a concentration dependent manner in ARPE-19 cells, **figure 17A**. The quantification indicates that DCFH fluorescence levels were significantly increased (p. valor < 0.05) in all treated groups compared to non-treated group. This fact reflects the 'redox state' of the cell, **figure 17B**. On the same way, **figure 17C** shows this significant increase of ROS in hRPE cells under EtOH treatment.

Fitting with this, significant increases of superoxide anions (measured with DHE), were also observed. All EtOH treated groups increased the amount of superoxide anions in a dose-dependent manner, **figure 17D**. Superoxide anions are significantly increased in EtOH-treated groups, **figure 17E**. The positive correlation (R^2=0.887) represented in **figure 17F** confirm the relationship between the increase of OS and cell death.

A

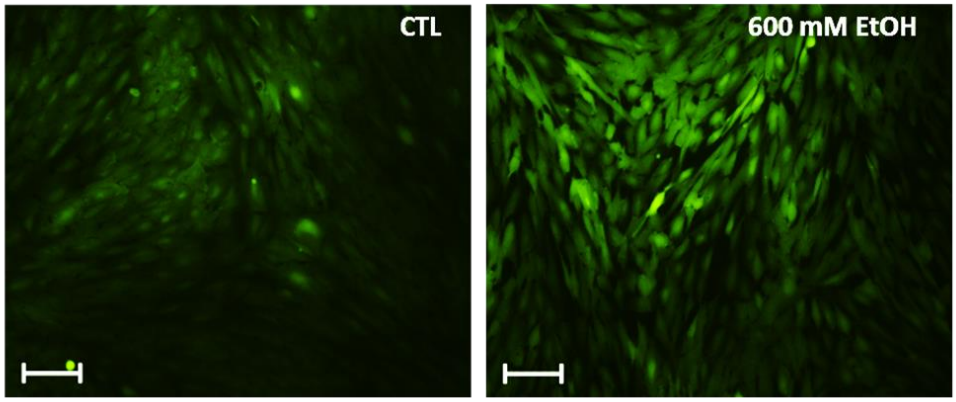
CTL
600 mM EtOH

B

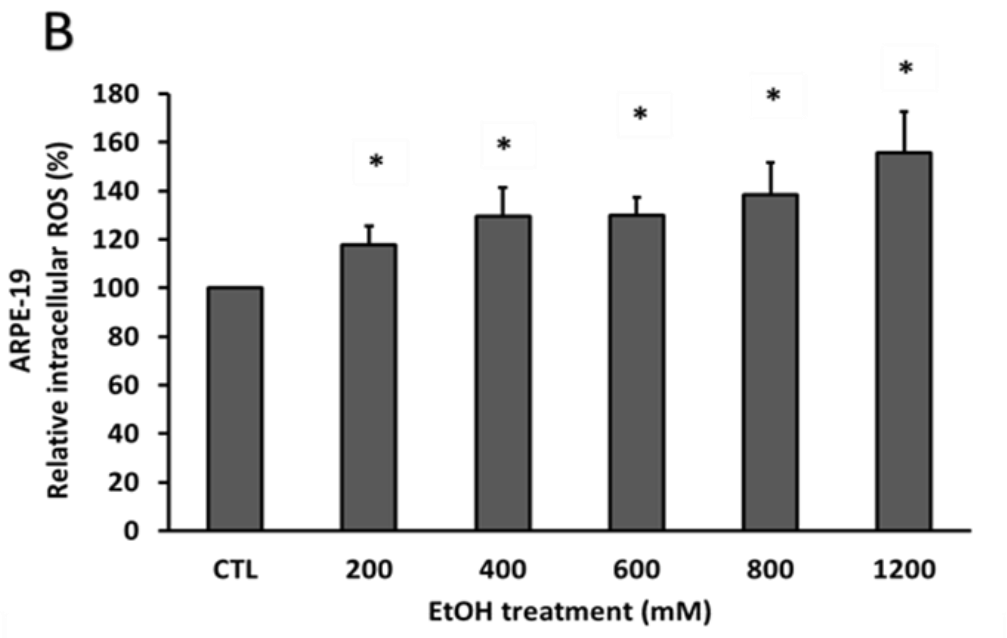
ARPE-19
Relative intracellular ROS (%)
180
160
140
120
100
80
60
40
20
0
*
*
*
*
*
CTL
200
400
600
800
1200
EtOH treatment (mM)

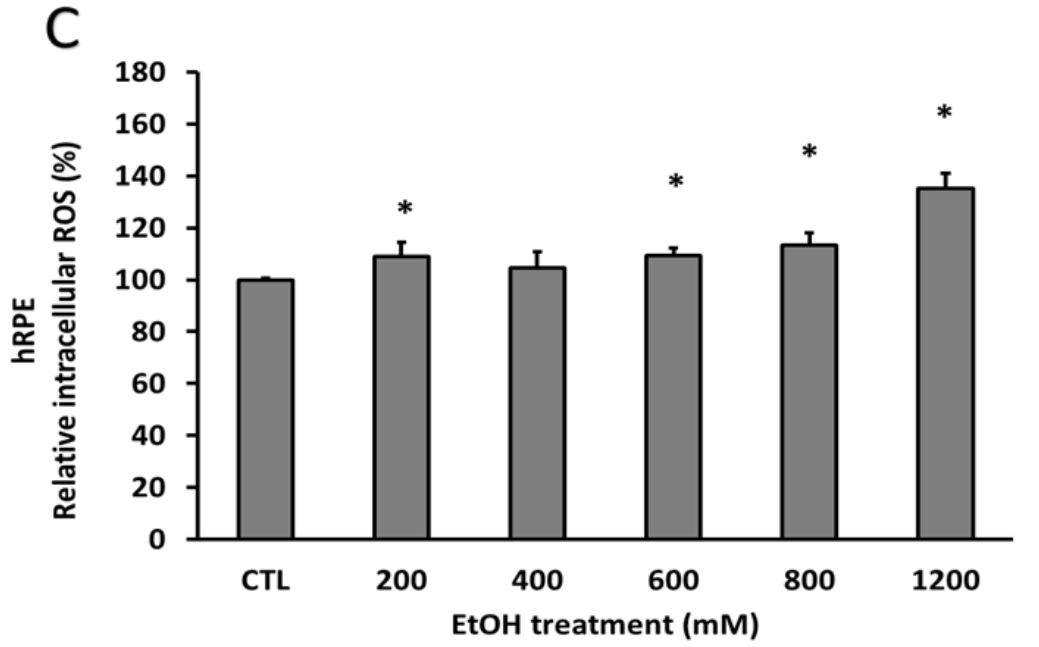
C
hRPE
Relative intracellular ROS (%)
180
160
140
120
100
80
60
40
20
0
*
*
*
*
CTL
200
400
600
800
1200
EtOH treatment (mM)

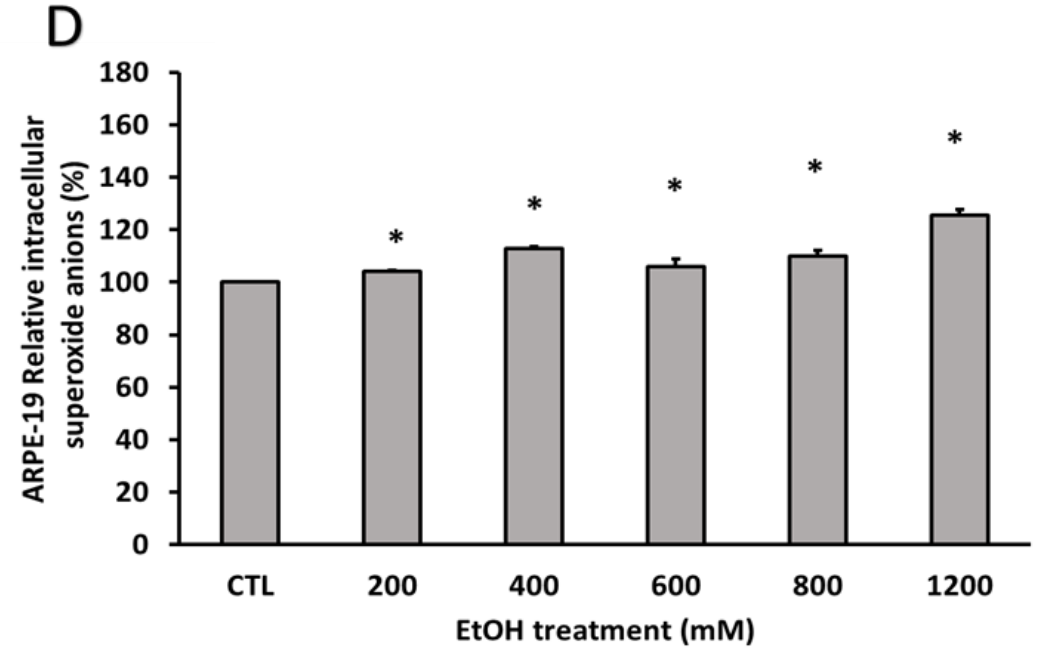
D
ARPE-19 Relative intracellular superoxide anions (%)
180
160
140
120
100
80
60
40
20
0
*
*
*
*
*
CTL
200
400
600
800
1200
EtOH treatment (mM)

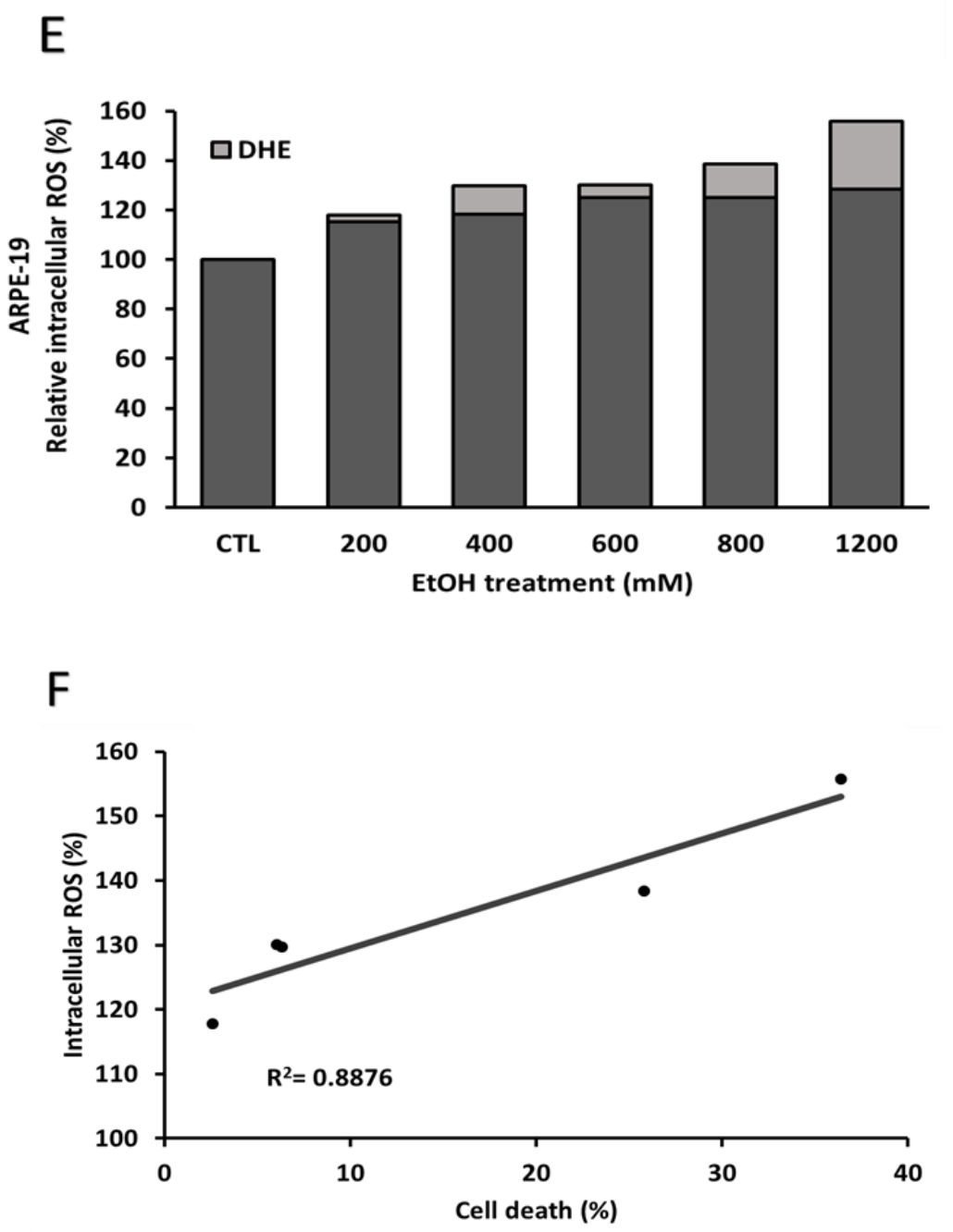

Figure 17. EtOH induces intracellular ROS. Total intracellular ROS measured with DCFH increased significantly in a concentration dependent manner after 24 hours of EtOH treatment in ARPE-19 cells (**A**). The quantification of DCFH fluorescence reveals the same result in ARPE-19 cells (**B**), and hRPE (**C**). At the same way superoxide anions measured by DHE were increased in ARPE-19 (**D**). The increase of ROS was caused by the implication of superoxide anions in total of ROS production (**E**). There is a positive correlation between the increase of total intracellular ROS and the increase of cell death measured by XTT (**F**). Values are expressed as mean ± SEM (N=3). Statistical significance was determined by means of 1-and-2-way ANOVA, and Student's t-test. Statistically significant differences were set at *p<0.05 vs. CTL group.

3. EtOH TREATMENT INDUCES APOPTOSIS MARKERS IN ARPE-19 CELLS IN A CONCENTRATION-DEPENDENT MANNER

With the aim to understand which process is implicated in ARPE-19 cell death under EtOH treatment, the most important apoptosis markers were studied, **figure 18**. The pro-apoptotic (Caspase-3 and Bax) and pro-survival (Bcl-2) markers were quantified by western blot 24 h after 200, 400 and 600 mM EtOH treatment. The **figure 18A** shows that 600 mM EtOH promoted significant increase, about 20% of Caspase-3 protein levels (p. value 0.01). Similar results were found with the other pro-apoptotic marker Bax, at 400 mM and 600 mM EtOH (p. value < 0.01), **figure 18B**.

On the other hand, 400 mM and 600 mM EtOH significantly enhanced, even two-fold the basal expression of the pro-survival marker Bcl-2 (p. value < 0.05), **figure 18C**.

Cell viability calcein-EthD-1 assay in ARPE-19 cells after EtOH treatment, confirmed previous results. As seen in **figure 18D**, increased EthD-1 (red dye) labelling (around 4%, indicate with arrows), can be observed at 600 mM EtOH treated cells. A decrease (around 16%) of the esterase activity (green dye) in all EtOH groups is also showed.

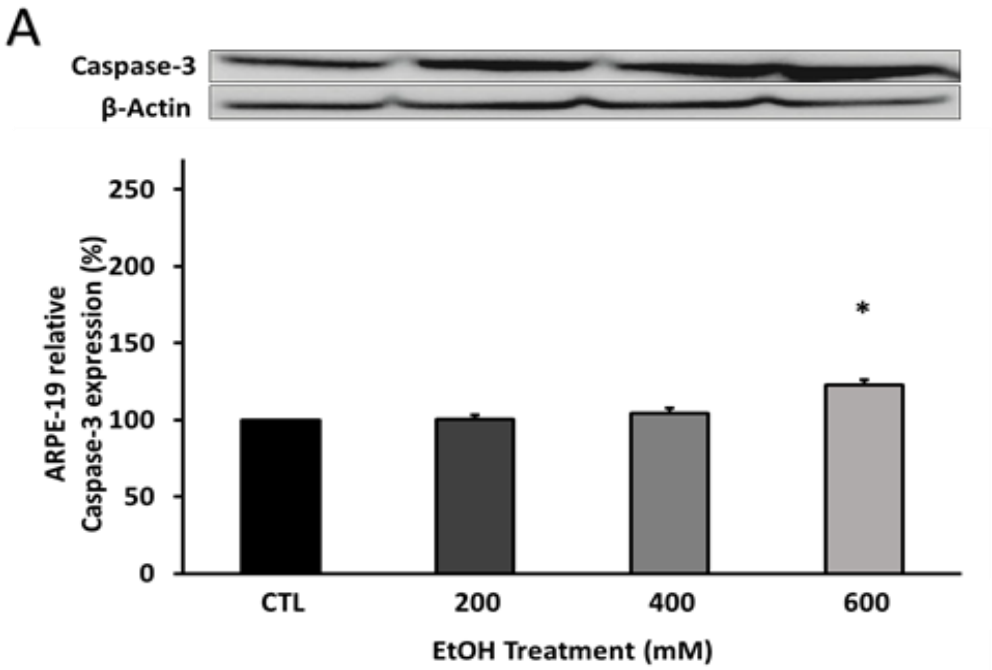

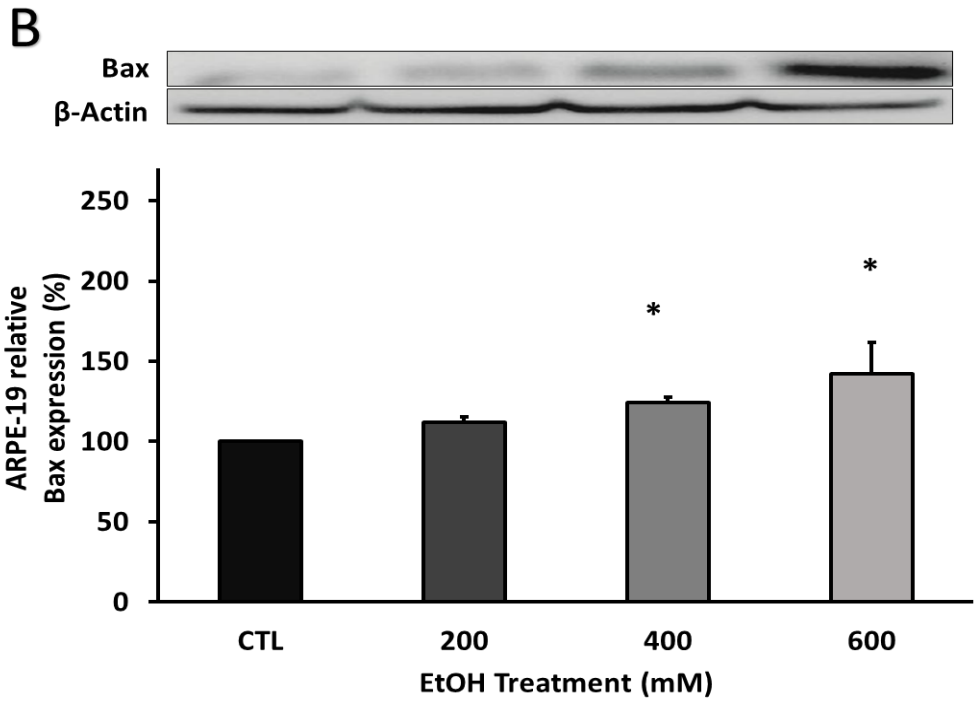
B
Bax
β-Actin
ARPE-19 relative Bax expression (%)
250
200
150
100
50
0
*
*
CTL
200
400
600
EtOH Treatment (mM)

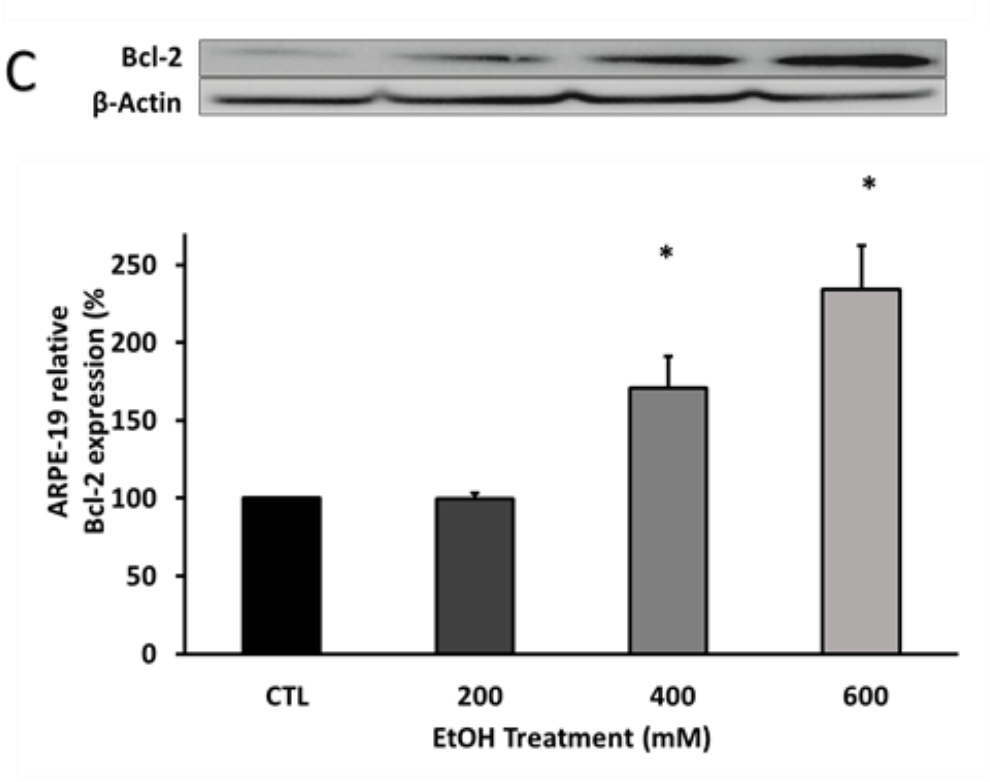
C
Bcl-2
β-Actin
ARPE-19 relative Bcl-2 expression (%
250
200
150
100
50
0
*
*
CTL
200
400
600
EtOH Treatment (mM)

D

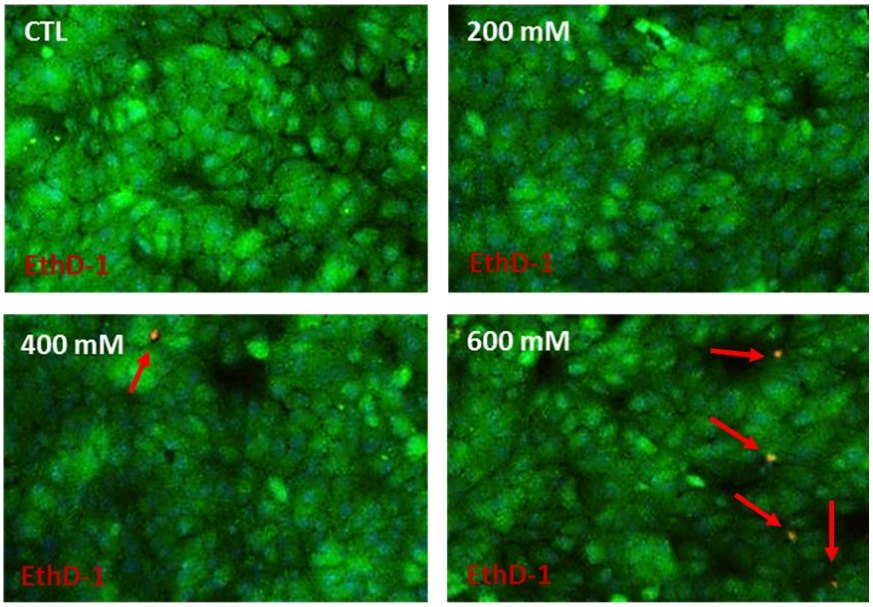

Figure 18. EtOH treatment induces apoptosis in ARPE-19 cells. Apoptotic markers in ARPE-19 after EtOH treatment during 24h were measured by WB. Exist and increase of Caspase-3 (**A**), Bax (**B**) and Bcl-2 (**C**) protein expression in a concentration dependent manner. Immunofluorescence with calcein and EthD-1 indicate loss of plasma membrane integrity with EtOH treatment (**D**). Protein expression was normalized by β-Actin. Values are expressed as mean ± SEM (N=3). Statistical significance was determined by means of 1-and-2-way ANOVA, and Student's t-test. Statistically significant differences were set at *p<0.05 vs. CTL group.

4. EtOH INDUCES CHANGES IN RPE BARRIER FUNCTION

4.1. EtOH DECREASES INTERCELLULAR JUNCTIONS INTEGRITY IN ARPE-19 CELLS.

ZO-1 is one of the most important proteins in tight junctions presents in RPE tissue. Considering the role of ZO-1 for the RPE barrier maintenance, an immunofluorescence against ZO-1 was performed. A significant decrease of ZO-1 expression (in green) can be observed in **figure 19A and 19B**. Those differences are significantly decreased, in a concentration dependent manner, from 200 mM (p. value < 0.01) to 600 mM (p. value < 0.0001).

TER is a technique to measure the integrity of TJ in epithelial monolayers. TER values are strong indicators of the integrity of the cellular barriers. TER assay with mature ARPE-19 cells validated previous results, **figure 19C**. EtOH exposure promoted a significant decrease of cell membrane electrical resistance after 600 mM and 1200mM EtOH challenge (p. value 0.001, p. value < 0.0001 resp.).

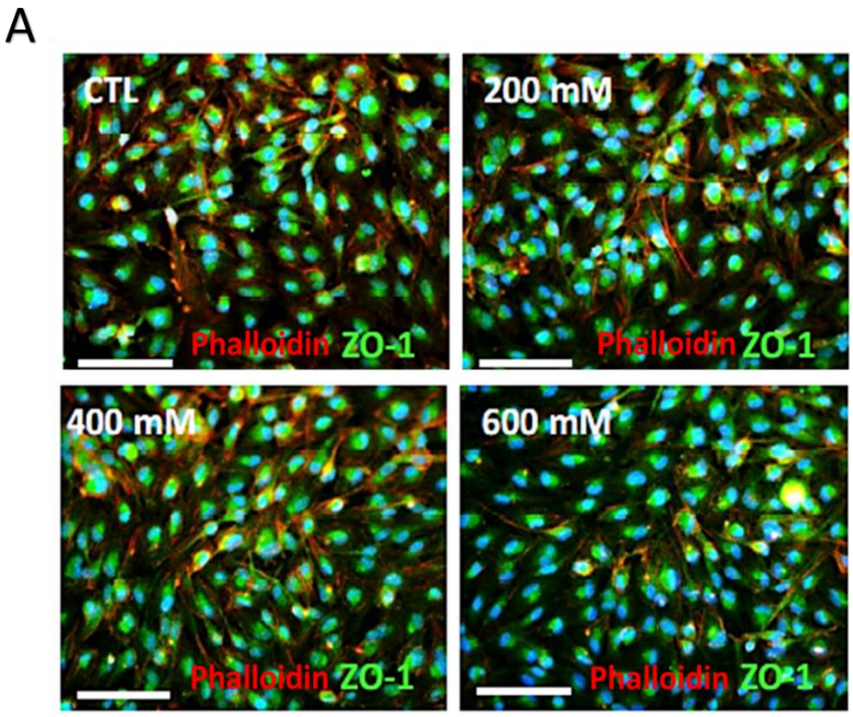

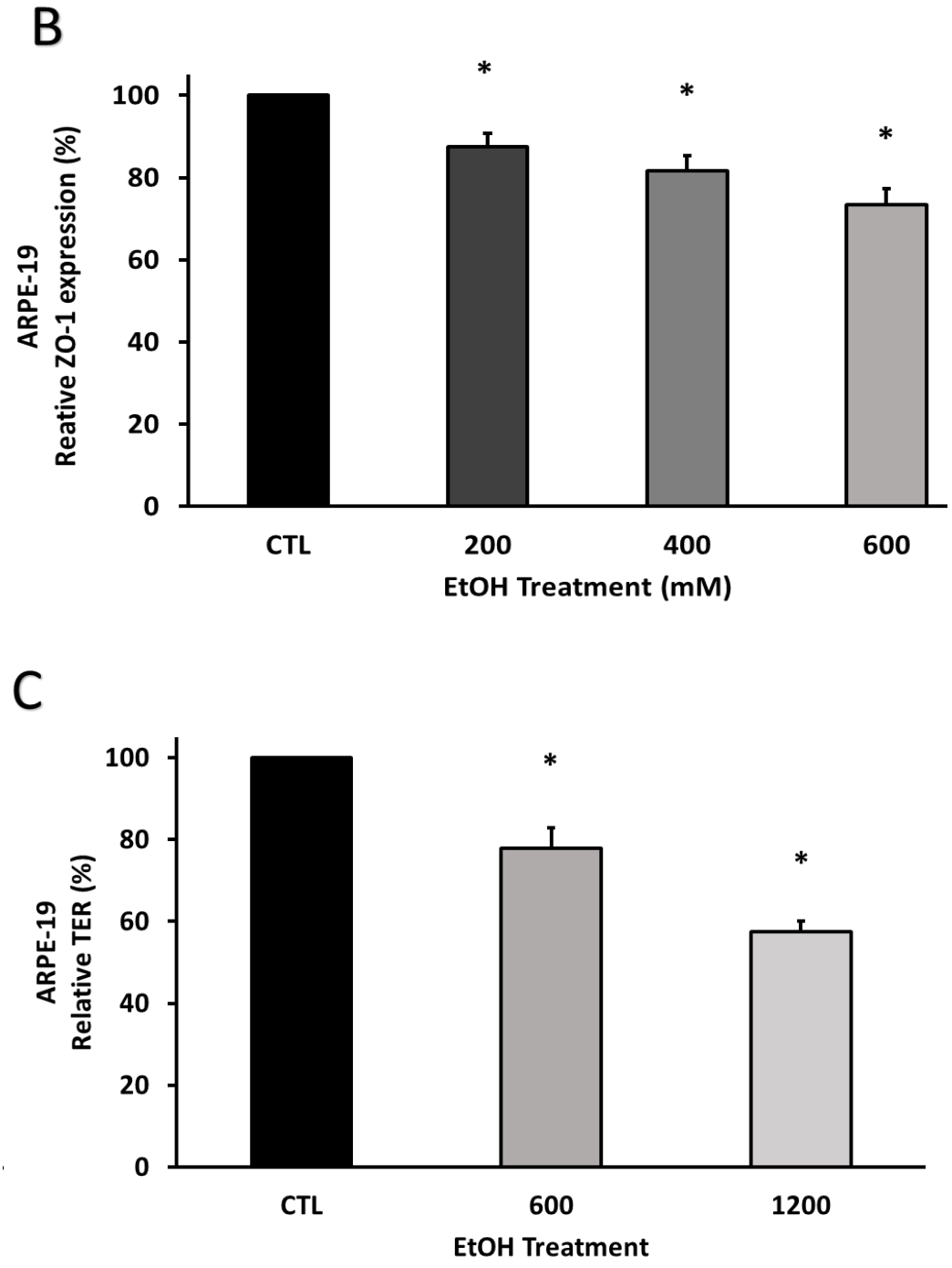

Figure 19. EtOH decrease ARPE-19 barrier function. EtOH treatment during 24 hours decreases ZO-1 expression in ARPE-19 cells (**A**). The immunofluorescence quantification shows a significant difference between EtOH treatment and control group (**B**). The TER assay showed the same also with high EtOH concentrations treatment (**C**). Values are expressed as mean ± SEM (N=3). Statistical significance was determined by means of 1-and-2-way ANOVA, and Student's t-test. Statistically significant differences were set at *p<0.05 vs. CTL group.

4.2. EtOH MODIFIES THE PROTEOME PROFILE IN ARPE-19 CELLS

4.2.1. PRO-INFLAMMATORY RELATED PROTEINS

Pro-inflammatory related protein detection is shown in **figure 20** after different EtOH concentrations. EtOH promoted a differential protein expression on the RPE-related factors and RPE-released proteins. GM-CSF, IGFBP-1, IL-1β, MCP-1, MIP-1α, PTX-3, TIMP-1, TIMP-4, MMP-8 and MMP-9 protein expression was enhanced after EtOH, **figure 20A**. But nevertheless, other RPE-related factors and RPE-released proteins were decreased; Activin, Amphiregulin, DPPIV, EGF, FGF, IL-8, TGF-β1 and Prolactin), **figure 20B**. In this latter group, the EGF expression decreased about 80% compared to CTL. Similar results were found for Activin with a 50% decreased at 600 mM EtOH.

4.2.2. ANGIOGENESIS RELATED PROTEINS

The same array was performed to detect agiogenic-related proteins in ARPE-19 cells under EtOH treatment, **figure 21.**

All proteins showed changes in their expression profile under EtOH treatment. Some of them decreased their expression in a concentration dependent manner, **figure 21A** (End/Coll XVIII, FGF-7, HGF, PDGF-AB/BB, PF4 and VEGF). But nevertheless, others suffered an increased, **figure 22B** (HB-EGF, Vasohibin, uPA and VEGF-C). Surprisingly, the VEGF-C and uPA expression increased around 5-fold at 600 mM of EtOH compared to each CTL groups.

In **figure 21C** and **D** are represented some proteins with a two-phase response. The profile expression is modified in term of EtOH concentration used. In all of these, 200 mM of EtOH was the inflection point. ADMATS-1, PDGF-AA, IGFBP-3, Serpin B5, PEDF and TSP-1, increased its expression in a concentrations above 200 mM EtOH, **figure 21C**. On the other hand, Ang/Plasm, EG-VEGF, FGF-4, IGFBP-2, PD-ECGF and PlGF showed a decreased, **figure 21D**.

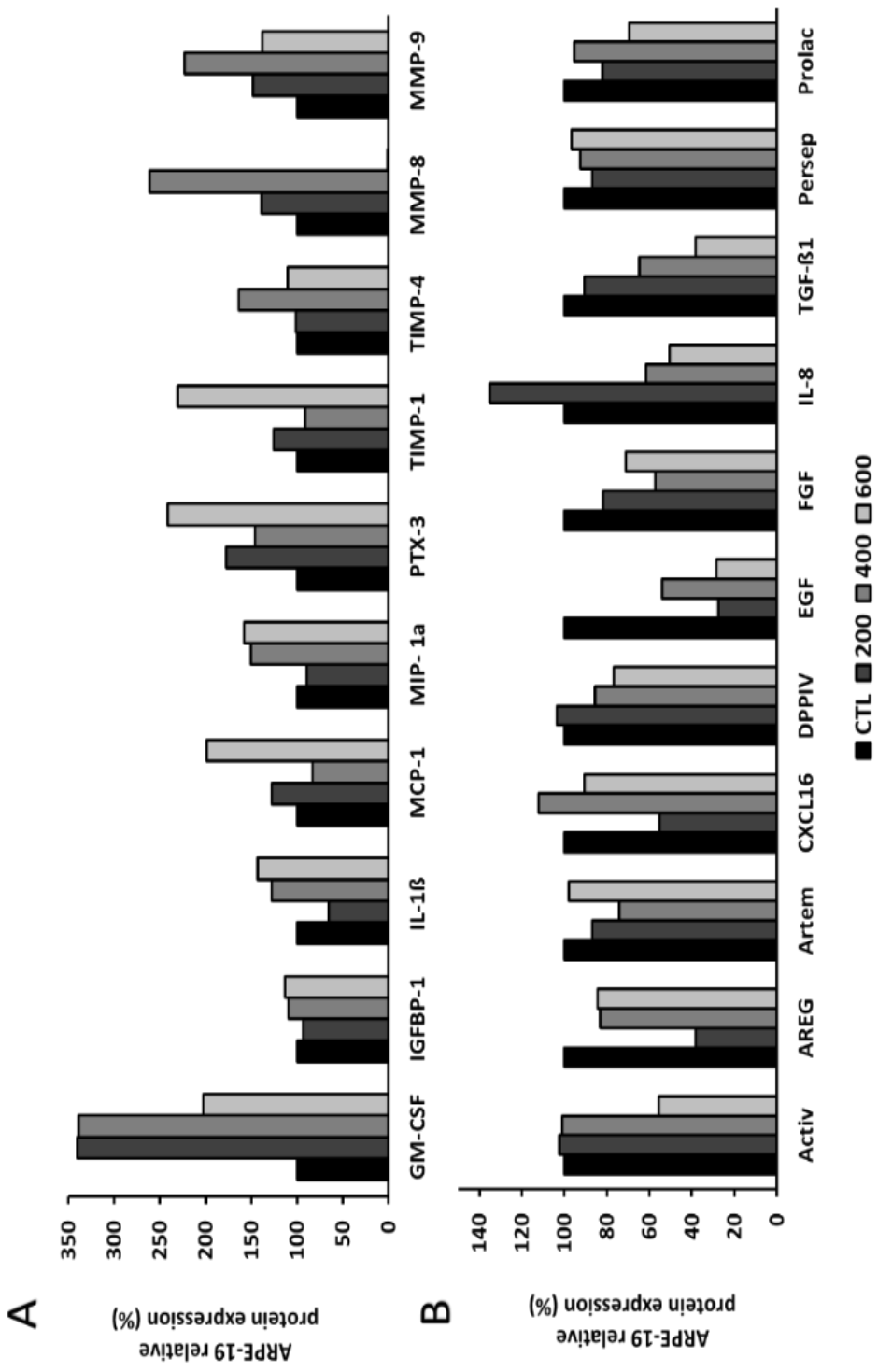

Figure 20. ARPE-19 inflammation markers profile after EtOH treatment. After 24 hours of EtOH treatment, the ARPE-19 cell inflammation markers profile was increased (**A**) or decreased (**B**) depending on the concentrations used. Values are expressed as average of an N= 3 samples pooled.

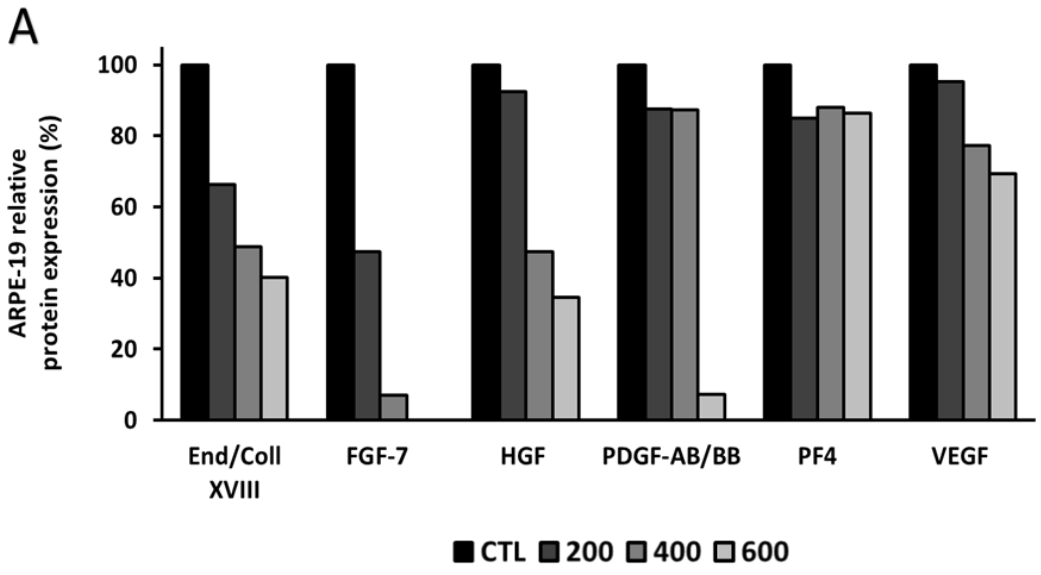
A
ARPE-19 relative protein expression (%)
100
80
60
40
20
0
End/Coll XVIII
FGF-7
HGF
PDGF-AB/BB
PF4
VEGF
CTL
200
400
600

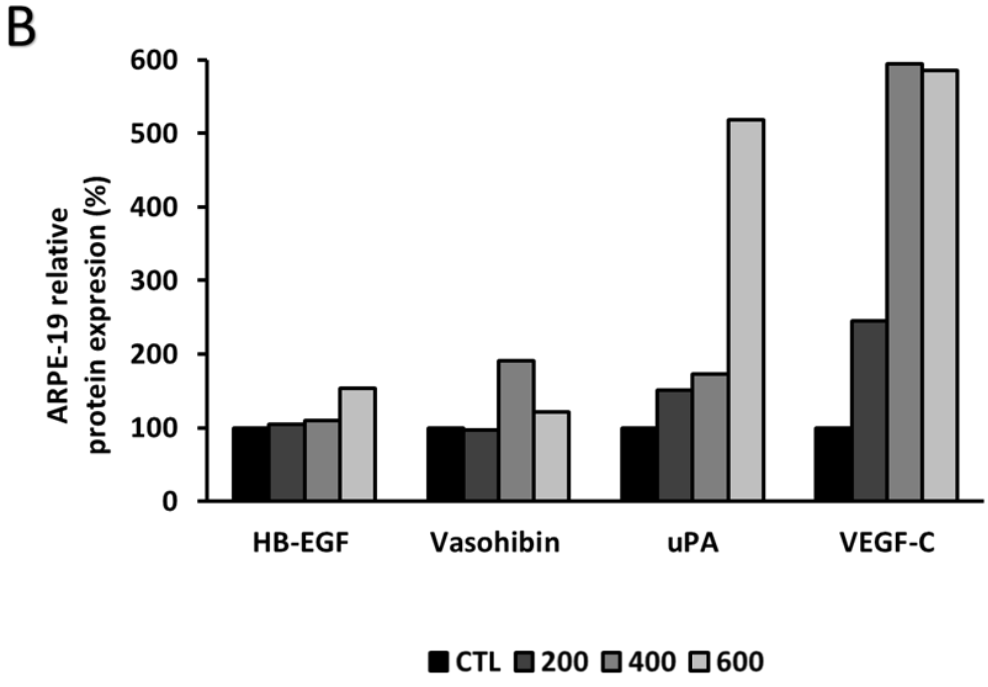
B
ARPE-19 relative protein expresion (%)
600
500
400
300
200
100
0
HB-EGF
Vasohibin
uPA
VEGF-C
CTL
200
400
600

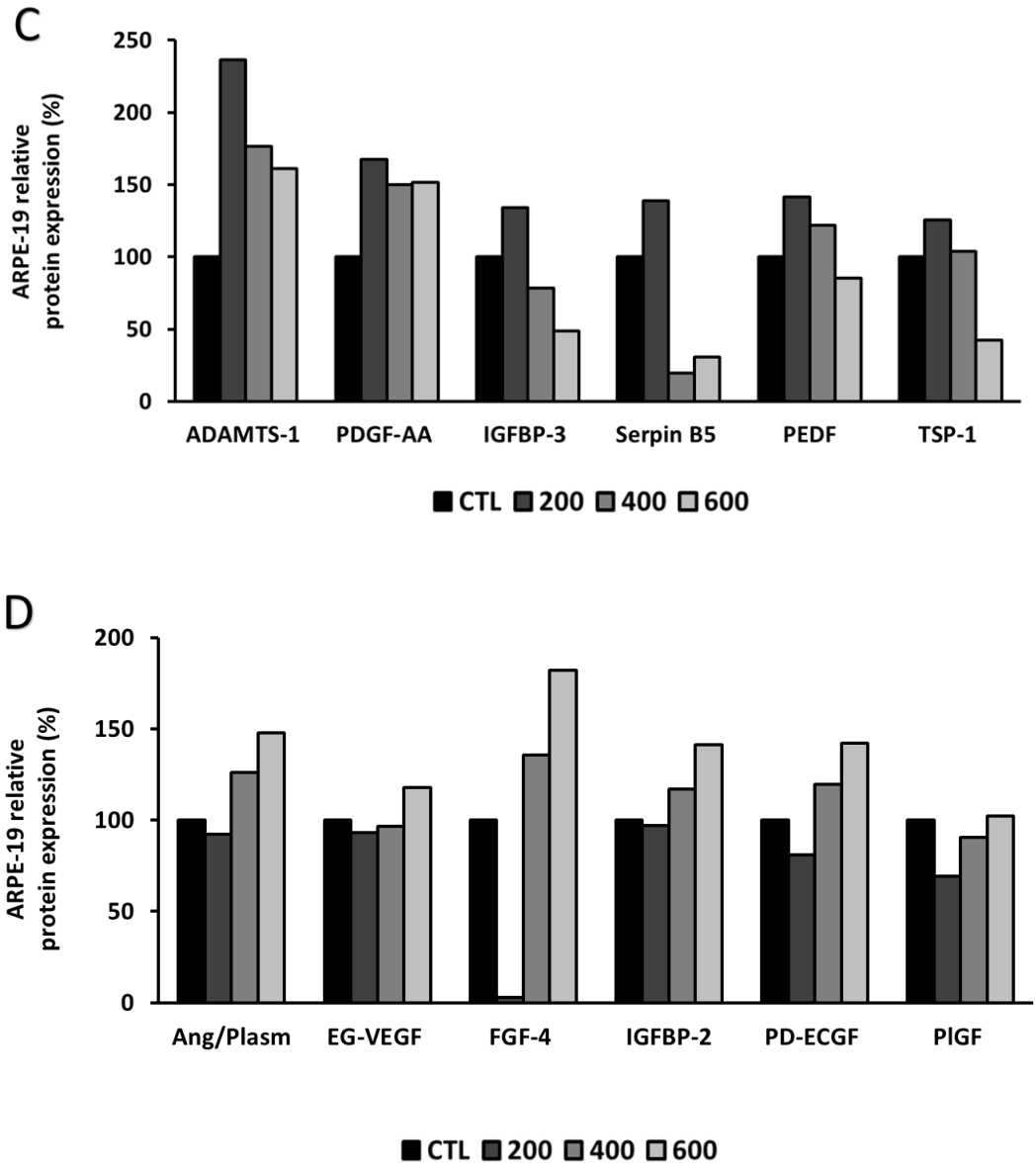

Figure 21. ARPE-19 angiogenesis markers profile after EtOH treatment. After 24 hours of EtOH treatment, the ARPE-19 cell angiogenesis markers profile was decreased (**A** and **C**) or increased (**B** and **D**) depending on the concentrations used. Values are expressed as average of an N= 3 samples pooled.

4.3. EtOH-INDUCED CHANGES IN VEGF AND PEDF EXPRESSION

One of the most important roles of the RPE is the release of growth factors for retinal maintenance. VEGF and PEDF are specific biomarkers of RPE barrier. Taking into account previous results, a study of their expression was carried out. The **figure 22A** and **22B** shows that EtOH treatment resulted on a significant decrease of VEGF and PEDF mRNA expression in ARPE-19 cells. Being statistically significant in case of PEDF (p. value < 0.05), **figure 22B**.

In contrast with this, both markers were overexpressed at 200 mM EtOH when compared with the CTL group. VEGF mRNA levels were significantly increased with 200mM EtOH (p. value 0.0001), **figure 22A** and PEDF mRNA was overexpressed around 150% (p. value < 0.05), **figure 22B**. VEGF receptor proteins showed significant differences, **figure 22C** and **22D.** VEGFR-1 decreased its expression in all EtOH treated groups (p. value < 0.001), **figure 22C**. In contrast, VEGFR-2 protein expression, **figure 22D**, was increased at 200 mM EtOH followed by a significant reduction at higher EtOH concentrations (p. value < 0.05).

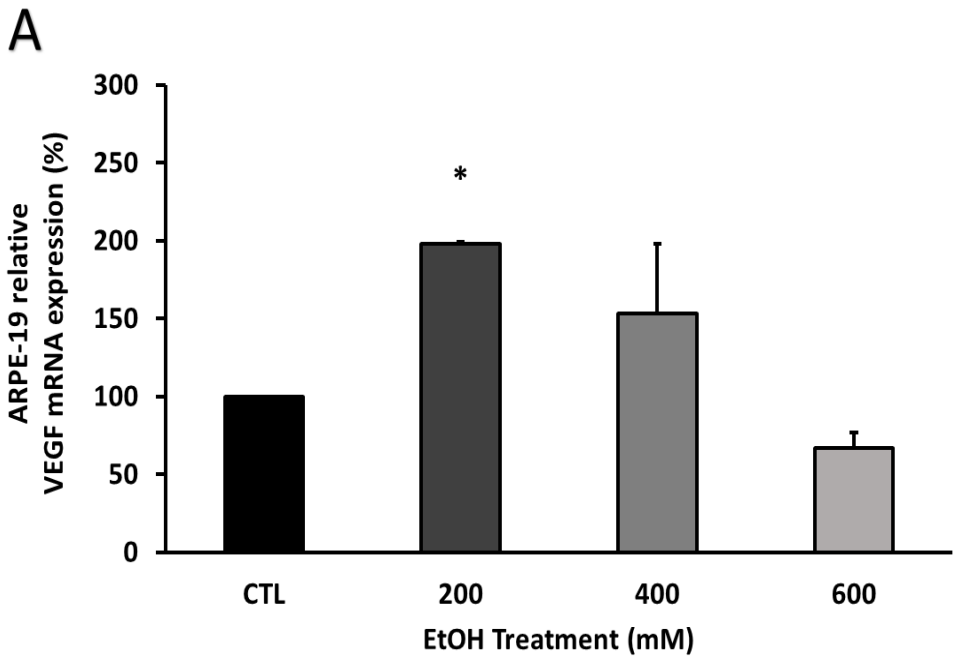

B

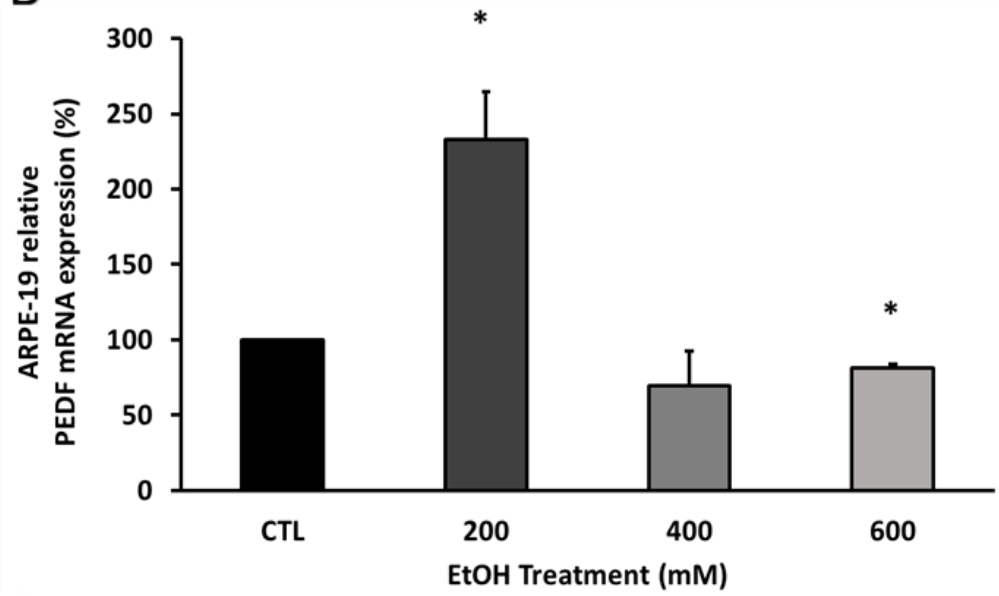
ARPE-19 relative
PEDF mRNA expression (%)
300
250
200
150
100
50
0
*
*
CTL
200
400
600
EtOH Treatment (mM)

C

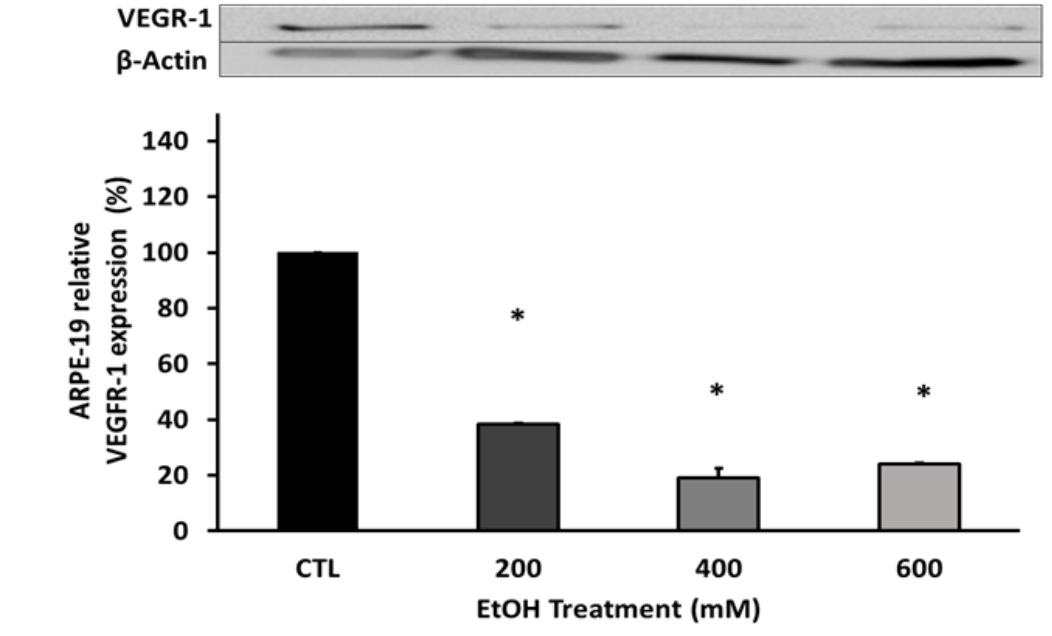
VEGR-1
β-Actin
ARPE-19 relative
VEGFR-1 expression (%)
140
120
100
80
60
40
20
0
*
*
*
CTL
200
400
600
EtOH Treatment (mM)

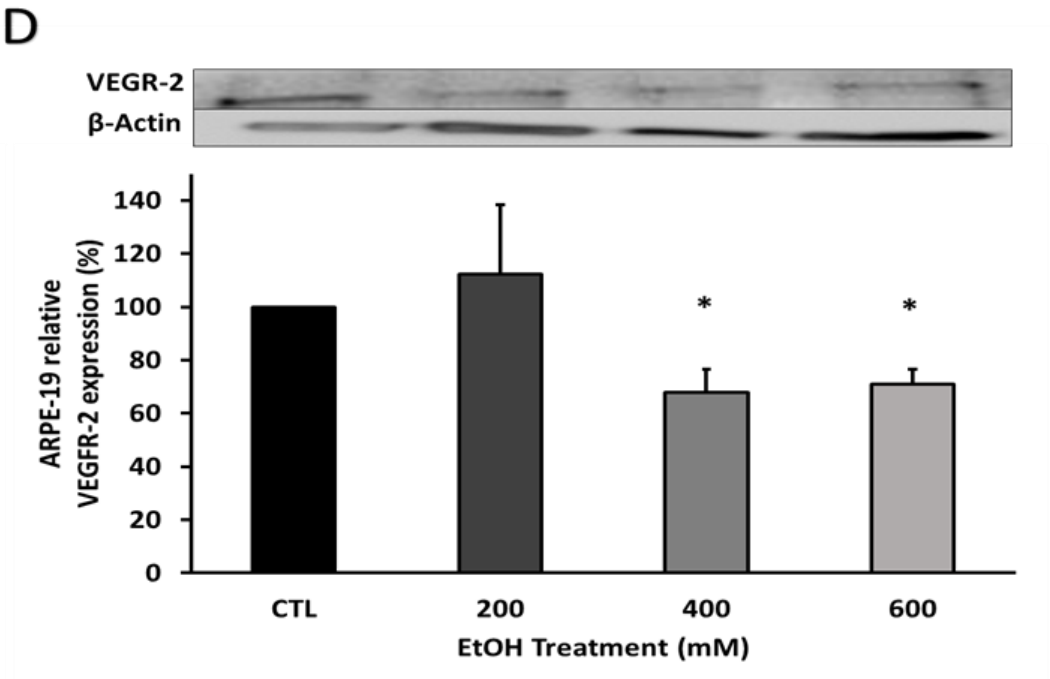

Figure 22. EtOH induces changes in ARPE-19 angiogenesis markers expression mRNA expression quantification by qPCR in ARPE-19 after EtOH treatment. Different VEGF (**A**) and PEDF (**B**) profile expression after different EtOH concentrations used. The same occurs with the protein expression measured by WB in VEGFR-1 (**C**) and VEGFR-2 (**D**). Gene expression of CYP2E1 was normalized by GAPDH gene expression. Protein expression was normalized by β-Actin. Values are expressed as mean ± SEM (N=3). Statistical significance was determined by means of 1-and-2-way ANOVA, and Student's t-test. Statistically significant differences were set at *p<0.05 vs. CTL group.

4.4. EtOH-INDUCED CHANGES IN MPPs EXPRESSION

EtOH exposure promoted a significant change on MMPs expression in ARPE-19 cells, (detected by ELISA). **Figure 23B** summarizes the MMPs values.

As seen in **figure 23B**, MMP-2 levels reached the highest value, 6.4 pg/ml at 400 mM EtOH. All MMPs were grouped according to their cellular function. Among collagenases, **figure 23C,** MMP-8 shows a marked expression in a dose dependent manner. The **figure 23D**, represents the gelatinases family. MMP-2 and MMP-9 increased their expression in all EtOH treated groups compared to control. Significant differences in MMP-2 protein expression could be set at 400 and 600 mM EtOH (p. values < 0.05 and 0.01 respectively). Nevertheless, MMP-9 exhibited these differences at 400 mM EtOH (p. value 0.05).

No significant differences were observed in the matrilysin MMP-7, **figure 23E**. Stromelysin MMP-3 expression was enhanced after EtOH treatment. Significant differences were observed in all EtOH concentrations used (p. value <0.01), **figure 23F**.

A

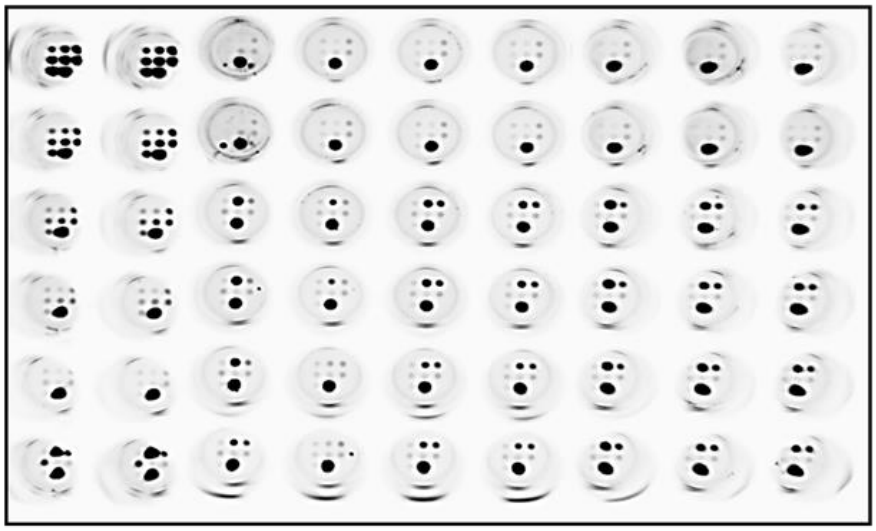

B

[MMPs] (pg/ml)	EtOH TREATMENT			
	CTL	200	400	600
MMP-1	0.077	0.080	0.101	0.081
MMP-2	3.712	4.933	6.040	4.713
MMP-3	0.040	0.056	0.059	0.067
MMP-7	0.004	0.004	0.006	0.006
MMP-8	0.030	0.031	0.048	0.058
MMP-9	0.053	0.051	0.069	0.060
MMP-13	0.025	0.024	0.029	0.027

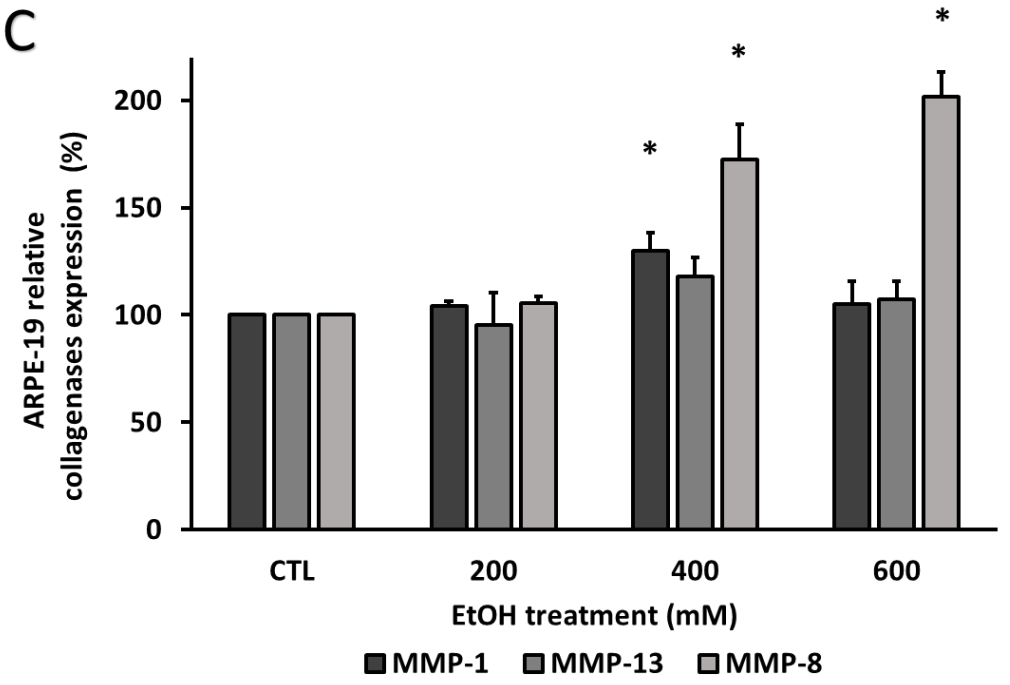
C
ARPE-19 relative collagenases expression (%)
200
150
100
50
0
*
*
*
CTL
200
400
600
EtOH treatment (mM)
MMP-1
MMP-13
MMP-8

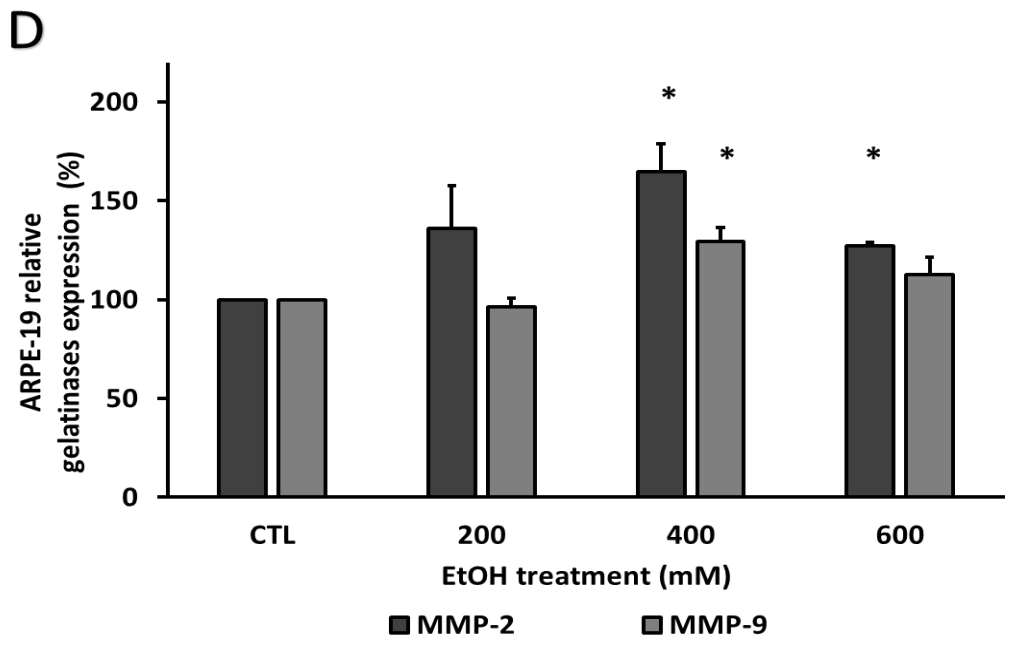
D
ARPE-19 relative gelatinases expression (%)
200
150
100
50
0
*
*
*
CTL
200
400
600
EtOH treatment (mM)
MMP-2
MMP-9

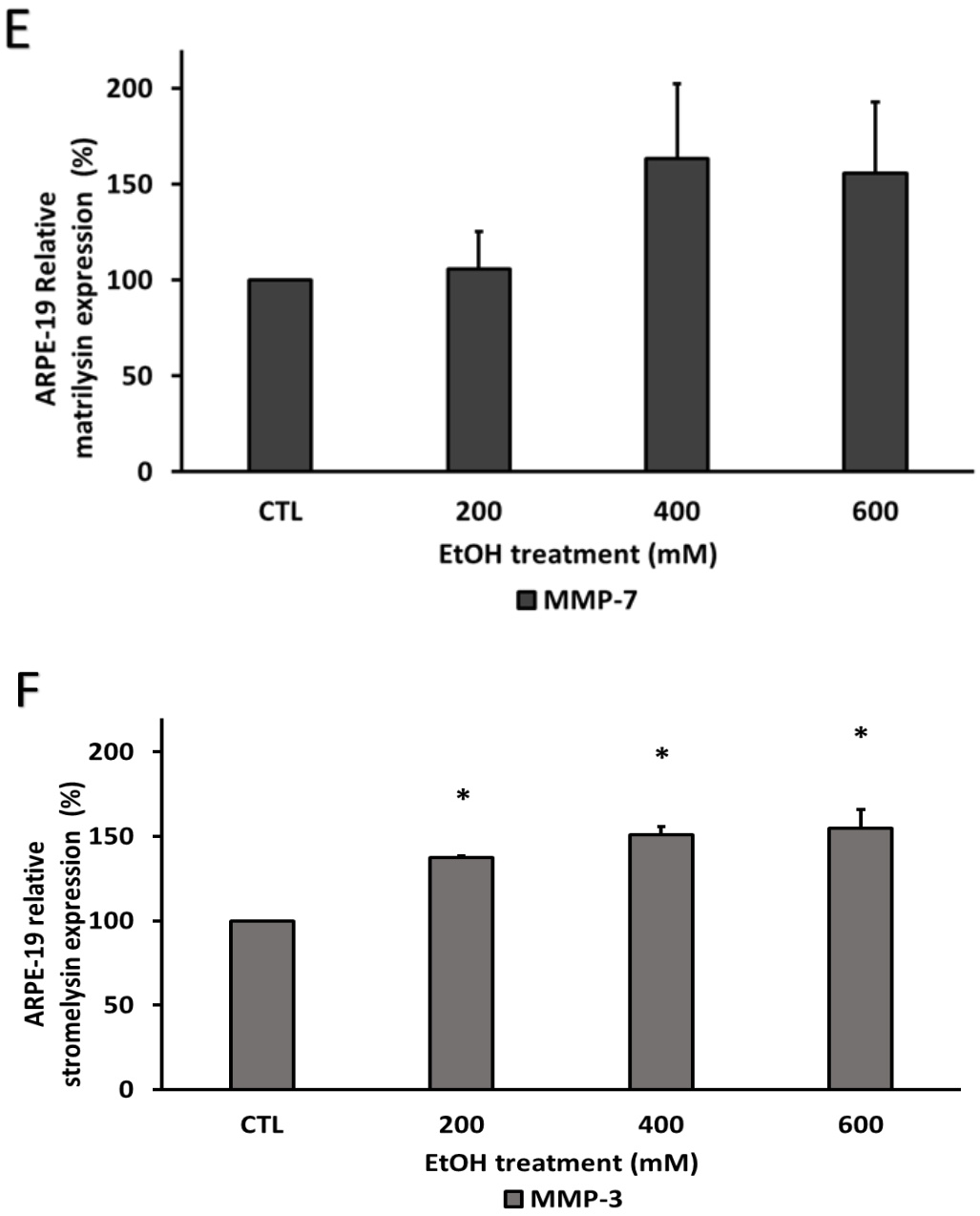

Figure 23. MMPs expression in ARPE-19 cells under EtOH treatment. The levels of MMPs were measured with ELISA assay in a 96 multiwell plate and the expression was quantify by chemiluminescence (**A**). The MPPs quantification expressed the values in pg/ml (**B**). The relative MMPs expression after EtOH treatment were represented by their functional classification; collagenases (**C**), gelatinases (**D**), matrilysin (**E**) and stromelysin (**F**). Values are expressed as mean ± SEM (N=3). Statistical significance was determined by means of 1-and-2-way ANOVA, and Student's t-test. Statistically significant differences were set at *p<0.05 vs. CTL group.

4.5. NFKB PROTEIN EXPRESSION IS MODIFIED BY ETOH

NFKB is one of the most important transcription factors that plays critical role in inflammation, angiogenesis and cell survival processes.

The figure **24A** show the NFKB protein quantification by western blot. After 24 hours of EtOH treatment, there is a significant increase of NFKB protein expression at 400 mM EtOH (p. value 0.05). However, 600 mM EtOH reduced its protein expression, below CTL levels (p. value < 0.05).

P65 NFKB immunofluorescence was carried out to identify nuclear translocation. To ensure that the experiment was successful, 100 mM of H_2O_2 was used as a positive control of p65 NFKB nuclear translocation, (**see the procedure on materials and methods, chapter 3**).

Figure 24B shows, that NFKB (green dye) did not undergo nuclear translocation in none of the cases studied. On the other hand, its expression was modified by EtOH treatment.

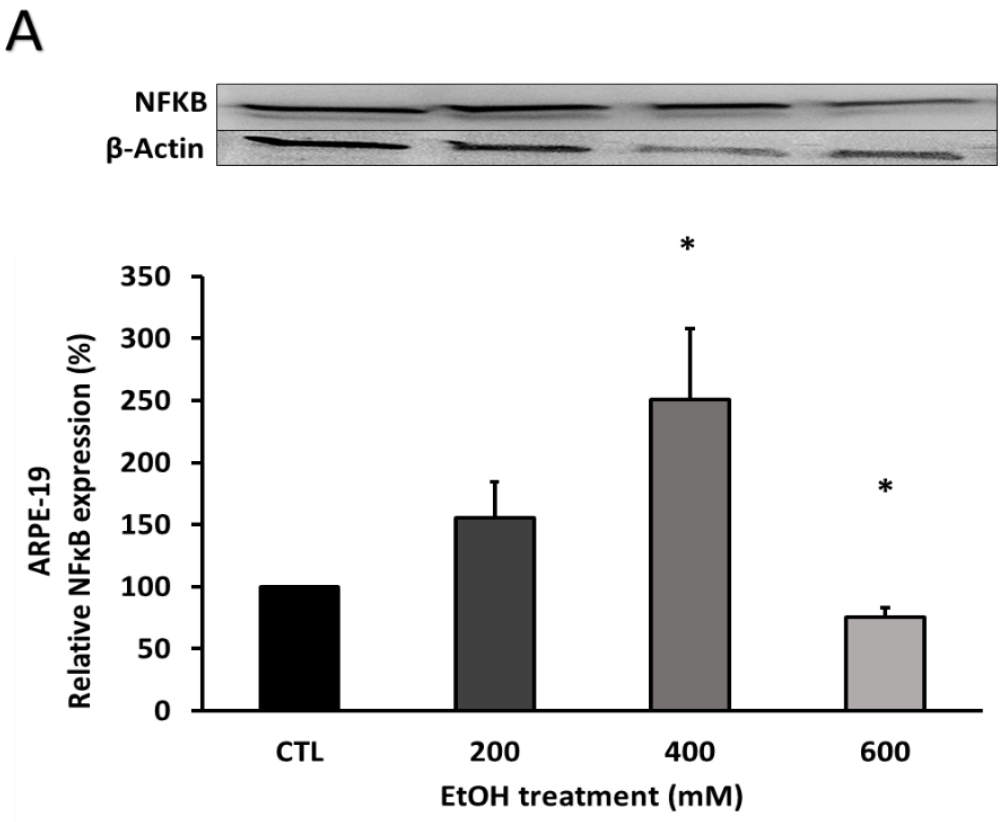

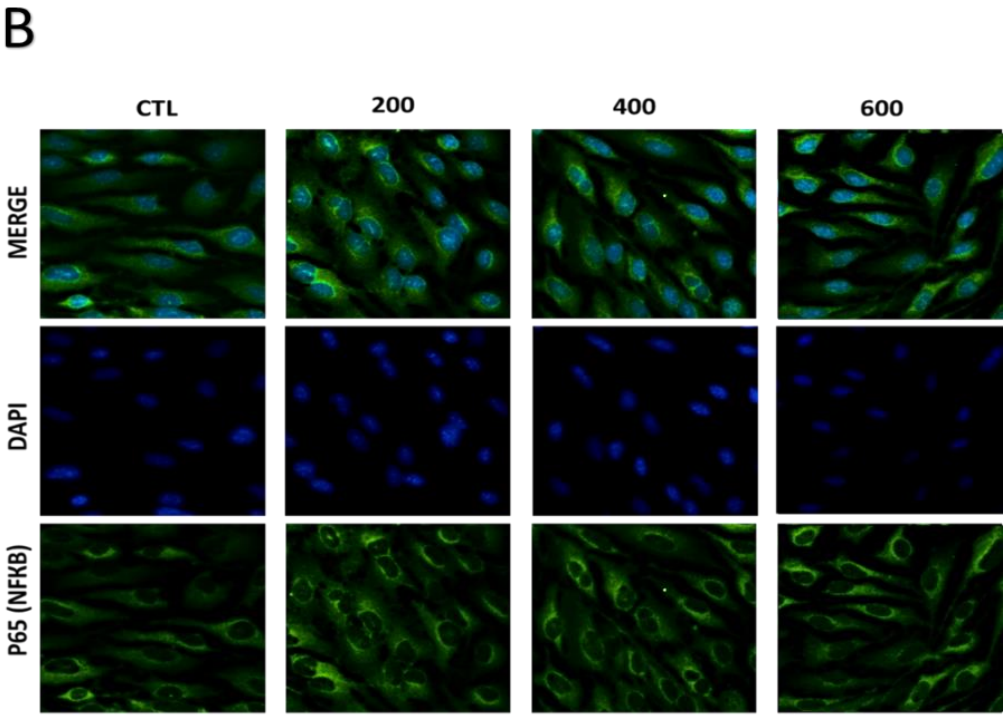

Figure 24. NFKB profile expression in ARPE-19 after EtOH treatment. P65 NFKB protein expression analyzed by WB (**A**) There is not NFKB nuclear translocation (**B**). Protein expression was normalized by β-Actin. Values are expressed as mean ± SEM (N=3). Statistical significance was determined by means of 1-and-2-way ANOVA, and Student's t-test. Statistically significant differences were set at *p<0.05 vs. CTL group.

5. CYP2E1 IS PRESENT IN RPE CELLS

With the aim to study the implication of the CYP2E1 in the metabolism of EtOH in ARPE-19 cells. CYP2E1 protein expression was checked by western blot, **figure 25A** and immunofluorescence, **figure 25B.**

PCR was performed to confirm previous results, **figure 25C.** CYP2E1 mRNA from HepG2 was used as positive control of mRNA expression (**see materials and methods, chapter 3**). The same CYP2E1 gene-specific primer and antibodies recognized all CYP2E1 and mRNA studied forms (ARPE-19, hRPE, and hiPSC-RPE).

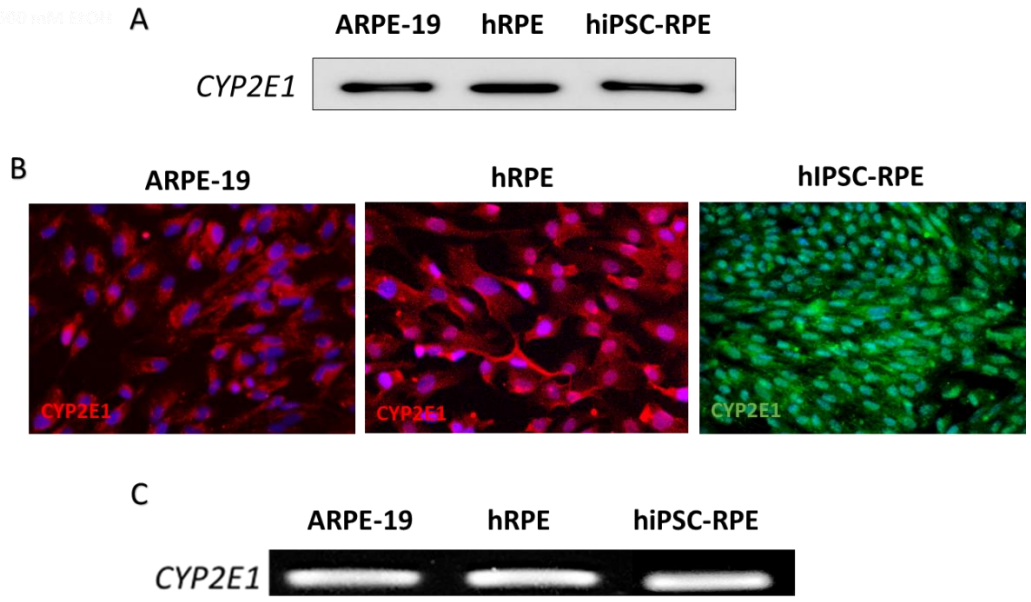

Figure 25. CYP2E1 expression in RPE cells. CYP2E1 protein was detected in all cellular RPE models studied by WB (**A**) and immunofluorescence (**B**). Also CYP2E1 gene was detected in same cells (**C**).

6. ETOH INDUCES CYP2E1 EXPRESSION IN RPE CELLS

CYP2E1 is overexpressed (induced) by high EtOH levels or chronic EtOH exposure. In order to characterize the expression of CYP2E1 in RPE after ETOH challenge, EtOH concentration and duration of the treatment were analyzed, **figure 26**.

6.1. CYP2E1 IS INDUCED IN A TIME- AND CONCENTRATION-DEPENDENT MANNER

Figure **26A** shows that CYP2E1 mRNA expression increased in a time dependent manner with a positive correlation (R^2 = 0.99) at 600 mM EtOH. Higher ethanol levels (1200 mM) decreased this correlation (**See figure 26A**).

CYP2E1 expression was analyzed by using 600 mM and 1200 mM of EtOH during 24 hours. The results in **figure 26C,** revealed a significant increment of CYP2E1 mRNA expression at 1200 mM EtOH (p. value < 0.01). Surprisingly, CYP2E1 protein levels were also significantly increased at 600 mM EtOH (p. value < 0.01), **figure 26D.** 1200 mM EtOH resulted on the highest CYP2E1 mRNA and protein expression. When compared ARPE-19 to HEPG2 cells, under control conditions (**figure 26E**), ARPE-19 cells presented significant lower CYP2E1 microsomal protein than the hepatic cell line.

Interestingly, microsomal CYP2E1 protein activity was significantly increased in ARPE-19 cells after 1200 mM EtOH. This expression was similar to the CYP2E1 activity from control levels in HEPG2 cells, the microsomal CYP2E1 protein activity was two-fold the control CYP2E1 ARPE-19 activity (p. value < 0.05), **figure 26E**. CYP2E1 activity was performed by the formation of 4NC in microsomes from ARPE-19 and HEPG2 cells (**see the procedure on materials and methods, chapter 3**).

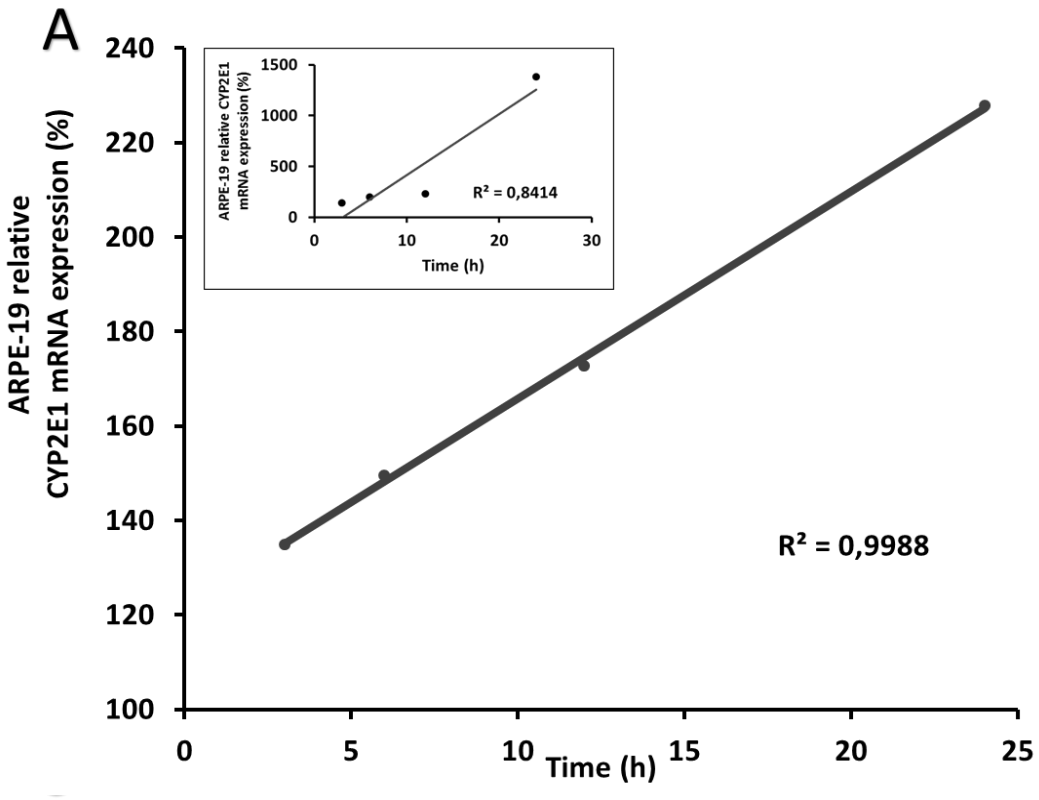
A
ARPE-19 relative CYP2E1 mRNA expression (%)
240
220
200
180
160
140
120
100
0
5
10
15
20
25
Time (h)
R² = 0,9988
ARPE-19 relative CYP2E1 mRNA expression (%)
1500
1000
500
0
0
10
20
30
Time (h)
R² = 0,8414

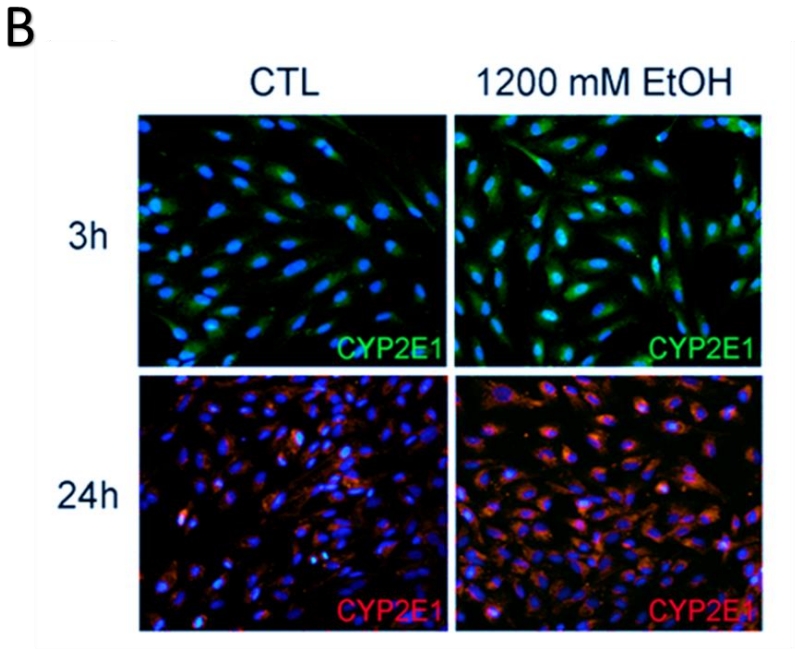
B
CTL
1200 mM EtOH
3h
24h
CYP2E1
CYP2E1
CYP2E1
CYP2E1

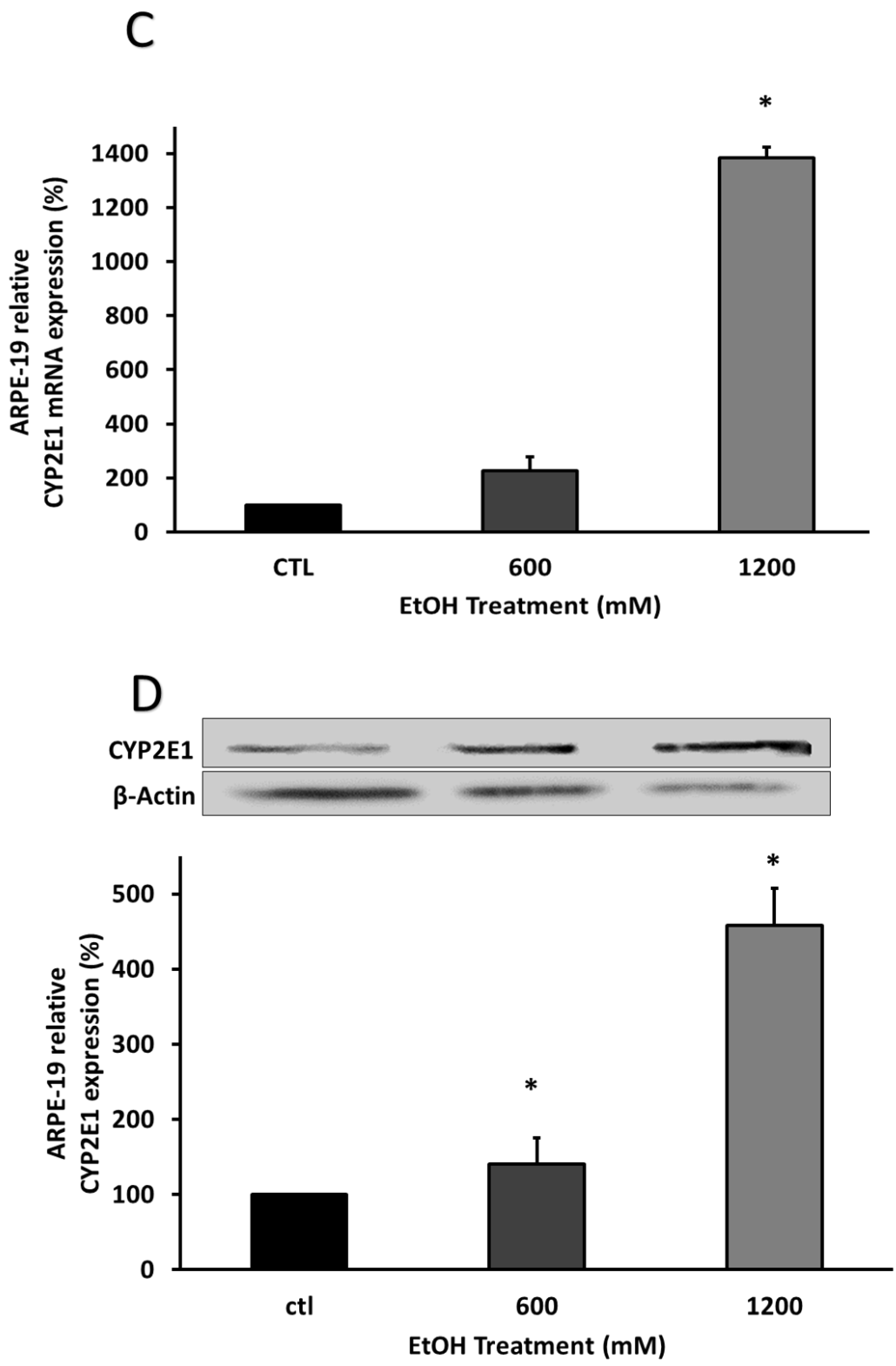
C
ARPE-19 relative CYP2E1 mRNA expression (%)
1400
1200
1000
800
600
400
200
0
*
CTL
600
1200
EtOH Treatment (mM)
D
CYP2E1
β-Actin
ARPE-19 relative CYP2E1 expression (%)
500
400
300
200
100
0
*
*
ctl
600
1200
EtOH Treatment (mM)

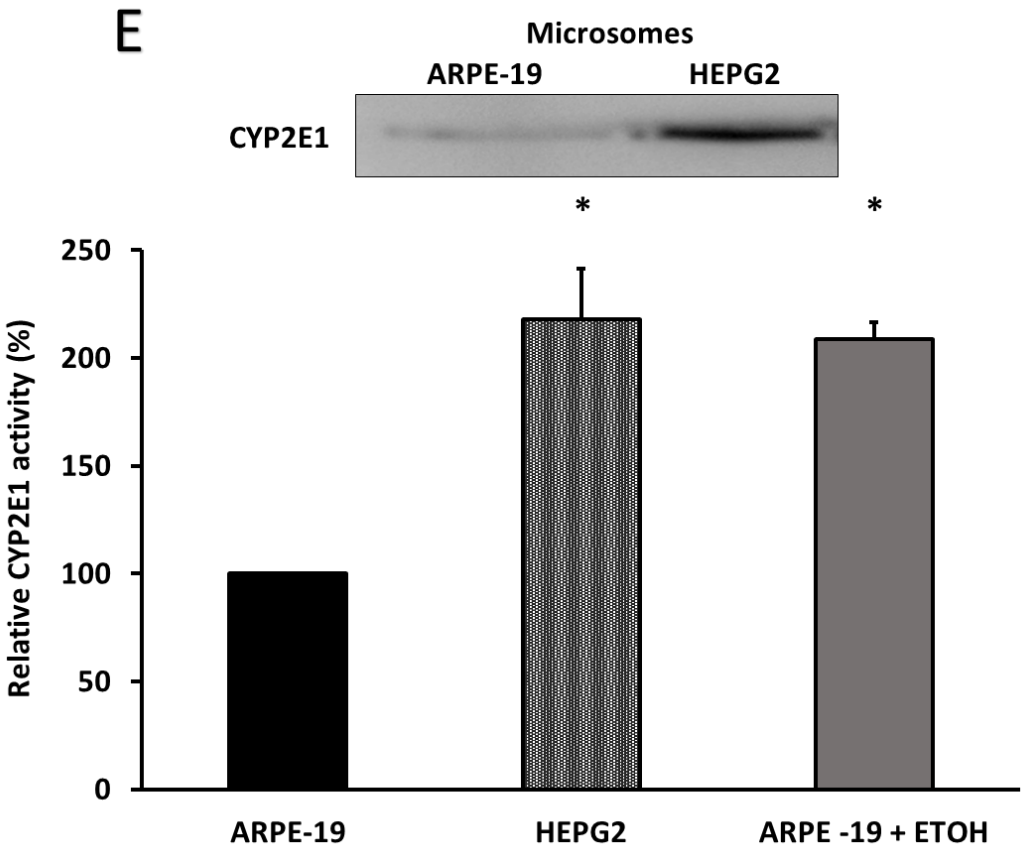

Figure 26. CYP2E1 expression and activity is increased under EtOH treatment. CYP2E1 mRNA expression measured was increased in a time dependent manner (**A**). Protein expression by immunofluorescence (**B**). CYP2E1 mRNA by qPCR (**C**) also protein expression by WB (**D**). CYP2E1 expression in ARPE-19 cells and HEPG2 microsomes by WB. EtOH increase CYP2E1 activity (HPLC) in ARPE-19 compared with HEPG2 cells (**E**). Gene expression of CYP2E1 was normalized by β-Actin and CREBBP gene expression. Protein expression was normalized by β-Actin. Values are expressed as mean ± SEM (N=3). Statistical significance was determined by means of 1-and-2-way ANOVA, and Student's t-test. Statistically significant differences were set at *$p<0.05$ vs. CTL group.

7. CYP2E1 IS IMPLICATED IN RPE CELL DEATH

After considering that CYP2E1 mRNA remains unaltered at 600 mM EtOH in ARPE-19 cells. Higher EtOH challenges were assayed on ARPE-19 cells.

7.1. APOPTOSIS PATHWAY IS ACTIVATED WITH CYP2E1 OVEREXPRESSION

Despite the differences in Caspase-3 expression at 600 and 800 mM EtOH **figure 27A,** the Bcl-2/Bax ratio was significantly increased, about 80% from CTL values at 600 mM EtOH (p. value < 0.01) with a marked decrease at 800 mM EtOH, **figure 27B**.

Figure 27C, shows the regular ARPE-19 cells with a typical cellular morphology. Evident morphological alterations are evident after 800 mM EtOH exposure and dramatic changes in shape; refringency, and plate detachment in 1200 mM EtOH-treated cells.

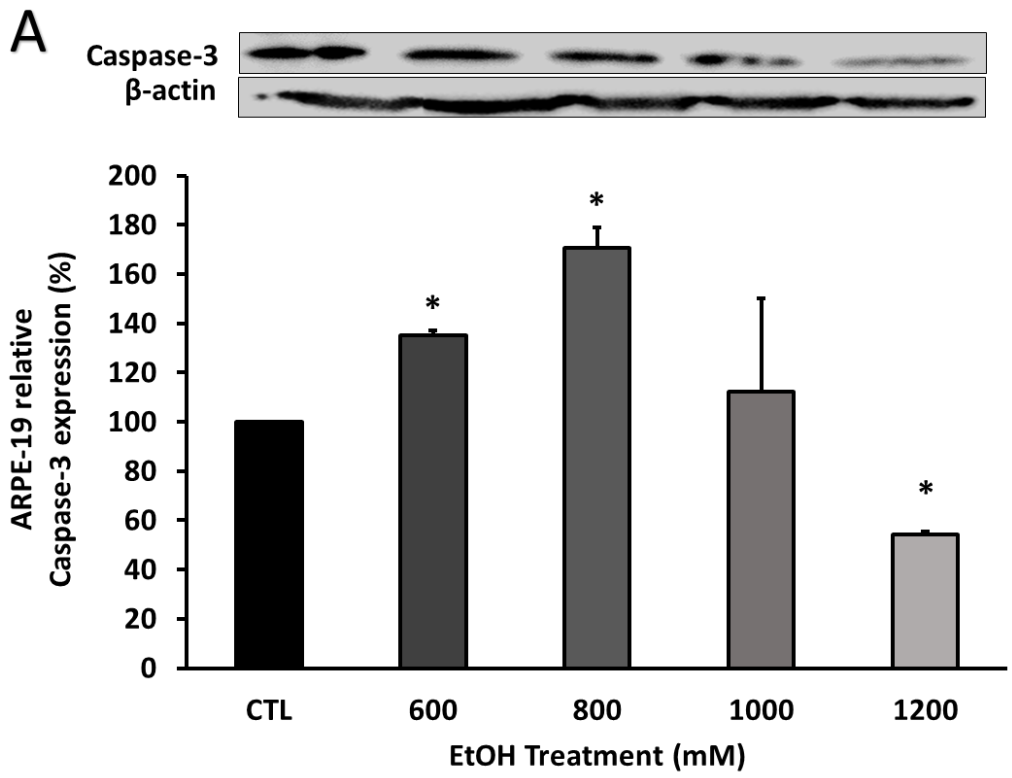

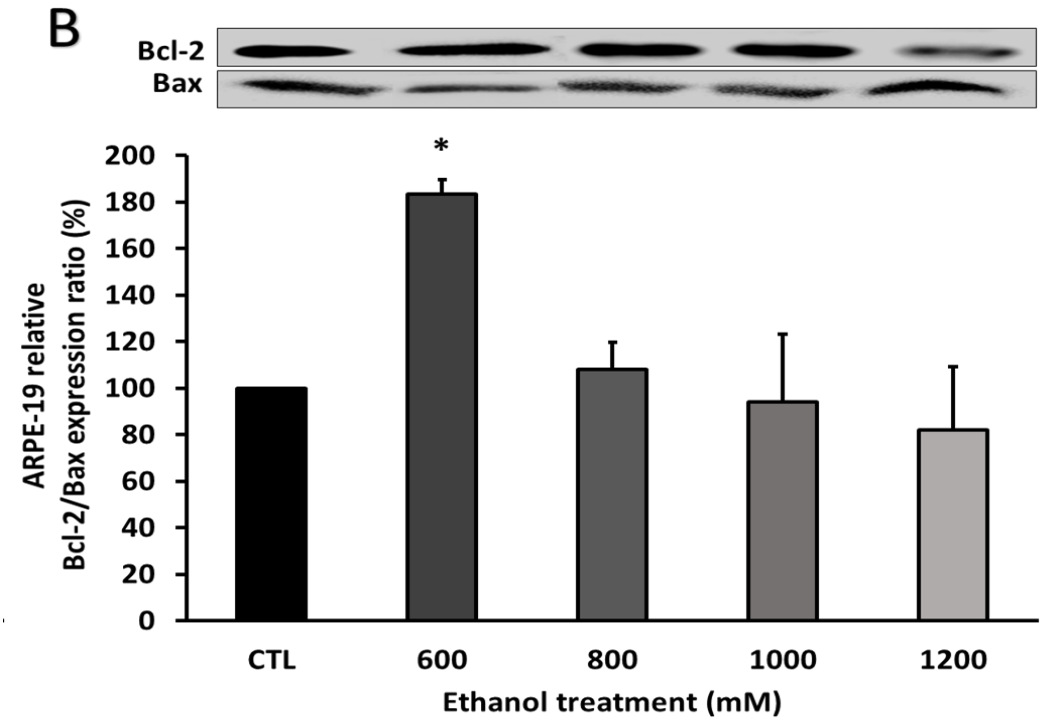

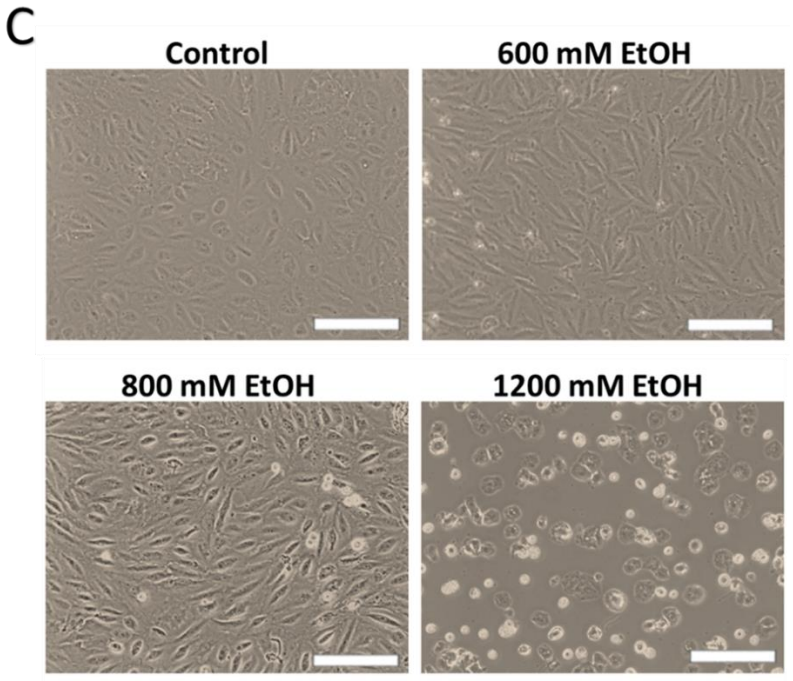

Figure 27. Apoptosis pathway activation in ARPE-19. Apoptosis markers were assayed, Caspase -3 (**A**), Bax and Bcl-2 that were represented as a ratio (**B**). Cellular morphology under phase-contrast microscopy after EtOH treatment (**C**). Protein expression was normalized by β-Actin. Values are expressed as mean ± SEM (N=3). Statistical significance was determined by means of 1-and-2-way ANOVA, and Student's t-test. Statistically significant differences were set at *p<0.05 vs. CTL group. Scale bar: 100 µm.

7.2. DAS REDUCES ETOH-INDUCED ROS PRODUCTION IMPROVING CELL VIABILITY OUTCOME

CYP2E1 metabolic activity is the major ROS producer during EtOH metabolism. Then CYP2E1 inhibitor DAS was used. As shown in **figure 28**, the selective CYP2E1 inhibition (20 mM DAS) is able to prevent the observed EtOH toxicity in RPE cells.

As described above, EtOH-induced intracellular ROS was significantly inhibited by DAS (p. value < 0.01) **figure 28A.** The use of DAS, led to a significant decrease on ROS formation in all treated groups. The effect of DAS, reached the basal values even below CTL group, **figure 28A**.

This CYP2E1 inhibition was accompanied by a significant increase in cell viability, **figure 28B**, without reaching the basal cell viability levels.

Phase-contrast microscopy images, seen in **figure 28C**, showed how 1200 mM EtOH promoted morphological alterations with much more evident refringency than control cells. Interestingly, DAS prevented those EtOH-induced morphological alterations. To confirm CYP2E1 activity inhibition after DAS treatment. ARPE-19 cells microsomes were incubated during 4 hours with 10 mM or 20 mM DAS. A significant inhibition of CYP2E1 activity could be observed with DAS (p. value < 0.01). **figure 28D**

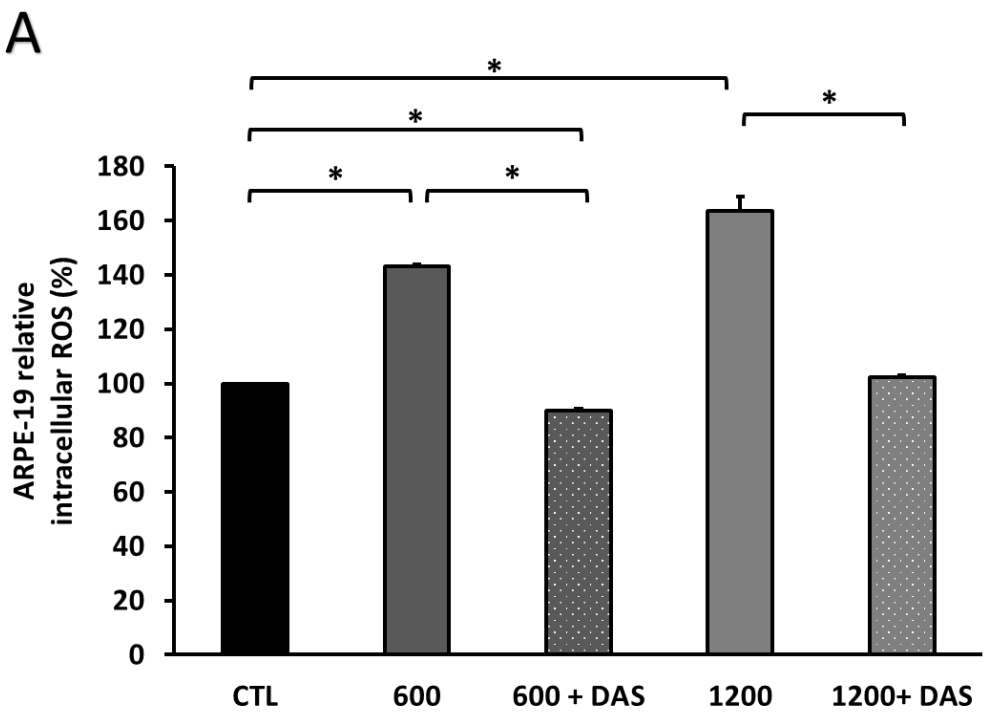

B

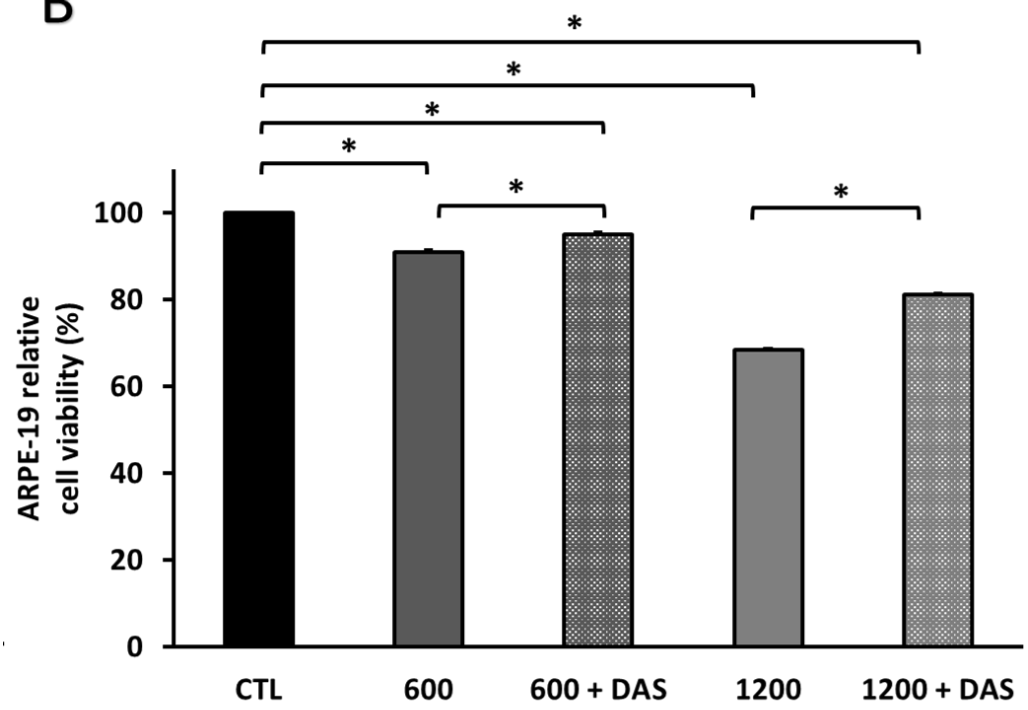
*
*
*
*
*
*
100
80
60
40
20
0
ARPE-19 relative cell viability (%)
CTL
600
600 + DAS
1200
1200 + DAS

C

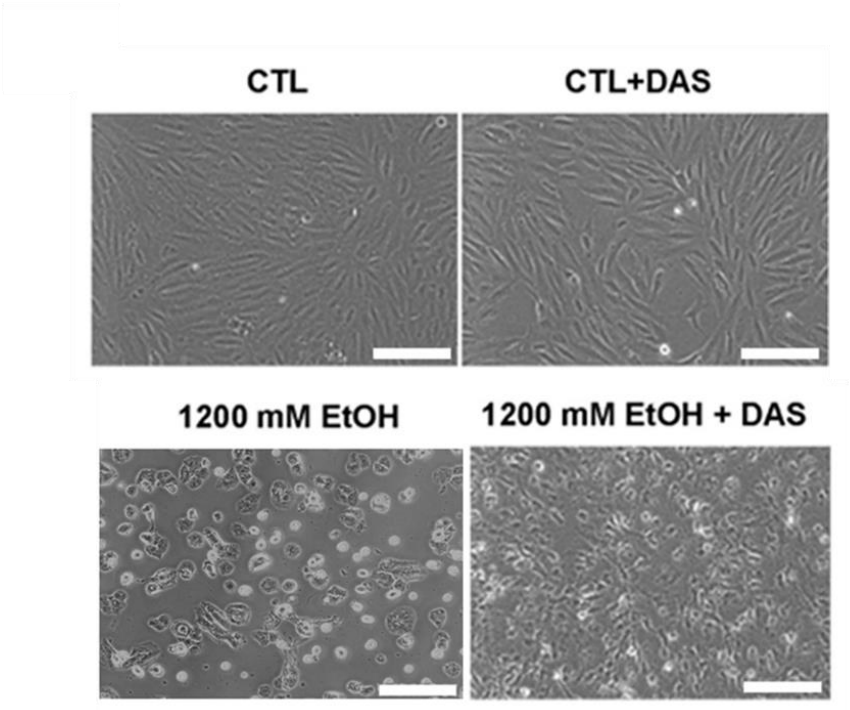
CTL
CTL+DAS
1200 mM EtOH
1200 mM EtOH + DAS

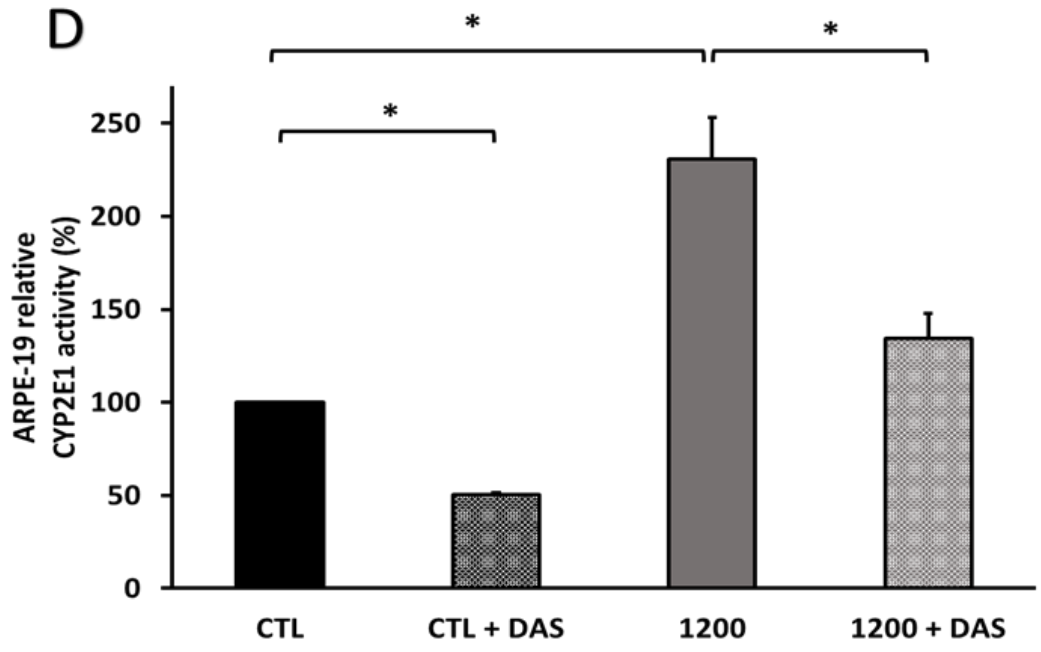

Figure 28. CYP2E1 is involved in EtOH-induced OS in ARPE-19 cells. DAS inhibits the EtOH-induced ROS production (**A**). DAS inhibits the EtOH-induced cell viability loss (**B**). Phase-contrast microscopy images of ARPE-19 cells morphology after 24 hours of 1200 mM EtOH exposure and DAS treatment (**C**). 4NC formation by CYP2E1 under inhibitory DAS treatment (**D**).Values are expressed as mean ± SEM (N=3). Statistical significance was determined by means of 1-and-2-way ANOVA, and Student's t-test. Statistically significant differences were set at *p<0.05. Scale bar: 100 µM.

7.3. DAS BLOCKS ETOH-INDUCED CYP2E1 mRNA AND PROTEIN EXPRESSION

The dramatic CYP2E1 protein overexpression observed at 1200 mM EtOH was significantly reduced by 20 mM DAS. (p. value < 0.05). Fitting with this fact, CYP2E1 mRNA overexpression was also decreased, **figure 29B**. CYP2E1 activity was almost undetectable after DAS addition in control cells. DAS provoked a reduction on CYP2E1 activity around 50% (p. value < 0.001), **figure 29C.**

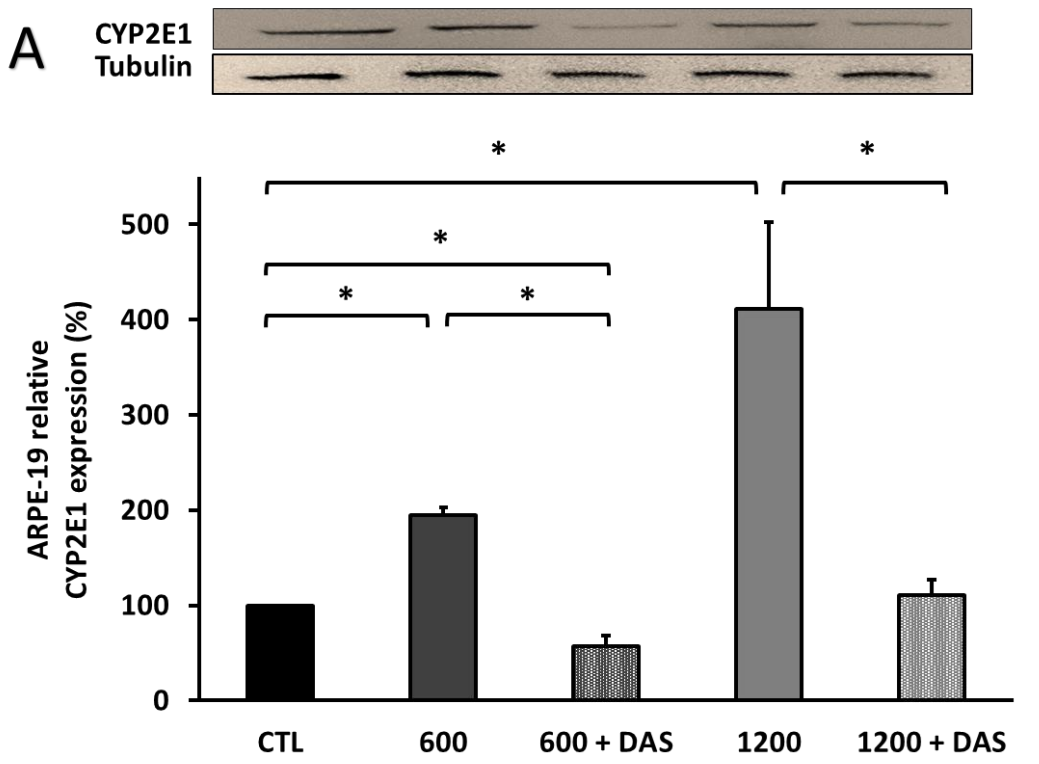
A
CYP2E1
Tubulin
ARPE-19 relative
CYP2E1 expression (%)
0
100
200
300
400
500
*
*
*
*
*
CTL
600
600 + DAS
1200
1200 + DAS

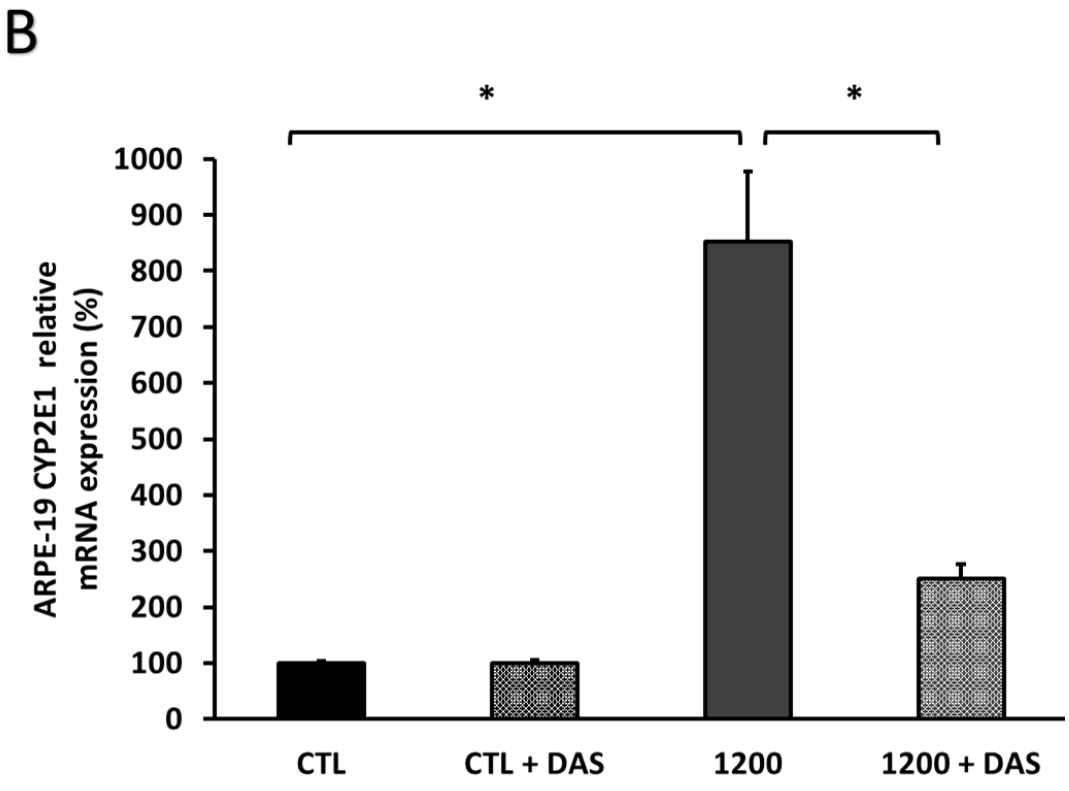
B
ARPE-19 CYP2E1 relative
mRNA expression (%)
0
100
200
300
400
500
600
700
800
900
1000
*
*
CTL
CTL + DAS
1200
1200 + DAS

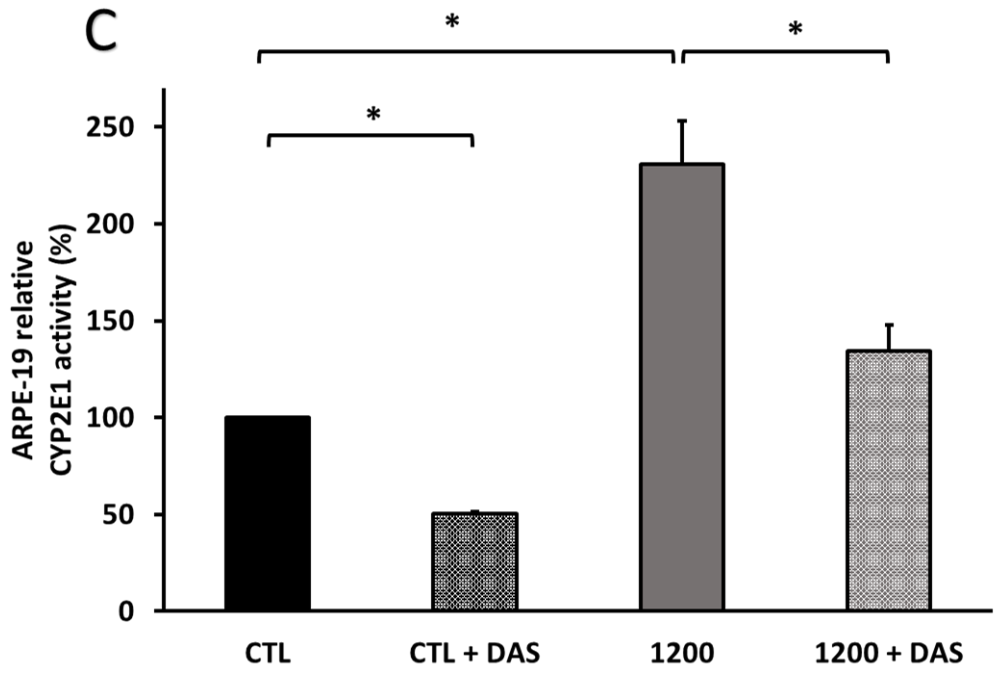

Figure 29. DAS reduced CYP2E1 mRNA and protein expression. EtOH-induced CYP2E1 protein expression also was reduced after 20 mM DAS (**A**). DAS at 20 mM inhibited EtOH-induced CYP2E1 mRNA expression to control levels (**B**). EtOH-induced CYP2E1 activity and the inhibitory effect of 20 mM DAS (**C**). Gene expression of CYP2E1 was normalized by β-Actin and CREBBP gene expression. Protein expression was normalized by Tubulin. Values are expressed as mean ± SEM (N=3). Statistical significance was determined by means of 1-and-2-way ANOVA, and Student's t-test. Statistically significant differences were set at *p<0.05

7.4. hRPE, MATURE ARPE- AND hiPSC-RPE CELLS PRESENT SIMILAR RESPONSES TO ARPE-19 UNDER EtOH EXPOSURE

In agreement with previous data (**See 1.1, figure 15B**), EtOH-induced cytotoxicity was likely observed in all studied RPE cell types. CYP2E1 inhibition by DAS was used in all RPE cell models.

20 mM DAS restored cell viability in hRPE after EtOH-treatment to basal levels (CTL group, p. value < 0.01), **Figure 30A**. EtOH-induced ROS formation was also demonstrated in hRPE cells, **figure 30B.** Similarly, 20 mM DAS blocked 100% of this EtOH-dependent ROS formation. Furthermore, EtOH exposure promoted CYP2E1 expression also in hRPE cells. The addition of DAS blocked this response.

Immunofluorescence against CYP2E1, **figure 30C**, showed a cytoplasmic location of CYP2E1 in hRPE cells. More CYP2E1-positive cells were labelled after 1200 mM EtOH exposure. Notably, 20 mM DAS reduced the number of CYP2E1–positive cells.

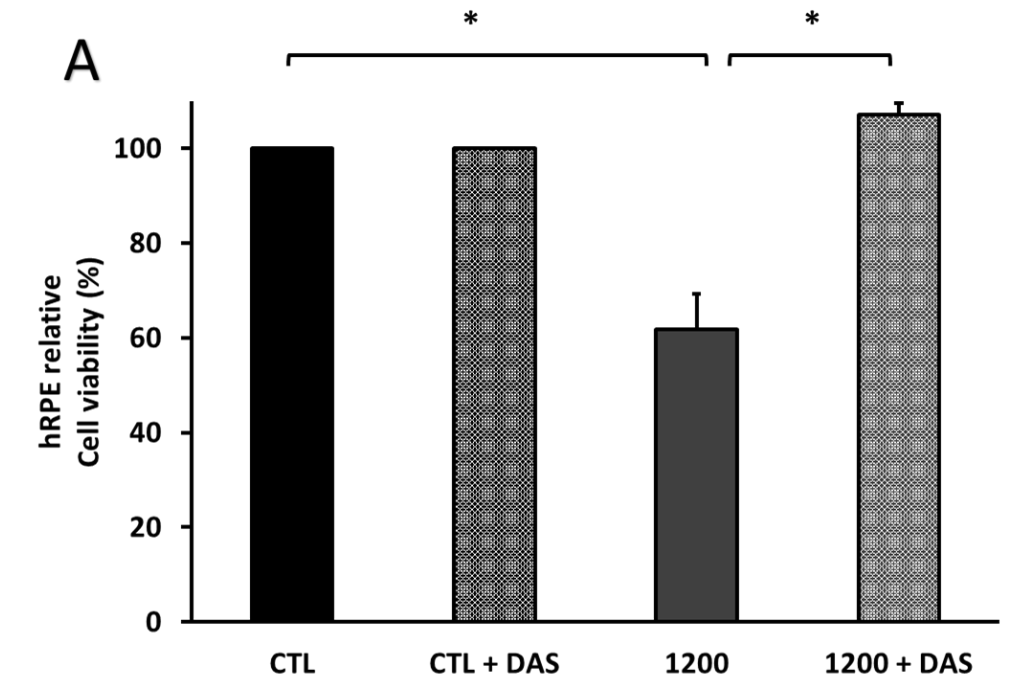
A
*
*
hRPE relative
Cell viability (%)
0
20
40
60
80
100
CTL
CTL + DAS
1200
1200 + DAS

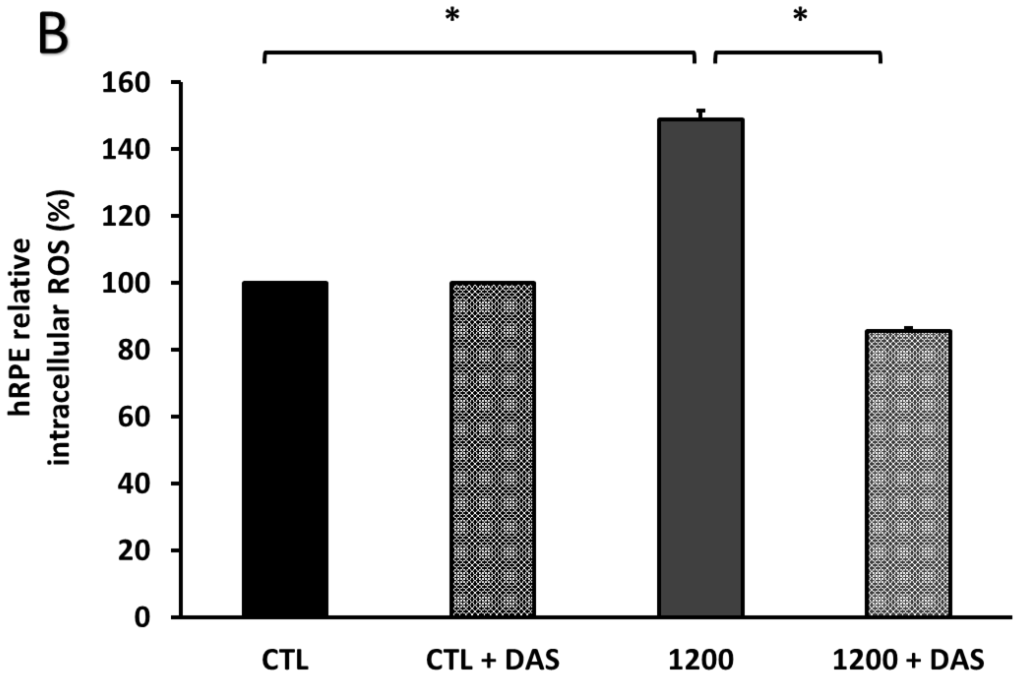
B
*
*
hRPE relative
intracellular ROS (%)
0
20
40
60
80
100
120
140
160
CTL
CTL + DAS
1200
1200 + DAS

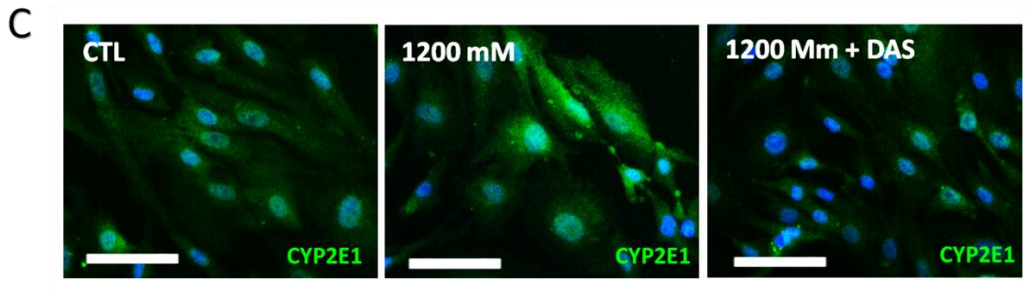

Figure 30. hRPE EtOH response. Human RPE cell viability (XTT assay) at 1200 mM of EtOH and DAS treatment (**A**). Inhibitory effect of DAS on EtOH-induced ROS production in hRPE cells, DCFH-DA fluorescence, (**B**). Immunofluorescence of CYP2E1 on hRPE cells after 24 hours of 1200 mM EtOH exposure and DAS treatment (**C**). Values are expressed as mean ± SEM (N=3). Statistical significance was determined by means of 1-and-2-way ANOVA, and Student's t-test. Statistically significant differences were set at *p<0.05. Scale bars*:* 100 µm.

Conversely, 600 mM EtOH did not affect hiPSC-RPE and mature ARPE-19 cell viability. As expected, 20 mM DAS was ineffective in any case, **figure 31**.

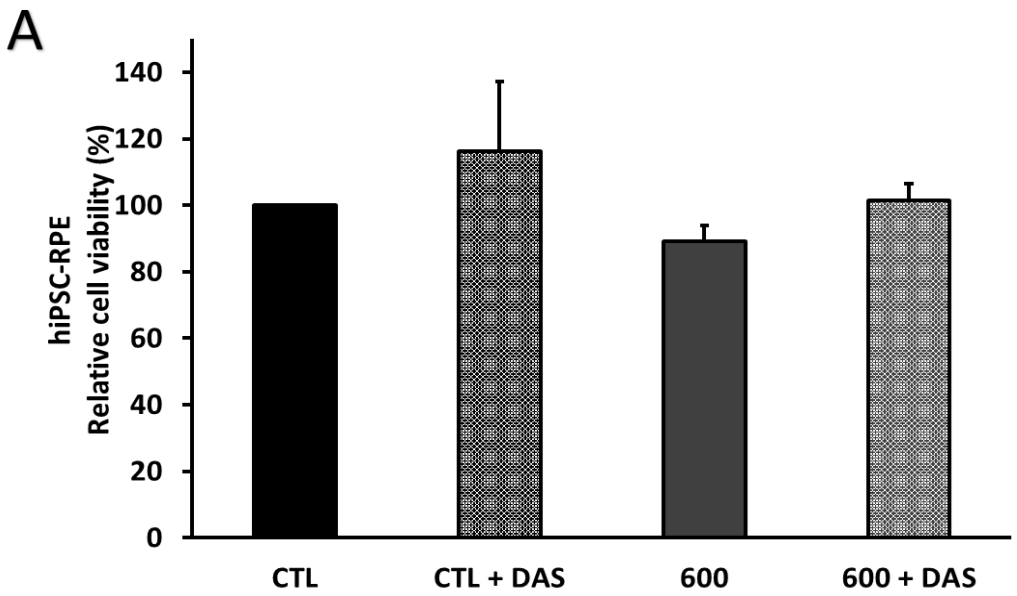

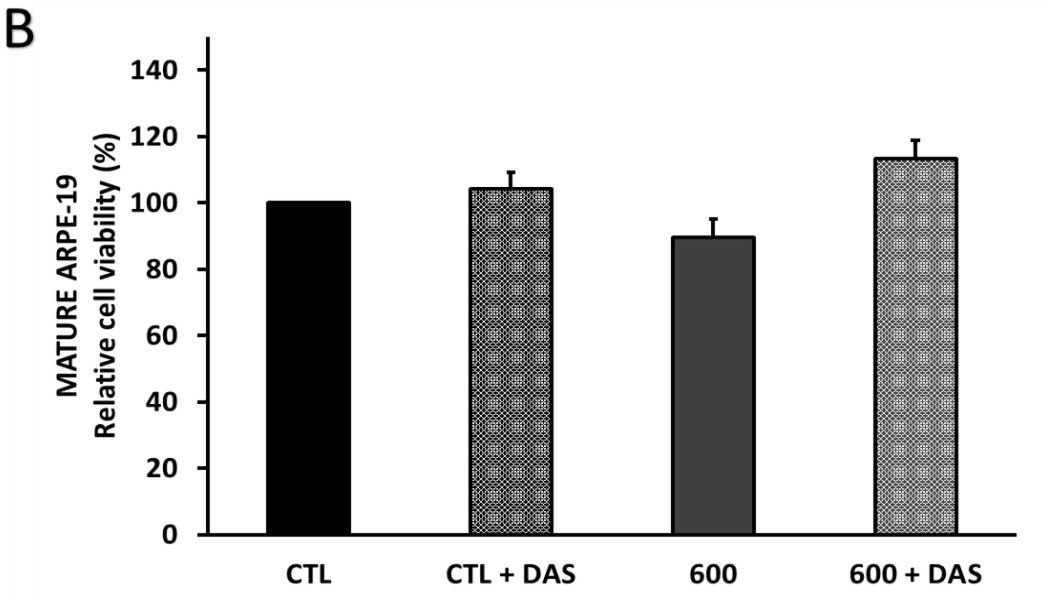

Figure 31. hiPSC-RPE and mature ARPE-19 cells EtOH response. HiPSC-RPE cell viability (XTT assay) (**A**) and mature ARPE-19 cells (**B**) at 600 mM of EtOH and 20 mM of DAS treatment (**A**). Inhibitory effect of DAS on EtOH-induced Values are expressed as mean ± SEM (N=3).

8. CYP2E1 IS IMPLICATED IN RPE CELL RESPONSE

8.1. DAS MODIFIES EtOH-INDUCED CELL STRESS BIOMARKERS

The treatment with 20 mM DAS did not modify the EtOH-induced changes in the expression of CITED-2, SIRT-2, P21/CIP1, HIF-1α, P27, p-P53 and PON2, **figure 32A**. However, Ethanol-induced biomarkers as CA9, CYT-C, HSP60 and P-JNK PAN were reduced after DAS exposure **figure 32B**. In these cases, CYP2E1 could be modulating cellular response against the OS generated by the EtOH.

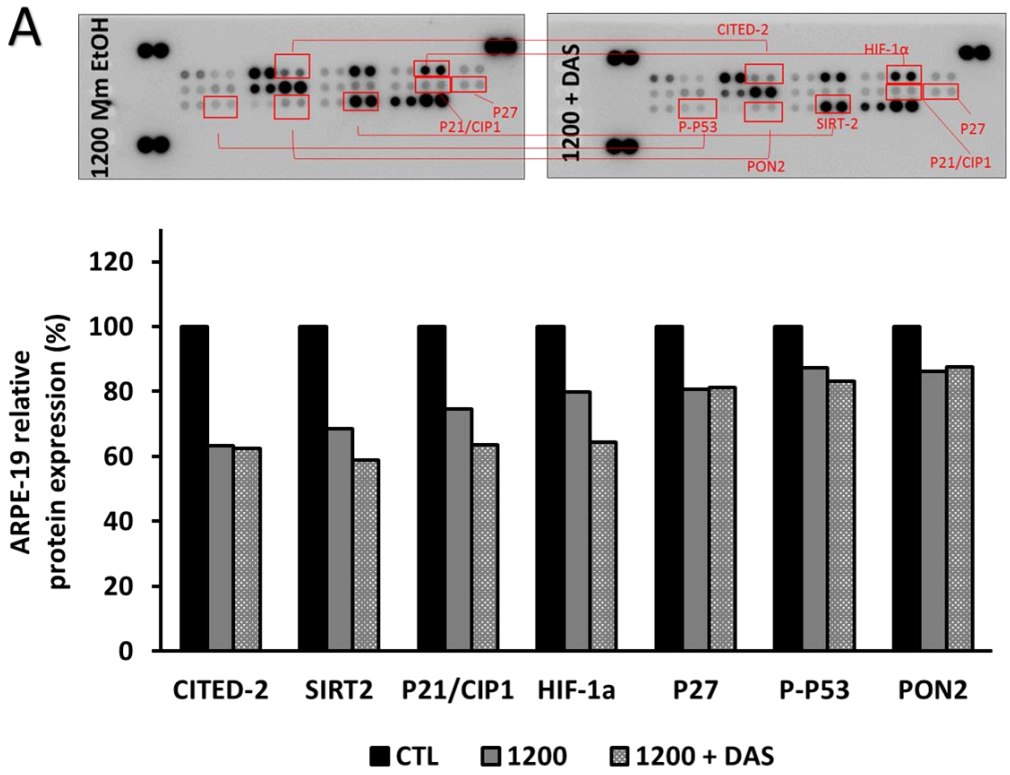

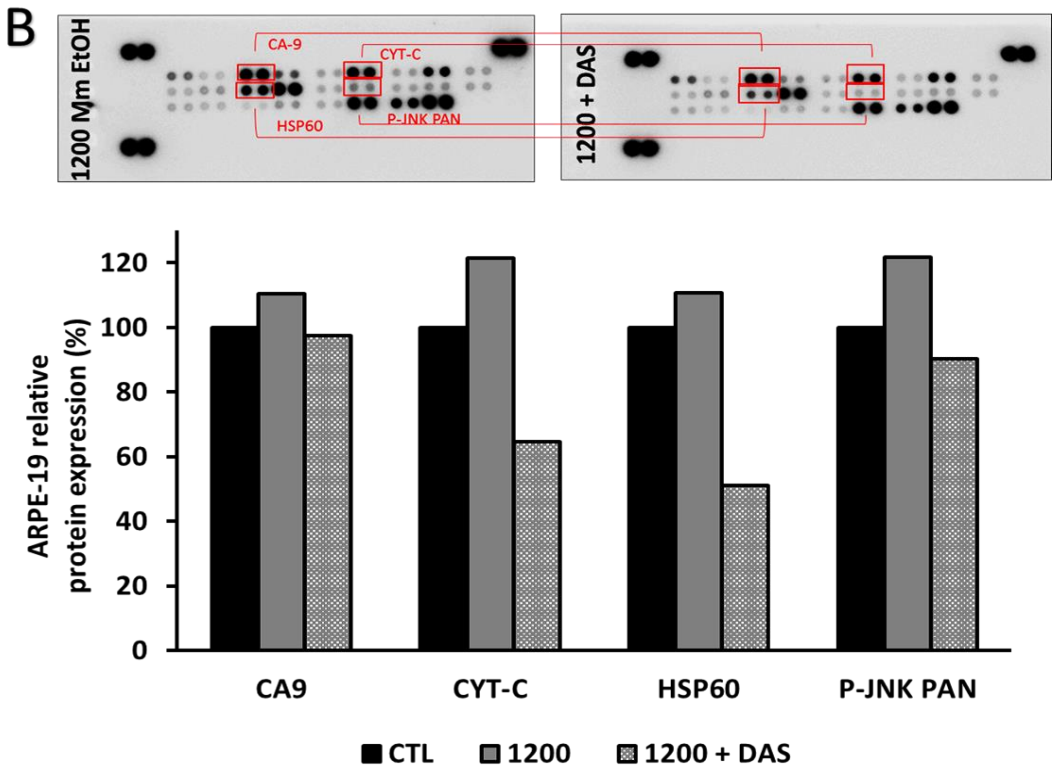

Figure 32. ARPE-19 cell stress profile after EtOH treatment. After 24 hours of EtOH treatment, the ARPE-19 cell survival and stress markers profile was decreased and DAS did not change the situation (**A**) Additionally in all OS markers studied 20 mM DAS modulated the EtOH cellular response (**B**). Values are expressed as average of an N= 3 samples pooled.

8.2. NFKB IS REGULATED BY CYP2E1

With the aim to study the effect of CYP2E1 in APRE-19 cell stress response. ARPE-19 cells were treated with 4 µM of the antioxidant NAC. The **figure 33** shows that CYP2E1 inhibition by DAS increased the expression of NFKB. On this line, NFKB quantification by western blot, **figure 33A** demonstrated higher NFKB levels in DAS treated cells compared to non-treated cells.

The use of NAC also reversed the effect of EtOH on NFkB. These data suggest that the expression of NFKB is regulated by CYPE21.

The representative pictures on **figure 33B** showed an increase of NFKB expression with 20 mM DAS. These results were higher than NAC treated group. No NFKB activation was observed in any case.

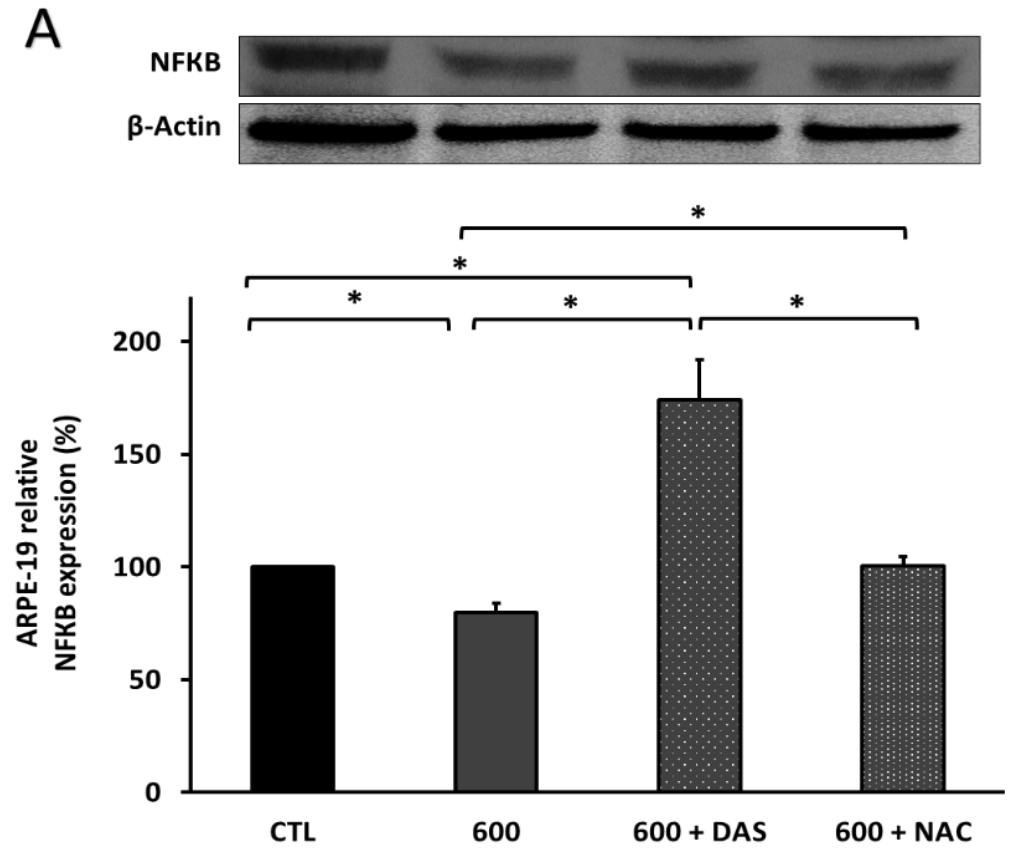

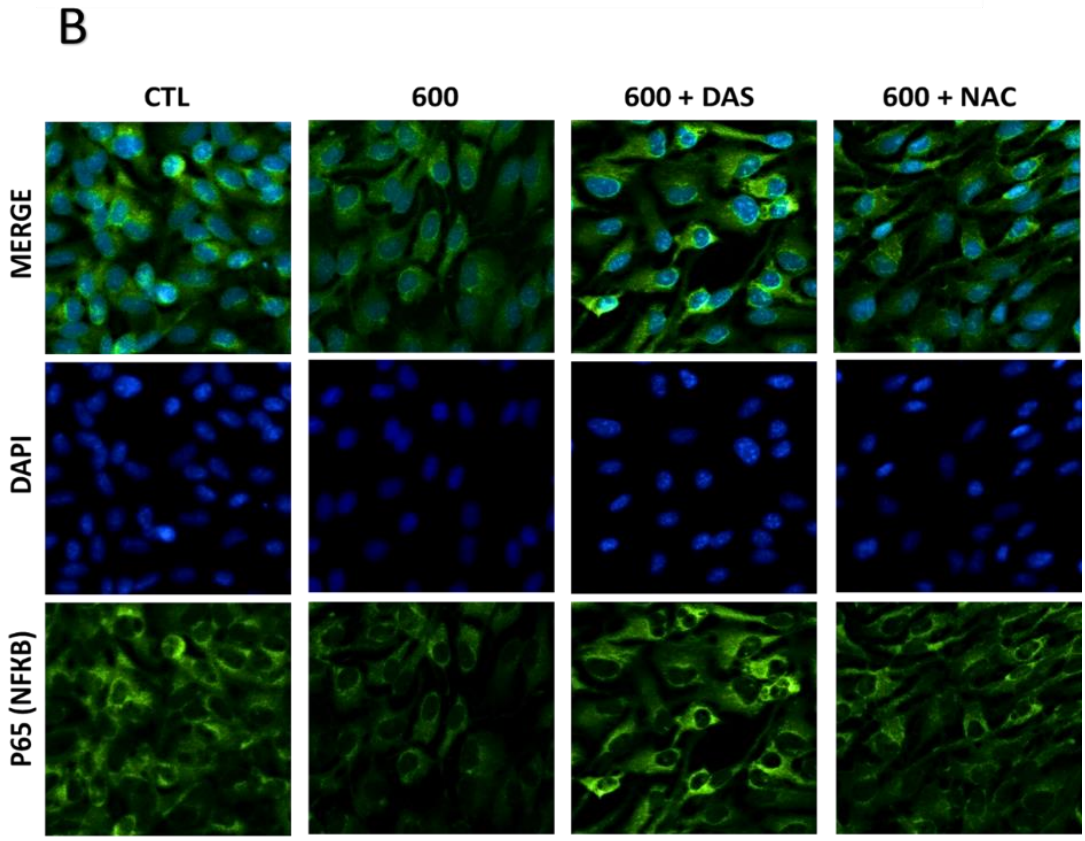

Figure 33. NFKB profile expression in ARPE-19 after EtOH and DAS treatment. Protein expression quantification by WB shows changes in NFKB profile expression blocking CYP2E1 with DAS and NAC treatment (**A**). The immunofluorescence showed that there is an enhanced of NFKB expression, but there is not nuclear translocation (**B**). Protein expression was normalized by β-Actin. Values are expressed as mean ± SEM (N=3). Statistical significance was determined by means of 1-and-2-way ANOVA, and Student's t-test. Statistically significant differences were set at *p<0.05 vs. control group.

9. CYP2E1 REGULATION IN RPE CELLS

9.1. INTRACELLULAR ROS IS REDUCED BY NAC IMPROVING CELL VIABILITY OUTCOME

The use of NAC attenuated EtOH-induced free radical damage, **figure 34**. 4 µM NAC improved cell viability, **figure 34A**, and reduced ROS levels (p. value < 0.01), **figure 34B**. Even so, it was possible to decrease around 20% intracellular ROS compared with CTL cells. Superoxide anions levels were less reduced by NAC **figure 34C.** The **figure 34D** shows that, superoxide anions did not represent the major free radicals increased in ARPE-19 cells under 600 mM EtOH treatment, however the use of NAC decreased almost all of them.

A

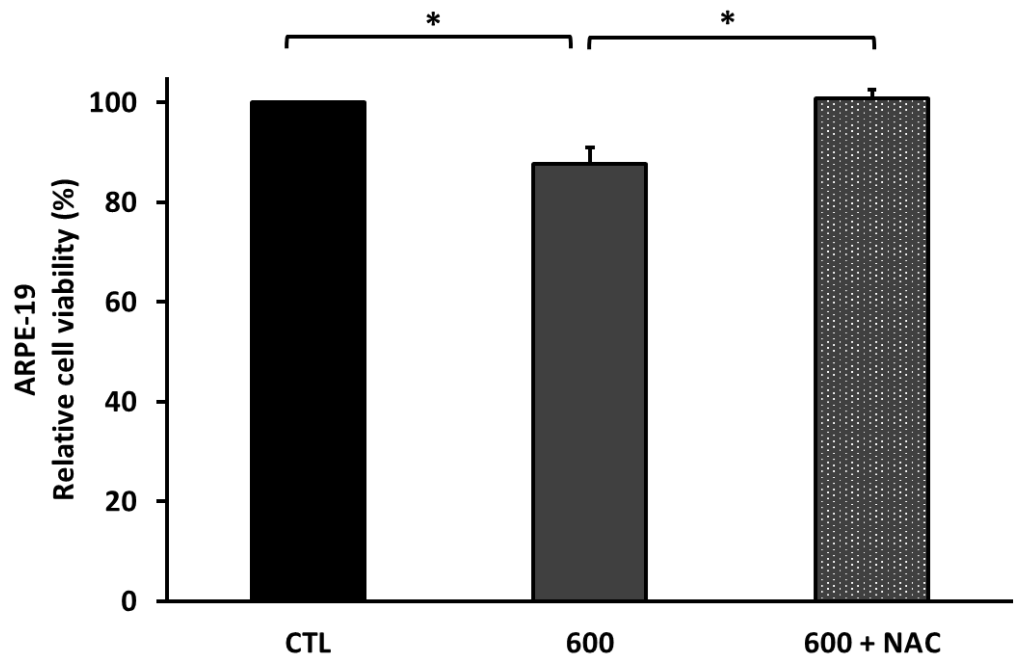

B

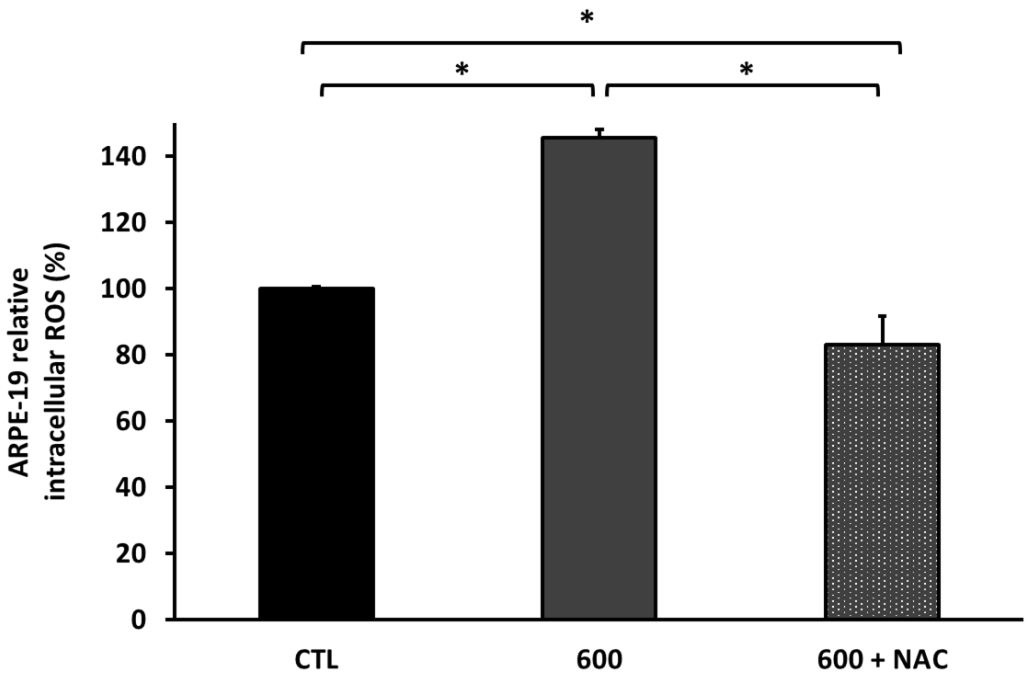
*
*
*
ARPE-19 relative intracellular ROS (%)
140
120
100
80
60
40
20
0
CTL
600
600 + NAC

C

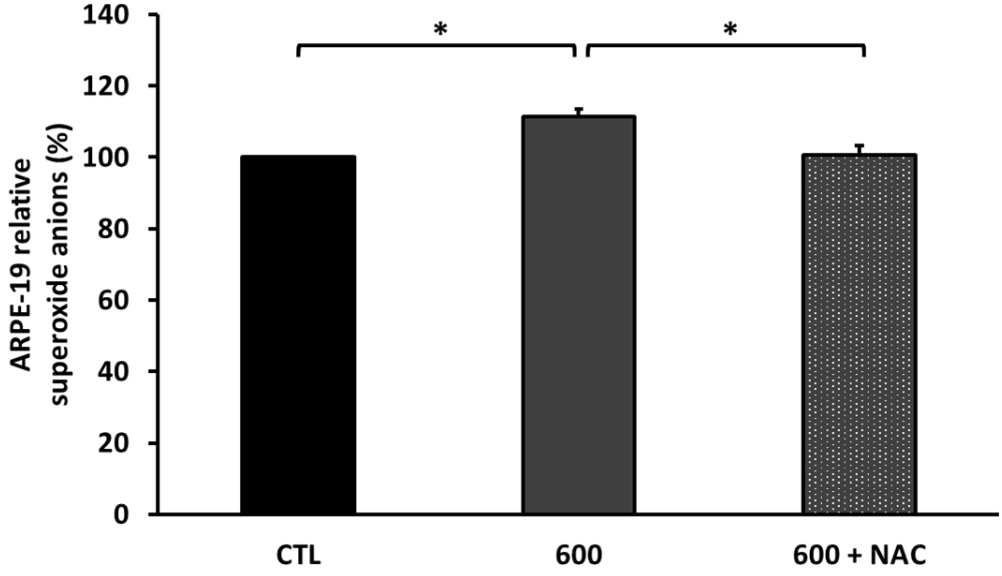
*
*
ARPE-19 relative superoxide anions (%)
140
120
100
80
60
40
20
0
CTL
600
600 + NAC

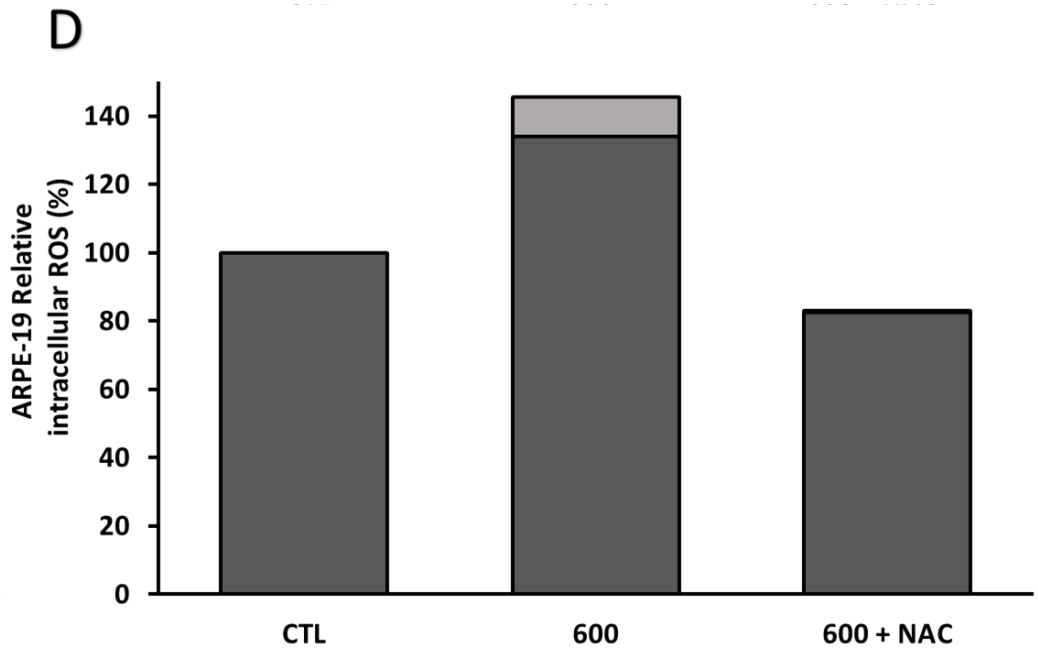

Figure 34. NAC decrease intracellular ROS. The cell viability assay (XTT) after 24 h 4 µM of NAC treatment (**A**). Total intracellular ROS (DCFH fluorescence) in ARPE-19 cells (**B**). At the same way superoxide anions measured by DHE (**C**). Superoxide anions versus the rest of free radical (**D**). Values are expressed as mean ± SEM (N=3). Statistical significance was determined by means of 1-and-2-way ANOVA, and Student's t-test. Statistically significant differences were set at *p<0.05.

9.2. ROS MODULATES CYP2E1 EXPRESSION

To understand the effect of ROS in the regulation of CYP2E1 protein expression. Western blot was assayed in ARPE-19 treated cells with 600 mM EtOH + 20 mM DAS or 4 µM NAC. As shown in **figure 35**, DAS and NAC promoted similar results.

NAC significantly decreased CYP2E1 protein expression (p. value < 0.001) around 150% compared to 600 mM EtOH. Also, there were not statistically significant differences between DAS and NAC. Blocking either the enzymatic CYP2E1 activity or the intracellular ROS reduced the EtOH-induced CYP2E1 overexpression in ARPE-19 cells.

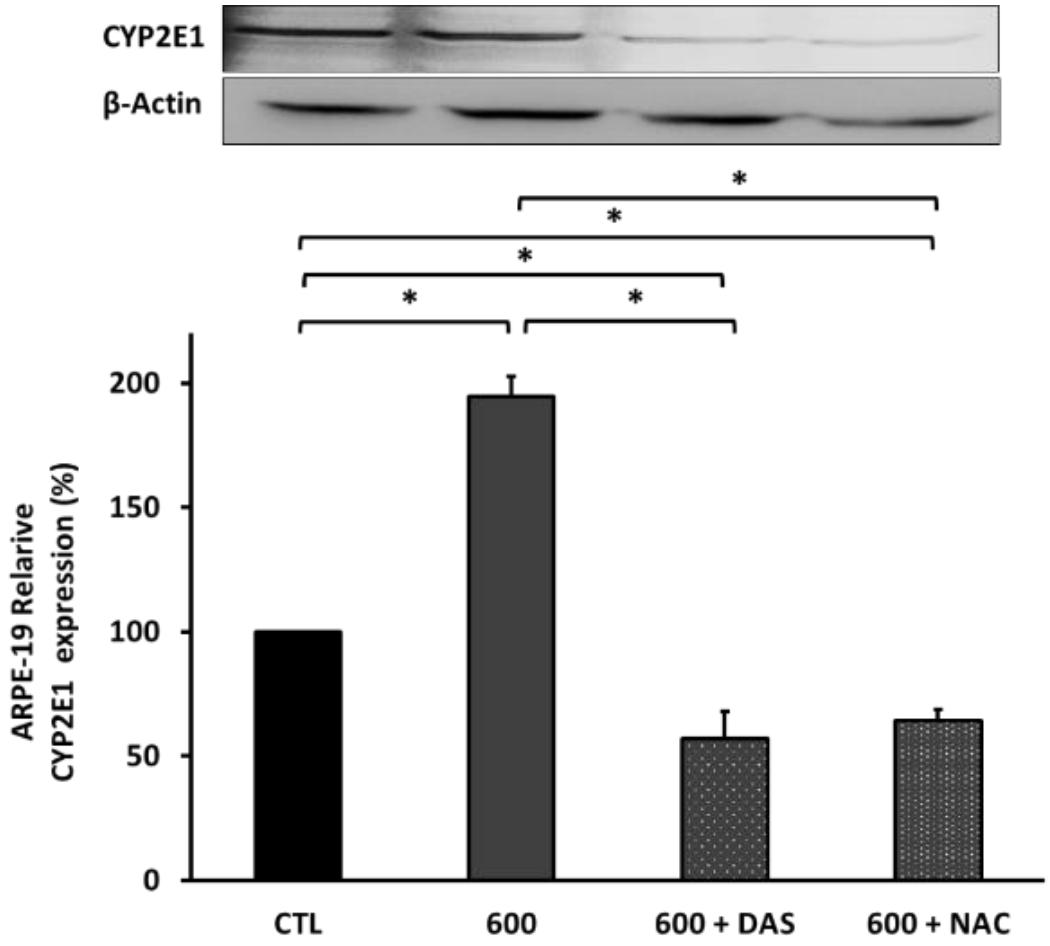

Figure 35. ROS regulates CYP2E1 expression in ARPE-19 cells. CYP2E1 expression in ARPE-19 after EtOH treatment with 20 mM of DAS and 4 μM of NAC during 24h were measured by WB. Protein expression was normalized by β-Actin. Values are expressed as mean ± SEM (N=3). Statistical significance was determined by means of 1-and-2-way ANOVA, and Student's t-test. Statistically significant differences were set at *p<0.05.

CHAPTER V

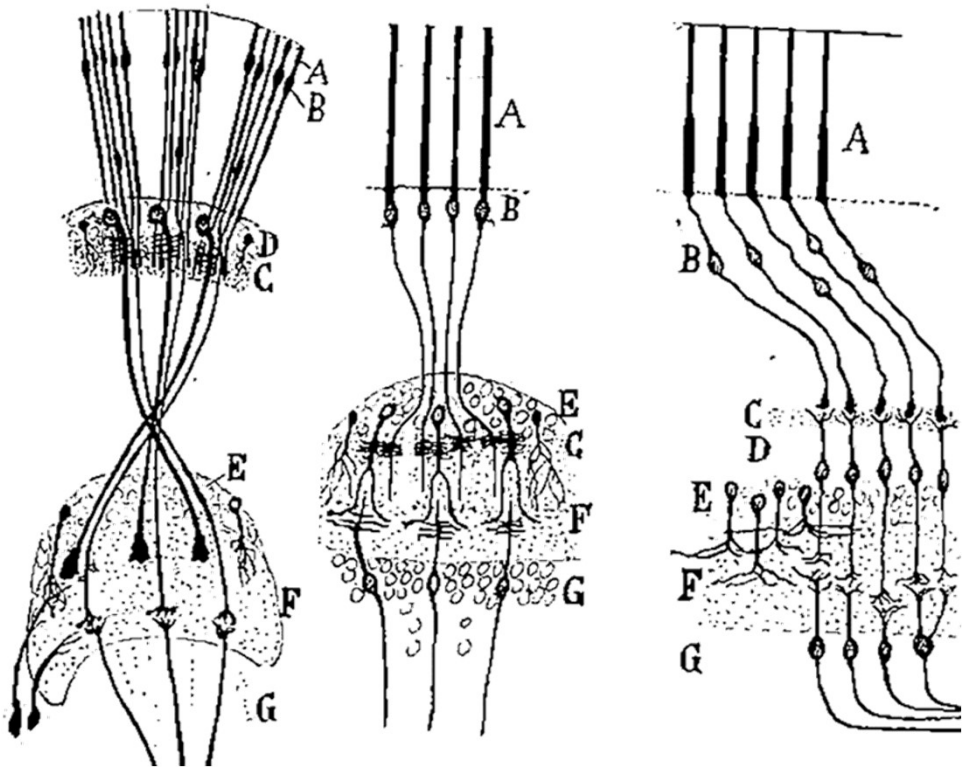

Homologous neurons in the retina of mammals (right), insects (left) and cephalopods (center)

S. Ramón y Cajal

Discussion

Considering RPE as a restrictive physiological part of the BRB, in this thesis we propose that the RPE dysfunction, due to OS generated by alcohol consumption, can lead to an overall deterioration of the retina. Any damage in the RPE will trigger damage to the retina or increasing the damage generated by other retinopathies.

Some epidemiological data support the suggestion that EtOH may affect the retina (193,194). Fitting with this, electroretinograms recorded from chronic EtOH-treated rats showed that the b-wave amplitude was significantly diminished. B-wave amplitude is attributable to depolarizing bipolar cell activity and Müller cells (195).

The presence of CYP2E1 and ADH (196, 197) in ARPE-19, hRPE and hiPSC-RPE cells strongly supports the proposal of a direct EtOH metabolism in RPE. Cytochrome p450 2E1 represents the major EtOH detoxifying isoform that furthermore is induced by EtOH, but paradoxically it is poorly expressed in RPE cells in basal conditions (198). CYP2E1 induction by ROS strongly suggests additional roles for CYP2E1 related to vision and cellular signaling modulating by OS. Additionally, EtOH and LPO metabolites inhibit the conversion of all-trans-retinol to all-*trans*-retinal (199) affecting visual cycle.

Besides, it is possible to detect a two-phase response in the release of growth factors by RPE as well as of inflammatory and cell stress biomarkers. This fact is dependent on ROS levels and CYP2E1 expression, giving us the key to reinforce the protective and regulatory role of this outer BRB under toxic treatment.

1. EtOH INDUCES SIMIAR CYTOTOXICITY PATTERN IN DIFFERENT RPE CELLS

Our first results reveal that ARPE-19 cells are an appropriate model for the study of cellular damage caused by EtOH-generated ROS (**See results, figure 14 and 15, chapter IV**). The EtOH cytotoxicity measured by XTT showed that there are not statistically significant citoxicity differences between ARPE-19 cells, RPE primary culture and mature ARPE-19 cells (**Figure 14D**). Alike, when ARPE-19 cells were compared with hiPSC-RPE cells, (**Figure 15F**) reinforces previous results.

EtOH represents an oxidative insult for our cells. In agreement with Brossas JY, et al. (200), 1200 mM EtOH exerts deleterious effects in ARPE-19 cells, hRPE cells and mature ARPE-19 cells (**Figure 14A, 14B and 14C respectively**). Surprisingly, hRPE cells show significant changes on cell viability already at 400 mM EtOH and mature ARPE-19 cells at 200 mM. This suggests that both types of cells are more susceptible to EtOH damage than ARPE-19 cells, where significant changes were found at 600 mM EtOH.

As noted by Flores-Bellver M, et al. (49) and Bonet-Ponce L, et al. (47), sublethal EtOH concentrations (below 600 mM EtOH) promote cellular alterations in terms of mitophagy and protein aggregation in ARPE-19 cells. Interestingly, this autophagic response seems to be related to cell protection.

On the other hand, hiPSC-RPE showed higher resistance to EtOH toxicity, 800 mM EtOH was required to detect cell death (**Figure 15B**). This fact suggests that hiPSC-RPE cells are more similar to ARPE-19 cells, than the other ones. The finding that mature ARPE-19 and hRPE cells were more sensitive to EtOH than ARPE-19 cells confirms that, ARPE-19 cells are very resistant to OS (200, 201). Being a commercial cell line, this difference could be explained in terms of OS resistance. Although, under this OS insult, ARPE-19 cells preserved the RPE structural and functional characteristics.

Interestingly, 100 mM EtOH promotes cell damage in an astrocytes, (161) whereas 200 to 600 mM EtOH levels are needed in mature ARPE-19, hRPE and ARPE-19, respectively, to decrease cell viability. Probably, the fact that RPE cells constitutively express ADH (202, 203) and CYP2E1, (**Figure 25**), might explain their resistance against xenobiotics and toxic agents, also EtOH.

The use of ARPE-19 as an RPE cellular model is extended in ophthalmology, cellular biology and physiology fields. Dunn KC, et al. (44), evidenced that ARPE-19 has structural and functional properties characteristic of RPE cells in vivo. Suggesting that this cell line will be valuable for *in vitro* studies of RPE physiology. Also, ARPE-19 cells have been used in studies about OS (48), cell signaling pathways (47), and inflammation diseases (50).

The present work demonstrates that in our EtOH toxicity study, ARPE-19 cells are an excellent model of RPE cells. The cells had the same cytotoxicity that the rest of RPE cells used.

Nevertheless, is relevant to keep in mind seeding and maintenance conditions developed in cell cultures. As Tian J, et al. demonstrated (204,205), both conditions may affect cell responsiveness and survival. The ARPE-19 cells behavior, differed according to seeding density (**Figure 15G**). The same happened with mature cells, since they are the same ARPE-19 cells maintained for 2 months in culture. The fact of experiencing this maturity condition makes them more sensitive to EtOH treatment (**Figure 14A versus 14C**).

One limitation of this study deals with the EtOH concentrations reaching the eye. Most probably, EtOH circulating levels will be lower than the initial concentrations used herein for cell cultures. Additionally, the presence of the choriocapillaris will affect the actual EtOH concentration finally reaching the eye. In this line, it is very interesting to note that vitreal EtOH levels are higher than those obtained from blood, (206) so it seems reliable that EtOH reaches the eye. As previously reported, 40 mM EtOH circulating blood levels significantly affected rat retina (142, 195, 207, 208). These EtOH levels are much lower than used initially for cell cultures (600 mM). Obviously, vaporization of EtOH in cultures is a significant phenomenon affecting the final EtOH concentration and, therefore, it is extremely difficult to confirm the actual EtOH concentration reaching the cultured cells (209).

2. EtOH ACTIVATES A ROS DEPENDENT CELLULAR RESPONSE IN RPE CELLS

The highest EtOH concentration used modified the cellular response in ARPE-19 cells (**See results, figure 16, chapter IV**). 40% of cell death was found at 1200 mM EtOH, provoked an activation of stress response of these cells.

Among the increased markers, it is possible to emphasize their implication on mitochondria maintaining function and activation of ROS-dependent cellular signaling pathways (**Figure 16A**). Knowing that mitochondria is one of the organelle more sensible to ROS presence in ARPE-19 cells (210) it is plausible to note how CYT-C and HSP60 are increased under EtOH treatment. It is noteworthy that studies performed on Caco-2 cells (human intestinal epithelial cells) HSP60 expression increased significantly at the concentration of 4% (700 mM) of EtOH (62). In agreement with previously published we found an increase of HSP60 under high EtOH concentrations on ARPE-19 cells (**Figure 16A**).

Previous publications showed that there is an activation of MAPK due to OS also by alcohol (79,174). In either *in vivo* or *in vitro* models of alcoholic liver disease, an increase of gene expression of the MAPK pathway was found. For example, in human monocytes, acute alcohol exposure increased JNK phosphorylation (211). P-JNK PAN was also increased in ARPE-19 cells under EtOH treatment (**Figure 16B**).

In a different way, the fact that the transcription factor HIF-1α was decreased, could be affecting the regulation of RPE growth factors expression, as well as a cellular stress response (76). One of the most diminished proteins was CITED-2, involved in the modulation of p53-mediated apoptosis, which was also decreased. ARPE-19 cells shown similar behavior in studies by Korthagen NM, et al. (212). After stimulation of inflammation by treatment with TNF-α, they observed that among the downregulated genes were transcription factors implicated in ocular development (SIX3, PAX6) and modulation of p53-mediated apoptosis (CITED-2) (212). Our data may lead us to suppose that the overexpression of certain markers, in turn favors the decrease of pro-apoptotic proteins. CITED-2 induces acetylation of p53 and enhances TNF-α induced apoptosis. Our results, once again reveal the specific downregulation of CITED-2 in ARPE-19 cells. This fact could be related to the resistance of these cells to the pro-apoptotic effects of OS (212).

The inhibition of SIRT-2 has been suggested to be neuroprotective. Indeed, reduced SIRT-2 expression is associated with increased photoreceptor survival in flies, although it is not yet clear whether SIRT-2 activation has negative effects in aging retinas (213).

SIRT-2 is also declining in our results. While studies of other groups showed that under conditions of OS, there is an increase of SIRT-2. Meléndez-García R, et al, (213), observed that prolactin maintains SIRT-2 levels contributing to RPE survival by reducing ROS levels. Conversely, under oxidizing conditions increased levels of SIRT-2, leading to RPE cell death (213). All of these results demonstrate that ARPE-19 cells could be activating different signaling pathways in response to the toxic effect of ROS generated by EtOH.

3. A ROS-DEPENDENT APOPTOSIS PATHWAY IS INDUCED BY EtOH

There are many reports that relate alcohol consumption with the increase of OS. Also there is a correlation in alcoholic patients between HNE adducts, suggesting that the latter catalyze LPO and HNE production (211). In addition, previous results in our group showed the increment of 4-HNE adducts and LPO in ARPE-19 cells under EtOH treatment (49).

The increase of ROS by EtOH treatment did grow significantly in RPE cells (**See results, figure 17, chapter IV**). 200 mM EtOH was enough to increase, almost 20%, intracellular ROS in ARPE-19 cells (**Figure 17A and 17B**) and hRPE cells (**Figure 17C**).

Superoxide anions did not represent the highest percentage of free radicals in the set of ROS produced by the cells. But they are the key, at higher EtOH concentrations, for the existence of significant differences (**Figure 17E**), coinciding with the concentrations that give rise to cell death.

In our cells, this increase of ROS generated by EtOH is directly related to cell death. (**Figure 17F**). As already observed Conde de la Rosa L, et al. (214), superoxide anions are responsible for the activation of caspase induced apoptosis in hepatocytes (214). In ARPE-19 cells there is an increase of apoptosis markers from 400 mM EtOH (**Figure 18A**). Which could be explained by the increase of the superoxide anions in those experimental groups.

However, the fact that OS was increased at 200 mM and 400 mM EtOH is not a cause for cell death. As shown in other published works (48, 49, 210), sublethal levels of ROS provoked an increase of autophagy (as a pro-survival processes) in ARPE-19 cells. This means that there is not cell death. In this way, after 400 mM EtOH, there is a greater increase of Bcl-2 (pro-survival) than Bax (pro-apoptotic) thus compensating the apoptosis activation (**Figure 18B and 18C respectively**).

Finally, it is important to remark that it is necessary a higher EtOH concentration than 600 mM during 24 h to loss plasma membrane integrity (**Figure 18D**) and activate apoptosis pathway, causing cell death.

4. EtOH INDUCES RPE BARRIER DYSFUNCTION

4.1. EtOH INCREASE RPE BARRIER PERMEABILTY

We should be aware that the increase of EtOH-mediated OS affects the permeability of the membrane (215-218). As already mentioned in the previous section, alcohol damages the plasma membrane integrity in RPE cells. Further, intercellular junctions could be affected too.

The most common methods to explore the function of the RPE barrier are measuring TER and content of the main TJ protein, ZO-1 (219). Our results showed a decrease of ZO-1 expression, which was dependent on EtOH concentration used (**See results, figure 19A and 19B, chapter IV**). Other authors pointed out that increased OS increases the expression of ZO-1 in ARPE-19 cells (220). This difference may be due to their treatment with tunicamycin (TM) or thapsigargin (TG) which generates endoplasmic reticulum (ER) stress. Moreover, Yoshikawa T, et al. (220), observed that this barrier damage was accompanied by an increase of VEGF, something that our results did not show either, (**Figure 22**).

As expected, TER assay revealed that the epithelial resistance decreases considerably with EtOH treatment (**Figure 19C**). TER measurement is a useful task to evaluate the establishment of an epithelial barrier function based on the formation of TJ. Changes in TER measurements can be used, then, to probe the integrity and RPE barrier function as an early marker of RPE injury (221).

It should be noted that at 1200 mM EtOH we found a considerably lower number of cells due to the significant increase in cell death which contributes to this result. On the other hand, the TER decline showed at 1200 mM in ARPE-19 cells could be explained because several pro-inflammatory cytokines act decreasing TER, increasing the permeability and altering the expression or content of TJ molecules (106,107,220).

4.2. EtOH MODIFIES THE PROFILE OF PROTEOME AND GROWTH FACTORS EXPRESSION

Inflammation and angiogenesis are the main responses presented in ocular diseases. In addition, these routes converge with each other. Namely, the activation of one depends on the other one (76, 98, 99). One of the RPE function is to maintain the correct concentrations of particular factors and proteins for retinal health (9, 28). Some of them are angiogenic factors (VEGF), inflammation biomarkers (ILs, TNF-α) even proteins involved in both processes (MMPs and TIMPs). It is important to have a complete pathway diagram to know how EtOH affects BRB function.

EtOH treatment modified the proteome profile in ARPE-19 cells (**Figures 20-24**). These results would be indicating that damage in the RPE barrier has occurred. Among different inflammation related proteins it should be noted that TIMP-1, TIMP-4 and MMP-8 and MMP-9 are enhanced in ARPE-19 cells after EtOH exposure (**Figure 20A**). As indicated, VEGF requires for its angiogenic action some enzymes like MMPs. TIMP-1 and TIMP-4 are natural inhibitors of MMPs. A correct balance between these and MMPs is necessary for the ECM integrity maintenance. The modification of the components of the ECM gives rise to inflammatory reactions and participates in the secretion of MMPs (222). The expression of MMPs is low in healthy tissues and its expression is elevated during inflammatory, autoimmune, degenerative, neoplastic and angiogenic lesions (223).

The increase of ROS promotes also the expression of TGF-β1, which induces the activation of NFKB (224). Nevertheless, EtOH treatment decreased the TGF-β1 expression in ARPE-19 cells (**Figure 20B**). In addition there was no NFKB activation, P65 translocation to the nucleus was not detected (**Figure 24**). Its regulatory function in inflammation and angiogenic process is complicated and controversial. Since, it has been implicated in different signaling pathways (225, 226, 227). While some studies support its role as a tumorigenic suppressor, others claim to act by promoting tumor formation (228, 229).

200 mM EtOH seems to be a critical concentration. At this dose, there is a modification in the profile expression of some ILs such as IL-8 (**Figure 20B**) or IL-1β. It is possible to find a clear decrease of IL-1β protein expression at 200 mM EtOH, followed by an increase, comparing to CTL group (**Figure 20A**). Some studies affirm that VEGF interacts with IL-1β in the angiogenic and inflammatory response (230, 231). IL-1β is able to activate the expression of some MMPs (232), such as MMP-3 (233). In addition, other authors affirm that IL-1β could induce tumor progression, since it contributes to the increase of vascularization (234).

Angiogenesis related proteins show clear modification after EtOH treatment too (**Figure 21**). HGF and FGF-7 were decreased at 600 mM EtOH (**Figure 21A**). HGF is secreted by the cells during inflammation process. Some studies show that it is able to promote the proliferation, activation and differentiation of endothelial and epithelial cells during angiogenesis, in intestine diseases (235, 236). Our results manifest a clear HGF protein expression decrease at 400 and 600 mM EtOH. Thus would be contributing to decrease angiogenesis process. This data is in agreement with the VEGF results (**Figure 21 and figure 22A**).

The fact that FGF-7 is expressed under hypoxia conditions (237) excludes this phenomenon in the RPE response to EtOH. In addition, previous study establishes the relationship between the activation of some inflammatory cytokines with the decrease of FGF-7 in different types of neoplasms (230). Therefore, our results would be suggested that EtOH treatment directly activate an inflammation process leading a loss of RPE barrier function.

Another specific marker of RPE barrier function is VEGF. This growth factor requires the action of different enzymes, e.g. plasmin system and the MMPs to induce activation, migration and proliferation in endothelial cells getting a new capillary formation (235, 238, 239). The key enzyme for the cell-plasmin union to take place is uPA (240). uPA exerts its effect by joining uPAR. Also uPA and its homologue tPA, are able to convert plasminogen to plasmin, a protease responsible for degrading the ECM (124). It appears that uPAR is involved in pathological angiogenesis and, it has been shown that anti-uPAR antibodies are be able to blocking angiogenesis in cornea. In addition, uPA-uPAR binding activates MMPs, breaking components of the ECM (124).

Our results demonstrate an increase of uPA expression after EtOH exposure on ARPE-19 cells, (**Figure 21B**). This data, could be contradictory with VEGF results, however, it is possible that uPA is related to some VEGF alternative isoforms, such as VEGF-C, which it was increased in our results (**Figure 21B**). Also, MMPs were overexpressed after EtOH treatment (**Figure 23**).

Previous results from our group showed an increase of multivesicular bodies at 80 mM EtOH. These release vesicles (exosomes) and acting as a cell communication system. 80 mM EtOH was enough to change their content stimulating angiogenesis in endothelial cells (54). According to these results, an increase of VEGF and VEGFR-2 was observed at 200 mM EtOH (**Figure 22**). In contrast, a significant decrease in VEGFR-1 (**Figure 22C**) was observed in all groups treated with EtOH. Nevertheless as **figures 21** and **22** demonstrate, 600 mM EtOH turned out a significant decrease in VEGF-A mRNA and protein expression.

Several authors claim that VEGF overexpression induces VEGFR-2 in different diseases e.g. atherosclerosis (241) arthritis (242), diabetes (243), sepsis, psoriasis and vascular inflammation (244). In contrast with this, our results reveals a decrease of VEGFR-2 expression in EtOH dose manner (**Figure 22C**).

This fact could be explained because while 200 mM EtOH, the lowest concentration employed, did not cause a decrease in cell viability, it did increase ROS significantly. This ROS is enough to activate an inflammatory response and also VEGF expression. 600 mM EtOH promotes the activation of apoptosis cell death. This fact could be blocking the VEGF/VEGFR-2 pathway (245).

PEDF would counteract the effect of VEGF imbalance in RPE cells. PEDF is considered a potent neurotropic and anti-inflammatory protein that protects neurons of the retina and photoreceptors against cell death (246, 247). Also, it is one of the major regulators of angiogenesis released by RPE. PEDF is able to inhibit the VEGF effect (246, 248, 249). It acts by binding to VEGFR-2 or by promoting the proteolysis of VEGFR-2 by the activation of α-secretase (250, 251).

Our data show an increase of PEDF at 200 mM EtOH, followed by a significant fall in dose dependent manner (**Figure 22B**). These data do not appear to be in agreement with VEGF results. However, could be justified considering that, the increase of PEDF would be compensating the VEGF overexpression. Thereby, the BRB homeostasis could be restored. Another explanation could be that RPE cells release PEDF in their apical side, whereas VEGF is secreted in the basolateral side, in our experiments, ARPE-19 cells were not polarized.

As mentioned before, MMPs are characteristic proteins of chronic inflammatory diseases (252) and also as a results to OS (253). MMP-1, MMP-2, MMP-3, MMP-8 and MMP-9 are associated with ECM degradation in ocular diseases. In our results, its inhibitors, e.g. TIMP-1 were also highly elevated (**Figure 20A**), this could be explain as an attempt to maintain physiological homeostasis (254). Studies on mature RPE cells revealed that, under normal conditions these cells express MMP-1, MMP-2, MMP-3 and MMP-9 at low concentrations (255). Our results demonstrate an increase of MMP-3 and MMP-8 after EtOH treatment, **figure 23**.

Regarding MMP-2, it is possible to find studies indicating that it is involved in chronic inflammatory processes, contributing to the inhibition of the degradation of the ECM, blocking the effect of MMP-9 (253). Our results reinforce the claim that MMP-2 is constitutively expressed in RPE, despite the presence of a higher expression than the rest of MMPs (**Figure 23B**). Nevertheless, its expression did not present significant variations after EtOH exposure.

The increase of MMP-3 expression observed after treatment (**Figure 23F**) would be related to ROS production and ECM degradation. Previous studies in cancer revealed the existence of a relationship between NFKB and ROS-induced MMP-3 (256). Also, elevated levels of this protein have been implicated in inflammatory diseases (257, 258, 259). In the eye, MMP-3 expression is induced by ROS and it has the ability to degrade several collagen types, most of which are found in the ECM surrounding the RPE and the membrane Bruch (258).

MMP-9 has been implicated in ocular diseases such as AMD, as well as damage caused by ROS (35) and hypoxia (260). Thereby the increase of MMP-9 expression in ARPE-19 cells after EtOH treatment, (**Figure 23D**) could be explained by the increase of inflammatory markers. The increase of MMP-8 expression (**Figure 23C**), corroborates the activation of inflammation process, also in eye (261, 262, 263).

The activation of MMPs, promotes a signaling cascade involving different proteins such as mTOR, NFKB and p53 (263). These can be regulated by several cytokines among which we find growth factors such as TNFα and IL-β (222). There is also a relationship between the increase of MMP and the degradation of the TJ that mainly affects ZO-1 (264-267). This fact, leads us to consider that some of them are involved in cell signaling after EtOH treatment, orchestrating the entire cellular response. In addition, certain inflammatory cytokines can protect RPE from death due to OS (268).

NFKB is a transcription factor that plays a key role regulating inflammation-induced angiogenesis. It comprises two subunits (p65 and p50), which upon activation translocate to the nucleus and activate the expression of genes associated with inflammation (269). Contrary to what we had expected, NFKB activation was not detected in ARPE-19. Any group suffered the translocation of P65 subunit towards cell nucleus under OS conditions generated by EtOH, (**Figure 24B**).These results can be explained because there is a direct NFKB regulation by ROS. For example, direct oxidation of NFKB by H_2O_2-induced ROS inhibits its DNA binding ability and this ROS also regulates the phosphorylation of IKBα (270). Besides, IKBα induced by P65 overexpression maintains NFKB in the cytoplasm (271).

The fact that, NFKB decreased at 600 mM EtOH is in agreement with the decrease of VEGF found in previous results. NFKB plays an important role in VEGF expression regulation in retina, constitutive VEGF secretion in the RPE/choroid seems to be regulated by the transcription factor NFKB (80).

5. EtOH INDUCES CYP2E1 EXPRESSION IN RPE CELLS

The presence of CYP2E1 enzyme in ARPE-19, hRPE and hiPSC-RPE cells, confirm the idea of a local EtOH-metabolism in RPE. (**See results, figure 25, chapter IV**). Due to the obvious difficulties to obtain hRPE from donors and hiPSC-RPE cells, the present work has been performed mostly on ARPE-19 cells as a model to assess the direct effects of EtOH on RPE (apart from the hepatic metabolism). The existence of CYP2E1 in all RPE cells studied reinforces the protective function of this tissue. Besides strongly suggests additional roles for CYP2E1 related to vision such as oxidation of retinoic acid to 4-Hydroxy-retinoic acid (23, 24).

It is of relevance, that 600 mM EtOH increases CYP2E1 mRNA expression in a time dependent manner with a linear correlation. Logically with the most toxic EtOH concentration (1200 mM) the linearity was lower. This fact fits with data shown in **figures 26A** and **26B**, suggesting that weak to moderate CYP2E1 overexpression could be related to a detoxifying-protective role. Whereas, maintained CYP2E1 overexpression (1200 mM EtOH) could be associated with EtOH-induced cellular toxicity (**Figures 26C and 26D**). In agreement with Badger TM, et al. (272), who reported hepatic CYP2E1 induction by EtOH, CYP2E1 mRNA expression was increased in a fast, progressive and maintained manner after EtOH exposure (600–1200 mM), in ARPE-19 cells.

CYP2E1 represents the major EtOH detoxifying isoform that furthermore is induced by EtOH, but paradoxically it is poorly expressed in RPE cells in basal conditions (198). As our results shown the induction of CYP2E1 with 1200 mM of EtOH, matched the activity with HEPG2 cells in basal conditions (**Figure 26E**). The presence and activity of CYP2E1 suggests that the RPE has a role on local EtOH metabolism, which is likely protective at low EtOH concentrations, whereas it is deleterious at higher ones.

6. CYP2E1 IS IMPLICATED IN RPE CELL DEATH

There is a close relationship between overexpression of CYP2E1 and apoptosis not only in hepatic tissue (273, 274). Zhang RH et al. (273), in their published work demonstrated that inhibiting CYP2E1 by DAS is possible to attenuate chronic alcohol intake-induced apoptosis (via caspase-3) (273). The adult male mice used were fed with a 4% EtOH in their diet for 6 weeks (273). According to this, we found an increase of caspase-3 expression in ARPE-19 under 600 mM and 800 mM EtOH. (**See results, figure 27A, chapter IV**).

Conversely, the most toxic amount of EtOH used that overexpressed CYP2E1, decrease caspase-3 expression. In this way, Perlman H, et al. (275), described that Bcl-2 expression in synovial fibroblasts is essential for maintaining mitochondrial homeostasis and cell viability, and the increased Bcl-2 expression can downregulated casapse-3 activation (275). The increase of Bcl-2/Bax ratio, (**Figure 27B**) the unapparent morphological cellular changes (**Figure 27C**), and the lack of CYP2E1 induction (at 600 mM EtOH) may well fit with our previous data, indicating that below 600 mM EtOH a protective autophagy/mitophagy response is activated in ARPE-19 cells (49, 210). This theory is in agreement with Chen G, et al. (276), who indicated the protective role of autophagy against EtOH exposure.

The results herein indicate that is possible to reduce intracellular ROS increasing cell viability by inhibiting CYP2E1 (**Figures 28, 30 and 31**). CYP2E1-derived ROS have been related directly to the inhibition of autophagy in liver, using a binge model of EtOH exposure in hepatic cell lines (277). Plausibly, EtOH-derived ROS are produced in a dose dependent manner leading to different autophagy related phenomena: from cell protection to cell death.

DAS as a competitive inhibitor of CYP2E1, which blocks ROS production by direct molecular interaction, decreasing its activity (**Figure 28D**). Indirectly, DAS could be inhibiting CYP2E1 transcription and translation (**Figure 29**). In agreement with this, it has been described that CYP2E1 gene transcription is ROS-mediated and consequently, CYP2E1 induction is accompanied by additional ROS production enhancing CYP2E1 transcription (161, 163).

7. CYP2E1 INHIBITION MODIFIED THE EtOH - INDUCED CELLULAR RESPONSE

As previously mentioned, EtOH caused modifications in the proteome expression profile in ARPE19 cells. To reverse this phenomenon, 20 mM DAS treatment was enough, (**See results, figure 32, chapter IV**).

As well as results published demonstrated the relationship between acute and chronic alcohol and HSP activation (177, 278) we found functional link between the increase of HSP60 and CYP2E1 activation (**Figure 32B**). DAS improves RPE mitochondrial status under acute EtOH exposure, favoring ARPE-19 cells survival (279). This could be explained by the decrease of CYT-C expression with 20 mM DAS.

It should be noted that not all proteins that their expression was increased by the EtOH, saw reversed this effect by DAS treatment. NFKB expression was significantly reduced by EtOH in ARPE-19 cells. This effect was reversed inhibiting CYP2E1, even surpassing CTL levels, (**Figure 33**).

The fact that the use of the NAC as antioxidant, reverses the effect of EtOH on NFKB expression, (**Figure 33**) means that part of our results were due to OS generated by EtOH. However, the effects with DAS are much higher, indicating that somehow overexpression of CYP2E1 could be regulating NFKB.

Is well known that exist the hypothesis that NFKB could be regulated by OS. Also there are many reports that demostrate a possible relationship between CYP2E1 and this transcription factor (167-169). DAS increased P65 NFKB protein expression surpassing the levels of control group. It is plausibly to hypothesize that CYP2E1 could be regulating VEGF expression through NFKB.

8. CYP2E1 IS REGULATED BY ROS

Previous authors demostrated that PKC/JNK/SP1 pathway is implicated in the regulation of CYP2E1 expression (161, 176). The use of DAS blocks its activation y and consequently the ROS-mediated positive feedback generated by CYP2E1.

Increasing ROS by CYP2E1 activity would trigger an activation of PKC/JNK/SP1 pathway by a positive feedback loop increasing the expression of CYP2E1 in monocytes and astrocytes (161). Our data suggest same scenario in RPE cells (**see results, figure 32B, chapter IV**). The use of NAC was able to decrease the OS generated by EtOH in the same way as the treatment with DAS, (**Figure 34**). This fact could be due because OS generated under EtOH treatment in ARPE-19 cells comes from the activity of CYP2E1. In addition same effects in terms of CYP2E1 protein expression were observed after NAC treatment (**Figure 35**). Both DAS and NAC were able to reduce enzyme overexpression in the same way. This reinforces the hypothesis that it is the OS itself that triggers an overexpression pathway of CYP2E1 (161).

In the previous section mentioned that CYP2E1 plays a fundamental role in the regulation of NFKB (72), but other researchers hypothesize the opposite. (165-167). In our data we cannot discriminate if NFKB is regulating CYP2E1 expression or vice versa because we did not use any NFKB inhibitor. However we can affirm that there is a direct relationship between them. It would be interesting to continue investigating this relationship. CYP2E1 and NFKB are directly involve in the development of different inflammatory diseases (280, 281).

Further recent findings suggest that NFKB is an important transcriptional regulator of neuroinflammation in retinal diseases as a glaucoma (280) and diabetic retinopathy (281) coulding be a new immunomodulation strategy for retinal diseases.

In summary, EtOH exposure in RPE cells caused different response depending on OS generation. This translates into a biphasic response of some inflammation and angiogenesis biomarkers. That could be regulating cell signaling, impeding the correct blood retinal barrier homeostasis. CYP2E1 would play a key role in the generation of ROS and thus in the regulation of cellular response (**Figure 36**).

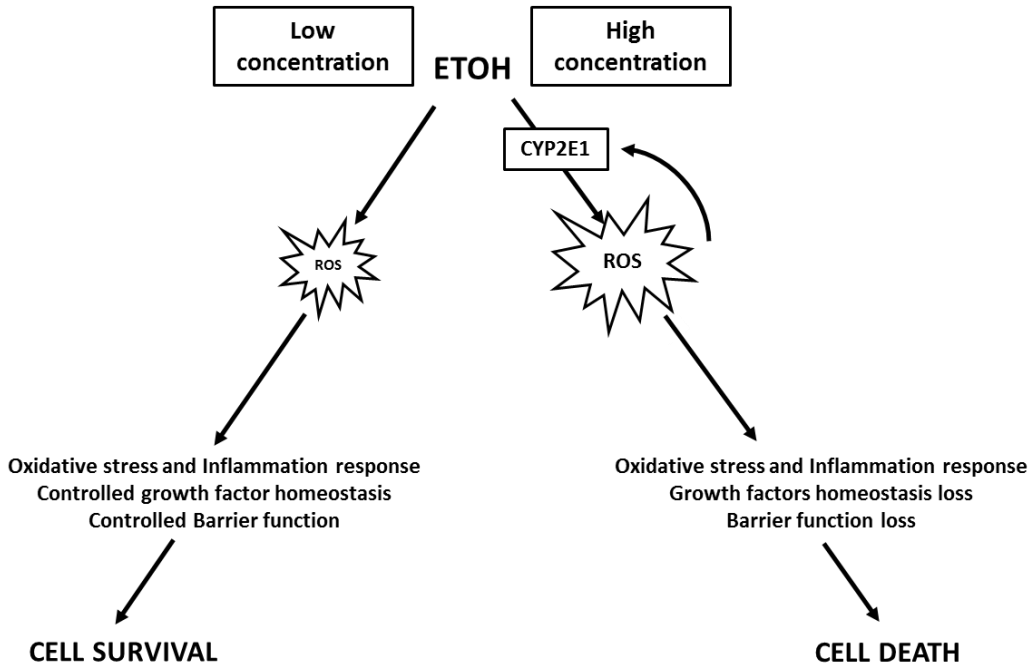

Figure 36. EtOH induces a two-phase response in RPE cells. Low EtOH concentration treatment induces ROS production in RPE cells activating oxidative stress response inducing cell survival. High EtOH concentration treatment in RPE induces more ROS than the lower used inducing RPE dysfunction and cell death.

CHAPTER VI

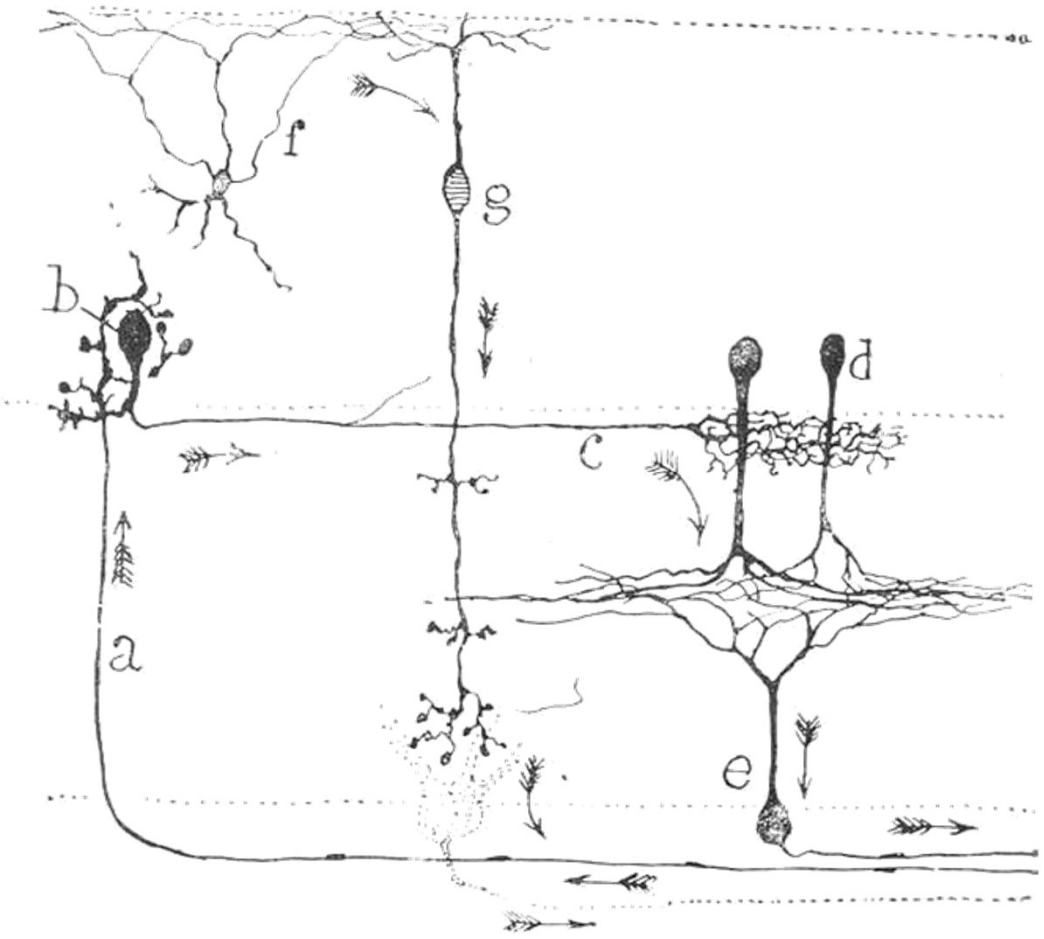

Bird retinal cells

S. Ramón y Cajal

Conclusions

In view of the results presented it can be concluded that alcohol intake could trigger RPE dysfunction promoting the formerly proposed 'alcoholic retinopathy'. Furthermore, it could even aggravate other retinal diseases by means of CYP2E1 activation. The present data would provide a valuable future tool and a significant piece of information for the further understanding of the pathophysiological mechanism of retinal diseases. CYP2E1 would play an important role in the generation of oxidative stress and thus in the regulation of retinal response and cell signaling activation.

1. ARPE-19 cells are an appropriate cellular model to study EtOH cytotoxicity in RPE. Seeding and culture conditions are important factors to consider.

2. RPE cells are resistant to EtOH-induced oxidative stress showing degeneration features only when EtOH concentration is above 600 mM.

3. Superoxide anions are the main species involved, in the significant increase of total intracellular ROS levels, at the highest EtOH concentrations used.

4. Superoxide anions are involved in the activation of EtOH-induced apoptosis pathway in ARPE-19 cells.

5. EtOH induces RPE barrier function degeneration, decreasing the integrity of intercellular junctions and modifying the expression profile of inflammatory and angiogenic factors in ARPE-19 cells.

6. EtOH treatment breaks the blood retinal barrier homeostasis unbalancing VEGF and PEDF expression, inducing RPE degeneration.

7. CYP2E1 is expressed in all RPE cells studied. CYP2E1 gene transcription, protein expression and activity are enhanced after EtOH exposure in ARPE-19 cells.

8. Inhibition of CYP2E1 with DAS, reverted oxidative stress damage and cell death in RPE cells. CYP2E1 is implicated in ARPE-19 cells apoptosis activation after EtOH exposure.

9. The expression of the transcriptional factor NFKB is down-regulated by CYP2E1-induced oxidative stress in ARPE-19 cells. The use of the antioxidant NAC reverted the values obtained after EtOH treatment. Nevertheless, treatment with DAS increased NFKB protein expression above baseline levels.

10. EtOH-induced oxidative stress regulates CYP2E1 expression in ARPE-19 cells. The use of DAS and NAC put back the results of CYP2E1 expression induced by EtOH, in the same way.

CHAPTER VII

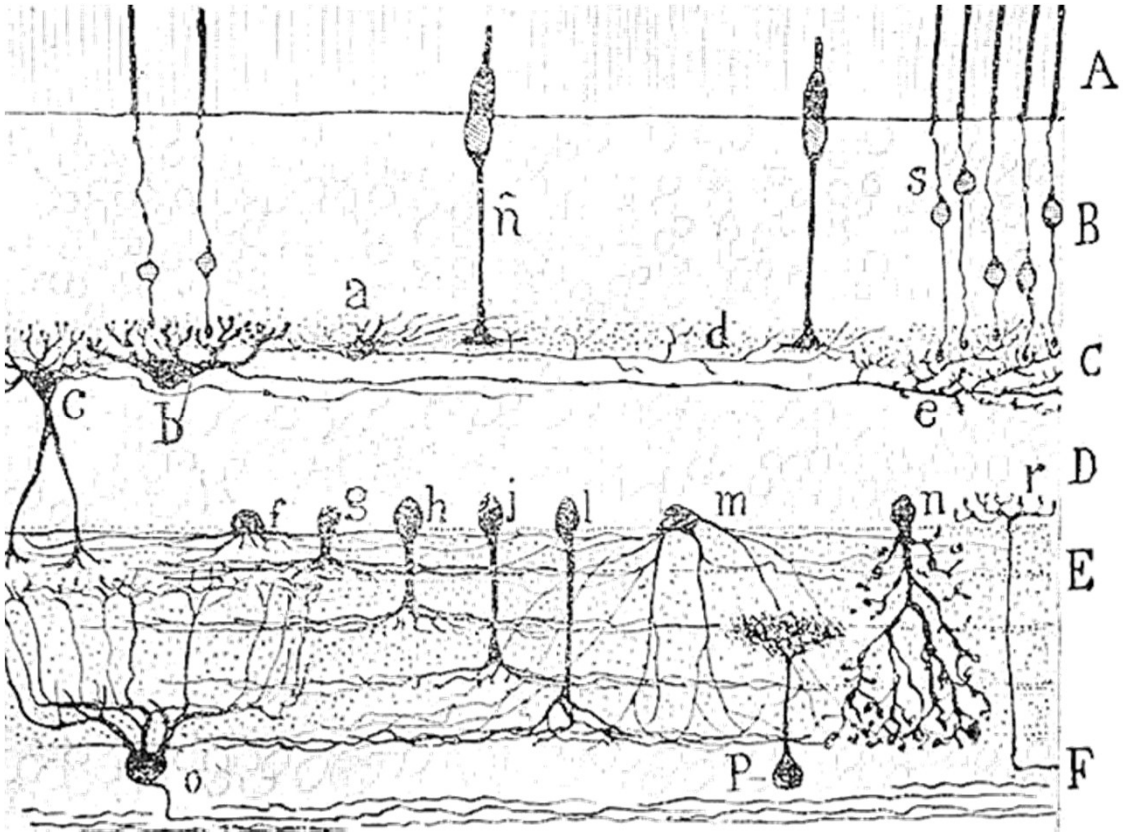

Mammals retinal layers

S. Ramón y Cajal

References

1. Benhar I, London A, Schwartz M. The privileged immunity of immune privileged organs: the case of the eye. Frontiers in immunology. 2012;3:296.

2. Tian J, Marziliano P, Baskaran M, Tun TA, Aung T. Automatic segmentation of the choroid in enhanced depth imaging optical coherence tomography images. Biomedical optics express. 2013;4(3):397-411.

3. Helga Kolb EF, and Ralph Nelson. Webvision The Organization of the Retina and Visual System 1995. Available from: http://webvision.med.utah.edu/.

4. Wiechers EG. El ojo: estructura y función. Oftalmología en la práctica de la medicina general: Universidad Nacional Autónoma de México; 2009. p. 14.

5. The retina reference. Available from: http://www.retinareference.com/anatomy/.

6. Th ebaultS. "El epitelio pigmentario retiniano como componente de la barrera hematoretiniana: implicación en la retinopatía diabética"2011; 12.

7. Nickla DL, Wallman J. The multifunctional choroid. Progress in retinal and eye research. 2010;29(2):144-68.

8. Yun C, Oh J, Choi KE, Hwang SY, Kim SW, Huh K. Peripapillary choroidal thickness after intravitreal ranibizumab injections in eyes with neovascular age-related macular degeneration. BMC ophthalmology. 2016;16:25.

9. Strauss O. The retinal pigment epithelium in visual function. Physiological reviews. 2005;85(3):845-81.

10. Panda-Jonas S, Jonas JB, Jakobczyk-Zmija M. Retinal pigment epithelial cell count, distribution, and correlations in normal human eyes. American journal of ophthalmology. 1996;121(2):181-9.

11. Sonoda S, Spee C, Barron E, Ryan SJ, Kannan R, Hinton DR. A protocol for the culture and differentiation of highly polarized human retinal pigment epithelial cells. Nature protocols. 2009;4(5):662-73.

12. Toops KA, Tan LX, Lakkaraju A. A detailed three-step protocol for live imaging of intracellular traffic in polarized primary porcine RPE monolayers. Experimental eye research. 2014;124:74-85.

13. Cunha-Vaz J, Bernardes R, Lobo C. Blood-retinal barrier. European journal of ophthalmology. 2011;21 Suppl 6:S3-9.

14. Liu Y, Zhang D, Wu Y, Ji B. Docosahexaenoic acid aggravates photooxidative damage in retinal pigment epithelial cells via lipid peroxidation. Journal of photochemistry and photobiology B, Biology. 2014;140:85-93.

15. Hamann S. Molecular mechanisms of water transport in the eye. International review of cytology. 2002;215:395-431.

16. Nandakumar N, Buzney S, Weiter JJ. Lipofuscin and the principles of fundus autofluorescence: a review. Seminars in ophthalmology. 2012;27(5-6):197-201.

17. Ozawa Y. Oxidative Stress in the RPE and Its Contribution to AMD Pathogenesis: Implication of Light Exposure. In: Nakazawa T KY, Harada T, editor. Neuroprotection and neuroregeneration for retinal diseases: Springer Japan; 2014. p. 239-53.

18. Wright AF, Chakarova CF, Abd El-Aziz MM, Bhattacharya SS. Photoreceptor degeneration: genetic and mechanistic dissection of a complex trait. Nature reviews Genetics. 2010;11(4):273-84.

19. Villegas-Perez MP. [Light exposure, lipofuscin and age-related macular degeneration]. Archivos de la Sociedad Espanola de Oftalmologia. 2005;80(10):565-8.

20. Perusek L, Maeda T. Vitamin A derivatives as treatment options for retinal degenerative diseases. Nutrients. 2013;5(7):2646-66.

21. Thompson DA, Gal A. Vitamin A metabolism in the retinal pigment epithelium: genes, mutations, and diseases. Progress in retinal and eye research. 2003;22(5):683-703.

22. Bavik C, Henry SH, Zhang Y, Mitts K, McGinn T, Budzynski E, et al. Visual Cycle Modulation as an Approach toward Preservation of Retinal Integrity. PloS one. 2015;10(5):e0124940.

23. Retinol Metabolism Covance Solution Made Real. Available from: http://cvd.pinpointdesign.com/map.php?mapid=881&item=9491.

24. Muindi JF, Young CW. Lipid hydroperoxides greatly increase the rate of oxidative catabolism of all-trans-retinoic acid by human cell culture microsomes genetically enriched in specified cytochrome P-450 isoforms. Cancer research. 1993;53(6):1226-9.

25. Bok D. The retinal pigment epithelium: a versatile partner in vision. Journal of cell science Supplement. 1993;17:189-95.

26. Sethna S, Chamakkala T, Gu X, Thompson TC, Cao G, Elliott MH, et al. Regulation of Phagolysosomal Digestion by Caveolin-1 of the Retinal Pigment Epithelium Is Essential for Vision. The Journal of biological chemistry. 2016;291(12):6494-506.

27. Nguyen-Legros J, Hicks D. Renewal of photoreceptor outer segments and their phagocytosis by the retinal pigment epithelium. International review of cytology. 2000;196:245-313.

28. Kay P, Yang YC, Paraoan L. Directional protein secretion by the retinal pigment epithelium: roles in retinal health and the development of age-related macular degeneration. Journal of cellular and molecular medicine. 2013;17(7):833-43.

29. Gerwins P, Skoldenberg E, Claesson-Welsh L. Function of fibroblast growth factors and vascular endothelial growth factors and their receptors in angiogenesis. Critical reviews in oncology/hematology. 2000;34(3):185-94.

30. Hollborn M, Iandiev I, Seifert M, Schnurrbusch UE, Wolf S, Wiedemann P, et al. Expression of HB-EGF by retinal pigment epithelial cells in vitreoretinal proliferative disease. Current eye research. 2006;31(10):863-74.

31. Jin M, Yaung J, Kannan R, He S, Ryan SJ, Hinton DR. Hepatocyte growth factor protects RPE cells from apoptosis induced by glutathione depletion. Investigative ophthalmology & visual science. 2005;46(11):4311-9.

32. Sporn MB, Roberts AB, Wakefield LM, Assoian RK. Transforming growth factor-beta: biological function and chemical structure. Science. 1986;233(4763):532-4.

33. Blobe GC, Schiemann WP, Lodish HF. Role of transforming growth factor beta in human disease. The New England journal of medicine. 2000;342(18):1350-8.

34. Dvashi Z, Goldberg M, Adir O, Shapira M, Pollack A. TGF-beta1 induced transdifferentiation of rpe cells is mediated by TAK1. PloS one. 2015;10(4):e0122229.

35. Bandyopadhyay M, Rohrer B. Matrix metalloproteinase activity creates pro-angiogenic environment in primary human retinal pigment epithelial cells exposed to complement. Investigative ophthalmology & visual science. 2012;53(4):1953-61.

36. Sánchez-Ramos Roda C. Filtros contra el efecto fototóxico del espectro visible en la retina: Experimentación animal. Universidad Europea de Madrid; 2010.

37. Yla-Herttuala S, Rissanen TT, Vajanto I, Hartikainen J. Vascular endothelial growth factors: biology and current status of clinical applications in cardiovascular medicine. Journal of the American College of Cardiology. 2007;49(10):1015-26.

38. Choi HY, Jung J, Name SB, Lee JE, Byon IS, Seo JH. The effects of vascular endothelial growth factor (VEGF) on human orbital preadipocyte. Orbit. 2016;35(1):6-10.

39. Wang H, Geisen P, Wittchen ES, King B, Burridge K, D'Amore PA, et al. The role of RPE cell-associated VEGF(1)(8)(9) in choroidal endothelial cell transmigration across the RPE. Investigative ophthalmology & visual science. 2011;52(1):570-8.

40. Sharma K, Sharma NK, Singh R, Anand A. Exploring the role of VEGF in Indian Age related macular degeneration. Annals of neurosciences. 2015;22(4):232-7.

41. Courtenay MD, Cade W, Schwartz SG, Kovach JL, Agarwal A, Wang G, et al. Set-based joint test of interaction between SNPs in the VEGF pathway and exogenous estrogen finds association with age-related macular degeneration. Investigative ophthalmology & visual science. 2014.

42. Bouck N. PEDF: anti-angiogenic guardian of ocular function. Trends in molecular medicine. 2002;8(7):330-4.

43. Subramanian P, Locatelli-Hoops S, Kenealey J, DesJardin J, Notari L, Becerra SP. Pigment epithelium-derived factor (PEDF) prevents retinal cell death via PEDF Receptor (PEDF-R): identification of a functional ligand binding site. The Journal of biological chemistry. 2013;288(33):23928-42.

44. Dunn KC, Aotaki-Keen AE, Putkey FR, Hjelmeland LM. ARPE-19, a human retinal pigment epithelial cell line with differentiated properties. Experimental eye research. 1996;62(2):155-69.

45. Kuznetsova AV, Kurinov AM. Cell models to study regulation of cell transformation in pathologies of retinal pigment epithelium. Journal of ophthalmology . 2014;2014:801787.

46. Srinivasan B, Kolli AR, Esch MB, Abaci HE, Shuler ML, Hickman JJ. TEER measurement techniques for in vitro barrier model systems. Journal of laboratory automation. 2015;20(2):107-26.

47. Bonet-Ponce L, Saez-Atienzar S, da Casa C, Sancho-Pelluz J, Barcia JM, Martinez-Gil N, et al. Rotenone Induces the Formation of 4-Hydroxynonenal Aggresomes. Role of ROS-Mediated Tubulin Hyperacetylation and Autophagic Flux Disruption. Molecular neurobiology. 2016;53(9):6194-208.

48. Atienzar-Aroca S, Flores-Bellver M, Serrano-Heras G, Martinez-Gil N, Barcia JM, Aparicio S, et al. Oxidative stress in retinal pigment epithelium cells increases exosome

secretion and promotes angiogenesis in endothelial cells. Journal of cellular and molecular medicine. 2016;20(8):1457-66.

49. Flores-Bellver M, Bonet-Ponce L, Barcia JM, Garcia-Verdugo JM, Martinez-Gil N, Saez-Atienzar S, et al. Autophagy and mitochondrial alterations in human retinal pigment epithelial cells induced by ethanol: implications of 4-hydroxy-nonenal. Cell death & disease. 2014;5:e1328.

50. Kozlowski MR. The ARPE-19 cell line: mortality status and utility in macular degeneration research. Current eye research. 2015;40(5):501-9.

51. Flores-Bellver M. Retinal Pigment Epithelium: A major role in retinal oxidative stress: Universidad Católica de Valencia; 2015.

52. Zhong X, Gutierrez C, Xue T, Hampton C, Vergara MN, Cao LH, et al. Generation of three-dimensional retinal tissue with functional photoreceptors from human iPSCs. Nature communications. 2014;5:4047.

53. Sies H. Oxidative stress: a concept in redox biology and medicine. Redox biology. 2015;4:180-3.

54. Naito TYaY. What Is Oxidative Stress? . Japan Medical Association Journal. 2002;45(7):5.

55. Holmstrom KM, Finkel T. Cellular mechanisms and physiological consequences of redox-dependent signalling. Nature reviews Molecular cell biology. 2014;15(6):411-21.

56. Koop DR, Morgan ET, Tarr GE, Coon MJ. Purification and characterization of a unique isozyme of cytochrome P-450 from liver microsomes of ethanol-treated rabbits. The Journal of biological chemistry. 1982;257(14):8472-80.

57. Lieber CS, DeCarli LM. Hepatic microsomal ethanol-oxidizing system. In vitro characteristics and adaptive properties in vivo. The Journal of biological chemistry. 1970;245(10):2505-12.

58. Ho E, Karimi Galougahi K, Liu CC, Bhindi R, Figtree GA. Biological markers of oxidative stress: Applications to cardiovascular research and practice. Redox biology. 2013;1:483-91.

59. Ayala A, Munoz MF, Arguelles S. Lipid peroxidation: production, metabolism, and signaling mechanisms of malondialdehyde and 4-hydroxy-2-nonenal. Oxidative medicine and cellular longevity. 2014;2014:360438.

60. Berlett BS, Stadtman ER. Protein oxidation in aging, disease, and oxidative stress. The Journal of biological chemistry. 1997;272(33):20313-6.

61. Eva Babusikova AE, Jozef Hatok, Dusan Dobrota and Jana Jurecekova Oxidative Changes and Possible Effects of Polymorphism of Antioxidant Enzymes in Neurodegenerative Disease, Neurodegenerative Diseases. Dr Uday Kishore (Ed), InTech. 2013.

62. Park SC, Lim JY, Jeen YT, Keum B, Seo YS, Kim YS, et al. Ethanol-induced DNA damage and repair-related molecules in human intestinal epithelial Caco-2 cells. Molecular medicine reports. 2012;5(4):1027-32.

63. Sharma A, Sharma R, Chaudhary P, Vatsyayan R, Pearce V, Jeyabal PV, et al. 4-Hydroxynonenal induces p53-mediated apoptosis in retinal pigment epithelial cells. Archives of biochemistry and biophysics. 2008;480(2):85-94.

64. van Leeuwen IM, Higgins M, Campbell J, McCarthy AR, Sachweh MC, Navarro AM, et al. Modulation of p53 C-terminal acetylation by mdm2, p14ARF, and cytoplasmic SirT2. Molecular cancer therapeutics. 2013;12(4):471-80.

65. Chou YT, Hsieh CH, Chiou SH, Hsu CF, Kao YR, Lee CC, et al. CITED2 functions as a molecular switch of cytokine-induced proliferation and quiescence. Cell death and differentiation. 2012;19(12):2015-28.

66. Birben E, Sahiner UM, Sackesen C, Erzurum S, Kalayci O. Oxidative stress and antioxidant defense. The World Allergy Organization journal. 2012;5(1):9-19.

67. Jackson BC, Thompson DC, Charkoftaki G, Vasiliou V. Dead enzymes in the aldehyde dehydrogenase gene family: role in drug metabolism and toxicology. Expert opinion on drug metabolism & toxicology. 2015;11(12):1839-47.

68. Pilat A, Herrnreiter AM, Skumatz CM, Sarna T, Burke JM. Oxidative stress increases HO-1 expression in ARPE-19 cells, but melanosomes suppress the increase when light is the stressor. Investigative ophthalmology & visual science. 2013;54(1):47-56.

69. de Andrade KQ, Moura FA, dos Santos JM, de Araujo OR, de Farias Santos JC, Goulart MO. Oxidative Stress and Inflammation in Hepatic Diseases: Therapeutic Possibilities of N-Acetylcysteine. International journal of molecular sciences. 2015;16(12):30269-308.

70. Yin J, Thomas F, Lang JC, Chaum E. Modulation of oxidative stress responses in the human retinal pigment epithelium following treatment with vitamin C. Journal of cellular physiology. 2011;226(8):2025-32.

71. Rao PS, Midde NM, Miller DD, Chauhan S, Kumar A, Kumar S. Diallyl Sulfide: Potential Use in Novel Therapeutic Interventions in Alcohol, Drugs, and Disease Mediated Cellular Toxicity by Targeting Cytochrome P450 2E1. Current drug metabolism. 2015;16(6):486-503.

72. Pintea DR A, Pop R Bunea A, Socaciu C, and Horst A. Diehl. Antioxidant Effect of Trans-Resveratrol in Cultured Human Retinal Pigment Epithelial Cells. Journal of Ocular Pharmacology and Therapeutics 2011;27(4):6.

73. Fang Y, Su T, Qiu X, Mao P, Xu Y, Hu Z, et al. Protective effect of alpha-mangostin against oxidative stress induced-retinal cell death. Scientific reports. 2016;6:21018.

74. Lu L, Hackett SF, Mincey A, Lai H, Campochiaro PA. Effects of different types of oxidative stress in RPE cells. Journal of cellular physiology. 2006;206(1):119-25.

75. Bazan NG. Survival signaling in retinal pigment epithelial cells in response to oxidative stress: significance in retinal degenerations. Advances in experimental medicine and biology. 2006;572:531-40.

76. Mateos MV, Tenconi PE, Giusto NM, Salvador GA. Inflammation and oxidative stress in retinal diseases: the role of intracellular signaling in the retinal pigment epithelium. International Journal of Ophthalmology and Clinical Research. 2015;2(3):7.

77. Son Y, Kim S, Chung HT, Pae HO. Reactive oxygen species in the activation of MAP kinases. Methods in enzymology. 2013;528:27-48.

78. Roth S, Shaikh AR, Hennelly MM, Li Q, Bindokas V, Graham CE. Mitogen-activated protein kinases and retinal ischemia. Investigative ophthalmology & visual science. 2003;44(12):5383-95.

79. Qiu Y, Tao L, Lei C, Wang J, Yang P, Li Q, et al. Downregulating p22phox ameliorates inflammatory response in Angiotensin II-induced oxidative stress by regulating MAPK and NF-kappaB pathways in ARPE-19 cells. Scientific reports. 2015;5:14362.

80. Klettner A, Westhues D, Lassen J, Bartsch S, Roider J. Regulation of constitutive vascular endothelial growth factor secretion in retinal pigment epithelium/choroid organ cultures: p38, nuclear factor kappaB, and the vascular endothelial growth factor receptor-2/phosphatidylinositol 3 kinase pathway. Molecular vision. 2013;19:281-91.

81. Faghiri Z, Bazan NG. PI3K/Akt and mTOR/p70S6K pathways mediate neuroprotectin D1-induced retinal pigment epithelial cell survival during oxidative stress-induced apoptosis. Experimental eye research. 2010;90(6):718-25.

82. Hector S, Prehn JH. Apoptosis signaling proteins as prognostic biomarkers in colorectal cancer: a review. Biochimica et biophysica acta. 2009;1795(2):117-29.

83. Bruce Alberts AJ, Julian Lewis, Martin Raff, Keith Roberts, and Peter Walter. The Cell Cycle and Programmed Cell Death. Molecular Biology of the Cell. 4 ed: New York: Garland Science; 2002.

84. Xu J, Zhu D, Sonoda S, He S, Spee C, Ryan SJ, et al. Over-expression of BMP4 inhibits experimental choroidal neovascularization by modulating VEGF and MMP-9. Angiogenesis. 2012;15(2):213-27.

85. Ho TC, Yang YC, Cheng HC, Wu AC, Chen SL, Chen HK, et al. Activation of mitogen-activated protein kinases is essential for hydrogen peroxide -induced apoptosis in retinal pigment epithelial cells. Apoptosis : an international journal on programmed cell death. 2006;11(11):1899-908.

86. Pasparakis M, Vandenabeele P. Necroptosis and its role in inflammation. Nature. 2015;517(7534):311-20.

87. Trichonas G, Murakami Y, Thanos A, Morizane Y, Kayama M, Debouck CM, et al. Receptor interacting protein kinases mediate retinal detachment-induced photoreceptor necrosis and compensate for inhibition of apoptosis. Proceedings of the National Academy of Sciences of the United States of America. 2010;107(50):21695-700.

88. Murakami Y, Matsumoto H, Roh M, Giani A, Kataoka K, Morizane Y, et al. Programmed necrosis, not apoptosis, is a key mediator of cell loss and DAMP-mediated inflammation in dsRNA-induced retinal degeneration. Cell death and differentiation. 2014;21(2):270-7.

89. Onodera J, Ohsumi Y. Autophagy is required for maintenance of amino acid levels and protein synthesis under nitrogen starvation. The Journal of biological chemistry. 2005;280(36):31582-6.

90. Frost LS, Mitchell CH, Boesze-Battaglia K. Autophagy in the eye: implications for ocular cell health. Experimental eye research. 2014;124:56-66.

91. Szatmari-Toth M, Kristof E, Vereb Z, Akhtar S, Facsko A, Fesus L, et al. Clearance of autophagy-associated dying retinal pigment epithelial cells - a possible source for inflammation in age-related macular degeneration. Cell death & disease. 2016;7(9):e2367.

92. Boya P, Esteban-Martinez L, Serrano-Puebla A, Gomez-Sintes R, Villarejo-Zori B. Autophagy in the eye: Development, degeneration, and aging. Progress in retinal and eye research. 2016;55:206-45.

93. Medzhitov R. Origin and physiological roles of inflammation. Nature. 2008;454(7203):428-35.

94. Mittal M, Siddiqui MR, Tran K, Reddy SP, Malik AB. Reactive oxygen species in inflammation and tissue injury. Antioxidants & redox signaling. 2014;20(7):1126-67.

95. Ashley NT WZ, Nelson RJ. . Inflammation: Mechanisms, Costs, and Natural Variation. ecolsysannualreviewsorg. 2012;43(1):21.

96. Schindler R, Mancilla J, Endres S, Ghorbani R, Clark SC, Dinarello CA. Correlations and interactions in the production of interleukin-6 (IL-6), IL-1, and tumor necrosis factor (TNF) in human blood mononuclear cells: IL-6 suppresses IL-1 and TNF. Blood. 1990;75(1):40-7.

97. Armstrong AW, Voyles SV, Armstrong EJ, Fuller EN, Rutledge JC. Angiogenesis and oxidative stress: common mechanisms linking psoriasis with atherosclerosis. Journal of dermatological science. 2011;63(1):1-9.

98. Blasiak J, Petrovski G. Oxidative stress, hypoxia, and autophagy in the neovascular processes of age-related macular degeneration. 2014;2014:768026.

99. Wilkinson-Berka JL, Rana I, Armani R, Agrotis A. Reactive oxygen species, Nox and angiotensin II in angiogenesis: implications for retinopathy. Clinical science (London, England : 1979). 2013;124(10):597-615.

100. Vatsyayan R, Lelsani PC, Chaudhary P, Kumar S, Awasthi S, Awasthi YC. The expression and function of vascular endothelial growth factor in retinal pigment epithelial (RPE) cells is regulated by 4-hydroxynonenal (HNE) and glutathione S-transferaseA4-4. Biochemical and biophysical research communications. 2012;417(1):346-51.

101. Li X, Cai Y, Wang YS, Shi YY, Hou W, Xu CS, et al. Hyperglycaemia exacerbates choroidal neovascularisation in mice via the oxidative stress-induced activation of STAT3 signalling in RPE cells. PloS one. 2012;7(10):e47600.

102. Angosto MC Á-GJ. Metaloproteinasas, matriz extracelular y cáncer. Anales de la Real Academia Nacional de Farmacia. 2010;76(1):25.

103. Haurigot V, Villacampa P, Ribera A, Bosch A, Ramos D, Ruberte J, et al. Long-term retinal PEDF overexpression prevents neovascularization in a murine adult model of retinopathy. PloS one. 2012;7(7):e41511.

104. Kale G, Naren AP, Sheth P, Rao RK. Tyrosine phosphorylation of occludin attenuates its interactions with ZO-1, ZO-2, and ZO-3. Biochemical and biophysical research communications. 2003;302(2):324-9.

105. Omri S, Omri B, Savoldelli M, Jonet L, Thillaye-Goldenberg B, Thuret G, et al. The outer limiting membrane (OLM) revisited: clinical implications. Clinical ophthalmology. 2010;4:183-95.

106. Krizbai IA, Bauer H, Bresgen N, Eckl PM, Farkas A, Szatmari E, et al. Effect of oxidative stress on the junctional proteins of cultured cerebral endothelial cells. Cellular and molecular neurobiology. 2005;25(1):129-39.

107. Ferreira SM, Lerner SF, Brunzini R, Evelson PA, Llesuy SF. Oxidative stress markers in aqueous humor of glaucoma patients. American journal of ophthalmology. 2004;137(1):62-9.

108. Santosa S, Jones PJ. Oxidative stress in ocular disease: does lutein play a protective role? CMAJ : Canadian Medical Association journal = journal de l'Association medicale canadienne. 2005;173(8):861-2.

109. Wakamatsu TH, Dogru M, Tsubota K. Tearful relations: oxidative stress, inflammation and eye diseases. Arquivos brasileiros de oftalmologia. 2008;71(6 Suppl):72-9.

110. Heath NEINIo. Facts About Retinitis Pigmentosa 2014. Available from: https://nei.nih.gov/health/pigmentosa/pigmentosa_facts.

111. Openshaw A, Branham K, Heckenlively J. Understanding Retinitis Pigmentosa. In: Center UoMKE, editor. University of Michigan. 2008. p. 28.

112. Shen J, Yang X, Dong A, Petters RM, Peng YW, Wong F, et al. Oxidative damage is a potential cause of cone cell death in retinitis pigmentosa. Journal of cellular physiology. 2005;203(3):457-64.

113. Carmody RJ, Cotter TG. Oxidative stress induces caspase-independent retinal apoptosis in vitro. Cell death and differentiation. 2000;7(3):282-91.

114. Komeima K, Rogers BS, Lu L, Campochiaro PA. Antioxidants reduce cone cell death in a model of retinitis pigmentosa. Proceedings of the National Academy of Sciences of the United States of America. 2006;103(30):11300-5.

115. Tah V, Orlans HO, Hyer J, Casswell E, Din N, Sri Shanmuganathan V, et al. Anti-VEGF Therapy and the Retina: An Update. Journal of ophthalmology. 2015;2015:627674.

116. Grossniklaus HE, Kang SJ, Berglin L. Animal models of choroidal and retinal neovascularization. Progress in retinal and eye research. 2010;29(6):500-19.

117. Wang H, Han X, Wittchen ES, Hartnett ME. TNF-alpha mediates choroidal neovascularization by upregulating VEGF expression in RPE through ROS-dependent beta-catenin activation. Molecular vision. 2016;22:116-28.

118. Manning BD, Cantley LC. AKT/PKB signaling: navigating downstream. Cell. 2007;129(7):1261-74.

119. van den Beucken T, Koritzinsky M, Niessen H, Dubois L, Savelkouls K, Mujcic H, et al. Hypoxia-induced expression of carbonic anhydrase 9 is dependent on the unfolded protein response. The Journal of biological chemistry. 2009;284(36):24204-12.

120. Guilak F BD, Goldstein SA, Baaijens FPT. . Biomechanics and mechanobiology in functional tissue engineering. Journal of biomechanics. 2014;47(9):7.

121. Plafker SM. Oxidative stress and the ubiquitin proteolytic system in age-related macular degeneration. Advances in experimental medicine and biology. 2010;664:447-56.

122. Jimenez Cuenca B. [Mechanism of inhibition of tumoral angiogenesis by thrombospondin-1]. Nefrologia : publicacion oficial de la Sociedad Espanola Nefrologia. 2003;23 Suppl 3:49-53.

123. Doll JA, Reiher FK, Crawford SE, Pins MR, Campbell SC, Bouck NP. Thrombospondin-1, vascular endothelial growth factor and fibroblast growth factor-2 are key functional regulators of angiogenesis in the prostate. The Prostate. 2001;49(4):293-305.

124. Blasi F, Carmeliet P. uPAR: a versatile signalling orchestrator. Nature reviews Molecular cell biology. 2002;3(12):932-43.

125. Martinez-Ezquerro JD, Herrera LA. Angiogénesis: VEGF/VEGFRs como blancos terapéuticos en el tratamiento contra el cáncer. In: (UNAM) UNAdM, editor. Cancerología. México 2006. p. 12.

126. Al Gwairi O, Thach L, Zheng W, Osman N, Little PJ. Cellular and Molecular Pathology of Age-Related Macular Degeneration: Potential Role for Proteoglycans. 2016;2016:2913612.

127. Nita M, Grzybowski A. The Role of the Reactive Oxygen Species and Oxidative Stress in the Pathomechanism of the Age-Related Ocular Diseases and Other Pathologies

of the Anterior and Posterior Eye Segments in Adults. Oxidative medicine and cellular longevity. 2016;2016:3164734.

128. Frank RN. Diabetic retinopathy. The New England journal of medicine. 2004;350(1):48-58.

129. Madsen-Bouterse SA, Mohammad G, Kanwar M, Kowluru RA. Role of mitochondrial DNA damage in the development of diabetic retinopathy, and the metabolic memory phenomenon associated with its progression. Antioxidants & redox signaling. 2010;13(6):797-805.

130. Chiu CJ, Taylor A. Dietary hyperglycemia, glycemic index and metabolic retinal diseases. Progress in retinal and eye research. 2011;30(1):18-53.

131. Room R, Babor T, Rehm J. Alcohol and public health. Lancet. 2005;365(9458):519-30.

132. Guo R, Ren J. Alcohol and acetaldehyde in public health: from marvel to menace. International journal of environmental research and public health. 2010;7(4):1285-301.

133. Baliunas DO, Taylor BJ, Irving H, Roerecke M, Patra J, Mohapatra S, et al. Alcohol as a risk factor for type 2 diabetes: A systematic review and meta-analysis. Diabetes care. 2009;32(11):2123-32.

134. George A, Figueredo VM. Alcohol and arrhythmias: a comprehensive review. Journal of cardiovascular medicine. 2010;11(4):221-8.

135. Ohkubo T, Metoki H, Imai Y. Alcohol intake, circadian blood pressure variation, and stroke. Hypertension. 2009;53(1):4-5.

136. Cederbaum AI, Lu Y, Wu D. Role of oxidative stress in alcohol-induced liver injury. Archives of toxicology. 2009;83(6):519-48.

137. Seitz HK, Becker P. Alcohol metabolism and cancer risk. Alcohol research & health : the journal of the National Institute on Alcohol Abuse and Alcoholism. 2007;30(1):38-41, 4-7.

138. Morris MJ. Alcohol breath testing in patients with respiratory disease. Thorax. 1990;45(10):717-21.

139. Marinho V, Laks J, Engelhardt E, Conn D. Alcohol abuse in an elderly woman taking donepezil for Alzheimer disease. Journal of clinical psychopharmacology. 2006;26(6):683-5.

140. Holford NH. Clinical pharmacokinetics of ethanol. Clinical pharmacokinetics. 1987;13(5):273-92.

141. Bondy SC, Guo SX. Regional selectivity in ethanol-induced pro-oxidant events within the brain. Biochemical pharmacology. 1995;49(1):69-72.

142. Bosch-Morell F, Martinez-Soriano F, Colell A, Fernandez-Checa JC, Romero FJ. Chronic ethanol feeding induces cellular antioxidants decrease and oxidative stress in rat peripheral nerves. Effect of S-adenosyl-L-methionine and N-acetyl-L-cysteine. Free radical biology & medicine. 1998;25(3):365-8.

143. Ramachandran V, Watts LT, Maffi SK, Chen J, Schenker S, Henderson G. Ethanol-induced oxidative stress precedes mitochondrially mediated apoptotic death of cultured fetal cortical neurons. Journal of neuroscience research. 2003;74(4):577-88.

144. Sun AY, Chen YM, James-Kracke M, Wixom P, Cheng Y. Ethanol-induced cell death by lipid peroxidation in PC12 cells. Neurochemical research. 1997;22(10):1187-92.

145. Israel Y, Rivera-Meza M, Karahanian E, Quintanilla ME, Tampier L, Morales P, et al. Gene specific modifications unravel ethanol and acetaldehyde actions. Frontiers in behavioral neuroscience. 2013;7:80.

146. Hernandez JA, Lopez-Sanchez RC. Lipids and Oxidative Stress Associated with Ethanol-Induced Neurological Damage. 2016;2016:1543809.

147. Cederbaum AI. Alcohol metabolism. Clinics in liver disease. 2012;16(4):667-85.

148. Wall TL, Luczak SE, Hiller-Sturmhofel S. Biology, Genetics, and Environment: Underlying Factors Influencing Alcohol Metabolism. Alcohol research : current reviews. 2016;38(1):59-68.

149. Zakhari S. Alcohol metabolism and epigenetics changes. Alcohol research : current reviews. 2013;35(1):6-16.

150. Yang SP, Medling T, Raner GM. Cytochrome P450 expression and activities in rat, rabbit and bovine tongue. Comparative biochemistry and physiology Toxicology & pharmacology : CBP. 2003;136(4):297-308.

151. Zhang W, Lu D, Dong W, Zhang L, Zhang X, Quan X, et al. Expression of CYP2E1 increases oxidative stress and induces apoptosis of cardiomyocytes in transgenic mice. The FEBS journal. 2011;278(9):1484-92.

152. Ye XH, Song L, Peng L, Bu Z, Yan SX, Feng J, et al. Association between the CYP2E1 polymorphisms and lung cancer risk: a meta-analysis. Molecular genetics and genomics : MGG. 2015;290(2):545-58.

153. Nakamura K, Fujiki T, Tamura HO. Age, gender and region-specific differences in drug metabolising enzymes in rat ocular tissues. Experimental eye research. 2005;81(6):710-5.

154. Nakano M, Mohri T, Fukami T, Takamiya M, Aoki Y, McLeod HL, et al. Single-Nucleotide Polymorphisms in Cytochrome P450 2E1 (CYP2E1) 3'-Untranslated Region Affect the Regulation of CYP2E1 by miR-570. Drug metabolism and disposition: the biological fate of chemicals. 2015;43(10):1450-7.

155. Koop DR. Alcohol metabolism's damaging effects on the cell: a focus on reactive oxygen generation by the enzyme cytochrome P450 2E1. Alcohol research & health : the journal of the National Institute on Alcohol Abuse and Alcoholism. 2006;29(4):274-80.

156. Porubsky PR, Meneely KM, Scott EE. Structures of human cytochrome P-450 2E1. Insights into the binding of inhibitors and both small molecular weight and fatty acid substrates. The Journal of biological chemistry. 2008;283(48):33698-707.

157. King M. The Medical Biochemistry Page. Available from: http://themedicalbiochemistrypage.org/.

158. Bansal S, Srinivasan S, Anandasadagopan S, Chowdhury AR, Selvaraj V, Kalyanaraman B, et al. Additive effects of mitochondrion-targeted cytochrome CYP2E1 and alcohol toxicity on cytochrome c oxidase function and stability of respirosome complexes. The Journal of biological chemistry. 2012;287(19):15284-97.

159. Lu Y, Cederbaum AI. CYP2E1 and oxidative liver injury by alcohol. Free radical biology & medicine. 2008;44(5):723-38.

160. Cederbaum AI. Molecular mechanisms of the microsomal mixed function oxidases and biological and pathological implications. Redox biology. 2015;4:60-73.

161. Jin M, Ande A, Kumar A, Kumar S. Regulation of cytochrome P450 2e1 expression by ethanol: role of oxidative stress-mediated pkc/jnk/sp1 pathway. Cell death & disease. 2013;4:e554.

162. Roberts BJ, Song BJ, Soh Y, Park SS, Shoaf SE. Ethanol induces CYP2E1 by protein stabilization. Role of ubiquitin conjugation in the rapid degradation of CYP2E1. The Journal of biological chemistry. 1995;270(50):29632-5.

163. Rao PS, Kumar S. Chronic Effects of Ethanol and/or Darunavir/Ritonavir on U937 Monocytic Cells: Regulation of Cytochrome P450 and Antioxidant Enzymes, Oxidative Stress, and Cytotoxicity. Alcoholism, clinical and experimental research. 2016;40(1):73-82.

164. Abdel-Razzak Z, Garlatti M, Aggerbeck M, Barouki R. Determination of interleukin-4-responsive region in the human cytochrome P450 2E1 gene promoter. Biochemical pharmacology. 2004;68(7):1371-81.

165. Travis L. The regulation of CYP2E1 gene expression and its role in breast cancer: University of Manchester; 2012.

166. Zangar RC, Davydov DR, Verma S. Mechanisms that regulate production of reactive oxygen species by cytochrome P450. Toxicology and applied pharmacology. 2004;199(3):316-31.

167. Zordoky BN, El-Kadi AO. Role of NF-kappaB in the regulation of cytochrome P450 enzymes. Current drug metabolism. 2009;10(2):164-78.

168. Roman J, Colell A, Blasco C, Caballeria J, Pares A, Rodes J, et al. Differential role of ethanol and acetaldehyde in the induction of oxidative stress in HEP G2 cells: effect on transcription factors AP-1 and NF-kappaB. Hepatology. 1999;30(6):1473-80.

169. Szuster-Ciesielska A, Mizerska-Dudka M, Daniluk J, Kandefer-Szerszen M. Butein inhibits ethanol-induced activation of liver stellate cells through TGF-beta, NFkappaB, p38, and JNK signaling pathways and inhibition of oxidative stress. Journal of gastroenterology. 2013;48(2):222-37.

170. Chen Q, Cederbaum AI. Cytotoxicity and apoptosis produced by cytochrome P450 2E1 in Hep G2 cells. Molecular pharmacology. 1998;53(4):638-48.

171. Arfian N, Muflikhah K, Soeyono SK, Sari DC, Tranggono U, Anggorowati N, et al. Vitamin D Attenuates Kidney Fibrosis via Reducing Fibroblast Expansion, Inflammation, and Epithelial Cell Apoptosis. The Kobe journal of medical sciences. 2016;62(2):E38-44.

172. Maurel DB, Boisseau N, Benhamou CL, Jaffre C. Alcohol and bone: review of dose effects and mechanisms. Osteoporosis international : a journal established as result of cooperation between the European Foundation for Osteoporosis and the National Osteoporosis Foundation of the USA. 2012;23(1):1-16.

173. Akbar M, Baick J, Calderon F, Wen Z, Kim HY. Ethanol promotes neuronal apoptosis by inhibiting phosphatidylserine accumulation. Journal of neuroscience research. 2006;83(3):432-40.

174. Wu D, AI Cederbaum. Inhibition of autophagy promotes CYP2E1-dependent toxicity in HepG2 cells via elevated oxidative stress, mitochondria dysfunction and activation of p38 and JNK MAPK. Redox biology. 2013;5(1):13.

175. Schattenberg JM, Czaja MJ. Regulation of the effects of CYP2E1-induced oxidative stress by JNK signaling. Redox biology. 2014;3:7-15.

176. Ahmad I, Shukla S, Singh D, Chauhan AK, Kumar V, Singh BK, et al. CYP2E1-mediated oxidative stress regulates HO-1 and GST expression in maneb- and paraquat-treated rat polymorphonuclear leukocytes. Molecular and cellular biochemistry. 2014;393(1-2):209-22.

177. Mandrekar P, Ambade A. Immunity and inflammatory signaling in alcoholic liver disease. Hepatology international. 2014;8 Suppl 2:439-46.

178. Peragallo J, Biousse V, Newman NJ. Ocular manifestations of drug and alcohol abuse. Current opinion in ophthalmology. 2013;24(6):566-73.

179. Adams MK, Chong EW, Williamson E, Aung KZ, Makeyeva GA, Giles GG, et al. 20/20--Alcohol and age-related macular degeneration: the Melbourne Collaborative Cohort Study. American journal of epidemiology. 2012;176(4):289-98.

180. Piermarocchi S, Tognetto D, Piermarocchi R, Masetto M, Monterosso G, Segato T, et al. Risk Factors and Age-Related Macular Degeneration in a Mediterranean-Basin Population: The PAMDI (Prevalence of Age-Related Macular Degeneration in Italy) Study--Report 2. Ophthalmic research. 2016;55(3):111-8.

181. Ghanayem BI. Inhibition of urethane-induced carcinogenicity in cyp2e1-/- in comparison to cyp2e1+/+ mice. Toxicological sciences : an official journal of the Society of Toxicology. 2007;95(2):331-9.

182. George J, Liddle C, Murray M, Byth K, Farrell GC. Pre-translational regulation of cytochrome P450 genes is responsible for disease-specific changes of individual P450 enzymes among patients with cirrhosis. Biochemical pharmacology. 1995;49(7):873-81.

183. Jimenez-Garza O, Baccarelli AA, Byun HM, Marquez-Gamino S, Barron-Vivanco BS, Albores A. CYP2E1 epigenetic regulation in chronic, low-level toluene exposure: Relationship with oxidative stress and smoking habit. Toxicology and applied pharmacology. 2015;286(3):207-15.

184. Howard LA, Miksys S, Hoffmann E, Mash D, Tyndale RF. Brain CYP2E1 is induced by nicotine and ethanol in rat and is higher in smokers and alcoholics. British journal of pharmacology. 2003;138(7):1376-86.

185. Hubacek JA, Pelclova D, Seidl Z, Vaneckova M, Klempir J, Ruzicka E, et al. Rare alleles within the CYP2E1 (MEOS system) could be associated with better short-term health outcome after acute methanol poisoning. Basic & clinical pharmacology & toxicology. 2015;116(2):168-72.

186. Toler SM. Oxidative stress plays an important role in the pathogenesis of drug-induced retinopathy. Experimental biology and medicine. 2004;229(7):607-15.

187. Yanai R, Mulki L, Hasegawa E, Takeuchi K, Sweigard H, Suzuki J, et al. Cytochrome P450-generated metabolites derived from omega-3 fatty acids attenuate neovascularization. Proceedings of the National Academy of Science. 2014;111(26):9603-8.

188. Zhu M, Provis JM, Penfold PL. Isolation, culture and characteristics of human foetal and adult retinal pigment epithelium. Australian and New Zealand journal of ophthalmology. 1998;26 Suppl 1:S50-2.

189. Abas L, Luschnig C. Maximum yields of microsomal-type membranes from small amounts of plant material without requiring ultracentrifugation. Analytical biochemistry. 2010;401(2):217-27.

190. Chang TK, Crespi CL, Waxman DJ. Spectrophotometric analysis of human CYP2E1-catalyzed p-nitrophenol hydroxylation. Methods in molecular biology. 2006;320:127-31.

191. Elbarbry F, Wilby K, Alcorn J. Validation of a HPLC method for the determination of p-nitrophenol hydroxylase activity in rat hepatic microsomes. Journal of chromatography B, Analytical technologies in the biomedical and life sciences. 2006;834(1-2):199-203.

192. Tassaneeyakul W, Veronese ME, Birkett DJ, Gonzalez FJ, Miners JO. Validation of 4-nitrophenol as an in vitro substrate probe for human liver CYP2E1 using cDNA expression and microsomal kinetic techniques. Biochemical pharmacology. 1993;46(11):1975-81.

193. Klein R, Lee KE, Gangnon RE, Klein BE. Relation of smoking, drinking, and physical activity to changes in vision over a 20-year period: the Beaver Dam Eye Study. Ophthalmology. 2014;121(6):1220-8.

194. Li Z, Xu K, Wu S, Sun Y, Song Z, Jin D, et al. Alcohol consumption and visual impairment in a rural Northern Chinese population. Ophthalmic epidemiology. 2014;21(6):384-90.

195. Sancho-Tello M, Muriach M, Barcia J, Bosch-Morell F, Genoves JM, Johnsen-Soriano S, et al. Chronic alcohol feeding induces biochemical, histological, and functional alterations in rat retina. Alcohol and alcoholism. 2008;43(3):254-60.

196. Martras S, Alvarez R, Martinez SE, Torres D, Gallego O, Duester G, et al. The specificity of alcohol dehydrogenase with cis-retinoids. Activity with 11-cis-retinol and localization in retina. European journal of biochemistry. 2004;271(9):1660-70.

197. Holmes RS, Popp RA, VandeBerg JL. Genetics of ocular NAD+-dependent alcohol dehydrogenase and aldehyde dehydrogenase in the mouse: evidence for genetic identity with stomach isozymes and localization of Ahd-4 on chromosome 11 near trembler. Biochemical genetics. 1988;26(3-4):191-205.

198. Nakano M, Kelly EJ, Wiek C, Hanenberg H, Rettie AE. CYP4V2 in Bietti's crystalline dystrophy: ocular localization, metabolism of omega-3-polyunsaturated fatty acids, and functional deficit of the p.H331P variant. Molecular pharmacology. 2012;82(4):679-86.

199. Khalighi M, Brzezinski MR, Chen H, Juchau MR. Inhibition of human prenatal biosynthesis of all-trans-retinoic acid by ethanol, ethanol metabolites, and products of lipid peroxidation reactions: a possible role for CYP2E1. Biochemical pharmacology. 1999;57(7):811-21.

200. Brossas JY, Tanguy R, Brignole-Baudouin F, Courtois Y, Torriglia A, Treton J. L-DNase II associated with active process during ethanol induced cell death in ARPE-19. Molecular vision. 2004;10:65-73.

201. Kurz T, Karlsson M, Brunk UT, Nilsson SE, Frennesson C. ARPE-19 retinal pigment epithelial cells are highly resistant to oxidative stress and exercise strict control over their lysosomal redox-active iron. Autophagy. 2009;5(4):494-501.

202. Simon A, Hellman U, Wernstedt C, Eriksson U. The retinal pigment epithelial-specific 11-cis retinol dehydrogenase belongs to the family of short chain alcohol dehydrogenases. The Journal of biological chemistry. 1995;270(3):1107-12.

203. Suzuki Y, Ishiguro S, Tamai M. Identification and immunohistochemistry of retinol dehydrogenase from bovine retinal pigment epithelium. Biochimica et biophysica acta. 1993;1163(2):201-8.

204. Tian J, Ishibashi K, Honda S, Boylan SA, Hjelmeland LM, Handa JT. The expression of native and cultured human retinal pigment epithelial cells grown in different culture conditions. The British journal of ophthalmology. 2005;89(11):1510-7.

205. Tian J, Ishibashi K, Handa JT. The expression of native and cultured RPE grown on different matrices. Physiological genomics. 2004;17(2):170-82.

206. Honey D, Caylor C, Luthi R, Kerrigan S. Comparative alcohol concentrations in blood and vitreous fluid with illustrative case studies. Journal of analytical toxicology. 2005;29(5):365-9.

207. Johnsen-Soriano S, Bosch-Morell F, Miranda M, Asensio S, Barcia JM, Roma J, et al. Ebselen prevents chronic alcohol-induced rat hippocampal stress and functional impairment. Alcoholism, clinical and experimental research. 2007;31(3):486-92.

208. Johnsen-Soriano S, Genoves JM, Romero B, Garcia-Delpech S, Muriach M, Sancho-Tello M, et al. [Chronic ethanol feeding induces oxidative stress in the rat retina: treatment with the antioxidant ebselen]. Archivos de la Sociedad Espanola de Oftalmologia. 2007;82(12):757-62.

209. Eysseric H, Gonthier B, Soubeyran A, Bessard G, Saxod R, Barret L. There is not simple method to maintain a constant ethanol concentration in long-term cell culture: keys to a solution applied to the survey of astrocytic ethanol absorption. Alcohol. 1997;14(2):111-5.

210. Bonet-Ponce L, Saez-Atienzar S, da Casa C, Flores-Bellver M, Barcia JM, Sancho-Pelluz J, et al. On the mechanism underlying ethanol-induced mitochondrial dynamic disruption and autophagy response. Biochimica et biophysica acta. 2015;1852(7):1400-9.

211. Yang L, Wu D, Cederbaum AI. CYP2E1, oxidative stress and MAPK signaling pathways in alcohol-induced hepatotoxicity. Journal of Biochemical and Pharmacological Research. 2014;2(2):16.

212. Korthagen NM, van Bilsen K, Swagemakers SM, van de Peppel J, Bastiaans J, van der Spek PJ, et al. Retinal pigment epithelial cells display specific transcriptional responses upon TNF-alpha stimulation. The British journal of ophthalmology. 2015;99(5):700-4.

213. Melendez Garcia R, Arredondo Zamarripa D, Arnold E, Ruiz-Herrera X, Noguez Imm R, Baeza Cruz G, et al. Prolactin protects retinal pigment epithelium by inhibiting sirtuin 2-dependent cell death. EBioMedicine. 2016;7:35-49.

214. Conde de la Rosa L, Schoemaker MH, Vrenken TE, Buist-Homan M, Havinga R, Jansen PL, et al. Superoxide anions and hydrogen peroxide induce hepatocyte death by different mechanisms: involvement of JNK and ERK MAP kinases. Journal of hepatology. 2006;44(5):918-29.

215. Laing JG, Chou BC, Steinberg TH. ZO-1 alters the plasma membrane localization and function of Cx43 in osteoblastic cells. Journal of cell science. 2005;118(Pt 10):2167-76.

216. Musch MW, Walsh-Reitz MM, Chang EB. Roles of ZO-1, occludin, and actin in oxidant-induced barrier disruption. American journal of physiology Gastrointestinal and liver physiology. 2006;290(2):G222-31.

217. Fukui A, Naito Y, Handa O, Kugai M, Tsuji T, Yoriki H, et al. Acetyl salicylic acid induces damage to intestinal epithelial cells by oxidation-related modifications of ZO-1. American journal of physiology Gastrointestinal and liver physiology. 2012;303(8):G927-36.

218. Laing JG, Koval M, Steinberg TH. Association with ZO-1 correlates with plasma membrane partitioning in truncated connexin45 mutants. The Journal of membrane biology. 2005;207(1):45-53.

219. Garcia-Ramirez M, Villarroel M, Corraliza L, Hernandez C, Simo R. Measuring permeability in human retinal epithelial cells (ARPE-19): implications for the study of diabetic retinopathy. Methods in molecular biology. 2011;763:179-94.

220. Yoshikawa T, Ogata N, Izuta H, Shimazawa M, Hara H, Takahashi K. Increased expression of tight junctions in ARPE-19 cells under endoplasmic reticulum stress. Current eye research. 2011;36(12):1153-63.

221. Thurman JM, Renner B, Kunchithapautham K, Ferreira VP, Pangburn MK, Ablonczy Z, et al. Oxidative stress renders retinal pigment epithelial cells susceptible to complement-mediated injury. The Journal of biological chemistry. 2009;284(25):16939-47.

222. Eichler W, Friedrichs U, Thies A, Tratz C, Wiedemann P. Modulation of matrix metalloproteinase and TIMP-1 expression by cytokines in human RPE cells. Investigative ophthalmology & visual science. 2002;43(8):2767-73.

223. Abu El-Asrar AM, Mohammad G, Nawaz MI, Siddiquei MM, Van den Eynde K, Mousa A, et al. Relationship between vitreous levels of matrix metalloproteinases and vascular endothelial growth factor in proliferative diabetic retinopathy. PloS one. 2013;8(12):e85857.

224. Tobar N, Villar V, Santibanez JF. ROS-NFkappaB mediates TGF-beta1-induced expression of urokinase-type plasminogen activator, matrix metalloproteinase-9 and cell invasion. Molecular and cellular biochemistry. 2010;340(1-2):195-202.

225. Benito-Almazan MJ. Papel del Factor de Crecimiento Transformante Beta (TGF-β) y eficacia de las moléculas inhibidoras en la respuesta inflamatoria de la superficie ocular. Universidad de Valladolid; 2012.

226. Fang S, Pentinmikko N, Ilmonen M, Salven P. Dual action of TGF-beta induces vascular growth in vivo through recruitment of angiogenic VEGF-producing hematopoietic effector cells. Angiogenesis. 2012;15(3):511-9.

227. Isenberg JS, Martin-Manso G, Maxhimer JB, Roberts DD. Regulation of nitric oxide signalling by thrombospondin 1: implications for anti-angiogenic therapies. Nature reviews Cancer. 2009;9(3):182-94.

228. Principe DR, Doll JA, Bauer J, Jung B, Munshi HG, Bartholin L, et al. TGF-beta: duality of function between tumor prevention and carcinogenesis. Journal of the National Cancer Institute. 2014;106(2):djt369.

229. Dobaczewski M, Chen W, Frangogiannis NG. Transforming growth factor (TGF)-beta signaling in cardiac remodeling. Journal of molecular and cellular cardiology. 2011;51(4):600-6.

230. Andaluz A, Yeste M, Rodriguez-Gil JE, Rigau T, Garcia F, Rivera del Alamo MM. Pro-inflammatory cytokines: Useful markers for the diagnosis of canine mammary tumours? Veterinary journal. 2016;210:92-4.

231. Szubert M, Suzin J, Duechler M, Szulawska A, Czyz M, Kowalczyk-Amico K. Evaluation of selected angiogenic and inflammatory markers in endometriosis before and after danazol treatment. Reproduction, fertility, and development. 2014;26(3):414-20.

232. Petrella BL, Armstrong DA, Vincenti MP. Interleukin-1 beta and transforming growth factor-beta 3 cooperate to activate matrix metalloproteinase expression and invasiveness in A549 lung adenocarcinoma cells. Cancer letters. 2012;325(2):220-6.

233. Tian J, Chen JW, Gao JS, Li L, Xie X. Resveratrol inhibits TNF-alpha-induced IL-1beta, MMP-3 production in human rheumatoid arthritis fibroblast-like synoviocytes via modulation of PI3kinase/Akt pathway. Rheumatology international. 2013;33(7):1829-35.

234. Badawi MA, Abouelfadl DM, El-Sharkawy SL, El-Aal WE, Abbas NF. Tumor-Associated Macrophage (TAM) and Angiogenesis in Human Colon Carcinoma. Open access Macedonian journal of medical sciences. 2015;3(2):209-14.

235. Tahara Y, Ido A, Yamamoto S, Miyata Y, Uto H, Hori T, et al. Hepatocyte growth factor facilitates colonic mucosal repair in experimental ulcerative colitis in rats. The Journal of pharmacology and experimental therapeutics. 2003;307(1):146-51.

236. Visconti RP, Richardson CD, Sato TN. Orchestration of angiogenesis and arteriovenous contribution by angiopoietins and vascular endothelial growth factor (VEGF). Proceedings of the National Academy of Sciences of the United States of America. 2002;99(12):8219-24.

237. Taylor KR, Rudisill JA, Gallo RL. Structural and sequence motifs in dermatan sulfate for promoting fibroblast growth factor-2 (FGF-2) and FGF-7 activity. The Journal of biological chemistry. 2005;280(7):5300-6.

238. Kim M, Park HJ, Seol JW, Jang JY, Cho YS, Kim KR, et al. VEGF-A regulated by progesterone governs uterine angiogenesis and vascular remodelling during pregnancy. EMBO molecular medicine. 2013;5(9):1415-30.

239. Arjaans M, Schroder CP, Oosting SF, Dafni U, Kleibeuker JE, de Vries EG. VEGF pathway targeting agents, vessel normalization and tumor drug uptake: from bench to bedside. Oncotarget. 2016;7(16):21247-58.

240. Brooks RC, Hasley PB, Jasti H, Macpherson D. Update in general internal medicine: evidence published in 2011. Annals of internal medicine. 2012;156(9):649-53.

241. Viita H, Markkanen J, Eriksson E, Nurminen M, Kinnunen K, Babu M, et al. 15-lipoxygenase-1 prevents vascular endothelial growth factor A- and placental growth factor-induced angiogenic effects in rabbit skeletal muscles via reduction in growth factor mRNA levels, NO bioactivity, and downregulation of VEGF receptor 2 expression. Circulation research. 2008;102(2):177-84.

242. Scaldaferri F, Vetrano S, Sans M, Arena V, Straface G, Stigliano E, et al. VEGF-A links angiogenesis and inflammation in inflammatory bowel disease pathogenesis. Gastroenterology. 2009;136(2):585-95.e5.

243. Kunstfeld R, Hirakawa S, Hong YK, Schacht V, Lange-Asschenfeldt B, Velasco P, et al. Induction of cutaneous delayed-type hypersensitivity reactions in VEGF-A transgenic mice results in chronic skin inflammation associated with persistent lymphatic hyperplasia. Blood. 2004;104(4):1048-57.

244. Leppanen P, Koota S, Kholova I, Koponen J, Fieber C, Eriksson U, et al. Gene transfers of vascular endothelial growth factor-A, vascular endothelial growth factor-B, vascular endothelial growth factor-C, and vascular endothelial growth factor-D have no

effects on atherosclerosis in hypercholesterolemic low-density lipoprotein-receptor/apolipoprotein B48-deficient mice. Circulation. 2005;112(9):1347-52.

245. Yang Z, Mo X, Gong Q, Pan Q, Yang X, Cai W, et al. Critical effect of VEGF in the process of endothelial cell apoptosis induced by high glucose. Apoptosis: an international journal on programmed cell death. 2008;13(11):1331-43.

246. He X, Cheng R, Benyajati S, Ma JX. PEDF and its roles in physiological and pathological conditions: implication in diabetic and hypoxia-induced angiogenic diseases. Clinical science. 2015;128(11):805-23.

247. Zhang SX, Wang JJ, Gao G, Shao C, Mott R, Ma JX. Pigment epithelium-derived factor (PEDF) is an endogenous antiinflammatory factor. FASEB journal : official publication of the Federation of American Societies for Experimental Biology. 2006;20(2):323-5.

248. Becerra SP, Notario V. The effects of PEDF on cancer biology: mechanisms of action and therapeutic potential. Nature reviews Cancer. 2013;13(4):258-71.

249. Zhang SX, Wang JJ, Gao G, Parke K, Ma JX. Pigment epithelium-derived factor downregulates vascular endothelial growth factor (VEGF) expression and inhibits VEGF-VEGF receptor 2 binding in diabetic retinopathy. Journal of molecular endocrinology. 2006;37(1):1-12.

250. Ablonczy Z, Prakasam A, Fant J, Fauq A, Crosson C, Sambamurti K. Pigment epithelium-derived factor maintains retinal pigment epithelium function by inhibiting vascular endothelial growth factor-R2 signaling through gamma-secretase. The Journal of biological chemistry. 2009;284(44):30177-86.

251. Johnston EK, Francis MK, Knepper JE. Recombinant pigment epithelium-derived factor PEDF binds vascular endothelial growth factor receptors 1 and 2. In vitro cellular & developmental biology Animal. 2015;51(7):730-8.

252. Dufour A, Overall CM. Missing the target: matrix metalloproteinase antitargets in inflammation and cancer. Trends in pharmacological sciences. 2013;34(4):233-42.

253. Chau KY, Sivaprasad S, Patel N, Donaldson TA, Luthert PJ, Chong NV. Plasma levels of matrix metalloproteinase-2 and -9 (MMP-2 and MMP-9) in age-related macular degeneration. Eye. 2007;21(12):1511-5.

254. Kimura K, Orita T, Liu Y, Yang Y, Tokuda K, Kurakazu T, et al. Attenuation of EMT in RPE cells and subretinal fibrosis by an RAR-gamma agonist. Journal of molecular medicine. 2015;93(7):749-58.

255. Juuti-Uusitalo K, Nieminen M, Treumer F, Ampuja M, Kallioniemi A, Klettner A, et al. Effects of Cytokine Activation and Oxidative Stress on the Function of the Human Embryonic Stem Cell-Derived Retinal Pigment Epithelial Cells. Investigative ophthalmology & visual science. 2015;56(11):6265-74.

256. Cichon MA, Radisky DC. ROS-induced epithelial-mesenchymal transition in mammary epithelial cells is mediated by NF-kB-dependent activation of Snail. Oncotarget. 2014;5(9):2827-38.

257. Sun S, Bay-Jensen AC, Karsdal MA, Siebuhr AS, Zheng Q, Maksymowych WP, et al. The active form of MMP-3 is a marker of synovial inflammation and cartilage turnover in inflammatory joint diseases. BMC musculoskeletal disorders. 2014;15:93.

258. Kernt M, Hirneiss C, Wolf A, Liegl R, Rueping J, Neubauer A, et al. Indocyanine green increases light-induced oxidative stress, senescence, and matrix metalloproteinases 1 and 3 in human RPE cells. Acta ophthalmologica. 2012;90(6):571-9.

259. Kofla-Dlubacz A, Matusiewicz M, Krzystek-Korpacka M, Iwanczak B. Correlation of MMP-3 and MMP-9 with Crohn's disease activity in children. Digestive diseases and sciences. 2012;57(3):706-12.

260. Bauer AT, Burgers HF, Rabie T, Marti HH. Matrix metalloproteinase-9 mediates hypoxia-induced vascular leakage in the brain via tight junction rearrangement. Journal of cerebral blood flow and metabolism : official journal of the International Society of Cerebral Blood Flow and Metabolism. 2010;30(4):837-48.

261. Demeestere D, Dejonckheere E, Steeland S, Hulpiau P, Haustraete J, Devoogdt N, et al. Development and Validation of a Small Single-domain Antibody That Effectively Inhibits Matrix Metalloproteinase 8. Molecular therapy : the journal of the American Society of Gene Therapy. 2016;24(5):890-902.

262. Dejonckheere E, Vandenbroucke RE, Libert C. Matrix metalloproteinase8 has a central role in inflammatory disorders and cancer progression. Cytokine & growth factor reviews. 2011;22(2):73-81.

263. Craig VJ, Quintero PA, Fyfe SE, Patel AS, Knolle MD, Kobzik L, et al. Profibrotic activities for matrix metalloproteinase-8 during bleomycin-mediated lung injury. Journal of immunology. 2013;190(8):4283-96.

264. Chen J, Crawford R, Xiao Y. Vertical inhibition of the PI3K/Akt/mTOR pathway for the treatment of osteoarthritis. Journal of cellular biochemistry. 2013;114(2):245-9.

265. Feng S, Cen J, Huang Y, Shen H, Yao L, Wang Y, et al. Matrix metalloproteinase-2 and -9 secreted by leukemic cells increase the permeability of blood-brain barrier by disrupting tight junction proteins. PloS one. 2011;6(8):e20599.

266. Cao L, Wang H, Wang F. Amyloid-beta-induced matrix metalloproteinase-9 secretion is associated with retinal pigment epithelial barrier disruption. International journal of molecular medicine. 2013;31(5):1105-12.

267. Kim JY, Ko AR, Hyun HW, Kang TC. ETB receptor-mediated MMP-9 activation induces vasogenic edema via ZO-1 protein degradation following status epilepticus. Neuroscience. 2015;304:355-67.

268. Juel HB, Faber C, Svendsen SG, Vallejo AN, Nissen MH. Inflammatory cytokines protect retinal pigment epithelial cells from oxidative stress-induced death. PloS one. 2013;8(5):e64619.

269. Prosser HC, Tan JT, Dunn LL, Patel S, Vanags LZ, Bao S, et al. Multifunctional regulation of angiogenesis by high-density lipoproteins. Cardiovascular research. 2014;101(1):145-54.

270. Morgan MJ, Liu ZG. Crosstalk of reactive oxygen species and NF-kappaB signaling. Cell research. 2011;21(1):103-15.

271. Scott ML, Fujita T, Liou HC, Nolan GP, Baltimore D. The p65 subunit of NF-kappa B regulates I kappa B by two distinct mechanisms. Genes & development. 1993;7(7a):1266-76.

272. Badger TM, Huang J, Ronis M, Lumpkin CK. Induction of cytochrome P450 2E1 during chronic ethanol exposure occurs via transcription of the CYP 2E1 gene when blood alcohol concentrations are high. Biochemical and biophysical research communications. 1993;190(3):780-5.

273. Zhang RH, Gao JY, Guo HT, Scott GI, Eason AR, Wang XM, et al. Inhibition of CYP2E1 attenuates chronic alcohol intake-induced myocardial contractile dysfunction and apoptosis. Biochimica et biophysica acta. 2013;1832(1):128-41.

274. Xu Y, Feng Y, Li H, Gao Z. Ferric citrate CYP2E1-independently promotes alcohol-induced apoptosis in HepG2 cells via oxidative/nitrative stress which is attenuated by pretreatment with baicalin. Food and chemical toxicology : an international journal published for the British Industrial Biological Research Association. 2012;50(9):3264-72.

275. Perlman H, Georganas C, Pagliari LJ, Koch AE, Haines K, 3rd, Pope RM. Bcl-2 expression in synovial fibroblasts is essential for maintaining mitochondrial homeostasis and cell viability. Journal of immunology. 2000;164(10):5227-35.

276. Chen G, Ke Z, Xu M, Liao M, Wang X, Qi Y, et al. Autophagy is a protective response to ethanol neurotoxicity. Autophagy. 2012;8(11):1577-89.

277. Wu D, Wang X, Zhou R, Yang L, Cederbaum AI. Alcohol steatosis and cytotoxicity: the role of cytochrome P4502E1 and autophagy. Free radical biology & medicine. 2012;53(6):1346-57.

278. Sidorik L, Kyyamova R, Bobyk V, Kapustian L, Rozhko O, Vigontina O, et al. Molecular chaperone, HSP60, and cytochrome P450 2E1 co-expression in dilated cardiomyopathy. Cell biology international. 2005;29(1):51-5.

279. Corsetti G, Stacchiotti A, Tedesco L, D'Antona G, Pasini E, Dioguardi FS, et al. Essential amino acid supplementation decreases liver damage induced by chronic ethanol consumption in rats. International journal of immunopathology and pharmacology. 2011;24(3):611-9.

280. Yang X, Hondur G, Tezel G. Antioxidant Treatment Limits Neuroinflammation in Experimental Glaucoma. Investigative ophthalmology & visual science. 2016;57(4):2344-54.

281. Kowluru RA, Mishra M, Kumar B. Diabetic retinopathy and transcriptional regulation of a small molecular weight G-Protein, Rac1. Experimental eye research. 2016;147:72-7.

ANNEX

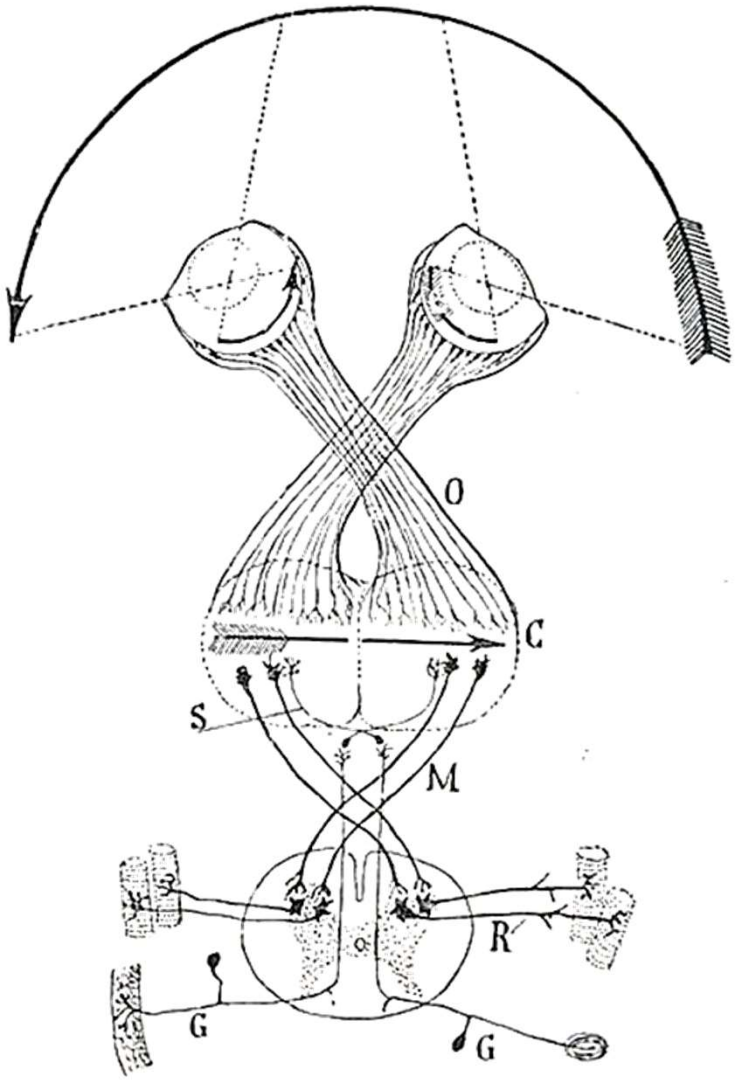

Optic nerves cross-linking
in lower vertebrates

S. Ramón y Cajal

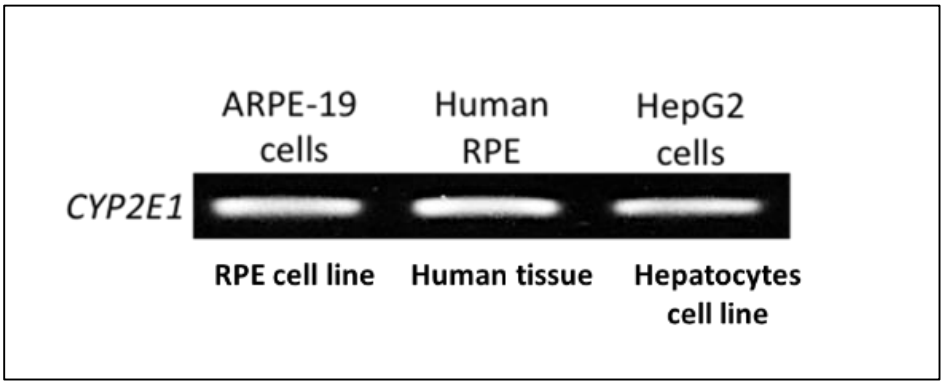

Figure 1. HEPG2 as a positive control of CYP21E expression. Same primers used in PCR assay amplified same CYP2E1 sequence in RPE compared with HEPG2 cells.

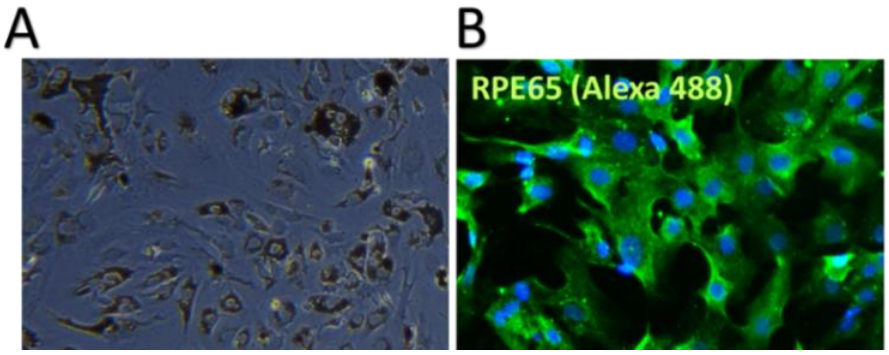

Figure 2. hRPE cells present RPE typical morphology and pigmentation **(A).** hRPE cells has a positive labeling of RPE65 in hRPE cells **(B).**

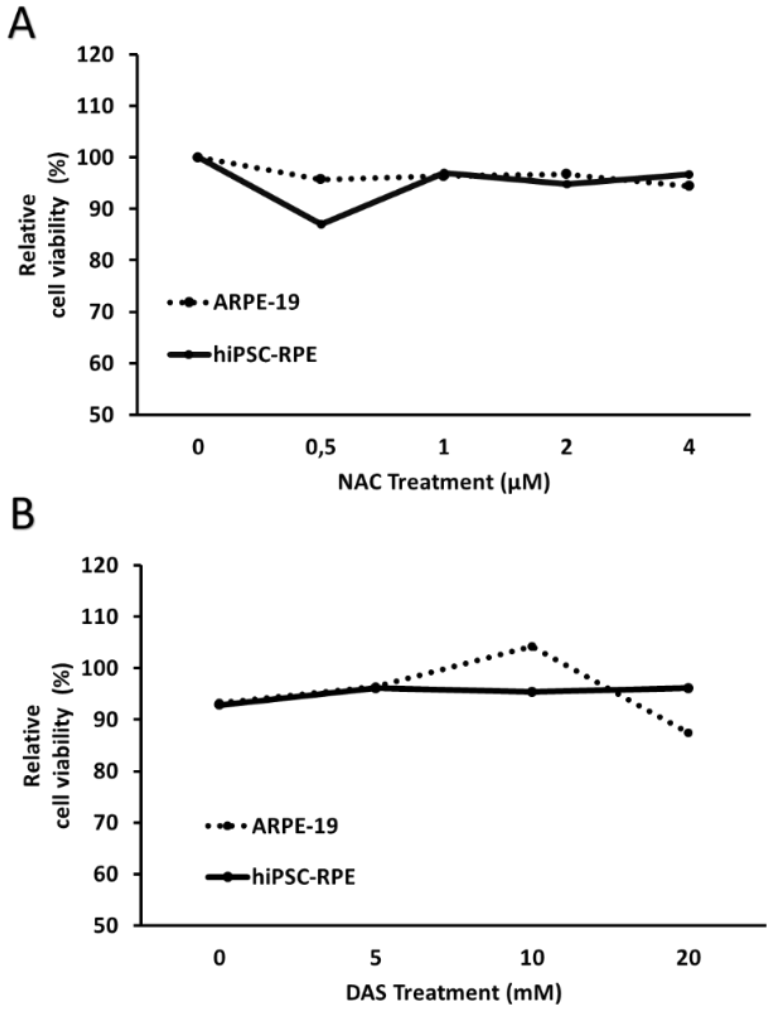

Figure 3. Drugs toxicity assay. XTT was assayed to evaluate the NAC treatment toxicity (A) and DAS (B). None of the concentrations used resulted in significant cell death. Values are expressed as mean (N=3). Statistical significance was determined by ANOVA and t-Student analysis.

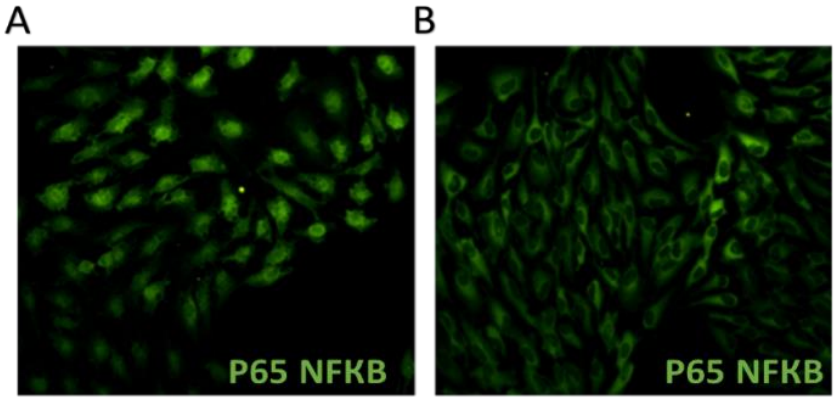

Figure 4. NFKB Immunocytochemistry. 100 mM of H_2O_2 induces P65 NFKB translocation (**A**). On the other hand, 100 µM did not promote it (**B**)

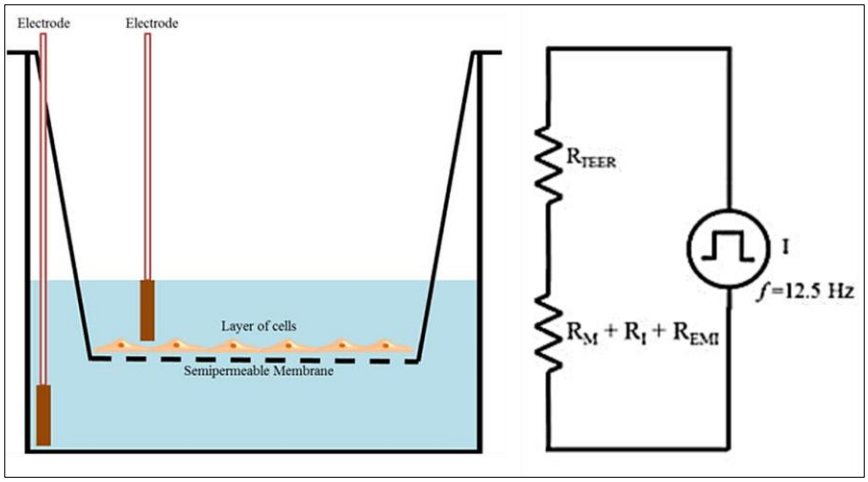

Figure 5. TER measurement with chopstick electrodes. Obtained and modified from Srinivasan B et al., 2015 (46).

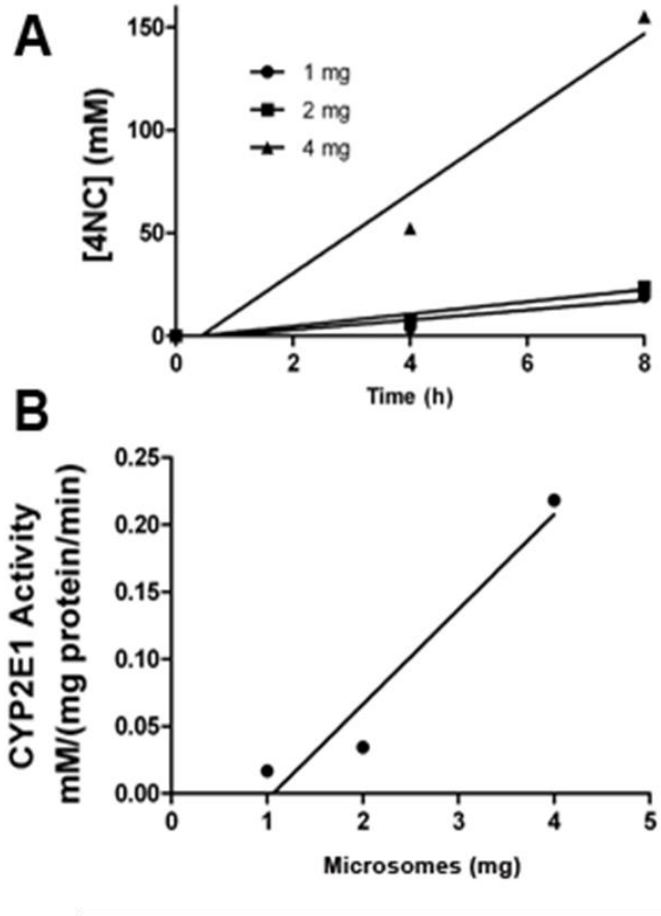

Figure 6. CYP2E1 activity. Time course of 4NC formation on microsomal-CYP2E1 from ARPE-19 cells (**A**). Graphical representation of the CYP2E1 activity versus different amounts of ARPE-microsomes, along 4 hours, (**B**). Values are expressed as mean. Activity of CYP2E1 was calculated by 4NC formation by the incubation time and microsomal protein content (nmol/min.mg).

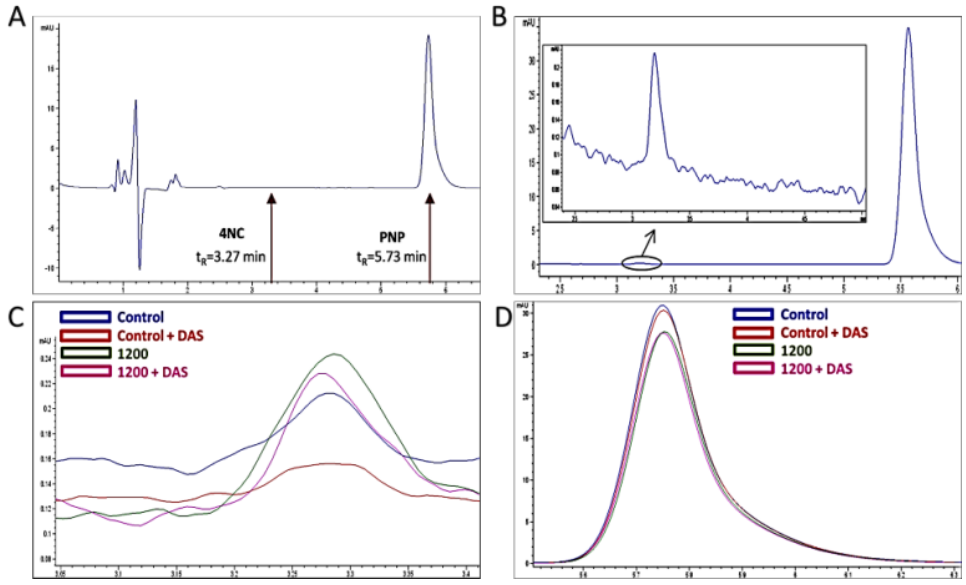

Figure 7. HPLC chromatogram of CYP2E1 activity. Blank chromatogram (**A**). Chromatogram corresponding to the time course of 16 h using 2 mg microsome (**B**). Overlapped chromatograms where it can be seen the apparition of the product 4NC (t_R = 3.27 min) (**C**). Consumption of the product PNP (t_R = 5.73 min), (**D**).

The work developed in this thesis has allowed to publish the following journal articles:

- Flores-Bellver M, Bonet-Ponce L, Barcia JM, Garcla-Verdugo JM, **Martinez-Gil N**, Saez-Atienzar S, Sancho-Pelluz J, Jordan J, Galindo M, Romero FJ. "Autophagy and mitochondrial alterations in human retinal pigment epithelial cells induced by ethanol. Implications of 4-hydroxy-nonenal"Cell Death Dis. 2014

- Barcia JM, Flores-Bellver M, Muriach M, Sancho-Pelluz J, Lopez-Malo D, Urdaneta AC, **Martinez-Gil N,** Atienzar-Aroca S, Romero FJ "Matching diabetes and alcoholism: oxidative stress, inflammation and neurogenesis are commonly involved" Mediat Inflamm. 2015

- **Martinez-Gil N**, Flores-Bellver M, Atienzar-Aroca S, Lopez-Malo D, Urdaneta AC, Sancho-Pelluz J, Peris C, Bonet-Ponce L, Romero FJ, Barcia JM "CYP2E1 in the human retinal pigment epithelium: expression, activity and induction by etanol" Invest Ophthalmol Vis Sci. 2015

- Bonet-Ponce L, Saez-Atienzar S, da Casa C, Sancho-Pelluz J, Barcia JM, **Martinez-Gil N**, Nava E, Jordan J, Romero FJ, Galindo MF. "Rotenone Induces the Formation of 4-Hydroxynonenal Aggresomes. Role of ROS-Mediated Tubulin Hyperacetylation and Autophagic Flux Disruption" Mol Neurobiol. 2016

- Atienzar-Aroca S, Flores-Bellver M, Serrano-Heras G, **Martinez-Gil N**, Barcia JM, Aparicio S, Perez-Cremades D, Garcia-Verdugo JM, Diaz-Llopis M, Romero FJ, Sancho-Pelluz J "Oxidative stress in retinal pigment epithelium cells increases exosome secretion and promotes angiogenesis in endothelial cells." J Cell Mol Med. 2016

The work developed in this thesis has been presented at the following national and international meetings and conferences:

- Romero FJ, Flores-Bellver M, Bonet-Ponce L, **Martínez-Gil N**, Barcia JM, Johnsen-Soriano S, Arnal E. "Alcohol exposure induces toxicity in a human RPE model" Association for Research in Vision and Ophtalmology (ARVO) Annual Meeting Seattle, Washington (EE.UU) 2013

- Bonet-Ponce L, Flores-Bellver M, **Martínez-Gil N**, Sancho-Pelluz J, Barcia JM; Romero FJ. "Ethanol exposure induces cell death by oxidative stress in human RPE in vitro model" Young Researcher Vision Camp 2013 Leibertingen, Germany. 2013

- **Martínez-Gil N**, Atienzar-Aroca S, Flores-Bellver M, Bonet-Ponce L, Sancho-Pelluz J, Barcia JM, Romero FJ. "CYP2E1 mediated ethanol metabolism in ARPE-19 cells" Association for Research in Vision and Ophtalmology (ARVO) Annual Meeting. Orlando, Florida (EE.UU). 2014

- Bonet-Ponce L, Flores-Bellver M, **Martínez-Gil N**, Saez-Atienzar S, Sancho-Pelluz J, Barcia JM, Jordan J,Galindo M, Romero FJ. "Effects of Ethanol on ARPE-19 cells: Autophagy and Oxidative Stress" Association for Research in Vision and Ophtalmology (ARVO) Annual Meeting Orlando, Florida (EE.UU). 2014

- **Martinez-Gil N**, Atienzar-Aroca S, Flores-Bellver M, Barcia JM, Garcia Verdugo JM, Sancho-Pelluz J, Serrano-Heras G, Romero FJ "Relationship between Autophagy and exosomes derived ARPE cells: Relevance of Ethanol in the RPE metabolism." Annual Meeting of the American Society for Exosomes and Microvesicles.Pacific Grove, CA (EE.UU). 2014

- Flores-Bellver M, Atienzar-Aroca S, **Martinez-Gil N**, Barcia JM, Garcia Verdugo JM, Sancho-Pelluz J, Serrano-Heras G, Romero FJ. "Retinal pigment epithelium-derived exosomes contain VEGF receptors after an oxidative insult." Annual Meeting of the American Society for Exosomes and Microvesicles. Pacific Grove, CA (EE.UU). 2014

- Atienzar-Aroca S, Flores-Bellver M, Serrano-Heras G, **Martinez-Gil N**, Barcia JM, Garcia Verdugo JM, ancho-Pelluz J, Romero FJ. "Ethanol induced liberation of VEGF and VEGF receptors in exosomes from Retinal Pigment Epithelium" Annual Meeting of the American Society for Exosomes and Microvesicles.
  Pacific Grove, CA (EE.UU). 2014

- **Martínez-Gil N**, Atienzar S, Flores-Bellver M, López-Malo D, Morillas-Carrasco N, Urdaneta AC, Sancho- Pelluz J, Barcia JM, Romero FJ. "CYP2E1 mediated ethanol metabolism in ARPE-19 cells" I Congress of PhD Students in Biomedicine. Valencia. 20147

- Atienzar-Aroca S, Flores-Bellver M, Serrano-Heras G, **Martinez-Gil N**, Barcia JM, Garcia Verdugo JM, Sancho-Pelluz J, Romero FJ. "Retinal pigment epithelium-derived exosomes contain vegf receptors following an oxidative insult."
  I Congress of PhD Students in Biomedicine. Valencia. 2014

- Flores-Bellver M, Bonet-Ponce L, Barcia JM, Garcia-Verdugo JM, **Martinez-Gil N**, Saez-Atienzar S, Sancho-Pelluz J, Jordan J, Galindo MJ, Romero JF."Autophagy and mitochondrial alterations in human retinal pigment epithelial cells induced by ethanol. Implications of 4-hydroxy-nonenal. I Congress of PhD Students in Biomedicine. Valencia. 2014

- Atiénzar-Aroca S, Flores-Bellver M, Serrano-Heras G, **Martinez-Gil N**, Barcia JM, Garcia-Verdugo JM, Sancho-Pelluz J, Romero FJ. "Stressed human retinal pigment epithelium-derived exosomes induce angiogenesis in vitro" World Congress on Angiogenesis. Boston, MA (EE.UU). 2015

- Sancho-Pelluz J, Atienzar-Aroca S, Flores-Bellver F, Serrano-Heras G, **Martinez-Gil N,** Barcia JM, Aparicio S, Perez-Cremades D, Garcia-Verdugo JM, Romero FJ. "Characterization of exosomes liberated from damaged RPE: implication in new blood vessel formation due to overexpression of VEGF receptor 1 and 2" Association for Research in Vision and Ophtalmology (ARVO) Annual Meeting Denver, Colorado (EE.UU). 2015

- Barcia JM, **Martinez-Gil N**, Flores-Bellver M, Atienzar-Aroca S, López-Malo D, Urdaneta AC, Morillas- Carrasco N, Sancho-Pelluz J, Romero FJ. "CYP2E1 activity on ARPE-19 cells: New approach to RPE ethanol metabolism" Association for Research in Vision and Ophtalmology (ARVO) Annual Meeting. Denver, Colorado (EE.UU). 2015

- Romero FJ, Flores-Bellver M, **Martinez-Gil N**, Atienzar-Aroca S, Morillas-Carrasco N, López-Malo D, Sancho-Pelluz J, Barcia JM "Alcohol-induced Oxidative Stress in RPE is linked to the Metabolism of Ethanol" Association for Research in Vision and Ophtalmology (ARVO) Annual Meeting Denver, Colorado (EE.UU). 2015

- **Martinez-Gil N**; Flores-Bellver Miguel; Atienzar-Aroca, S; Lopez-Malo, D; Urdaneta, AC.; Sancho-Pelluz, J; Peris-Martinez, C; Bonet-Ponce, L; Romero, FJ; Barcia, J M. "Ethanol is metabolized in the human retinal pigment epithelium: role of the cytochrome P450-2E1". OCC World Congress. Valencia, Spain. 2015

- Bonet-Ponce, L; Flores-Bellver, M; **Martinez-Gil, N**; Atienzar-Aroca, S Barcia,JM.; Sancho-Pelluz, J; Jordan J;Romero, FJ. "Autophagy and oxidative stress in human retinal pigment epithelium-derived ARPE-19 cells" OCC World Congress. Valencia, Spain. 2015

- **Martinez-Gil N**, Atiénzar-Aroca S, Flores-Bellver M, Serrano-Heras G, Perez-Cremades D, Barcia JM, Garcia Verdugo JM, Sancho-Pelluz J, Romero FJ "Retinal pigment epithelium-derived exosomes contain VEGF receptors and induces the formation of new vessels by oxidative stress.4th International Conference on Translational Medicine. Baltimore, MD EE.UU. 2015

- **Martinez-Gil N**, Flores-Bellver M, Aparicio S, Vergara MN, Barcia JM,Canto-Soler MV, Romero FJ. "hiPSC-derived RPE as a model of human RPE cells in CYP2E1 expression studies".13th Stem Cell and Regenerative Medicine Conference.. Boston, MA EE.UU. 2016

- **Martínez-Gil N**, Vidal-Gil L, Flores-Bellver M, Aparicio S, Vergara MN, Canto-Soler MV, Romero FJ, Barcia JM. "Use of hiPSC-derived RPE as a model of RPE cells" IIII Congreso de estudiantes predoctorales de Valencia y I Congreso Nacional Biomedicina Jóvenes Investigadores en Valencia. Valencia. 2016

- Vidal-Gil, L, **Martinez-Gil N**, Lopez-Malo, D., Atienzar-Aroca, S, Morillas, N., Perez-Pastor, G.M.A., Barcia, J.M., Romero, F.J., Sancho-Pelluz FJ. "Oxidative stress generated by Ethanol promotes an inflammatory response in the RPE" IIII Congreso de estudiantes predoctorales de Valencia y I Congreso Nacional Biomedicina Jóvenes Investigadores en Valencia. Valencia. 2016

The retinal pigment epithelium (RPE) is essential for the vision. As a part of blood retinal barrier its main role is the retinal and choroid homeostasis maintenance. Alcohol has become the more socially accepted addictive drug. The CYP2E1 enzyme has a high ethanol affinity. Its catalytic activity results in the increase of oxidative stress in cells generating large amounts of reactive oxygen species. In spite of CYP2E1 could be implicated in a RPE visual cycle, nothing is known about its role under alcohol intake.

Our results demonstrate that ethanol increased levels of reactive oxygen species in RPE cells triggering cell death. Alcohol induced RPE barrier dysfunction. increasing CYP2E1 expression. The use of DAS (CYP2E1 inhibitor) and NAC (antioxidant molecule) reverted RPE cellular damage indicating that CYP2E1 is regulated by oxidative stress.. Finally, the presence of CYP2E1 reinforces the protective role of RPE and strongly suggests additional CYP2E1 roles related to vision.